Dossier présenté en vue de l'obtention de l'Habilitation à Diriger des Recherches

Marceau Coupechoux

1. Curriculum Vitae
2. Mémoire d'habilitation
3. Résumés en français et en anglais
4. Sélection d'articles

Institut Mines-Telecom

Telecom ParisTech

Curriculum Vitae

Marceau Coupechoux
Maître de Conférences
Telecom ParisTech, CNRS LTCI
23, avenue d'Italie
75013 Paris, France
marceau.coupechoux@telecom-paristech.fr
http:perso.telecom-paristech.fr/~coupecho
Tél : +33 1 45 81 75 88
Mob. : +33 6 95 96 75 85

Positions

- **Sept. 2011 – août 2012** : Scientifique invité par le Prof. Anurag KUMAR, Indian Institute of Science, ECE dpt., Bangalore, Inde.
- **Depuis déc. 2005** : Maître de Conférences à Telecom ParisTech, Paris, France.
- **Juil. 2004 – déc. 2005** : Ingénieur, Alcatel-Lucent, Dimensionnement des réseaux cellulaires, Vélizy, France.
- **Avr. 2000 – juin 2004** : Ingénieur de Recherche, Alcatel-Lucent Bell Labs, Marcoussis, France.
- **Août 1999 – mars 2000** : Stagiaire, Alcatel-Lucent Bell Labs, Stuttgart, Allemagne.
- **Juil. 1998 – août 1998** : Stagiaire, Alcatel-Lucent, Berlin, Allemagne.

Éducation

- **2004** : **Thèse de Doctorat** (Très Honorable).
  Titre : « Protocoles d'accès au medium pour réseaux ad hoc fortement chargés ».
  Sous la supervision du Prof. Christian BONNET, Institut Eurecom, Sophia Antipolis, France.
  Réalisée chez Alcatel-Lucent Bell Labs, Marcoussis, France.
  Disponible à l'adresse : http://perso.telecom-paristech.fr/~coupecho/publis/thesis.pdf.
  Rapporteurs :
  Prof. Mario GERLA (UCLA, États-Unis).
  Prof. Xavier LAGRANGE (Telecom Bretagne, France).
  Éxaminateurs :
  Prof. Jean-Claude BELFIORE (Telecom ParisTech, France).
  Prof. Bruno BAYNAT (UPMC, France).
  Dr. Vinod KUMAR (Alcatel-Lucent, France).

- **2000** : Dipl-Ing., Université de Stuttgart, Allemagne.
  Studienarbeit (3 mois) : « Interférences entre symboles dans le systéme DAB ».
  Diplomarbeit (8 mois) : « Comparaison de deux techniques de diversité : le codage spatio-temporel et la combinaison par rapport maximal (MRC) », sous la supervision du Prof. Paul KÜHN et du Dr. Volker BRAUN, prix du meilleur Diplomarbeit de l'Université de Stuttgart.

- **1999** : Diplôme d'Ingénieur de Telecom ParisTech.
  Dominantes : Communications, Traitement du signal, Réseaux.

- **1998** : Maîtrise (AB) en mathématiques fondamentales, UPMC, France.

- **1993 - 1996** : Classes préparatoires, Lycée Henri IV, Paris.

- **1993** : Baccalauréat (TB), Lycée Descartes, Antony.

Projets de recherche

- Projet « Urbanisme des radio communications (URC) » (représentant Telecom ParisTech), FUI Pôle de compétitivité SYSTEMATIC, 2006-2009,
- Projet « Terminals for opportunistic radio applications (TEROPP) » (responsable du sous-projet 1), Instituts Carnots, 2008-2011,
- Projet « Qualité de service dans les réseaux ad hoc », DGA/COGYSIS, 2007-2008,

- Contrat industriel « Dimensionnement des réseaux WiMAX », Alcatel-Lucent, 2006-2009,
- Contrat industriel « Dimensionnement des réseaux MIMO », Orange Labs, 2009-2012.
- Projet « Dimensionnement des réseaux ad hoc », LIP6/LTCI, 2009-2012.
- Contrat industriel « Dimensionnement et Qualité de Service pour Réseaux OFDMA dans un Environnement Réel - Application au LTE », Orange Labs, 2010-2013.
- Projet « Femtocell Enabled Roaming and Resource Allocation for a more Resilient Interconnection », LIP6/LTCI, 2012-2014.
- Projet « D2D Communications for LTE-Advanced Cellular Networks », franco-indien CEFIPRA, 2014-2017.
- Projet « Orchestration d'algorithmes d'apprentissage distribués pour la gestion des ressources dans les réseaux mobiles (NETLEARN) » (coordinateur), ANR, 2013-2016.
- Projet « Infrastructure low cost pour le développement des pays émergents », FUI Pôle de compétitivité SYSTEMATIC, 2014-2017.

Membre TPC

IEEE Globecom 2011 (Intl. Workshop on M2M Communications), Future Network and Mobile Summit 2011 (European Workshop on Broadband Femto cell Networks), IEEE ICCCN 2011 (FlexBWAN Workshop), IEEE IWCRN 2012, IEEE WCNC 2012 (Workshop on Hybrid Optical-Wireless Access Networks), IEEE Globecom 2012 (Intl. Workshop on M2M Communications), IEEE ICC 2013 (Wireless Communications Symposium), IEEE WiOpt 2013, IEEE RAWNET 2013, IEEE PIMRC 2013 (Fundamental and PHY Track), IEEE WiCOM 2013, IEEE ICC 2014 (Wireless Communications Symposium), IEEE WiOpt 2014, IEEE RAWNET 2014, IEEE WNC3 2014, IEEE SPCOM 2014, ITS 2014.

Jurys de thèse

- Hicham ANOUAR (Institut Eurecom, 13 novembre 2006).
- Jean-Marc KÉLIF (Telecom ParisTech, 11 février 2008).
- Aymen BELGHITH (Telecom Bretagne, 26 mars 2009).
- François MÉRIAUX (Supélec, 26 novembre 2013).
- Luis SUAREZ (Telecom Bretagne, 13 décembre 2013).

Comité de sélection

- MCF 0068 université de Cergy-Pontoise (2011), sections 27-61, Traitement de l'information et systèmes, équipe Information, Communications, Imagerie du laboratoire ETIS (UMR 8051).

Références

Prof. Philippe GODLEWSKI : Télécom ParisTech, Paris, France.
Dept. Informatique et Réseaux
Tél : +33 1 45 81 73 41
Mèl : philippe.godlewski@telecom-paristech.fr

Prof. Christian BONNET : Institut Eurecom, Sophia-Antipolis, France.
Mobile Communications Dept.
Tél : +33 4 93 00 81 08
Mèl : christian.bonnet@eurecom.fr

Prof. Bruno BAYNAT : Université Pierre et Marie Curie (UMPC), Paris, France.
Laboratoire d'Informatique de Paris 6.
Tél : +33 1 44 27 87 89
Mèl : bruno.baynat@lip6.fr
Dr. Vinod KUMAR : Alcatel-Lucent Bell Labs, Villarceaux, France.
Tél : +33 1 69 63 43 65
Mèl : vinod.kumar@alcatel-lucent.fr
Dr. Jean-Marc KELIF : Orange Labs, Issy-les Moulineaux, France.
Tél : +33 1 45 29 61 79
Mèl : jeanmarc.kelif@orange-ftgroup.com
Prof. Anurag KUMAR : Indian Institute of Science, Bangalore, Inde.
Tél : +91 80 2360 0855
Mèl : anurag@ece.iisc.ernet.in

Encadrement

Post-doctorants

- Muriel MABIALA (2007-2008, 6 mois) : « Qualité de service dans les réseaux ad hoc. »Post-Doctorante (projet DGA),
- Lin CHEN (2009, 8 mois) : « Enchères sur le spectre pour les réseaux radio cognitifs. »Post-Doctorant (projet TEROPP).

Doctorants

- Masood MAQBOOL (2006-2009) : « Ingénierie radio des réseaux d'accès OFDMA. »Thèse soutenue le 9 novembre 2009, co-encadrée avec Philippe GODLEWSKI (Télécom ParisTech) et Véronique CAPDEVIELLE (Alcatel-Lucent),
- Hany KAMAL (2007-2010) : « Allocation dynamique du spectre dans les réseaux d'accès cellulaires. »Thèse soutenue le 7 décembre 2010, co-encadrée avec Philippe GODLEWSKI,
- Dorra BEN CHEIKH (2009-2012) : « Formules de probabilités de coupure pour les réseaux cellulaires : contributions pour les fonctionnalités MIMO, CoMP et de retournement temporel. »Thèse soutenue le 6 juillet 2012, co-encadrée avec Jean-Marc KÉLIF (Orange) et Philippe GODLEWSKI,
- Jing CHI (2008, 1 an) : « Accès aléatoire dans les réseaux IEEE 802.16 »Doctorante de L'Université de Pékin des Postes et Télécommunications (BUPT), en séjour doctoral à Télécom ParisTech, co-encadrée avec Philippe MARTINS (Télécom ParisTech),
- Mattia MINELLI (2010-2013) : « Dimensionnement des réseaux cellulaires avec relais. » Thèse en cours, co-dirigée avec Philippe GODLEWSKI et Ma MAODE (NTU, Singapore),
- Stefano IELLAMO (2011-2014) : « Allocation de ressource dans les réseaux radio cognitifs. »Thèse en cours, co-dirigée avec Philippe GODLEWSKI et Lin CHEN (University of Paris XI Orsay),
- Arpan CHATTOPADYAY (2011-2012) : j'ai travaillé un an avec Arpan, étudiant en thèse d'Anurag KUMAR, sur les relais coopératifs quand j'étais en séjour sabbatique à l'IISc de Bangalore.

Masters

- Yougourtha BOUHANIK (2006) : « Dimensionnement des réseaux 3G : étude du facteur f dans les réseaux cellulaires CDMA. »Master STN (UMPC/TPT),
- Sébastien MARTIN (2007) : « Problèmes combinatoires dans les réseaux sans-fil : conception et performances. »Master IAD (UPMC), co-encadré avec Pierre FOUILHOUX (UMPC, LIP6),

- Hilaire CHEVREAU (2009) : « Gestion centralisée et orchestrée de l'activation de liaisons avec contrôle de puissance dans un réseau WiFi mesh. »Master IAD (UPMC) co-encadré avec Pierre FOUILHOUX (UMPC/LIP6),
- Oussama HABACHI (2009) : « Dimensionnement des réseaux OFDMA : simulateur multi-trafic. »Master Réseaux (UPMC), co-encadré avec Bruno BAYNAT (UMPC, LIP6),
- Nardjesse MILOUDI (2009) : « Dimensionnement des réseaux OFDMA : études de trafic multi-cellulaires. »Master Réseaux (UMPC), co-encadré avec Bruno BAYNAT (UMPC, LIP6),
- Stefano IELLAMO (2009) : « Opportunistic Spectrum Access for Cognitive Radio Networks. » Thesi de Laurea Magistrale (Politecnico di Milano), co-encadré avec Lin CHEN (TPT),
- Abhishek SINHA (2011-2012) : « Optimal Impromptu Deployment of a Multi-hop Wireless Network on a Random Lattice Path. »Master IISc, co-encadré avec Anurag KUMAR (IISc),
- Reuben G. STEPHEN (2011-2012) : « Pilot Allocation and Receive Antenna Selection : A Markov Decision Theoretic Approach. »Master IISc, co-encadré avec Chandra MURTHY (IISc),
- Iyad CHERIF (2013) : « Algorithmes d'apprentissage distribués pour les réseaux femto. »Master SAR (Supelec), co-encadré avec Stefano Iellamo (TPT).

Enseignement

J'ai dispensé quelques cours pendant ma thèse (à l'UPMC, à l'ENSTA, à l'ISEP, à l'Université Paris XIII) mais j'ai acquis l'essentiel de mon expérience à Télécom ParisTech (TPT). Dans cette école, les enseignements sont structurés en Unités d'Enseignement (UE) de 40 ou 60 heures. Je suis intervenu et j'interviens dans les Unités d'Enseignement suivantes :

RES101 (L3) : Réseaux (2006-2011),

RES200 (M1) : Cycle d'harmonisation Réseaux (2006-2013),

RES222 (M1) : Accès au medium et ordonnancement (2006-2013),

RES841 (M1) : Foundations of Computer Networks (*Master of Science*) (2008-2013),

RES340 (M2) : Communications sans fil et réseaux autonomes (2006-2008),

RES341 (M2) : Ingénierie des réseaux radio-mobiles (2005-2013),

RES345 (M2) : Réseaux radio-mobiles cellulaires (2005-2013),

RES390 (M2) : Interfaces radio haut débit (semaine Athènes) (2007)

COM944 (M2) : Simulation de Systèmes Mobiles et Implémentation des Systèmes Numériques (Master STN UMPC/TPT) (2009-2011).

Je suis intervenu et j'interviens dans les sessions de formation continue suivantes :

FCK53 : Systèmes cellulaires : du GSM à l'UMTS (2005-2006),

FCK55 : UMTS : une nouvelle technique radio et une convergence vers l'IP (2006-2007),

FCG57 : Principes de la téléphonie sur IP et de la voix sur IP (2006-2010),

FCK59 : WiFi et ses technologies connexes (2007),

FCS62 : Radio cognitive opportuniste : enjeux, contraintes et perspectives (2010),

FCK69 : De la 3G+ à la 4G : HSPA, 3G-LTE, LTE-Advanced (2008-2013).

Je donne chaque année 6 heures de cours et 6 heures de TD en anglais aux élèves de troisième année de l'ISEP sur le thème « Performances et théorie des files d'attente ». J'ai donné pendant plusieurs années 3 heures de cours par an à l'Université Paris XIII sur le thème « Introduction aux WLAN ».

J'assure en alternance la coordination de l'Unité d'Enseignement RES222 depuis 2006, de l'UE RES345 depuis 2007 et de l'UE RES200 depuis 2008. Je coordonne la session de formation continue FCK69 (voir *supra*).

Le tableau 1 donne les heures équivalent TD (HETD) que j'ai effectuées depuis 2005 [1]. On obtient une moyenne de 219 HETD par an hors première année et année sabbatique.

TABLE 1 – Volumes horaires d'enseignement

Années scolaires	**HETD**
2005-2006	176
2006-2007	255
2007-2008	232
2008-2009	331
2009-2010	184
2010-2011	179
2011-2012	0
2012-2013	138

1. Avec la règle suivante : 1 heure de cours = 1,5 HETD, 1 heure de TP = 1 HETD, 1 projet libre (3 mois) = 10 HETD, 1 mini-projet dans une UE de 60h = 5 HETD. La valeur pour 2012-2013 est une estimation. 2011-2012 correspond à mon année sabbatique.

Publications

Journaux

[1] M. Minelli, M. Ma, M. Coupechoux, J.-M. Kélif, M. Sigelle, and Ph. Godlewski. Optimal relay placement in cellular networks. *IEEE Trans. on Wireless Communications*, 2014. to appear.

[2] R. G. Stephen, Ch. R. Murthy, and M. Coupechoux. A markov decision theoretic approach to pilot allocation and receive antenna selection. *IEEE Trans. on Wireless Communications*, 12(8) :3813–3823, August 2013.

[3] S. Iellamo, L. Chen, and M. Coupechoux. Proportional and Double Imitation Rules for Spectrum Access in Cognitive Radio Networks. *Elsevier Computer Networks*, 57(8) :1863–1879, June 2013.

[4] D. Ben Cheikh, J.-M. Kélif, M. Coupechoux, and Ph. Godlewski. Analytical Joint Processing Multi-Point Cooperation Performance in Rayleigh Fading. *IEEE Wireless Communications Letters*, 1(4) :272–275, Aug. 2012.

[5] D. Ben Cheikh, J.-M. Kélif, M. Coupechoux, and Ph. Godlewski. Multi-cellular Alamouti Scheme Performance in Rayleigh and Shadow Fading. *Springer Annals of telecommunications*, 68(5-6) :345–358, June 2012.

[6] J.-M. Kélif, M. Coupechoux, and Ph. Godlewski. On the Dimensioning of Cellular OFDMA Networks. *Elsevier Physical Communication*, 5(1) :10–21, Mar. 2012.

[7] M. Minelli, M. Coupechoux, J.-M. Kélif, M. Ma, and Ph. Godlewski. SIR Estimation in Hexagonal Cellular Networks with Best Server Policy. *Kluwer Wireless Personnal Communications*, 69(1) :133–152, Mar. 2012.

[8] H. Kamal, M. Coupechoux, and Ph. Godlewski. Tabu Search for Dynamic Spectrum Allocation (DSA) in Cellular Networks. *European Transactions on Telecommunications*, 23(6) :508–521, Jan. 2012.

[9] D. Ben Cheikh, J.-M. Kélif, M. Coupechoux, and Ph. Godlewski. SIR Distribution Analysis in Cellular Networks Considering the Joint Impact of Path-loss, Shadowing and Fast Fading. *EURASIP Journal on Wireless Communications and Networking*, 2011(137) :1–10, Oct. 2011.

[10] L. Chen, S. Iellamo, M. Coupechoux, and Ph. Godlewski. Spectrum Auction with Interference Constraint for Cognitive Radio Networks with Multiple Primary and Secondary Users. *Springer Wireless Networks*, 17(5) :1355–1371, May 2011.

[11] H. Kamal, M. Coupechoux, Ph. Godlewski, and J.-M. Kélif. Optimal, Heuristic and Q-learning Based DSA Policies for Cellular Networks with Coordinated Access Band. *European Transactions on Telecommunications*, 21(8) :694–703, Dec. 2010.

[12] J.-M. Kélif, M. Coupechoux, and Ph. Godlewski. A Fluid Model for Performance Analysis in Cellular Networks. *EURASIP Journal on Wireless Communications and Networking*, 2010(435189) :1–11, July 2010.

[13] S. Doirieux, B. Baynat, M. Maqbool, and M. Coupechoux. An Efficient Analytical Model for the Dimensioning of WiMAX Networks Supporting Multi-profile Best Effort Traffic. *Elsevier Computer Communications*, 33(10) :1162–1179, June 2010.

[14] M. Maqbool, Ph. Godlewski, M. Coupechoux, and J.-M. Kélif. Analytical Performance Evaluation of Various Frequency Reuse and Scheduling Schemes in Cellular OFDMA Networks. *Performance Evaluation*, 67(4) :318–337, Apr. 2010.

[15] M. Coupechoux, B. Baynat, Ch. Bonnet, and V. Kumar. CROMA : An Enhanced Slotted MAC Protocol for MANETs. *ACM/Kluwer Mobile Networks and Applications*, 10(1-2) :183–197, June 2005.

[16] M. Cohen, D. Rouffet, L. Brignol et M. Coupechoux. Internet rapide en zones peu denses. *Alcatel Telecommunication Review*, (3) :377–381, Dec. 2004.

[17] M. Coupechoux and B. Baynat and T. Lestable and V. Kumar and C. Bonnet. Improving the MAC Layer of Multi-Hop Networks. *Kluwer Wireless Personal Communications*, 29(1-2) :71–100, Apr. 2004.

Livre et chapitres de livre

[18] Marceau Coupechoux et Philippe Martins. *Vers les systèmes radiomobiles de quatrième génération, de l'UMTS au LTE.* Collection IRIS. Springer, 2012.

[19] M. Maqbool, M. Coupechoux, Ph. Godlewski, and V. Capdevielle. Achieving Frequency Reuse 1 in WiMAX Networks with Beamforming. In *WiMAX, New Developments*. In-Tech, 2009.

[20] G. Nogueira, B. Baynat, M. Maqbool, and M. Coupechoux. Performance evaluation and dimensioning of wimax. In *WiMAX Networks Planning and Optimization*. CRC Press, 2008.

[21] M. Coupechoux and T. Lestable and C. Bonnet and V. Kumar. Throughput of the Multi-hop Slotted Aloha with Multi-Packet Reception. In *Wireless On-demand Network Systems*, volume 2928 of *Lecture Notes in Computer Science*, pages 239–243. Springer, 2004.

Conférences avec actes

[22] S. Iellamo, L. Chen, and M. Coupechoux. Retrospective spectrum access protocol : A payoff-based learning algorithm for cognitive radio networks. In *IEEE International Conference on Communications (ICC)*, Sydney, Australia, June 2014.

[23] M. Minelli, M. Ma, M. Coupechoux, and Ph. Godlewski. A geometrical approach for power optimization in relay-based cellular networks. In *IEEE National Conference on Communications (NCC)*, pages 1–6, Kanpur, India, February 2014.

[24] J.-M. Kélif, S. Senecal, and M. Coupechoux. Impact of small cells location on performance and qos of heterogeneous cellular networks. In *IEEE International Symposium on Personal, Indoor and Mobile Radiocommunications (PIMRC)*, London, UK, September 2013.

[25] M. Minelli, M. Ma, J.-M. Kélif, M. Coupechoux, and M. Sigelle. A fluid approach for performance analysis of lte-a networks with relays. In *IEEE International Symposium on Personal, Indoor and Mobile Radiocommunications (PIMRC), Workshop on Cooperative and Heterogeneous Cellular Networks*, pages 1–5, London, UK, September 2013.

[26] R. G. Stephen, Ch. R. Murthy, and M. Coupechoux. Pilot Allocation and Receive Antenna Selection : A Markov Decision Theoretic Approach. In *IEEE International Conference on Communications (ICC)*, June 2013.

[27] A. Chattopadhyay, M. Coupechoux, and A. Kumar. Measurement based impromptu deployment of a multi-hop wireless relay network. In *International Symposium on Modeling and Optimization in Mobile, Ad Hoc and Wireless Networks (WiOpt)*, Tsukuba Science City, Japan, May 2013.

[28] S. Iellamo, L. Chen, M. Coupechoux, and A. V. Vasilakos. Imitation-based Spectrum Access Policy for Cognitive Radio Networks. In *International Symposium on Wireless Communication Systems (ISWCS)*, Aug. 2012. Invited Paper.

[29] A. Chattopadhyay, A. Sinha, M. Coupechoux, and A. Kumar. Optimal Capacity Relay Node Placement in a Multi-hop Network on a Line. In *International workshop on Resource Allocation and Cooperation in Wireless Networks (RAWNET) in conjunction with WiOpt*, May 2012.

[30] S. Iellamo, L. Chen, and M. Coupechoux. Imitation-based Spectrum Access Policy for CSMA/CA-based Cognitive Radio Networks. In *IEEE Wireless Communications and Networking Conference (WCNC)*, Apr. 2012.

[31] L. Chen, S. Iellamo, and M. Coupechoux. Opportunistic Spectrum Access with Channel Switching Cost for Cognitive Radio Networks. In *IEEE International Conference on Communications (ICC)*, June 2011.

[32] D. Ben Cheikh, J.-M. Kélif, M. Coupechoux, and Ph. Godlewski. Dynamic System Performance of SISO, MISO and MIMO Alamouti Schemes. In *IEEE Sarnoff Symposium*, May 2011.

[33] D. Ben Cheikh, J.-M. Kélif, M. Coupechoux, and Ph. Godlewski. Multicellular Zero Forcing Precoding Performance in Rayleigh and Shadow Fading. In *IEEE Vehicular Technology Conference (VTC Spring)*, May 2011.

[34] M. Coupechoux and J.-M. Kélif. How to Set the Fractional Power Control Compensation Factor in LTE ? In *IEEE Sarnoff Symposium*, May 2011.

[35] M. Minelli, M. Coupechoux, J.-M. Kélif, M. Ma, and Ph. Godlewski. Relays-Enhanced LTE-Advanced Networks Performance Studies. In *IEEE Sarnoff Symposium*, May 2011.

[36] H. Kamal, M. Coupechoux, and Ph. Godlewski. A Tabu Search DSA Algorithm for Reward Maximization in Cellular Networks. In *IEEE International Conference on Wireless and Mobile Computing, Networking and Communications (WiMob)*, Oct. 2010.

[37] H. Kamal, M. Coupechoux, and Ph. Godlewski. An Efficient Tabu Search DSA Algorithm for Heterogeneous Traffic in Cellular Networks. In *IFIP Wireless Days*, Oct. 2010.

[38] J.-M. Kélif, M. Coupechoux, and F. Marache. Limiting Power Transmission of Green Cellular Networks : Impact on Coverage and Capacity. In *IEEE International Conference on Communications (ICC)*, May 2010.

[39] D. Ben Cheikh, J.-M. Kélif, M. Coupechoux, and Ph. Godlewski. Outage Probability in a Multi-Cellular Network Using Alamouti Scheme. In *IEEE Sarnoff Symposium*, Apr. 2010.

[40] L. Chen, S. Iellamo, M. Coupechoux, and Ph. Godlewski. An Auction Framework for Spectrum Allocation with Interference Constraint in Cognitive Radio Networks. In *IEEE INFOCOM*, Mar. 2010.

[41] M. Minelli, M. Coupechoux, and J.-M. Kélif. Average SIR Estimation in Cellular Networks with Best Server Policy. In *IFIP Wireless Days*, Oct. 2010.

[42] H. Kamal, M. Coupechoux, and Ph. Godlewski. Inter-Operator Spectrum Sharing for Celullar Networks using Game Theory. In *IEEE Personal, Indoor and Mobile Radio Communications Symposium (PIMRC)*, Sept. 2009.

[43] S. Doirieux, B. Baynat, M. Maqbool, and M. Coupechoux. An Analytical Model for WiMAX Networks with Multiple Traffic Profiles and Throttling Policy. In *Intl. Symposium on Modeling and Optimization in Mobile, Ad Hoc, and Wireless Networks (WiOpt)*, June 2009.

[44] H. Kamal, M. Coupechoux, and Ph. Godlewski. Traffic Studies for DSA Policies in a Simple Cellular Context with Packet Services. In *IEEE/ICST Int. Conf. on Cognitive Radio Oriented Wireless Networks and Communications (CrownCom)*, June 2009.

[45] J. M. Kélif and M. Coupechoux. Cell Breathing, Sectorization and Densification in Cellular Networks. In *Intl. Symposium on Modeling and Optimization in Mobile, Ad Hoc, and Wireless Networks (WiOpt)*, June 2009.

[46] J. M. Kélif and M. Coupechoux. Impact of Topology and Shadowing on the Outage Probability of Cellular Networks. In *IEEE International Conference on Communications (ICC)*, June 2009.

[47] B. Baynat, G. Nogueira, M. Maqbool, and M. Coupechoux. An Efficient Analytical Model for the Dimensioning of WiMAX Networks. In *IFIP/TC6 Networking*, May 2009.

[48] M. Coupechoux, H. Kamal, Ph. Godlewski, and J. M. Kélif. Optimal and Heuristic DSA Policies for Cellular Networks with Coordinated Access Band. In *IEEE European Wireless (EW)*, May 2009. Best Paper Award.

[49] M. Maqbool, M. Coupechoux, and Ph. Godlewski. Reuse 1 in WiMAX Networks with Beamforming. In *Wireless World Research Forum, WWRF22*, May 2009.

[50] J. Chi, P. Martins, and M. Coupechoux. A Novel Mechanism for Contention-based Initial Ranging in IEEE 802.16e Networks. In *IEEE Wireless Communications and Networking Conference (WCNC)*, Apr. 2009.

[51] J. M. Kélif and M. Coupechoux. On the Impact of Mobility on Outage Probability in Cellular Networks. In *IEEE Wireless Communications and Networking Conference (WCNC)*, Apr. 2009.

[52] M. Maqbool, M. Coupechoux, and P. Godlewski. A Semi-analytical Method to Model Effective SINR Spatial Distribution in WiMAX Networks. In *IEEE Sarnoff Symposium*, Mar. 2009.

[53] M. Maqbool, M. Coupechoux, Ph. Godlewski, S. Doirieux, B. Baynat, and V. Capdevielle. Dimensioning Methodology for OFDMA Networks. In *Wireless World Research Forum, WWRF22*, May 2009.

[54] Ph. Godlewski, M. Maqbool, M. Coupechoux, and J. M. Kélif. Analytical Evaluation of Various Frequency Reuse Schemes in Cellular OFDMA Networks. In *ACM International Conference on Performance Evaluation Methodologies and Tools (Valuetools)*, Oct. 2008.

[55] B. Baynat, S. Doirieux, G. Nogueira, M. Maqbool, and M. Coupechoux. An Efficient Analytical Model for WiMAX Networks with Multiple Traffic Profiles. In *ACM International Workshop on Performance and Analysis of Wireless Networks (PAWN)*, Sept. 2008.

[56] J. Chi, P. Martins, and M. Coupechoux. A Novel Waiting-time Dependent Mechanism for Contention-based Initial Ranging in IEEE 802.16e Networks. In *IFIP EUNICE Open European Summer School*, Sept. 2008.

[57] M. Maqbool, M. Coupechoux, and Ph. Godlewski. Effect of Distributed Subcarrier Permutation on Adaptive Beamforming in WiMAX Networks. In *IEEE Vehicular Technology Conference (VTC Fall)*, Sept. 2008.

[58] M. Coupechoux, J. M. Kélif, and Ph. Godlewski. SMDP Approach for JRRM Analysis in Heterogeneous Networks. In *IEEE European Wireless (EW)*, June 2008.

[59] M. Coupechoux, J. M. Kélif, and Ph. Godlewski. Network Controlled Joint Radio Resource Management for Heterogeneous Networks. In *IEEE Vehicular Technology Conference (VTC Spring)*, May 2008.

[60] M. Maqbool, M. Coupechoux, and Ph. Godlewski. Comparison of Various Frequency Reuse Patterns for WiMAX Networks with Adaptive Beamforming. In *IEEE Vehicular Technology Conference (VTC Spring)*, May 2008.

[61] J. M. Kélif, M. Coupechoux, and Ph. Godlewski. Effect of Shadowing on Outage Probability in Fluid Cellular Radio Networks. In *Intl. Symposium on Modeling and Optimization in Mobile, Ad Hoc, and Wireless Networks (WiOpt)*, Mar. 2008.

[62] J. M. Kélif, M. Coupechoux, and Ph. Godlewski. Fluid Model of the Outage Probability in Sectored Wireless Networks. In *IEEE Wireless Communications and Networking Conference (WCNC)*, Mar. 2008.

[63] J. M. Kélif, M. Coupechoux, and Ph. Godlewski. Spatial Outage Probability for Cellular Networks. In *IEEE Global Communications Conference (GLOBECOM)*, Nov. 2007.

[64] J. M. Kélif, M. Coupechoux, and Ph. Godlewski. Spatial Outage Probability Formula for CDMA Networks. In *IEEE Vehicular Technology Conference (VTC falls)*, Sept. 2007.

[65] M. Coupechoux and T. Lestable. On the Capacity of the Channel Aware Slotted Aloha over Rayleigh and Nakagami-m Channels. In *Intl. Symposium on Modeling and Optimization in Mobile, Ad Hoc, and Wireless Networks (WiOpt)*, Mar. 2004. Poster.

[66] M. Coupechoux and V. Kumar and L. Brignol. Voice over IEEE 802.11b Capacity. In *ITC Specialist Seminar*, Oct. 2004.

[67] M. Coupechoux and B. Baynat and C. Bonnet and V. Kumar. CROMA - A Slotted MAC Protocol with Multi-Slot Communications. In *Wireless Networking and Communications Group Conference (WNCG)*, Oct. 2003.

[68] M. Coupechoux and B. Baynat and C. Bonnet and V. Kumar. Modeling a Slotted MAC Protocol for MANETs. In *Workshop on Mobile Ad Hoc Networking and Computing (MADNET)*, Dec. 2003.

[69] M. Coupechoux and J. Brouet and L. Brignol and V. Kumar. Suggested Solutions for the Near-Far Effect in Multimode WLANs. In *Wireless World Research Forum, WWRF10*, Oct. 2003.

[70] V. Capdevielle and T. Lestable and M. Coupechoux and M.L. Alberi-Morel and L. Brignol. Multi-Hop Coverage Extension of an IEEE 802.11b WLAN in a Corporate Environment. In *Wireless Networking and Communications Group Conference (WNCG)*, Oct. 2003.

[71] M. Coupechoux and C. Bonnet and V. Kumar. A Scheduling Policy for Dense and Highly Mobile Networks. In *Workshop on Mobile Ad Hoc Network (WMAN)*, Mar. 2002.

[72] M. Coupechoux and C. Bonnet and V. Kumar. CROMA - a New Collision-free Receiver Oriented MAC Protocol for MANETs. In *World Telecommunication Congress (WTC)*, Sept. 2002.

[73] M. Coupechoux and C. Bonnet and V. Kumar. A Scheduling Policy for Dense and Highly Mobile Networks. In *Wireless*, July 2001.

[74] V. Braun and M. Coupechoux. Viterbi Equalization of Space-Time Coded Signals in GSM-like Systems. In *IEEE Workshop on Convolutional Codes*, Oct. 2001.

[75] M. Coupechoux and V. Braun. Space-Time Coding for the EDGE Downlink. In *IEEE Intl. Conference on Personal Wireless Communications (ICPWC)*, Dec. 2000.

Rapports de recherche

[76] A. Chattopadhyay, M. Coupechoux, and A. Kumar. Measurement Based Impromptu Deployment of a Multi-Hop Wireless Relay Network. *CoRR*, abs/1301.3302, 2013.

[77] A. Chattopadhyay, A. Sinha, M. Coupechoux, and A. Kumar. Optimal Capacity Relay Node Placement in a Multi-hop Network on a Line. *CoRR*, abs/1204.4323, 2012.

[78] A. Sinha, A. Chattopadhyay, K. P. Naveen, M. Coupechoux, and A. Kumar. Optimal Sequential Wireless Relay Placement on a Random Lattice Path. *CoRR*, abs/1207.6318, 2012.

[79] S. Iellamo, L. Chen, and M. Coupechoux. Let Cognitive Radios Imitate : Imitation-based Spectrum Access for Cognitive Radio Networks. *CoRR*, abs/1101.6016, 2011.

[80] J.-M. Kélif and M. Coupechoux. Impact conjoint de l'affaiblissement de parcours, de l'effet de masque et des évanouissemnts rapides - Une formule de la probabilité de dépassement pour les réseaux sans fil. Technical Report 2010D001, Telecom ParisTech, Jan. 2010.

[81] J.-M. Kélif and M. Coupechoux. Joint Impact of Pathloss Shadowing and Fast Fading - An Outage Formula for Wireless Networks. *CoRR*, abs/1001.1110, 2010.

[82] M. Maqbool, M. Coupechoux, and P. Godlewski. Méthode de semi-analytique pour la modélisation de la distribution spatiale du sinr effectif dans les réseaux wimax. Technical Report 2009D005, Telecom ParisTech, Jan. 2009.

[83] M. Mabiala and M. Coupechoux. Etude de trois mécanismes de qualité de service dans les réseaux ad hoc multi-bonds. Technical report, Telecom ParisTech, June 2008. Projet DGA "Etude de la Gestion de la Qualité de Service en Environnements Contraints".

[84] M. Coupechoux, P. Godlewski, P. Martins, C. Riou, V. Capdevielle, V. Kumar, M. Alberi-Morel, N. Broqua, and J. Marzoni. Méthodes d'allocation du spectre radio dans les systèmes de communications mobiles terrestres. Technical Report URC-CPV 602, Telecom ParisTech, Jan. 2008.

[85] M. Maqbool, M. Coupechoux, and P. Godlewski. Comparaison de différents schémas de réutilisation fréquentielle pour les réseaux cellulaires wimax. Technical Report 2008D005, Telecom ParisTech, Apr. 2008.

[86] M. Maqbool, M. Coupechoux, and P. Godlewski. Types de permutations de sous-porteuses en ieee 802.16e. Technical Report 2008D004, Telecom ParisTech, July 2008.

Brevets

[87] M. Coupechoux and V. Kumar. Method of Selecting of a Path to Establish a Telecommunication Link. Patent US 7,302,230B2, Nov. 2007.

[88] M. Coupechoux and L. Fiat. Method for Improving Handovers in a WLAN. Patent EP1648115A1 US2006/0077933A1, Apr. 2006.

[89] M. Coupechoux and J. Brouet. Wireless Mobile Terminal and Telecommunication System. Patent EP1585283A1 US2005/0243718A1, Oct. 2005.

[90] V. Kumar and M. Coupechoux. Fast Delivery of Multimedia Messages in Cellular Networks. Patent EP1511333A1 US2005/0048980A1, Mar. 2005.

[91] M. L. Alberi-Morel and M. Edimo and H. Maillard and T. Lestable and M. Coupechoux. Radio Frequency Device using Circulator and Echo Canceller for Cancelling Transmission Leakage Signal in the Reception Chain. Patent EP1508975A1, Feb. 2005.

[92] M. Coupechoux and V. Kumar. A Method of Selecting a Path to Establish a Telecommunication Link. Patent EP1448011A1, Aug. 2004.

[93] V. Kumar and M. Coupechoux and H. Maillard. Method for Establishing a Connection between Terminals Having a Short-Range Wireless Communication Interface. Patent EP1333627A1, Aug. 2003.

[94] V. Kumar and M. Coupechoux. Mobile Station with Two Communication Interfaces. Patent EP1289320A1 US2003/0045294A1, Mar. 2003.

[95] V. Kumar and M. Coupechoux. Method for Providing Access to a Data-Network for a Vehicle Travelling on a Road. Patent EP1233575A1, Aug. 2002.

Séminaires sans actes

[96] M. Coupechoux, S. Iellamo, and L. Chen. Retrospective spectrum access protocol : A completely uncoupled learning algorithm for cognitive networks. In *CEFIPRA Workshop on New Avenues for Network Models*, Bangalore, India, January 2014.

[97] S. Iellamo, E. Alekseeva, L. Chen, M. Coupechoux, and Y. A. Kochetov. A hybrid matheuristics algorithm for the competitive base stations location problem in cognitive radio networks. In *European Conference on Operational Research (EURO-INFORMS)*, Roma, July 2013.

[98] S. Iellamo, L. Chen, and M. Coupechoux. Self-imitation in cognitive radio networks. In *Workshop on Algorithmic Game Theory : Learning Algorithms and Dynamics in Distributed Systems (AlgoGT), Invited presentation*, Grenoble, France, July 2013.

[99] M. Minelli, M. Ma, M. Coupechoux, J.-M. Kélif, and M. Sigelle. Simulated annealing algorithm for optimal relay placement in cellular networks. In *Workshop on Algorithmic Game Theory : Learning Algorithms and Dynamics in Distributed Systems (AlgoGT), Invited poster*, Grenoble, France, July 2013.

[100] R. G. Stephen, Ch. R. Murthy, and M. Coupechoux. A pomdp approach to pilot allocation and receive antenna selection. In *LINCS seminar*, Paris, France, July 2013.

[101] M. Coupechoux, S. Iellamo, and L. Chen. Imitation Policies for Cognitive Radio Networks. In *Alcatel-Lucent Bell Labs Seminar*, Bangalore, India, July 2012. Invited Presentation.

[102] S. Iellamo, L. Chen, M. Coupechoux, and Y. A. Kochetov. Strategic Planning in Cognitive Radio Networks : a Competitive Facility Location Game Perspective. In *The Fith All-Russia Conference on Optimization Problems and their Economical Applications*, Omsk, Russia, July 2012.

[103] M. Coupechoux, J.-M. Kélif, and F. Marache. Impact on Coverage and Capacity of Reduced Transmit Power in Cellular Networks. In *Green Telecom and IT Workshop, Indian Institute of Science*, Bangalore, India, Apr. 2012. Invited Presentation.

[104] M. Minelli, M. Ma, M. Coupechoux, and Ph. Godlewski. Radio Engineering of Relay-Based OFDMA Networks. In *Alcatel-Lucent Bell Labs Seminar*, Villarceaux, France, Apr. 2012. Invited Presentation.

[105] M. Coupechoux, D. Ben Cheikh, J.-M. Kélif, and Ph. Godlewski. Outage Probability for Joint Processing Coordinated Multi-Point (JP-CoMP) Performance Analysis in LTE-Advanced Networks. In *Communication Networks Seminar, Indian Institute of Science*, Bangalore, India, Mar. 2012. Invited Presentation.

[106] L. Chen M. Coupechoux et Y. A. Kochetov S. Iellamo, E. Alekseeva. A Bi-Level Competitive Facility Location Problem for the Design of Cognitive Networks. In *International Conference on Performance Evaluation Methodologies and Tools (VALUETOOLS)*, Oct. 2012. Invited Presentation.

[107] S. Iellamo, L. Chen, and M. Coupechoux. Imitation in CSMA/CA based Cognitive Networks. In *Workshop on Algorithmic Game Theory : Dynamics and Convergence in Distributed Systems, AlgoGT*, Grenoble, France, June 2011. Invited Presentation.

[108] S. Iellamo, L. Chen, and M. Coupechoux. Population games for cognitive radios : Evolution through imitation. In *GDR ISIS*, Paris, France, May 2011.

[109] M. Coupechoux, H. Kamal, and Ph. Godlewski. Some Optimization Problems in Dynamic Spectrum Allocation. In *Sagemcom TECHDAYS Seminar*, Rueil-Malmaison, France, Fev. 2011. Invited Presentation.

[110] L. Chen, S. Iellamo, and M. Coupechoux. Game Theoric Spectrum Access in Cognitive Radio Networks. In *York-Zhejiang Summer School on Cognitive Communications*, Zhejiang, China, Oct. 2010.

[111] M. Coupechoux, H. Kamal, and Ph. Godlewski. Quelques problèmes d'optimisation dans le domaine de l'accès dynamique au spectre. In *Journée Optimisation des Réseaux*, Paris, France, June 2010. Invited Presentation.

[112] H. Chevreau, M. Coupechoux, and P. Fouilhoux. Optimisation des protocoles ofdma orchestrés pour les réseaux sans-fil maillés. In *Congrès de la Société Française de Recherche Opérationnelle et d'Aide à la Décision (ROADEF)*, Toulouse, France, Fev. 2010.

[113] M. Coupechoux, P. Fouilhoux, and S. Martin. Combinatorial Problems and Integer Formulations in Wireless Mesh Network Design. In *International Conference on Non-Convex Programming*, Rouen, France, Dec. 2007.

Autre publication

[114] M. Coupechoux, P. Godlewski, P. Martins, and P. Ciblat. Projet urc : vers une gestion flexible et régulée du spectre radio en ile-de-france. *La Lettre Techniques de l'Ingénieur*, (11) :5–6, January 2008.

Radio Engineering of Wireless Networks

Dimensionning, performance evaluation and algorithm design

Marceau Coupechoux

Institut Mines-Telecom

Telecom ParisTech

CONTENTS

LIST OF ACRONYMS

HSPA .... High Speed Packet Access *Page 18*

ICT .... Information and Communication Technologies *Page 70*

IFFT .... Inverse Fast Fourier Transform *Page 7*

IFR .... Integer Frequency Reuse *Page 8*

JP-CoMP ...... Joint Processing CoMP *Page 14*

LOS .... Line-Of-Sight *Page 39*

LTE .... Long Term Evolution *Page 7*

LTE-A .... Long Term Evolution Advanced *Page 7*

MAB .... Multi-Armed Bandit *Page 50*

MCS .... Modulation and Coding Scheme *Page 4*

MDP .... Markov Decision Process *Page 61*

MIC .... Mean Instantaneous Capacity *Page 9*

MIMO .... Multiple Input Multiple Output *Page 1*

MISO .... Multiple Input Single Output *Page 41*

MMSE .... Minimum Mean Square Error *Page 13*

MRC .... Maximum Ratio Combining *Page 12*

MRT .... Maximum Ratio Transmission *Page 14*

MS .... Mobile Station *Page 3*

MU-MIMO .... Multi-User MIMO *Page 13*

NE .... Nash Equilibrium *Page 53*

NLOS .... Non Line-Of-Sight *Page 39*

OCIF .... Other Cell Interference Factor *Page 6*

OFDM .... Orthogonal Frequency Division Multiplexing *Page 7*

OFDMA .... Orthogonal Frequency Division Multiple Access *Page 1*

OSLA .... One Step Look Ahead *Page 61*

OSTBC .... Orthogonal STBC *Page 39*

POMDP .... Partially Observable Markov Decision Process *Page 42*

PU .... Primary User *Page 48*

RAN .... Radio Access Network *Page 49*

RAT .... Radio Access Technology *Page 52*

RB .... Resource Block *Page 8*

RF .... Radio Frequency *Page 47*

RoF .... Radio over Fiber *Page 69*

RV .... Random Variable *Page 3*

SDR .... Software Defined Radio *Page 47*

SFR .... Soft Frequency Reuse *Page 8*

SINR .... Signal to Interference plus Noise Ratio *Page 1*

SISO .... Single Input Single Output *Page 11*

SMDP .... Semi-Markov Decision Process *Page 52*

SNR .... Signal to Noise Ratio *Page 10*

STBC .... Space-Time Block Codes *Page 12*

SU .... Secondary User *Page 48*

SU-MIMO ..... Single User MIMO *Page 12*

TDD .... Time Division Duplex *Page 15*

TLPC .... Two Level Power Control *Page 8*

TTI .... Transmission Time Interval *Page 7*

ULA .... Uniform Linear Array *Page 11*

UMTS .... Universal Mobile Telecommunications System *Page 6*

WiMAX .... Worldwide Interoperability for Microwave Access *Page 7*

WLAN .... Wireless Access Network *Page 59*

ZF .... Zero Forcing *Page 40*

ZFBF .... Zero Forcing Beamforming *Page 13*

1 INTRODUCTION

This thesis is a summary of my work and contributions in the domain of the radio engineering of wireless networks as well as my research project for the next few years. Since I joined Telecom ParisTech (end of 2005), I have been working on the dimensioning and the performance evaluation of cellular networks.

After some studies on CDMA (Code Division Multiple Access) networks, which are widely used in todays third generation cellular networks, I have focused on OFDMA (Orthogonal Frequency Division Multiple Access), which is the access scheme of the fourth generation and appears today as the preferred access scheme for most of the wireless standards. I have then extended my studies to MIMO (Multiple Input Multiple Output) features in a cellular context.

The general approach for performance evaluation of these networks is presented in the first chapter of this thesis. It focuses on the outage probability of the SINR (Signal to Interference plus Noise Ratio) or, equivalently, on its distribution. It is indeed a central parameter for coverage as well as capacity studies. The first chapter, which is a short lecture on the dimensioning of cellular networks, also presents the tools and models used in my works.

Recently, I have started working on a new research area called *cognitive radio*, which is an approach for better utilizing the frequency spectrum. In particular, cognitive radios are able to sense and analyze their environment, and take decisions to adapt their transmission parameters to this environment in a decentralized way.

Under the term *spontaneous networks*, I gather networks that are characterized by a possible short-lived deployment, the use of unlicensed frequencies, the possible lack of infrastructure, a distributed mode of operation, etc, i.e., a counterexample of cellular networks. Most of my contributions in this field have been done during my PhD thesis that I devoted to access protocols for ad hoc networks. I have however recently tackled some issues in sensor networks during my sabbatical sojourn at the Indian Institute of Science in Bangalore.

Every chapter makes a short review of the literature in the domain, lists my contributions and gives conclusions and perspectives. The thesis ends with few research axes I want to study in the next few years, namely, 'towards very high data rates', which includes the performance evaluation of future cellular networks, 'a better spectrum usage', which is related to cognitive radio and 'green communications', which is a transverse theme that I want to develop.

2 MODELS FOR CELLULAR NETWORK PLANNING

2.1 Introduction

In this chapter, we provide a set of models used for the dimensioning and the performance evaluation of cellular networks. In the planning of such networks, there are several phases, typically an initial dimensioning study, the propagation parameter calibration with drive tests, and a detailed radio planning on digitized maps using ray tracing techniques or empirical statistical propagation models. In this thesis, we focus on the first phase. This means that we imagine an ideal network deployment of base stations and we make simple assumptions on the radio propagation and the generated traffic pattern. This allows us to develop simple analytical forms or simple Monte Carlo simulators to quickly evaluate the performance of a network. Even if such an approach is not so accurate than the detailed radio planning, it permits to derive generic conclusions and insights for the design of a cellular network. This chapter is useful to understand the kind of models I use but can be skipped for a first reading.

2.2 Propagation

We consider a set $\mathcal{B}$ of BS (Base Station) and a set $\mathcal{U}$ of MS (Mobile Station) or users and we focus mainly on the downlink, i.e., the communication link from a BS to a MS. The modeling of the path-gain $g_{b,u}$ between a BS b and a MS u is a research area *per se*. We adopt here a typical and simplified statistical model, called the three stage model, well adapted to analytical studies.

The first part is a deterministic part that models the long term signal attenuation as a function of the distance and other environment parameters. The second part is a log-normal shadowing mask, which models the presence of obstacles between the transmitter and the receiver. The third part is a very short term model of the coherent addition of several paths of the signal at the receiver resulting in fast fading. The statistical model can be summarized as:

$$g_{b,u}(r,\theta) = \frac{KA(\theta)}{r^{\eta}} 10^{\frac{\xi}{10}} X, \tag{2.1}$$

where K is a constant, $A(\theta)$ is the BS antenna pattern, (r,θ) is the polar coordinate of user u with respect to the BS location and BS antenna boresight direction, η is the path-loss exponent, ξ is a zero mean Gaussian RV (Random Variable) with standard deviation σ representing the shadowing and X represents the fast fading, usually modeled as an exponential RV (corresponding to the Rayleigh distribution of the signal amplitude).

Equation (2.1) is valid for r sufficiently large. It can be replaced by:

$$\min\{mcl, KA(\theta)/r^{\eta} 10^{\frac{\xi}{10}} X\},$$

where $mcl \leqslant 1$ is called the minimum coupling loss and accounts for the minimum loss observed at the BS location. Some studies have also observed in small urban cells an *absorption* term under the form of an exponential $e^{-\rho r}$ [14].

The values of K, η and σ depend mainly on the considered environment (urban, suburban, rural, indoor, picocell, etc), on the transmitter and receiver antenna heights and on the signal carrier frequency. Detailed models exist in the literature to provide these figures. One of the best known in macro cells is the Okumura-Hata model [2], which is valid between 150 and 1500 MHz, it has been extended to 2000 MHz in the COST 231-Hata model [1].

2.3 SINR and Outage Probability

The most important metric to evaluate the quality of a received signal is the SINR. Let us define the following quantities:

- P_b, the BS b total transmit power;
- $P_{b,u}$, the BS b transmit power dedicated to user u;
- $p_{b,u} = P_{b,u} g_{b,u}$ the power received by u from b.

It is common to split the system received power in two terms: $p_{int,u} + p_{ext,u}$, where $p_{int,u}$ is the *internal* (or own-cell) received power and $p_{ext,u}$ is the *external* (or other-cell) interference. Then, the SINR in u can be written as:

$$\gamma_u = \frac{p_{b,u}}{\alpha(p_{int,u} - p_{b,u}) + p_{ext,u} + N_0 W_u}, \tag{2.2}$$

where $N_0 W_u$ is the thermal noise power, $N_0/2$ is the noise power spectral density, W_u is the bandwidth allocated to user u, and $\alpha \in [0, 1]$ is called the orthogonality factor of the system. The first term of the denominator is called the external interference, the second is the internal interference.

Circuit-switched services (voice, visio-conference, streaming, but also data transfer in UMTS) are subject to a *hard interference requirement* : below a certain SINR threshold γ_u^*, the service is not accessible, while above this level, there is no significant increase of the service quality. In contrast, data traffic services are subject to a *soft interference requirement*, where interference can be tolerated without a hard threshold. A higher level of interference however induces a soft degradation of the user throughput.

In this case, a model is needed for the mapping between SINR and user throughput. A typical function is the traditional Shannon formula. An upper bound on the user throughput can be written as: $C_u(\gamma_u) = W_u \log_2(1 + \gamma_u)$. In this approach, interference is treated as noise for simplicity because the Shannon capacity in presence of interference is an open problem in information theory [41]. When analyzing a specific system, another approach is to consider the set of MCS (Modulation and Coding Scheme) of the system. In this case, there is a mapping between MCS (and so user throughput) and intervals of SINR values. We have for MCS n, $C_u(\gamma_u) = C_n$ for $\gamma^{(n-1)} \leqslant \gamma_u \leqslant \gamma^{(n)}$, where $\gamma^{(n-1)}$ and $\gamma^{(n)}$ are delimiting the range of use of MCS n, and C_n is the throughput achieved by a user using MCS n. This results in a increasing step function. An intermediate approach is to fit the step function by a Shannon-like system specific formula as proposed in [27] for LTE:

$$C(\gamma_u) = \begin{cases} 0 & \text{if } 10\log\gamma_u < -10\text{dB} \\ 0.6\log_2(1+\gamma_u) & \text{if } -10 \leqslant 10\log\gamma_u \leqslant 22\text{dB} \\ 4.4 & \text{if } 10\log\gamma_u > 22\text{dB}. \end{cases} \quad (2.3)$$

Keeping in mind that C_u is a RV, network design can be interested in two possible performance parameters [41]. The first one is the *ergodic capacity*. Assuming channel state information at the receiver, this is $\mathbb{E}[C_u]$, where the expectation is taken over SINR variations. The second one is called *outage capacity* and is defined as $C_{out} = (1 - P_{out})W_u \log_2(1 + \gamma_{out})$, where γ_{out} is a threshold below which data cannot be decoded without errors, and

$$P_{out} = \mathbb{P}[\gamma_u < \gamma_{out}] \quad (2.4)$$

is called the *outage probability*. As (2.4) is also the CDF (Cumulative Distribution Function) of the SINR (involved in the computation of the ergodic capacity), the outage probability appears as a central performance parameter for the design of cellular networks.

2.4 Multiplexing Scheme

The multiplexing scheme of a system has a decisive impact on how radio resources are organized, how they can be reused from a cell to another and how the SINR is computed.

2.4.1 *F/TDMA*

In GSM (Global System for Mobile Communications), GPRS (General Packet Radio Service) and EDGE (Enhanced Data rates for Global Evolution) networks, F/TDMA (Frequency/Time Division Multiple Access) is used. As voice is the main service, users are subject to a hard interference constraint, which is managed thanks to the frequency planning. Cells are organized in clusters within which frequencies are used only once, as shown in figure 2.1 (a). The number of cells in a cluster is called *reuse factor*. The high SINR target (around 9 dB) imposes a reuse factor strictly greater than 1, typically 7 or 9. In a cell, there is an orthogonal allocation of radio resources to users in time and frequency, so that there is no internal interference. At a given instant, the whole power of a transceiver is dedicated to a single user. Every user is served by a single BS, from which it receives the whole transceiver power. Assume that u is served by BS b. Equation (2.2) reduces to:

$$\gamma_u = \frac{P_b g_{b,u}}{\sum_{k \neq b, k \in \mathcal{F}_b} P_k g_{k,u} + N_0 W_u}, \quad (2.5)$$

where $\mathcal{F}_b \subset \mathcal{B}$ is the set of cells using the same frequency as b. W_u is here the downlink channel bandwidth of the system.

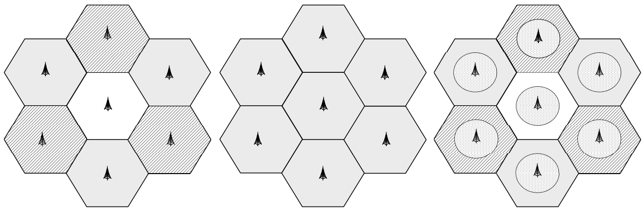

Figure 2.1: Possible frequency plannings: (a) F/TDMA with reuse factor 3, (b) CDMA with reuse factor 1, and (c) OFDMA with fractional frequency reuse.

2.4.2 *CDMA*

The case of CDMA, used in UMTS (Universal Mobile Telecommunications System), is shown in figure 2.1 (b): the same frequency is reused in all cells. The downlink of adjacent cells is distinguished thanks to different scrambling codes. As there are 512 different scrambling codes, the cell code planning is not an issue in UMTS. Within a cell, on the downlink, the radio resource control allocates different channelization codes to users and signals of different users are transmitted simultaneously using the whole system bandwidth, so that $W_u = W$ for all u. With such an access scheme, interference should be managed carefully and the system relies on power control to allow the coexistence of concurrent transmissions on the same carrier frequency. Moreover, users are subject to a hard interference constraint because of the dedicated channels structure defined in the standard.

The total transmit power of a BS b is the sum of the power dedicated to common control channels P_{cch} and the powers to users served by b. We ignore here the case of soft-handover and macro diversity. We define the OCIF (Other Cell Interference Factor) in u, as the ratio of total power received from other BSs to the total power received from the serving BS b as:

$$f_u = \frac{p_{ext,u}}{p_{int,u}} = \frac{\sum_{j \neq b} g_{j,u}}{g_{b,u}}, \tag{2.6}$$

where it has been assumed that all BSs transmit with the same power P_b.

Although UMTS is able to transport packet services, its radio interface is fundamentally based on circuits characterized by a SINR threshold that depends on the user service. This threshold, denoted γ_u^*, is a priori different from the SINR γ_u evaluated at u. However, we assume perfect power control, so that $\gamma_u = \gamma_u^*$ for all users. With the introduced notations, the SINR experimented by u can thus be derived:

$$\gamma_u^* = \frac{p_{b,u}}{\alpha(p_{int,u} - p_{b,u}) + p_{ext,u} + N_0 W}. \tag{2.7}$$

From this relation, from $P_{b,u} = p_{b,u}/g_{b,u}$, and from the definition of f_u, we can express the transmitted power for user u :

$$P_{b,u} = \frac{\gamma_u^*}{1 + \alpha\gamma_u^*}(\alpha P_b + f_u P_b + N_0 W/g_{b,u}). \tag{2.8}$$

From this relation, the output power of BS b can be computed as follows:

$$P_b = P_{cch} + \sum_u P_{b,u}, \tag{2.9}$$

and so, according to (2.8),

$$P_b = \frac{P_{cch} + \sum_u \frac{\gamma_u^*}{1+\alpha\gamma_u^*} \frac{N_0 W}{g_{b,u}}}{1 - \sum_u \frac{\gamma_u^*}{1+\alpha\gamma_u^*}(\alpha + f_u)}. \tag{2.10}$$

The output power appears as a RV that depends on the number of users and on their channel variations. It is possible to define the outage probability for the downlink of UMTS as follows: $P_{out} = \mathbb{P}[P_b > P_{max}]$, where P_{max} is the maximum allowed transmit power. If noise is neglected, if we assume a single service network ($\gamma_u^* = \gamma^*$ for all u) and when there are n MSs per cell, we deduce from (2.10):

$$P_{out}^{(n)} = \Pr\left[\sum_{u=0}^{n-1}(\alpha + f_u) > \frac{1-\varphi}{\beta}\right], \tag{2.11}$$

where $\varphi = P_{cch}/P_{max}$ and $\beta = \gamma^*/(1+\alpha\gamma^*)$.

For a given number n of MSs per cell, a spatial outage probability can also be defined. In this case, it is assumed that n MSs have already been accepted by the system, i.e., the output power needed to serve them does not exceed the maximum allowed power. The spatial outage probability at location r_u is the probability that maximum power is exceeded if a new MS is accepted in r_u:

$$P_{sout}^{(n)} = \Pr\left[(\alpha + f_u) + \sum_{v=0}^{n-1}(\alpha + f_v) > \frac{1-\varphi}{\beta} \middle| \sum_{v=0}^{n-1}(\alpha + f_v) \leqslant \frac{1-\varphi}{\beta}\right], \tag{2.12}$$

$$= \frac{\Pr\left[\frac{1-\varphi}{\beta} - (\alpha + f_u) < \sum_{v=0}^{n-1}(\alpha + f_v) \leqslant \frac{1-\varphi}{\beta}\right]}{\Pr\left[\sum_{v=0}^{n-1}(\alpha + f_v) \leqslant \frac{1-\varphi}{\beta}\right]}. \tag{2.13}$$

In HSDPA (High Speed Downlink Packet Access), equations (2.7) and (2.10) are valid for each TTI (Transmission Time Interval). Parameter γ_u^* should be now interpreted as an experienced SINR and not any more as a target. Sums are done on the number of scheduled users per TTI. If a single user is scheduled per TTI (which is a common case), sums reduce to a single term. Even in this case, parameter α has to be considered since common control channels and traffic channels are not perfectly orthogonal due to multi-path.

2.4.3 *OFDMA*

OFDMA is the multiplexing access scheme of WiMAX (Worldwide Interoperability for Microwave Access) and, on the downlink, of LTE (Long Term Evolution) and LTE-A (Long Term Evolution Advanced). It is based on the OFDM (Orthogonal Frequency Division Multiplexing) transmission technique, which consists in dividing the system bandwidth in orthogonal subcarriers, whose bandwidth is very small compared to the signal coherence bandwidth. This technique is efficiently implemented thanks to a FFT (Fast Fourier Transform) and its inverse, an IFFT (Inverse Fast Fourier Transform), and allows an almost complete removal on the inter-symbol interference. The OFDMA multiplexing allocates orthogonal groups of subcarriers and time slots to different users. In WiMAX, sub-channels are obtained by grouping subcarriers that are pseudo-randomly chosen on the whole bandwidth. In LTE/LTE-A, adjacent subcarriers and OFDM symbols form a RB (Resource Block), which is the smallest radio resource that can be allocated to a user.

A BS may or may not use a set of subcarriers, so that frequency planning is very flexible in OFDMA. GSM-like and CDMA-like frequency patterns can be easily implemented in OFDMA networks provided that the outage probability on the common control channels is not too high. The WiMAX literature has introduced a new terminology for describing a frequency plan used by sectored or omni-directional BSs. In [25], the frequency reuse pattern has been defined by the expression: $N_c \times N_t \times N_f$. N_c is the number of cells in the network cluster. It determines the inter-cellular frequency reuse. N_t represents the number of sectors in a cell and N_f demonstrates intra-cellular frequency reuse. Figure 2.2 shows six examples of such frequency patterns in WiMAX networks. We call IFR (Integer Frequency Reuse), patterns of type $N_c \times 1 \times 1$.

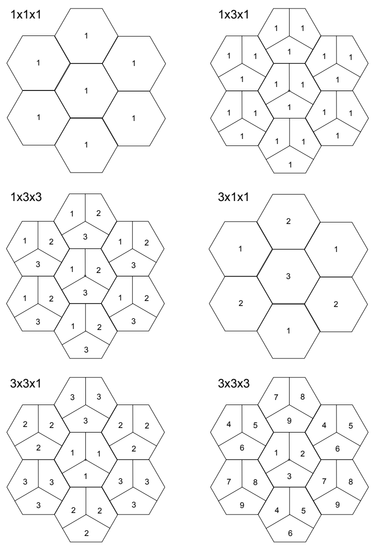

Figure 2.2: Examples of frequency patterns $N_c \times N_t \times N_f$ in WiMAX networks.

The users in the outer region of cell suffer from low SINR values especially for reuse patterns $1 \times 1 \times 1$, $1 \times 3 \times 1$ and $1 \times 3 \times 3$. To resolve this issue, FFR (Fractional Frequency Reuse) has been suggested in [20]. In this frequency reuse scheme, available bandwidth is divided among inner and outer regions in such a way that the former employs reuse 1 while the latter applies frequency reuse 3. Figures 2.1 (c) and 2.3 illustrates this concept. The notion of FFR can be generalized to SFR (Soft Frequency Reuse) [17, 26]. In SFR, the frequency reuse is 1 but bandwidth parts are allocated to different cell zones, in which a different maximum power is allowed.

We have also proposed and analyzed in [38] a TLPC (Two Level Power Control) scheme (see figure 2.4) to overcome the fact that in FFR it is not possible to use full network bandwidth in a cell. In TLPC, total bandwidth in a cell (equal to the system bandwidth) is divided into three equal parts: two parts allocated to inner region and one to the outer region. The output power per subcarrier in the inner region is P_i and that in the outer region is P_o. We define $\delta \geqslant 1$ as $\delta = P_o/P_i$.

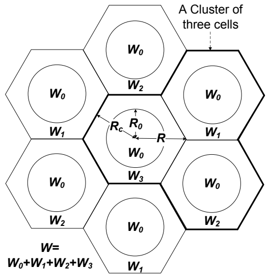

Figure 2.3: Fractional Frequency Reuse in OFDMA networks: system bandwidth is $W = W_0 + W_1 + W_2 + W_3$; inner cell uses W_0; outer cell uses alternatively W_1, W_2 and W_3 with a reuse factor of 3.

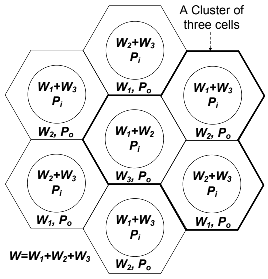

Figure 2.4: Two level power control case in OFDMA networks: bandwidth W is partitioned into three equal parts, i.e., $W_1 = W_2 = W_3$

The three spectrum parts W_1, W_2 and W_3 alternate from cell to cell in such a way that there is a pseudo-reuse 3 scheme between outer regions. Neighboring cells contribute in fact to interference in the outer region but with a reduced power P_i. The consequence is that the total network bandwidth is used in every cell but interference is expected to be reduced in outer regions.

In OFDMA networks, the SINR formulation in (2.5) is still valid provided that we consider a single subcarrier n:

$$\gamma_u^{(n)} = \frac{P_b^{(n)} g_{b,u}^{(n)}}{\sum_{k \neq b, k \in \mathcal{F}_b^{(n)}} P_k^{(n)} g_{k,u}^{(n)} + N_0 W_{sc}}, \tag{2.14}$$

where $P_b^{(n)}$ is the subcarrier transmit power, $g_{b,u}^{(n)}$ is the path-gain on subcarrier n, $\mathcal{F}_b^{(n)}$ is the set of BSs transmitting on subcarrier n and W_{sc} is the subcarrier bandwidth.

In order to predict the throughput achieved by a user on a sub-channel or a RB, we rely on a physical layer abstraction methodology. Such a methodology computes a single effective value of the SINR (γ_u^{eff}) and maps it to a BLER (Block Error Rate) value. The effective SINR vs. BLER mapping is obtained by link level simulations assuming a flat fading channel. The effective SINR can be seen as a compressed value of the vector of the received subcarrier SINR values [22]. Several physical layer abstraction models are given in [22] and [25]. The most convenient one is the MIC (Mean Instantaneous Capacity), which derives the effective SINR from the subcarrier SINR values as follows:

$$\gamma_u^{eff} = 2^{\frac{1}{N_{sc}} \sum_{n=1}^{N_{sc}} \log_2(1+\gamma_u^{(n)})} - 1. \tag{2.15}$$

In WiMAX, the subcarriers of a sub-channel are pseudo-randomly distributed over the whole system bandwidth. It is thus reasonable to consider that the RVs $\gamma_u^{(n)}$ are independent. In LTE/LTE-A however, the subcarriers of a RB are contiguous, so that it is necessary to consider correlated RVs. The correlation factor depends on the coherence bandwidth of the channel.

2.5 BS LOCATIONS

The model used for placing BSs in a cellular network mainly depends on the informations we have concerning the area to be covered. In a first phase of dimensioning, the detailed topography and radio propagation parameters are not known from the network designer. The only available information can be the environment type (urban, suburban, rural), which is supposed to be uniform resulting in an isotropic radio propagation. In this case, the hexagonal layout (as shown for example in figure 2.3) is the most traditional one. Some references adopt also the circular cell model (e.g. [18, 9]) but have to deal with the fact that cell areas are overlapping.

The hexagonal network model can be considered as too much idealized since in reality the BS location pattern is not so regular. This is due to the fact that some locations cannot be used (in the middle of a street or on a building where residents refuse the installation of an antenna) and some other are preferred (for example at the top of a hill). The BS layout can be then seen as a realization (or a snapshot) of a random model. The simplest model is the homogeneous Poisson point process. In such an approach, cells can be modeled using the Boolean model (that doesn't take into account interference), the Poisson-Voronoi tessellation (that associates to each BS, the set of closest points) or a more complex SINR coverage model, where interference is represented by a shot-noise field. Stochastic geometry analysis provides the average characteristics of a typical cell (see e.g. [8, 28, 40]).

2.6 MULTIPLE ANTENNAS

Antenna configuration plays a dominant role in the performance increase of todays cellular networks. By allowing the use of multiple antennas at the transmission and/or at the reception, MIMO techniques provide a higher reliability of the signal as well as an increase of the available data rates. Several gains are expected:

- The diversity gain: Independent copies of the same signal provide a higher reliability of the signal against fast fading effects. The diversity order d of a transmission is the number of independent received copies of the signal. It characterizes also the rapidity with which the bit error probability, P_e, decreases as a function of the SNR (Signal to Noise Ratio), γ [13]:

$$P_e(\gamma) \underset{\gamma \to +\infty}{\sim} \gamma^{-d}.$$

- The array gain: At the transmitter side, an antenna array focuses the energy in a given direction. At the receiver side, an antenna array receives more energy, so that the SINR is improved even in absence of fast fading. Antenna pattern

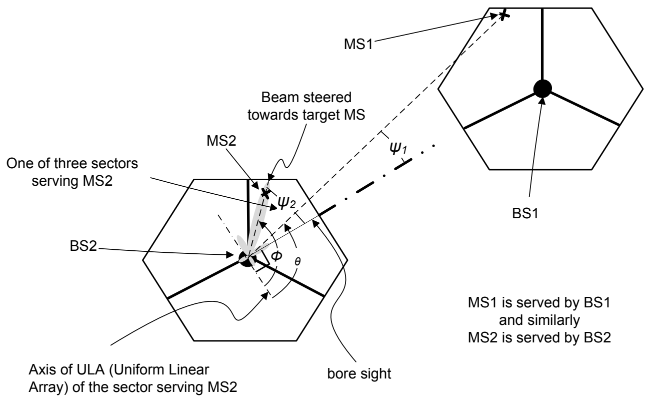

Figure 2.5: Example of beamforming transmission.

is obtained thanks to precoding or *beamforming* techniques that adapt the signal phase on each antenna of the array and sum these signal coherently.

- The multiplexing gain: A MIMO coding scheme can achieve a multiplexing gain r if the theoretical achievable throughout R can be written:

$$R(\gamma) \underset{\gamma \to +\infty}{\sim} r \log \gamma \text{ [bits/s/Hz]},$$

i.e., r times the capacity of a SISO (Single Input Single Output) system. For a $M \times N$ MIMO channel with independent Rayleigh fading, the capacity can be written [6]:

$$C(\gamma) \underset{\gamma \to +\infty}{\sim} \min(M, N) \log \gamma \text{ [bits/s/Hz]}.$$

Maximal values for d and r cannot be achieved simultaneously. There exists a function $d^*(r) = (M - r) \times (N - r)$, $r = 1, ..., \min\{M, N\}$, that represents the diversity/multiplexing trade-off [13].

2.6.1 *Beamforming*

A classical beamforming model is the delay and sum beamformer (or conventional beamformer) with ULA (Uniform Linear Array). The power radiation pattern for a conventional beamformer is a product of array factor and radiation pattern of a single antenna. The array factor for this power radiation pattern is given as [44]:

$$AF(\theta) = \frac{1}{n_t} \left| \frac{\sin(\frac{n_t \pi}{2}(\cos(\theta) - \cos(\phi)))}{\sin(\frac{\pi}{2}(\cos(\theta) - \cos(\phi)))} \right|^2, \tag{2.16}$$

where n_t is the number of transmit antennas at BS (with inter-antenna spacing equal to half wavelength), ϕ is the look direction (towards which the beam is steered) and θ is any arbitrary direction. Both these angles are measured with respect to array axis at BS (see figure. 2.5). The array factor is multiplied by the gain of a single antenna of the array to give the resultant beamforming gain, i.e., $A \leftarrow A \times AF$ in (2.1).

2.6.2 *SU-MIMO*

In SU-MIMO (Single User MIMO), the BS is equipped with several transmit antennas and the signal is received with multiple receive antennas. The transmission is done using space-time codes like STBC (Space-Time Block Codes). Many STBC were proposed in the literature to achieve full diversity (the Alamouti code [7] or DAST [11]), maximum multiplexing gain (V-BLAST code [6]) or an optimal diversity multiplexing tradeoff (the Golden code [15]). In this section, we focus on the Alamouti code at the transmission combined with the MRC (Maximum Ratio Combining) technique at the reception.

Alamouti code is a STBC [7] that achieves the full transmission diversity for two transmit antennas without requiring channel knowledge and is very simple to implement. It was adopted for the downlink transmission of WiMax (IEEE 802.16m), UMTS and CDMA2000 standards. In LTE, a "frequential" version of the Alamouti code as a transmit diversity scheme for the 2 transmit antenna case [30]. The Alamouti code matrix is given by [7]:

$$\mathbf{X} = \begin{bmatrix} s_1 & -s_2^* \\ s_2 & s_1^* \end{bmatrix}, \tag{2.17}$$

where $\{s_i\}_{i=1,2}$ are the transmitted complex symbols. It consists in transmitting the symbols s_1 and s_2 from the two antennas in the first channel use period and $-s_2^*$, s_1^* in the second channel use period. It is hence a rate 1 code since two symbols are transmitted during two channel use periods.

We now assume that the receiver is performing MRC with N antennas. At the receiver side, the signal can be written as:

$$\begin{aligned} \mathbf{y}_u &= \sqrt{\frac{p_{b,u}}{2}} \underbrace{\begin{bmatrix} h_{1,1,b} & h_{1,2,b} \\ h_{1,2,b}^* & -h_{1,1,b}^* \\ \cdot & \cdot \\ \cdot & \cdot \\ h_{N,1,b} & h_{N,2,b} \\ h_{N,2,b}^* & -h_{N,1,b}^* \end{bmatrix}}_{\mathbf{H}_b} \underbrace{\begin{bmatrix} s_{1,b} \\ s_{2,b} \end{bmatrix}}_{\mathbf{x}_0} \\ &+ \sum_{k \neq b} \sqrt{\frac{p_{k,u}}{2}} \begin{bmatrix} h_{1,1,k} & h_{1,2,k} \\ h_{1,2,k}^* & -h_{1,1,k}^* \\ \cdot & \cdot \\ \cdot & \cdot \\ h_{N,1,k} & h_{N,2,k} \\ h_{N,2,k}^* & -h_{N,1,k}^* \end{bmatrix} \underbrace{\begin{bmatrix} s_{1,k} \\ s_{2,k} \end{bmatrix}}_{\mathbf{x}_k} + \mathbf{n}, \end{aligned} \tag{2.18}$$

where $h_{i,j,k}$ is the Rayleigh flat fading channel between the i^{th} antenna of the receiver and the j^{th} antenna of the BS k, $p_{k,u}$ is the power received from BS k without fast fading, $s_{.,k}$ are the symbols transmitted by k, and $\mathbf{n}$ is the thermal noise vector. The $h_{i,j,k}$ are complex Gaussian distributed RVs, i.e., $h_{i,j,k} \in \mathcal{CN}(0,1)$.

The MRC receiver combines the received signals from the N antennas. The received signal is multiplied by the complex conjugate of the channel $\mathbf{H}_b$. The SINR per symbol is, hence, given by:

$$\gamma_u = \frac{\frac{p_{b,u}}{2}\sum_{n=1}^{N}(|h_{n,1,b}|^2+|h_{n,2,b}|^2)}{\sum_{k\neq b}\frac{p_{k,u}}{2}\left(\frac{|\sum_{n=1}^{N}h^*_{n,1,b}h_{n,1,k}+h_{n,2,b}h^*_{n,2,k}|^2+|\sum_{n=1}^{N}h^*_{n,1,b}h_{n,2,k}-h_{n,2,b}h^*_{n,1,k}|^2}{\sum_{n=1}^{N}(|h_{n,1,b}|^2+|h_{n,2,b}|^2)}\right)+N_0W}. \tag{2.19}$$

2.6.3 *MU-MIMO*

In a MU-MIMO (Multi-User MIMO) communication system, output antennas are distributed on different users. The spatial degrees of freedom of MIMO channels combined with multiuser multiplexing schemes can enhance considerably the system capacity.

In a multiuser communication, interference is the key performance limiting factor since it ultimately limits the system capacity. To mitigate multiuser interference, scheduling is generally combined with additional pre-transmit signal processing techniques. In this context, many precoding techniques were proposed in the literature among them we can mention: DPC (Dirty Paper Coding) [4, 12], ZFBF (Zero Forcing Beamforming) [21], MMSE (Minimum Mean Square Error) beamforming [23], random beamforming [19], codebook beamforming [24, 31]. In this section, we focus on ZFBF as an example of MU-MIMO scheme.

It is a linear transmission strategy allowing a multiuser transmission without generating multiuser interference and presenting the advantage of simplicity of implementation. However, it was shown in [21], that the ZFBF combined with an appropriate scheduling approaches the sum-capacity achieved by the DPC when the number of users is very large.

Consider a downlink, multicellular multiuser system. Each BS is equipped with M antennas and there are N users per cell with a single antenna each. ZFBF consists of multiplying the information vector by the ZF precoding matrix given by:

$$\mathbf{W} = \mathbf{H}^H(\mathbf{H}\mathbf{H}^H)^{-1}, \tag{2.20}$$

where $\mathbf{H}$ is the channel between the BS and the users served simultaneously. $\mathbf{H}$ is a $N \times M$ matrix with complex Gaussian distributed entries, i.e, $h_{i,j} \in \mathcal{CN}(0,1)$. Hence the transmitted signal is given by:

$$\mathbf{x} = \sqrt{P_b}\frac{\mathbf{Ws}}{\sqrt{\delta}}, \tag{2.21}$$

where P_b is the transmit power, $\mathbf{s} = [s_1, s_2, ...s_N]$ the symbol information vector intended to the N users and δ is a normalization factor introduced to satisfy the transmission power constraint and to ensure: $\|\mathbf{x}\|^2 = P_b$. δ is given by:

$$\delta = \|\mathbf{Ws}\|^2. \tag{2.22}$$

The maximum number of users that can be served by a BS is $N = M$. When $N > M$, M among the N users can be scheduled to be served by the BS simultaneously.

In a multicellular system, the signal received by a user u served by the BS b is given by:

$$y_u = \sqrt{p_{b,u}}\mathbf{h}_{b,u}\frac{\mathbf{W}_b\mathbf{s}_b}{\sqrt{\delta_b}} + \sum_{k\neq b}\sqrt{p_{k,u}}\mathbf{h}_{k,u}\frac{\mathbf{W}_k\mathbf{s}_k}{\sqrt{\delta_k}} + n_u, \tag{2.23}$$

$$= \frac{\sqrt{p_{b,u}}}{\sqrt{\delta_b}}s_{b,u} + \sum_{k\neq b}\sqrt{p_{k,u}}\mathbf{h}_{k,u}\frac{\mathbf{W}_k\mathbf{s}_k}{\sqrt{\delta_k}} + n_u, \tag{2.24}$$

where $\mathbf{h}_{k,u} \in \mathbb{C}^{1\times M}$ is the channel between the BS k and user u, $\mathbf{W}_k \in \mathbb{C}^{M\times N}$ is the precoding matrix used by k, $\mathbf{s}_k$ is the information symbol vector intended to the users of BS k, δ_k is the normalization factor used by k, $p_{k,u}$ is the power received from the BS k without fast fading, and n_u is the AWGN (Average White Gaussian Noise).

From (2.24) we can write the SINR at the user u:

$$\gamma_u = \frac{p_{b,u}}{\delta_b\left(\sum_{k\neq b} p_{k,u}\frac{\|\mathbf{h}_{k,u}\mathbf{W}_k\|^2}{\delta_k} + N_0 W\right)}. \tag{2.25}$$

2.6.4 *Multicell Cooperation*

Multicell cooperation is a paradigm, which aims at increasing cell edge user throughputs. Instead of trying to mitigate multicell interference, the multicell cooperation transforms it to a useful signal or at least to a less harmful signal. There are several terminologies in the literature for this technique: multicell processing, multicell MIMO, network MIMO or DAS (Distributed Antenna Systems). We use here CoMP (Coordinated Multipoint Transmission), which is the terminology of the 3GPP standardization body. CoMP is foreseen to be a key performance technique for LTE-A.

CoMP consists in a multicell cooperation scheme that takes advantage of the distributed antenna formed by the neighboring cells to mitigate multicell interference and to improve cell-edge and system throughput [39]. In the 3GPP LTE-A, two main schemes were highlighted [33]: the CB/S-CoMP (Coordinated Beamforming/Scheduling CoMP) and the JP-CoMP (Joint Processing CoMP). The former consists in coordinating the scheduling decisions of adjacent cells in order to mitigate co-channel interference. The latter consists in sharing information across coordinated BSs to serve users cooperatively. The surrounding BSs contribute to transmit the useful signal to the user instead of acting as inteferers. In this section, we focus on JP-CoMP.

Consider a downlink multicellular multiuser system (K active users) and consider multiple antenna BSs (M antennas) and single antenna user equipments. Let a *cluster* be a subset of BSs cooperating to serve a user. The clusters are disjoint. We assume a simple criterion for BS selection based on the minimization of the distance depending path-loss. A cluster of BSs transmits to a single user per TTI. BSs use the MRT (Maximum Ratio Transmission) scheme to transmit their data. We assume coherent multicell transmission which needs a tight synchronization across transmitting BSs (like in [34]) that can be ensured using low-latency and high-capacity backhaul communication. The information data intended to a user are shared by all BSs in its cooperation cluster. CSI (Channel State Information) between the considered user and the cooperating BSs are estimated using feedback for the FDD (Frequency Division Duplex) mode or uplink-downlink channel reciprocity for the TDD (Time Division Duplex) mode. The cluster of BSs serving a user u is denoted B_u. The signal received by a user u is given by [32]:

$$y_u = \sum_{b \in B_u} \sqrt{p_{b,u}} \mathbf{h}_{b,u} \mathbf{x}_{b,u} + \sum_{i \neq u} \sum_{k \in B_i} \sqrt{p_{k,u}} \mathbf{h}_{k,u} \mathbf{x}_{k,i} + n, \tag{2.26}$$

where $\mathbf{h}_{b,u} \in \mathbb{C}^{1 \times M}$ is the complex Gaussian channel between user u and BS b, n is the AWGN and $\mathbf{x}_{b,u} \in \mathbb{C}^{M \times 1}$ is the MRT data vector transmitted from BS b to the user u and is given by:

$$\mathbf{x}_{b,u} = \frac{\mathbf{h}_{b,u}^T}{\|\mathbf{h}_{b,u}\|} s_u, \tag{2.27}$$

where $s_u \in \mathbb{C}$ is the normalized information symbol intended to user u from BS b.

The output SINR perceived by a user u is given by:

$$\gamma_u = \frac{\left(\sum_{b \in B_u} \sqrt{p_{b,u}} \|\mathbf{h}_{b,u}\|\right)^2}{\sum_{i \neq u} \left| \sum_{k \in B_i} \sqrt{p_{k,u}} \mathbf{h}_{k,u} \frac{\mathbf{h}_{k,i}^T}{\|\mathbf{h}_{k,i}\|} \right|^2 + N_0 W}. \tag{2.28}$$

2.7 Fluid Model

The fluid model has been proposed by Kelif and Altman [18] to simplify the expression of the OCIF factor in CDMA networks. It is in fact a generic approach for computing an approximation of the interference at a given location in the cell. Due to its simplicity and to the fact that the computed interference depends only on the distance to the serving BS, it allows further analysis like capacity computation, admission control policy design, etc.

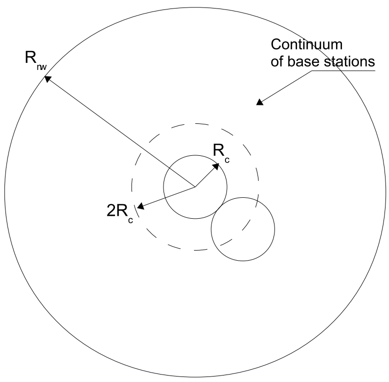

Figure 2.6: Network and cell of interest in the fluid model; the minimum distance between the BS of interest and interferers is $2R_c$ and the interfering network is made of a continuum of base stations.

The key modelling step of the model consists in replacing a given fixed finite number of interfering BSs by an equivalent continuum of transmitters, which are spatially distributed in the network. This means that the transmitting interference power is now considered as a continuum field all over the network. We focus on

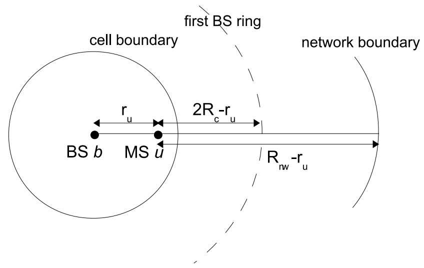

Figure 2.7: Integration limits for external interference computation.

a given cell and consider a round shaped network around this central cell with radius R_{nw}. In figure 2.6, the central disk represents the cell of interest, i.e., the area covered by its BS. The continuum of interfering BSs is located between the dashed circle and the outer circle. By analogy with the discrete regular network, where the half distance between two BSs is R_c, we consider that the minimum distance to interferers is $2R_c$.

Let us consider a mobile u at a distance r_u from its serving BS b. Each elementary surface $zdzd\theta$ at a distance z from u contains $\rho_{BS}zdzd\theta$ base stations which contribute to $p_{ext,u}$. Their contribution to the external interference is $\rho_{BS}zdzd\theta P_b K z^{-\eta}$. We approximate the integration surface by a ring with centre u, inner radius $2R_c - r_u$, and outer radius $R_{nw} - r_u$ (see figure 2.7).

$$\begin{aligned} p_{ext,u} &= \int_0^{2\pi}\int_{2R_c-r_u}^{R_{nw}-r_u} \rho_{BS} P_b K z^{-\eta} zdzd\theta \\ &= \frac{2\pi\rho_{BS}P_bK}{\eta-2}\left[(2R_c - r_u)^{2-\eta} - (R_{nw} - r_u)^{2-\eta}\right]. \end{aligned} \tag{2.29}$$

Now, the OCIF $f_u = p_{ext,u}/p_{int,u}$ can be expressed by:

$$f_u = \frac{2\pi\rho_{BS}r_u^\eta}{\eta-2}\left[(2R_c - r_u)^{2-\eta} - (R_{nw} - r_u)^{2-\eta}\right]. \tag{2.30}$$

If the network is large, i.e., R_{nw} is large compared to R_c, f_u can be further approximated by:

$$f_u = \frac{2\pi\rho_{BS}r_u^\eta}{\eta-2}(2R_c - r_u)^{2-\eta}. \tag{2.31}$$

This closed-form formula allows a quick computation of the performance parameters of a cellular network. If we compare this approximation with Monte Carlo simulations in an hexagonal network, we can note that there is a lack of accuracy at cell edge. In [37], we have thus proposed an extension of this formula to hexagonal networks by introducing a correction depending only on the path-loss exponent. The OCIF factor can be re-written as follows:

$$f_{hexa,u} = (1 + A_{hexa}(\eta))\frac{2\pi\rho_{BS}r_u^\eta}{\eta-2}(2R_c - r_u)^{2-\eta}, \tag{2.32}$$

where $A_{hexa}(\eta) = 0.15\eta - 0.32$ is a corrective term obtained by least-square fitting. For example, $A_{hexa}(2.5) = 0.055$ (the correction is tiny) and $A_{hexa}(4) = 0.28$ (the correction is significative). We have compared this formula to extensive Monte

Carlo simulations in [37] and shown that it is accurate for a wide range of path-loss exponents, cell radii and network sizes.

2.8 Traffic Models

Up to now, we have focused our discussion on the radio link quality through the expression of the SINR in various situations. This kind of study can be called *static* in the sense that we consider a static user at a given time instant. Several papers in the literature however study the user performance parameters in a *dynamic* environment, i.e., from a teletraffic point of view. In this approach, users are arriving in a cell according to a random process in time, according to a certain spatial distribution in the cell area, stay for a random duration and leave the system.

For circuit-switched services (voice, video-conference or even streaming), we have a loss system. Access to the service is possible as soon as the SINR is above a certain threshold. A call is usually characterized by a Poisson arrival and by a random duration (usually following an exponential distribution). The main performance parameter is the blocking probability, which can be obtained using the classical Erlang-B formula (single service), the multi-dimensional Erlang-B formula (several services), or the Kaufman-Robert's algorithm [3, 43] (see [10] for other algorithms for loss systems). There are various variations on this theme, see for example [5] for a teletraffic analysis of hierarchical networks with mobility.

For packet services, we have seen how the SINR translates into an instantaneous throughput is captured by the Shannon formula, an approximation of it or a mapping from SINR intervals to throughputs. A packet call is usually characterized by a Poisson arrival and by a random volume of data to be downloaded. Main performance parameters are the average packet call throughput and delay, and possibly the blocking probability in case of admission control. We now detail two possible approaches we have considered in our work.

2.8.1 *Multi-class Processor Sharing*

In this approach, a cell is modeled as a M/G/1/PS queue. If there are n clients in the system, the service rate of the BS is $\mu(n)$ ($0 < \mu(n) < \infty$ and $n\mu(n) < \infty$). The client arrival rate is λ. There are K classes of client with arrival rate $\lambda_k = p_k\lambda$ for the class k. Every arriving client in class k has a service requirement σ_k. These requirements are i.i.d. with mean β_k. The load of class k is $\rho_k = \lambda_k\sigma_k$. The total load is $\rho = \sum_k \rho_k$.

Then, the steady-state probabilities of the number of clients in each class knowing n, the total number of clients in the system, is [42]:

$$\pi(n_1, ..., n_K|n) = H^{-1}\phi(n)\prod_{k=1}^{K}\frac{\rho_k^{n_k}}{n_k!}, \tag{2.33}$$

where $\phi(n) = \left(\prod_{i=1}^{n}\mu(i)\right)^{-1}$, $n = n_1 + ... + n_K$ and $H = \sum_{n=0}^{\infty}\frac{\rho^n}{n!}\phi(n)$. The steady-state probabilities of the number of clients in the system is given by:

$$\pi(n) = H^{-1}\frac{\rho^n}{n!}\phi(n). \tag{2.34}$$

The expected number of clients in the system ($\bar{Q}$) and in class k ($\bar{Q}_k$) are given by:

$$\bar{Q} = H^{-1}\sum_{n=1}^{\infty}\frac{\rho^n\phi(n)}{(n-1)!}, \tag{2.35}$$

$$\bar{Q}_k = \frac{\rho_k}{\rho}\bar{Q}. \tag{2.36}$$

From Little's formula, we obtain the average sojourn time for a client of class k:

$$\bar{R}_k = \frac{\bar{Q}_k}{\lambda_k} \tag{2.37}$$

and its average throughput:

$$\bar{X}_k = \frac{\beta_k}{\bar{R}_k}. \tag{2.38}$$

These formulas are independent on the service requirement distribution.

Assume now that the BS uses a Round Robin scheduling algorithm and thus equally allocates radio resources to the active users. We have $\mu(n) = 1/n$, $\phi(n) = n!$ and $H^{-1} = 1-\rho$. We further assume that the cell is divided in K regions with an average data rate c_k for the region k. Packet call sizes are i.i.d. with mean B, then the service requirement of a user in region k is $\beta_k = B/c_k$. The total cell load is:

$$\rho = \sum_k \lambda B\frac{p_k}{c_k}. \tag{2.39}$$

The stability condition is given by $\rho < 1$ and thus the cell capacity is:

$$C = \left(\sum_k \frac{p_k}{c_k}\right)^{-1}. \tag{2.40}$$

The average sojourn time and the average throughput of a user in region k are respectively given by:

$$\bar{R}_k = \frac{B}{c_k(1-\rho)}, \tag{2.41}$$

$$\bar{X}_k = c_k(1-\rho). \tag{2.42}$$

This approach has been extended to Proportional Fair scheduling in [16], when the user data rate can be expressed as a linear function of the SINR. This assumption is valid for low SINR values as observed in UMTS or HSPA (High Speed Packet Access) networks. See [29, 35] for recent expressions of the average throughput assuming opportunistic scheduling and alpha-fairness scheduling.

2.8.2 *Engset-like Markovian Model*

An alternative to this approach has been developed in [36]. In this model, the number of MSs in a cell, N, is fixed and includes both active and inactive users. Every MS is assumed to generate an infinite length ON/OFF elastic traffic. ON periods are characterized by a random data volume, while OFF periods are characterized by a random duration (both with exponential distribution). Radio resources are organized in frames of N_S slots. There are K different MCSs and a slot can carry m_k bits with a MCS type k. MCS type 0 represents the outage state. The channel may change at every frame boundary. The probability that a user has MCS k is p_k.

The proposed model is based on a CTMC (Continuous Time Markov Chain) made of $N+1$ states and shown in figure 2.8. The rate at which a user ends its OFF period is $\lambda = 1/\bar{t}_{off}$, where $\bar{t}_{off}$ is the average OFF period. The departure rate $\mu(n)$ depends on the number of active users and on the scheduling policy.

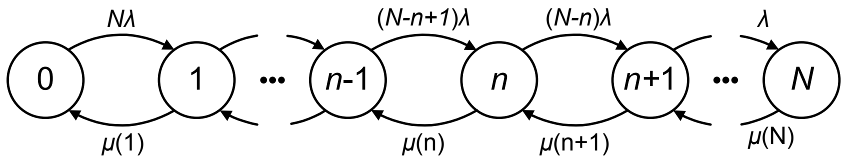

Figure 2.8: CTMC with departure rate depending on the number of active MS.

The generic expression for the departure rate is given by:

$$\mu(n) = \frac{\bar{m}(n) N_S}{\bar{x}_{on}\, T_F}, \tag{2.43}$$

where T_F is the duration of frame, $\bar{x}_{on}$ is the average volume of data and $\bar{m}(n)$ is the average number of bits per slot, when there are n active MSs.

For a scheduling fair in resource, we have:

$$\bar{m}(n) = \sum_{\substack{(j_0, j_1, \ldots, j_K) = (0,0,\ldots,0) | \\ j_0 + j_1 + \ldots + j_K = n \\ j_0 \neq n}}^{(n,n,\ldots,n)} \frac{n!}{n - j_0} \left(\sum_{k=1}^{K} m_k j_k \right) \left(\prod_{k=0}^{K} \frac{p_k^{j_k}}{j_k!} \right). \tag{2.44}$$

For a scheduling fair in throughput, we have:

$$\bar{m}(n) = \sum_{\substack{(j_0, j_1, \ldots, j_K) = (0,0,\ldots,0) | \\ j_0 + j_1 + \ldots + j_K = n \\ j_0 \neq n}}^{(n,n,\ldots,n)} \frac{(n - j_0)\, n! \prod_{k=0}^{K} \frac{p_k^{j_k}}{j_k!}}{\sum_{k=1}^{K} \frac{j_k}{m_k}}. \tag{2.45}$$

For an opportunistic scheduling, we have:

$$\bar{m}(n) = \sum_{i=1}^{K} \left(1 - \sum_{j=i+1}^{K} p_j \right)^n \left[1 - \left(1 - \frac{p_i}{\sum_{j=0}^{i} p_j} \right)^n \right] m_i. \tag{2.46}$$

Then, the stationary probabilities are given by:

$$\pi(n) = \frac{N!}{(N-n)!} \frac{\rho^n}{N_S^n \prod_{i=1}^{n} \bar{m}(i)} \pi(0), \tag{2.47}$$

where ρ is given by:

$$\rho = \frac{\bar{x}_{on}\, T_F}{\bar{t}_{off}}, \tag{2.48}$$

and $\pi(0)$ is given by:

$$\pi(0) = \frac{1}{1 + \sum_{n=1}^{N} \left(\prod_{i=1}^{n} \frac{(i-1)\lambda}{\mu(i)} \right)}. \tag{2.49}$$

The average number of active MSs is expressed as:

$$\bar{Q} = \sum_{n=1}^{N} n\,\pi(n). \tag{2.50}$$

The mean number of departures per time unit is given by the following equation:

$$\bar{X}_d = \sum_{n=1}^{N} \pi(n)\, N_S\, \mu(n). \tag{2.51}$$

Using Little's law, we can now derive the average duration $\bar{t}_{on}$ of an ON period:

$$\bar{t}_{on} = \frac{\bar{Q}}{\bar{X}_d}. \tag{2.52}$$

Finally, the average instantaneous user throughput during ON period is given as:

$$\bar{X} = \frac{\bar{x}_{on}}{\bar{t}_{on}}. \tag{2.53}$$

In [36], the performance parameters associated to a so called *throttling* policy are also given, where users have a target throughput but cannot go beyond a peak data rate. There is also an extension to a multi-profile traffic model, where each profile has its own traffic characteristics.

2.9 Conclusion

This chapter is a short lecture on cellular network dimensioning models. We have shown the central role played by the SINR and by the SINR outage probability in the performance evaluation of cellular networks. This role is central not only for coverage studies but also for traffic studies. We can easily express the SINR for different multiplexing schemes and MIMO transmission techniques. The fluid model is an approximate derivation of the interference in a cell as the function of the distance to the serving station. We have extensively used in our work these models and formulas to evaluate the performance of cellular networks.

Bibliography

[1] COST 231. Digital Mobile Radio Towards Future Generation Systems, Final Report. Technical report, COST. [Online] http://www.lx.it.pt/cost231.

[2] Y. Okumura, E. Ohmuri, T. Kawano, and K. Fukuda. Field Strength and its Variability in VHF and UHF Land Mobile Radio Service. *Review of the ECL*, 16:825–873, Sept.-Oct. 1968.

[3] J. S. Kaufman. Blocking in a Shared Environment. *IEEE Trans. on Communications*, 29(10):1474–1481, Oct. 1981.

[4] M. Costa. Writing on Dirty Paper (corresp.). *IEEE Trans. on Information Theory*, 29(3):439–441, May 1983.

[5] X. Lagrange and P. Godlewski. Teletraffic Analysis of a Hierarchical Cellular Network. In *Proc. of IEEE Vehicular Technology Conference (VTC)*, July 1995.

[6] G. J. Foschini. Layered Space-Time Architecture for Wireless Communication in a Fading Environment when Using Multi-element Antennas. *Bell Labs Tech. J.*, 1(2):41–49, Summer 1996.

[7] S. M. Alamouti. A Simple Transmit Diversity Technique for Wireless Communications. *IEEE Journal on Selected Areas in Communications*, 16(8):1451–1458, Oct. 1998.

[8] A. Frey and V. Schmidt. Marked Point Porcesses in the Plane I. *Advances in Performance Analysis*, 1(1):65–110, Jan. 1998.

[9] M.-S. Alouini and A. Goldsmith. Area Spectral Efficiency of Cellular Mobile Radio Systems. *IEEE Trans. on Vehicular Technology*, 48(4):1047–1066, July 1999.

[10] V. B. Iversen. Teletraffic Enginneering Handbook. Technical Report ITU-D SG 2/16 & ITC, ITU, June 2001.

[11] M. O. Damen, K. Abed-Meraim, and J.-C. Belfiore. Diagonal Algebraic Space-Time Block Codes. *IEEE Trans. on Information Theory*, 48(3):628–636, Mar. 2002.

[12] N. Jindal, S. Vishwanath, S. Jafar, and A. Goldsmith. Duality, Dirty Paper Coding and Capacity for Multiuser Wireless Channels. In *Proc. of DIMACS Workshop on Signal Processing for Wireless Transmisson*, Oct. 2002.

[13] L. Zheng and D. Tse. Diversity and Multiplexing: a Fundamental Tradeoff in Multiple Antenna Channels. *IEEE Trans. on Information Theory*, 49(5):1073–1096, May 2003.

[14] M. Franceschetti, J. Bruck, and L. J. Schulman. A Random Walk Model of Wave Propagation. *IEEE Trans. on Antennas and Propagation*, 52(5):1304–1327, May 2004.

[15] J-C. Belfiore, G. Rekaya, and E. Viterbo. The Golden Code: A 2×2 Full-Rate Code with Non-Vanishing Determinants. *IEEE Trans. on Information Theory*, 51(4):1432–1436, Jul. 2005.

[16] S. Borst. User-Level Performance of Channel-Aware Scheduling Algorithms in Wireless Data Networks. *IEEE/ACM Trans. on Networking*, 13(3):636–647, June 2005.

[17] Huawei. Soft Frequency Reuse Scheme for UTRAN LTE. Technical Report R1-050507, 3GPP, 2005.

[18] J.-M. Kelif and E. Altman. Downlink Fluid Model of CDMA Networks. In *Proc. of IEEE Vehicular Technology Conference (VTC)*, May 2005.

[19] M. Sharif and B. Hassibi. On the Capacity of MIMO Broadcast Channels with Partial Side Information. *IEEE Trans. on Information Theory*, 51(2):506–522, Feb. 2005.

[20] WiMAX Forum. Mobile WiMAX-Part II: A Comparative Analysis. Technical report, WiMAX Forum, May 2006.

[21] T. Yoo and A. Goldsmith. On the Optimality of Multiantenna Broadcast Scheduling Using Zero-Forcing Beamforming. *IEEE Journal on Selected Areas in Communications*, 24(3):528–541, Mar. 2006.

[22] R. Srinivasan. Draft IEEE 802.16m Evaluation Methodology Document. Technical report, IEEE 802.16 Broadband Wireless Access Working Group, Aug. 2007.

[23] F. Kaltenberger, M. Kountouris, L. Cardoso, R. Knopp, and D. Gesbert. Capacity of Linear Multi-User MIMO Precoding Schemes with Measured Channel Data. In *Proc. of IEEE Workshop on Signal Processing Advances in Wireless Communications (SPAWC)*, Jul. 2008.

[24] T.H. Kim, R.W Heath, and S. Choi. Multiuser MIMO Downlink with Limited Feedback Using Transmit-Beam Matching. In *Proc. of IEEE International Conference on Communications (ICC)*, May 2008.

[25] K. Ramadas and R. Jain. WiMAX System Evaluation Methodology. Technical Report v2.1, WiMAX Forum, July 2008.

[26] M. Bohge, J. Gross, and A. Wolisz. Optimal Power Masking in Soft Frequency Reuse based OFDMA Networks. In *Proc. of European Wireless Conference (EW)*, May 2009.

[27] J. Ellenbeck, J. Schmidt, U. Korger, and C. Hartmann. A Concept for Efficient System-Level Simulations of OFDMA Systems with Proportional Fair Fast Scheduling. In *Proc. of IEEE GLOBECOM Workshops*, Dec. 2009.

[28] M. Haenggi, J. G. Andrews, F. Baccelli, O. Dousse, and M. Franceschetti. Stochastic Geometry and Random Graphs for the Analysis and Design of Wireless Networks. *IEEE Journal on Selected Areas in Communications*, 27(7):1029–1046, Sept. 2009.

[29] M. Karray and B. Blaszczyszyn. Fading Effect on the Dynamic Performance Evaluation of OFDMA Cellular Networks. In *Proc. of IEEE International Conference on Communications and Networking (ComNet)*, Nov. 2009.

[30] J. Lee, J.-K. Han, and J. Zhang. MIMO Technologies in 3GPP LTE and LTE-Advanced. *EURASIP Journal on Wireless Communications and Networking*, 2009(Article ID 302092), 2009.

[31] F. Shu, W. Gang, X. Yue, and L. Shao-Qian. Multi-User MIMO Linear Precoding with Grassmannian Codebook. In *Proc. of International Conference on Communications and Mobile Computing (CMC)*, Jan. 2009.

[32] A. Tolli, H. Pennanen, and P. Komulainen. On the Value of Coherent and Coordinated Multi-cell Transmission. In *Proc. of IEEE International Communication Conference (ICC)*, June 2009.

[33] 3GPP TR 36.814. Evolved Universal Terrestrial Radio Access (E-UTRA); Further advancements for E-UTRA physical layer aspects. *Release 9 V9.0.0*, Mar. 2010.

[34] E. Bjornson, R. Zakhour, D. Gesbert, and B. Ottersten. Cooperative Multicell Precoding: Rate Region Characterization and Distributed Strategies With Instantaneous and Statistical CSI. *IEEE Trans. on Wireless Communications*, 58(8):4298–4310, Aug. 2010.

[35] R. Combes, Z. Altman, and E. Altman. On the Use of Packet Scheduling in Self-optimization Processes: Application to Coverage-Capacity Optimization. In *Proc. of International Symposium on Modeling and Optimization in Mobile, Ad Hoc, and Wireless Networks (WiOpt)*, May 2010.

[36] S. Doirieux, B. Baynat, M. Maqbool, and M. Coupechoux. An Efficient Analytical Model for the Dimensioning of WiMAX Networks Supporting Multi-Profile Best Effort Traffic. *Elsevier Computer Communications*, 33(10):1162–1179, June 2010.

[37] J.-M. Kélif, M. Coupechoux, and Ph. Godlewski. A Fluid Model for Performance Analysis in Cellular Networks. *EURASIP Journal on Wireless Communications and Networking*, 2010(Article ID 435189), 2010.

[38] M. Maqbool, Ph. Godlewski, M. Coupechoux, and J.-M. Kélif. Analytical Performance Evaluation of Various Frequency Reuse and Scheduling Schemes in Cellular OFDMA Networks. *Performance Evaluation*, 67(4):318–337, April 2010.

[39] M. Sawahashi, Y. Kishiyama, A. Morimoto, D. Nishikawa, and M. Tanno. Coordinated Multipoint Transmission/Reception Technique For LTE-Advanced. *IEEE Wireless Communications*, 17(3):26–34, Jun. 2010.

[40] F. Baccelli and B. Blaszczyszyn. *Stochastic Geometry and Wireless Networks: Volume I Theory*, volume 3 of *Foundations and Trends in Networking*. Now Publisher, 2009.

[41] A. Goldsmith. *Wireless Communications*. Cambridge University Press, Cambridge, 2005.

[42] F. P. Kelly. *Reversibility and Stochastic Networks*. John Wiley and Sons, Chichester, New York, Brisbane, Toronto, 1979.

[43] J. W. Roberts. *Performance of Data Communication Systems and their Applications*, chapter A Service System with Heterogeneous User Requirements - Applications to Multi-Service Telecommunication Systems. North-Holland Publ. Co., 1981.

[44] D. Tse and P. Viswanath. *Fundamentals of Wireless Communications*. Cambridge University Press, 2006.

3 CDMA NETWORKS

3.1 Introduction

As we have seen in the previous chapter, the estimation of cellular networks capacity and coverage mainly depends on the characterization of the interference. At a first glance, compared to the classical F/TDMA approach used in GSM, CDMA has simplified the network design. All cells indeed use the same carrier frequency and the whole system bandwidth. The number of scrambling codes needed to separate neighboring cells on the downlink is so large that the code planning is an easy task. The interference issue becomes however crucial and difficult to control and to evaluate for engineers: fast power control, intra-cell interference, soft-handover have been concepts brought by CDMA in the radio engineering of cellular networks.

3.2 Related Work

There is a large literature around the question of characterizing interference in CDMA networks. Pioneering works on the subject [3, 4, 19] mainly focuses on the uplink. [1, 3, 7] rely on numerical integration or Monte Carlo simulations. Such approaches are not satisfactory because of their computational time and because they provide very specific results for a given set of parameters.

Some analytical studies are proposed in the literature. For example, Chan and Hanly [5] approximate the distribution of the other-cell interference on the uplink using Edgeworth approximations. Abu-Dayya and Beaulieu [2] computes the outage probability in presence of multiple log-normal interferers, but assumes that all interference signals have the same statistics, which is not a realistic assumption in cellular networks. Moreover, thermal noise is often neglected for the computation of the outage probability (see e.g. [18]). This is a reasonable assumption for typical output powers and in urban environments. It is however questionable at high frequencies, in rural environments or when BS output power is decreased.

In contrast to previous works in the field, our approximations are based on the fluid model, which considers the discrete BS entities of a cellular network as a continuum. We thus revisit the traditional question of the outage probability in the light of the fluid model. There are similar approaches in the literature but in slightly different domains. For example, the authors of [8] describe a network in terms of macroscopic quantities such as node density. The same idea has been used in [6] for ad hoc networks. Both papers however assume a very high density of nodes and infinite networks. On the contrary, the fluid model is accurate even when the BS density is low and the network size is limited, as shown in [16].

3.3 Contributions

In collaboration with Orange Labs (Jean-Marc Kélif) and Philippe Godlewski, we have used the fluid model to characterize in a simple way the performance of CDMA networks.

- In [16], we have validated the fluid model through Monte Carlo simulations and proposed an extension of the original formula for hexagonal networks. As the original model assumes circular cells, a deviation is observed with simulations obtained in a traditional hexagonal network. This deviation depends mainly on the path-loss exponent. The new model adds thus a corrective term, depending on the path-loss exponent, to the original formula.
- In [9, 10], we have proposed global and spatial outage probability approximated formulas in absence of thermal noise and shadowing for the downlink of CDMA networks. Both formulas are direct applications of the fluid model and of the Central Limit Theorem applied to the total BS transmit power.
- In [11, 14], we have extended the previous formulas to environments characterized by shadowing using the fluid model and the Fenton-Wilkinson approximation of a sum of log-normal RVs. We have shown its negative impact on the network performance. The proposed approximation is accurate for standard deviations of the shadowing typically less than 6 dB. This is due to the inaccuracy of the Fenton-Wilkinson approach. A standard deviation of 8 dB can be achieved if shadowing RVs are supposed to be correlated.
- In [13], we have characterized analytically the notion of *cell breathing*, which is a phenomenon observed in CDMA networks when the traffic is increasing. It results in a reduction of the cell coverage. One way to combat cell breathing is to deploy new BSs through the process of *densification*. In this work, we have quantified the number of new BSs to be installed as a function of the traffic load.
- In [12], we have proposed an extension of the fluid model to tri-sectorized BSs. This new formula includes the antenna pattern of a BS sector.
- In [15], we have studied the influence of the user mobility on the outage probability and shown how cell capacity is decreasing with the mean radial user speed.
- In [17], we have studied the impact of a transmit power limitation on the coverage and the capacity of CDMA networks in a context where energy should be saved. This paper shows that it is possible to drastically reduce the BS transmit power without any loss of quality of service in a urban area. Transmit power can be further reduced if one accepts a small degradation of the service quality.

3.4 Conclusion

Although vanishing from research interests, CDMA is still the access scheme of the widely used 3G networks. These networks are characterized by fast power control, intra-cell interference and soft-handover. There has been a large literature for characterizing interference in such networks and our contributions consisted mainly in re-visiting traditional questions in the light of the fluid model with the aim of providing simpler formulas.

Bibliography

[1] K. S. Gilhousen, I. M. Jacobs, R. Padovani, A. J. Viterbi, L. A. Weaver, and C. E. Wheatley. On the Capacity of Cellular CDMA System. *IEEE Trans. on Vehicular Technology*, 40(2):303–312, May 1991.

[2] A. A. Abu-Dayya and N. C. Beaulieu. Outage Probabilities in the Presence of Correlated Lognormal Interferers. *IEEE Trans. on Vehicular Technology*, 43(1):164–173, Feb. 1994.

[3] A. J. Viterbi, A. M. Viterbi, and E. Zehavi. Other-Cell Interference in Cellular Power-Controlled CDMA. *IEEE Trans. on Communications*, 42(2/3/4):1501–1504, Feb./Mar./Apr. 1994.

[4] J. S. Evans and D. Everitt. Effective Bandwidth-Based Admission Control for Multiservice CDMA Cellular Networks. *IEEE Trans. on Vehicular Technology*, 48(1):36–46, Jan. 1999.

[5] C. C. Chan and S. V. Hanly. Calculating the Outage Probability in a CDMA Network with Spatial Poisson Traffic. *IEEE Trans. on Vehicular Technology*, 50(1):183–204, Jan. 2001.

[6] P. Jacquet. Geometry of Information Propagation in Massively Dense Ad hoc Networks. In *Proc. of ACM International Symposium on Mobile Ad Hoc Networking and Computing (MobiHoc)*, May 2004.

[7] S. E. Elayoubi and T. Chahed. Admission Control in the Downlink of WCDMA/UMTS. In *Wireless Systems and Mobility in Next Generation Internet*, volume 3427 of *Lecture Notes in Computer Science*, pages 136–151. Springer, 2005.

[8] S. Toumpis and L. Tassiulas. Packetostatics Deployment of Massively Dense Sensor Networks as an Electrostatics Problem. In *Proc. IEEE International Conference on Computer Communications (INFOCOM)*, Mar. 2005.

[9] J. M. Kélif, M. Coupechoux, and Ph. Godlewski. Spatial Outage Probability for Cellular Networks. In *Proc. of IEEE Global Communications Conference (GLOBECOM)*, Nov. 2007.

[10] J. M. Kélif, M. Coupechoux, and Ph. Godlewski. Spatial Outage Probability Formula for CDMA Networks. In *Proc. of IEEE Vehicular Technology Conference (VTC falls)*, Sept. 2007.

[11] J. M. Kélif, M. Coupechoux, and Ph. Godlewski. Effect of Shadowing on Outage Probability in Fluid Cellular Radio Networks. In *Proc. of International Symposium on Modeling and Optimization in Mobile, Ad Hoc, and Wireless Networks (WiOpt)*, Mar. 2008.

[12] J. M. Kélif, M. Coupechoux, and Ph. Godlewski. Fluid Model of the Outage Probability in Sectored Wireless Networks. In *Proc. of IEEE Wireless Communications and Networking Conference (WCNC)*, Mar. 2008.

[13] J. M. Kélif and M. Coupechoux. Cell Breathing, Sectorization and Densification in Cellular Networks. In *Proc. of International Symposium on Modeling and Optimization in Mobile, Ad Hoc, and Wireless Networks (WiOpt)*, June 2009.

[14] J. M. Kélif and M. Coupechoux. Impact of Topology and Shadowing on the Outage Probability of Cellular Networks. In *Proc. of IEEE International Conference on Commununications (ICC)*, June 2009.

[15] J. M. Kélif and M. Coupechoux. On the Impact of Mobility on Outage Probability in Cellular Networks. In *Proc. of IEEE Wireless Communications and Networking Conference (WCNC)*, Apr. 2009.

[16] J.-M. Kélif, M. Coupechoux, and Ph. Godlewski. A Fluid Model for Performance Analysis in Cellular Networks. *EURASIP Journal on Wireless Communications and Networking*, 2010(Article ID 435189), 2010.

[17] J.-M. Kélif, M. Coupechoux, and F. Marache. Limiting Power Transmission of Green Cellular Networks: Impact on Coverage and Capacity. In *Proc. of IEEE International Conference on Communications (ICC)*, May 2010.

[18] G.L. Stuber. *Principles of Mobiles Communications*. Norwell , MA. Kluwer, 1996.

[19] A. J. Viterbi. *CDMA - Principles of Spread Spectrum Communication*. Addison-Wesley, 1995.

4 OFDMA NETWORKS

4.1 Introduction

The dimensioning and performance evaluation of OFDMA networks have attracted a lot of interest in the past few years with the generalization of this access scheme in wireless standards, in particular in WiMAX and LTE. Whereas CDMA has been the common technology for third generation networks, OFDMA appears to be the unifying access scheme of the fourth generation. The long technical debate on the best multiple access technique researchers had ten years ago completely disappeared. Thanks to the (quasi) absence of inter-cell interference, OFDMA make the things easier for both design and operational engineers. It allows however a certain flexibility for the radio resource allocation (in terms of sub-carriers and time-slots), so that new engineering techniques have to be studied such as FFR.

4.2 Related Work

A significant part of the literature on the OFDMA access focuses on the resource allocation problem, which consists of allocating power and sub-carriers to multiple users in order to maximize the cell sum rate (see e.g. [11, 28, 33]). Most of these papers, which often rely on the computation of outage probabilities, however neglect inter-cell interference and focus on SNR variations. Two notable exceptions are references [43] and [38]. The former considers only a two cell network. The latter derives an expression of the SINR distribution conditionally on the average received powers and finally rely on Monte Carlo simulations at cell edge. Few papers are dealing with analytical approaches when inter-cell interference is considered, whereas there are many papers using simulations to find outage probability or SINR distribution, see e.g. [3, 4, 6, 13, 15, 27]. [7] proposes an analytical expression of the outage probability, which explicitly depends on the distances to every interferer. A simple planning procedure is proposed in [32] based on the evaluation of two averages of the SINR. Effective SINR is approximated by a Gaussian RV. The limitation of this study lies in the fact that the two involved averages are computed by simulations and have to be obtained for each user location. Contrary to the above mentioned papers, we have given in [48] an approximated formula of the outage probability in terms of effective SINR that depends only on the distance to the serving station.

An other open question in the radio quality of OFDMA networks evaluation is the analytical characterization of the SINR with the best server assumption. Most of the analytical works indeed assume that a user is attached to the closest BS. A more realistic assumption is the best server attachment, where users are served by the BS providing the best signal quality. Taking into account this assumption has been only recently tackled by the literature [42, 56]. We have proposed in [35] a semi-analytical approach to account for the best server assumption. We have also proposed an approximation of the SINR in this case in [41, 50].

Our work allows thus to obtain in a simple way the distribution of the SINR over the cell or the average SINR at a given distance from the BS. This a first step in the complete dimensioning methodology developed with Alcatel-Lucent Bell Labs and LIP6 for WiMAX networks. We can indeed quickly obtain the probability for a user to be served with a given MCS and derive from the Engset-like traffic model presented in Section 2.8.2 the average user throughput, the average delay or the average number of active users. In the literature, generic analytical traffic models for performance evaluation of cellular networks with varying channel conditions have been proposed in [1, 2, 5]. The models presented in these papers are mostly based on multi-class processor-sharing queues with each class corresponding to users having similar radio conditions and subsequently equal data rates, see Section 2.8.1. The variability of radio channel conditions at flow level is taken into account by considering a propagation model and a spatial distribution of users in a cell. These papers implicitly consider that users can only switch class between two successive data transfers, while in practice radio conditions and thus data rates of a particular user can change frequently during a data transfer. In addition, capacity of a WiMAX cell may vary as a result of varying radio conditions of users. Unlike existing models [1, 2, 5], the Engset-like model is adapted to WiMAX systems assumptions and is generic enough to integrate any appropriate scheduling policy. On the contrary, the classical M/G/1/PS approach is based on a Round Robin scheduler. Proportional fairness may be considered but only at low SINR, which is not a valid assumptions for OFDMA networks. Moreover, our approach makes it possible to consider the outage situation. A user experiencing outage is indeed not scheduled.

As explained in Section 2.4.3, OFDMA allows the deployment of smart frequency reuse schemes and it is a subject of research to understand the trade-offs involved in these schemes. In a nutshell, frequency reuse 1 (IFR1) should be preferred for operators willing to increase the cell capacity because the whole system bandwidth is available in every cell. On the other hand, frequency reuse 1 implies a bad radio signal quality at cell edges, outage probability may even attain unacceptable figures. FFR schemes have thus been proposed to improve the SINR at cell edge and at the same time to maintain a high cell capacity [8]. In our work, we have first studied through Monte Carlo simulations the possibility to deploy frequency reuse 1 in WiMAX networks using beamforming. At the time of our work, there was very few system level studies using beamforming in OFDMA networks. There was measurements campaigns not taking into account interference (see e.g. [19]). There was studies on frequency reuse schemes using MIMO but ignoring beamforming [21]. Existing beamforming simulations were neglecting important aspects of OFDMA networks like frequency diversity [18] or a physical abstraction model for the computation of the effective SINR [10, 16]. Our work has thus been the first one to systematically analyze frequency reuse schemes with beamforming and to account for the different channelizations patterns of the WiMAX standard. We have shown in which conditions, frequency reuse 1 was possible.

In absence of beamforming, the study of frequency reuse schemes has attracted the attention of a lot of researchers. Authors of [9] studied the performance of

FFR for 3GPP/3GPP2 OFDMA systems. Authors have used system level simulations in their analysis. In [17] and [16], the author has studied the FFR in a IEEE 802.16 based system in conjunction with an interference coordination algorithm. Performance is evaluated with simulations. Two new algorithms, FTR (Fractional Time Reuse) and FTFR (Fractional Time and Frequency Reuse), are proposed in [14] to cater for reduced capacity in the border area of cell because of FFR. In [20], authors have studied the capacity of a WiMAX system in presence of FFR. In [15] also, performance of a FFR system is analyzed through simulations. [23] proposes a Markov model to analyze different frequency reuse schemes but relies on simulations for the radio part of the study. Based on the fluid model, we have on the contrary proposed a simple analytical model for the SINR evaluation under different frequency reuse and scheduling schemes [24, 40].

At last, we have tackled some specific aspect of the heterogeneous networks, namely the optimal placement of relay nodes in a cellular networks. Hetnets are foreseen in the LTE-Advanced standard as a means of increasing the network capacity and improving coverage by adding to the macro BS layer smaller equipments like small BSs, femto BSs or relays. Relay related problems arise in various contexts like sensor networks [12], WLANs, or information theory. We have however focused on their deployment in cellular networks. In the literature, several authors study a single BS controlling several RNs (see e.g. [30, 44]) and thus ignore inter-cell interactions. In many papers considering multiple cell deployments and trying to solve combinatorial optimization problems, interference is not accurately modeled (see e.g. [34, 54, 47, 51]) and user locations are supposed to be known from the network planner [54]. This assumption is realistic in a WiMAX network but cannot be considered for a cellular network. The only papers that tries to take into account the effect of interference adopt a static approach where all buffers are always full [49, 52, 53]. On the contrary, our work assumes a dynamic traffic model. Based on an accurate modeling of the SINR, we solve the optimization problem with an enhanced Simulated Annealing algorithm [55].

4.3 Contributions

The following contributions have been obtained in collaboration with Alcatel-Lucent Bell Labs (Véronique Capdevielle, Vinod Kumar, Laurent Thomas), University of Paris VI (Sébastien Doirieux, George Nogueira, Bruno Baynat from LIP6 laboratory) and Orange Labs (Jean-Marc Kélif) in the framework of the thesis of Masood Maqbool (co-directed with Ph. Godlewski) and with NTU in the framework of the thesis of Mattia Minelli (co-directed with Ph. Godlewski and Ma Maode from NTU Singapore).

- We have first proposed some extensions of the fluid model for OFDMA networks. In [48], we have given an approximated formula of the outage probability in terms of effective SINR, see (2.15). This formula takes into account both shadowing and fast fading and assumes that channel gains on any two subcarriers of a sub-channel are independent (this is a valid assumption in the context of WiMAX networks). In [41, 50], we have further assumed that every user is served by the best server, i.e., the BS providing the highest receive power.

- In a series of papers, we have developed with LIP6 a complete dimensioning methodology for Alcatel-Lucent Bell Labs including traffic and coverage studies (see [37] for an overview). Traffic studies are based on the Engset-like approach presented in Section 2.8.2 and includes various scheduling policies like fair in throughput, fair in resource or opportunistic. A throttling policy is also proposed to limit the user peak rate (as foreseen by the standard) [22, 29, 31, 39]. The coverage study is based in a semi-analytical method that approximates the SINR spatial distribution by a Generalized Extreme Value distribution [35].

- We have evaluated the performance of several frequency reuse schemes for OFDMA networks either with simple analytical approaches [24, 40] or through Monte Carlo Simulations [25, 26, 36]. In particular, we have studied the possibility to use a frequency reuse 1 in WiMAX networks. On the one hand, frequency reuse 1 increases the cell capacity, on the other hand, it can lead to an unacceptable outage probability at cell edge. We have shown that reuse 1 is feasible only if beamforming is used in conjunction with the PUSC channelization. This kind of channelization is indeed the only one that can provide sufficient diversity on the interference signal and sufficient array gain on the useful signal.

- In the context of LTE networks, we have optimized the fractional power control parameter by using the fluid model on the uplink [45].

- We have shown the advantage of using relays in [46]. In [55], we have introduced a dynamic framework for the relay placement based on traffic analysis. Relays and BSs are modeled as M/G/1/PS queue and a fixed point iteration captures the interactions between transmitting nodes. Contrary to most of the literature, our framework takes into account non uniform traffic patterns. An extension of the fluid model has been proposed for relay based cellular networks. We have developed a dedicated Simulated Annealing algorithm that dynamically adapts temperature to energy variations and uses a combination of coarse and fine grids to accelerate the search for an optimal solution. Numerical results shows that out-of-band relays are preferably placed on the cell edge and are arranged in rings around the BS, when their number increases. In-band relays suffer from the poor quality of the backhaul link, especially in presence of shadowing and tends to be much closer to the BS. In both cases, cell capacity increases with the number of relays. The benefit is however small with in-band relays.

4.4 Conclusion

In this chapter, we focused on OFDMA cellular networks. At the time of the first studies, operators and manufacturers were working on dimensioning methodologies for these networks. This lead us to develop with LIP6 an approach spanning from the radio aspects to the traffic aspects for Alcatel-Lucent. At the radio level, an important question is to understand the trade-offs involved by FFR and to know whether it is possible to implement a frequency reuse 1. We have shown in which conditions it is possible to do a reuse 1 planning in WiMAX networks using beamforming techniques and analyzed FFR under various scheduling schemes. We have at last tackled the problem of optimally placing relays in a cellular network. Our current studies are related to interference coordination in heterogeneous networks and mobile relays.

Bibliography

[1] T. Bonald and A. Proutiere. Wireless Downlink Channels: User Performance and Cell Dimensioning. In *Proc. of ACM International Conference on Mobile Computing and Networking (Mobicom)*, Sept. 2003.

[2] S. Borst. User-level Performance of Channel-aware Scheduling Algorithms in Wireless Data Networks. In *Proc. of IEEE International Conference on Computer Communications (INFOCOM)*, Mar. 2003.

[3] C. F. Ball, E. Humburg, K. Ivanov, and R. Müllner. Rapid Estimation Method for Data Capacity and Spectrum Efficiency in Cellular Networks. In *Proc. of IST Mobile and Wireless Communications Summit*, June 2005.

[4] C. F. Ball, E. Humburg, K. Ivanov and F. Treml. Performance Analysis of IEEE802.16 Based Cellular MAN with OFDM-256 in Mobile Scenarios. In *Proc. of IEEE Vehicular Technology Conference (VTC)*, June 2005.

[5] S. Liu and J. Virtamo. Performance Analysis of Wireless Data Systems with a Finite Population of Mobile Users. In *Proc. of International Test Conference (ITC)*, Nov. 2005.

[6] Y.-J. Choi, C. S. Kim, and S. Bahk. Flexible Design of Frequency Reuse Factor in OFDMA Cellular Networks. In *Proc. of IEEE International Conference on Communications (ICC)*, June 2006.

[7] N. Damji and T. Le-Ngoc. Adaptive Downlink Resource Allocation Strategies for Real-Time Data Services in OFDM Cellular Systems. *EURASIP Journal on Wireless Communications and Networking*, 2006(Article ID 17526), 2006.

[8] WiMAX Forum. Mobile WiMAX-Part II: A Technical Overview and Performance Evaluation. Technical report, WiMAX Forum, Mar. 2006.

[9] G. Liu, J. Zhu, F. Jiang, B. Zhou, Y. Wang, and P. Zhang. Initial Performance Evaluation on TD-SCDMA Long Term Evolution System. In *Proc. of IEEE Vehicular Technology Conference (VTC)*, May 2006.

[10] M. C. Necker. Towards Frequency Reuse 1 Cellular FDM/TDM Systems. In *Proc. of ACM International Conference on Modeling, Analysis and Simulation of Wireless and Mobile Systems (MSWiM)*, October 2006.

[11] K. Seong, M. Mohseni, and J.M. Cioffi. Optimal Resource Allocation for OFDMA Downlink Systems. In *Proc. of IEEE International Symposium on Information Theory*, July 2006.

[12] K. Akkaya, M. Younis, and W. Youssef. Positioning of Base Stations in Wireless Sensor Networks. *IEEE Communications Magazine*, 45(4):96–102, Apr. 2007.

[13] M. Einhaus, O. Klein, B. Walke, and R. Halfmann. MAC Level Performance Comparison of Distributed and Adjacent OFDMA Subchannels in IEEE 802.16. In *Proc. of European Wireless (EW)*, April 2007.

[14] C. He, F. Liu, H. Yang, C. Chen, H. Sun, W. May, and J. Zhang. Co-channel Interference Mitigation in MIMO-OFDM System. In *Proc. of IEEE International Conference on Wireless Communications, Networking and Mobile Computing (WiCom)*, Sept. 2007.

[15] H. Jia, Z. Zhang, G. Yu, P. Cheng, and S. Li. On the Performance of IEEE 802.16 OFDMA System under Different Frequency Reuse and Subcarrier Permutation Patterns. In *Proc. of IEEE International Communication Conference (ICC)*, June 2007.

[16] M. C. Necker. Coordinated Fractional Frequency Reuse. In *Proc. of ACM International Conference on Modeling, Analysis and Simulation of Wireless and Mobile Systems (MSWiM)*, Oct. 2007.

[17] M. C. Necker. Local Interference Coordination in Cellular 802.16e Networks. In *Proc. of IEEE Vehicular Technology Conference (VTC)*, Oct. 2007.

[18] R. Pabst, J. Ellenbeck, M. Schinnenburg, and C. Hoymann. System Level Performance of Cellular WiMAX IEEE 802.16 with SDMA-enhanced Medium Access. In *Proc. of IEEE Wireless Communications and Networking Conference (WCNC)*, Mar. 2007.

[19] J. W. Porter, J. F. Kepler, T. P. Krauss, F. W. Vook, T. K. Blankenship, V. Desai, A. Schooler, and J. Thomas. An Experimental Adaptive Beamforming System for the IEEE 802.16e-2005 OFDMA Downlink. In *Proc. of IEEE Radio and Wireless Symposium*, Jan. 2007.

[20] C. Tarhini and T. Chahed. On Capacity of OFDMA-based IEEE802.16 WiMAX Including Adaptive Modulation and Coding (AMC) and Inter-cell Interference. In *Proc. of IEEE Workshop on LANMAN*, June 2007.

[21] F. Wang, A. Ghosh, C. Sankaran, and S. Benes. WiMAX System Performance with Multiple Transmit and Multiple Receive Antennas. In *Proc. of IEEE Vehicular Technology Conference (VTC)*, Apr. 2007.

[22] B. Baynat, S. Doirieux, G. Nogueira, M. Maqbool, and M. Coupechoux. An Efficient Analytical Model for WiMAX Networks with Multiple Traffic Profiles. In *Proc. of ACM International Workshop on Performance and Analysis of Wireless Networks (PAWN), in conjunction with Mobility Conference*, Sept. 2008.

[23] S-E. Elayoubi, O. Ben Haddada, and B. Fourestié. Performance Evaluation of Frequency Planning Schemes in OFDMA based Networks. *IEEE Trans. on Wireless Communications*, 7(5):1623–1633, May 2008.

[24] Ph. Godlewski, M. Maqbool, M. Coupechoux, and J. M. Kélif. Analytical Evaluation of Various Frequency Reuse Schemes in Cellular OFDMA Networks. In *Proc. of ACM International Conference on Performance Evaluation Methodologies and Tools (Valuetools)*, 2008.

[25] M. Maqbool, M. Coupechoux, and Ph. Godlewski. Comparison of Various Frequency Reuse Patterns for WiMAX Networks with Adaptive Beamforming. In *Proc. of IEEE Vehicular Technology Conference (VTC)*, May 2008.

[26] M. Maqbool, M. Coupechoux, and Ph. Godlewski. Effect of Distributed Subcarrier Permutation on Adaptive Beamforming in WiMAX Networks. In *Proc. of IEEE Vehicular Technology Conference (VTC)*, 2008.

[27] J.-W. So. Performance Analysis of VoIP Services in the IEEE 802.16e OFDMA System With Inband Signaling. *IEEE Trans. on Vehicular Technology*, 57(3):1876–1886, May 2008.

[28] I.C. Wong and B.L. Evans. Optimal Downlink OFDMA Resource Allocation With Linear Complexity to Maximize Ergodic Rates. *IEEE Trans. on Wireless Communications*, 7(3), Mar. 2008.

[29] B. Baynat, G. Nogueira, M. Maqbool, and M. Coupechoux. An Efficient Analytical Model for the Dimensioning of WiMAX Networks. In *Proc. of IFIP/TC6 Networking*, May 2009.

[30] C.-Y. Chang, C.-T. Chang, M.-H. Li, and C.-H. Chang. A Novel Relay Placement Mechanism for Capacity Enhancement in IEEE 802.16j WiMAX Networks. In *Proc. of IEEE Int. Conf. on Communications (ICC)*, June 2009.

[31] S. Doirieux, B. Baynat, M. Maqbool, and M. Coupechoux. An Analytical Model for WiMAX Networks with Multiple Traffic Profiles and Throttling Policy. In *Proc. of International Symposium on Modeling and Optimization in Mobile, Ad Hoc, and Wireless Networks (WiOpt)*, June 2009.

[32] R. Giulianoand and F. Mazzenga. Dimensioning of OFDM/OFDMA based Cellular Networks using Exponential Effective SINR. *IEEE Trans. on Vehicular Technology*, 58(8), Oct. 2009.

[33] J. Leinonen, J. Hamalainen, and M. Juntti. Performance Analysis of Downlink OFDMA Resource Allocation with Limited Feedback. *IEEE Trans. on Wireless Communications*, 8(6), June 2009.

[34] H.-C. Lu and W. Liao. Joint Base Station and Relay Station Placement for IEEE 802.16j Networks. In *Proc. of IEEE Global Conf. on Communications (Globecom)*, Nov. 2009.

[35] M. Maqbool, M. Coupechoux, and P. Godlewski. A Semi-analytical Method to Model Effective SINR Spatial Distribution in WiMAX Networks. In *Proc. of IEEE Sarnoff Symposium*, Mar. 2009.

[36] M. Maqbool, M. Coupechoux, and Ph. Godlewski. Reuse 1 in WiMAX Networks with Beamforming. In *Proc. of Wireless World Research Forum (WWRF22)*, May 2009.

[37] M. Maqbool, M. Coupechoux, Ph. Godlewski, S. Doirieux, B. Baynat, and V. Capdevielle. Dimensioning Methodology for OFDMA Networks. In *Proc. of Wireless World Research Forum (WWRF22)*, May 2009.

[38] C. Seol and K. Cheun. A Statistical Inter-Cell Interference Model for Downlink Cellular OFDMA Networks Under Log-Normal Shadowing and Multipath Rayleigh Fading. *IEEE Trans. on Communications*, 57(10), Oct. 2009.

[39] S. Doirieux, B. Baynat, M. Maqbool, and M. Coupechoux. An Efficient Analytical Model for the Dimensioning of WiMAX Networks Supporting Multi-Profile Best Effort Traffic. *Elsevier Computer Communications*, 33(10):1162–1179, June 2010.

[40] M. Maqbool, Ph. Godlewski, M. Coupechoux, and J.-M. Kélif. Analytical Performance Evaluation of Various Frequency Reuse and Scheduling Schemes in Cellular OFDMA Networks. *Performance Evaluation*, 67(4):318–337, April 2010.

[41] M. Minelli, M. Coupechoux, and J.-M. Kélif. Average SIR Estimation in Cellular Networks with Best Server Policy. In *Proc. of IFIP Wireless Days*, Oct. 2010.

[42] V. M. Nguyen and F. Baccelli. A Stochastic Geometry Model for the Best Signal Quality in a Wireless Network. In *Proc. of IEEE International Symposium on Modeling and Optimization in Mobile, Ad Hoc and Wireless Networks (WiOpt)*, May 2010.

[43] L.-C. Wang and W.-C. Li. Outage Performance Analysis for Fractional Frequency Reused TDD-OFDMA Systems with Asymmetric Traffics. In *Proc. of IEEE International Symposium on Information Theory and its Applications (ISITA)*, Oct. 2010.

[44] D. Yang, X. Fang, G. Xue, and J. Tang. Relay Station Placement for Cooperative Communications in WiMAX Networks. In *Proc. of IEEE Global Conf. on Communications (Globecom)*, Dec. 2010.

[45] M. Coupechoux and J.-M. Kélif. How to Set the Fractional Power Control Compensation Factor in LTE ? In *Proc. of IEEE Sarnoff Symposium*, May 2011.

[46] M. Minelli, M. Coupechoux, J.-M. Kélif, M. Ma, and Ph. Godlewski. Relays-Enhanced LTE-Advanced Networks Performance Studies. In *Proc. of IEEE Sarnoff Symposium*, May 2011.

[47] M. H. Islam, Z. Dziong, K. Sohraby, M. F. Daneshmand, and R. Jana. Capacity-Optimal Relay and Base Station Placement in Wireless Networks. In *Proc. of IEEE Int. Conf. on Information Networking (ICOIN)*, Feb. 2012.

[48] J.-M. Kélif, M. Coupechoux, and Ph. Godlewski. On the Dimensioning of Cellular OFDMA Networks. *Elsevier Physical Communication*, 5(1):10–21, Mar. 2012.

[49] S. Khakurel, M. Mehta, and A. Karandikar. Optimal Relay Placement for Coverage Extension in LTE-A Cellular Systems. In *Proc. of IEEE National Conf. on Communications (NCC)*, Feb. 2012.

[50] M. Minelli, M. Coupechoux, J.-M. Kélif, M. Ma, and Ph. Godlewski. SIR Estimation in Hexagonal Cellular Networks with Best Server Policy. *Wireless Personnal Communications*, 69(1):133–152, Mar. 2012.

[51] A. Bou Saleh, O. Bulakci, J. Hämäläinen, S. Redana, and B. Raaf. Analysis of the Impact of site Planning on the Performance of Relay Deployments. *IEEE Trans. on Vehicular Technology*, 61(7):3139–3150, Sept. 2012.

[52] K. Sambale and B. Walke. Decode-and-Forward Relay Placement for Maximum Cell Spectral Efficiency. In *Proc. of IEEE European Wireless*, Apr. 2012.

[53] W. Guo and T. O'Farrell. Relay Deployment in Cellular Networks: Planning and Optimization. *IEEE Journal on Selected Areas in Communications*, 2013. to appear.

[54] S. Wang, W. Zhao, and C. Wang. Approximation Algorithms for Cellular Networks Planning with Relay Nodes. In *Proc. of IEEE Wireless Communications and Networking Conf. (WCNC)*, Apr. 2013.

[55] M. Minelli, M. Ma, M. Coupechoux, J.-M. Kélif, M. Sigelle, and Ph. Godlewski. Optimal Relay Placement in Cellular Networks. *IEEE Trans. on Wireless Communications*, 2014. to appear.

[56] B. Blaszczyszyn and M. Karray. Quality of Service in Wireless Cellular Networks Subject to Log-Normal Shadowing. *IEEE Trans. on Communications*, to appear.

5 MIMO NETWORKS

5.1 Introduction

Multiple antenna systems have aroused many research considerations in recent years. The exploitation of the spatial dimension yielded through the use of multiple antennas at the transmitter and/or the receiver indeed permits to increase capacity [2, 4] and to improve reliability [42]. The originality of our work relies in the fact that we studied these systems in a multi-cellular context, whereas existing literature mainly focuses on point-to-point communications. This means that inter-cell interference is often neglected although it has a negative impact on the effectiveness of MIMO schemes.

5.2 Related Work

Our work in this domain is related to single user MIMO, multi-user MIMO, multi-cell cooperation and antenna selection.

Among single user MIMO schemes, OSTBC (Orthogonal STBC) [3] have been proposed to provide a reliability improvement through the diversity gain. Among the proposed codes, the Alamouti [1] scheme has attracted much attention thanks to its simple implementation and decoding. There are many papers that have studied the Alamouti code for a point-to-point communication in a single cell: in terms of outage capacity [17], of bit error rate [6], in presence of LOS (Line-Of-Sight) or NLOS (Non Line-Of-Sight) propagation, with a single receive antenna or two receive antennas [15], in an uplink multiuser context [18], etc. In [27], the authors showed that, in a single cell multiuser system, the Alamouti transmission approach combined with the MRC receiver provides high system throughputs, when there is a big unbalance in users channels gains. In [36], an analytical study of Almouti-MRC systems was derived in a single cell context. A closed form expression of the BER (Bit Error Rate) was proposed. Some papers have conducted MIMO Alamouti systems performance evaluations considering multicell interference. In [14], authors rely on Monte Carlo simulations, whereas in our contributions we propose an analytical study. In [12] and [20], authors mainly focus their investigation on a scenario, where interferers are received with equal average powers. An approximation of the SINR distribution is given for only two interferers received with unequal average powers. In our contributions, we analyze the performance of the full transmit diversity Alamouti scheme in a multi-cellular system with an MRC receiver. We consider a channel model taking into account Rayleigh fading, shadowing and path-loss. We derive an expression of the SINR cumulative distribution function or equivalently the outage probability for a $2 \times N$ multi-cellular Alamouti system with an MRC receiver.

Turning to multi-user MIMO, we have then studied the ZFBF precoding scheme. This technique is interesting because of the ease of implementation and because it was shown that for a MIMO broadcast channel and using an adequate user selection algorithm, the ZF (Zero Forcing) precoding approaches the performance of the DPC for a large number of users in the cell [11, 21]. We have studied the performance of this scheme in a multicellular context in terms of outage probability. In the literature, the ZF performance has been studied in a single cell context (see e.g. [13, 16]) without considering multicell interference and for a Rayleigh channel except in [26], where an asymptotic analysis of linear precoding techniques (ZF and MMSE) was conducted for small cells multiuser multicellular systems. It was shown that the inter-cell interference affects enormously the system performance. In our work, we have proposed an analytical study of the performance of the ZF precoding in a multiuser multicellular system.

As a third example of MIMO cellular network, we have studied the JP-CoMP transmission [28]. The JP-CoMP was deeply studied in the literature. In [22], a measurement study shows that multicell cooperation attains larger mean capacity than an isolated cell when considering a sufficiently high capacity and a low latency backbone. In [37], a field trial has been performed to confirm the throughput enhancement introduced by JP-CoMP strategy. In [9, 10], a numerical study of different joint processing schemes show the potential of this technique to enhance the overall system performance. In [35], the performance of the femtocell coordination strategy has been studied for the ZF and the MRT schemes. Two power allocation algorithms are proposed and compared. In [9, 22, 35, 37], authors performed simulation, measurement or field study but no theoretical studies were conducted. In [33], an analytical expression of the capacity outage probability was derived for an open-loop Alamouti-like CoMP downlink transmission in Rayleigh fading. The proposed SINR expression can only be achieved when using a distributed Alamouti for two cooperating BSs. In [34], an analytical study of a multicell multi-antenna cooperative MRT/MRC scheme was conducted. An analytical expression of the PDF of the SIR was derived considering path-loss, shadowing and Rayleigh fading. However, the authors resorted to many assumptions: a cell-edge user served in cooperation is at equal distances from the cooperative BSs, a Gamma distributed shadowing and a Poisson spatial distribution of interfering transmitters. Furthermore, there is a significant difference between simulation and theoretical results. Our main contribution has been to perform an analytical study of a downlink coherent multicell cooperation system using the MRT precoding technique.

Very recently, we have studied AS (Antenna Selection) [7, 8], which is is a popular technique for reducing the hardware costs at the transmitter and/or receiver of a multiple antenna wireless link. The idea is to use a limited number of radio frequency chains while adaptively switching to subsets of a larger number of available antenna elements. AS maintains the same diversity order as a system that uses all the available antenna elements, and only a small loss in data rate is suffered when the receiver uses the best possible subset [8]. AS can be employed at the transmitter, receiver or both ends; our work focuses on receive AS. Several algorithms for AS that assume perfect CSI at the receiver have been proposed earlier [29, and references therein]. However, in practice, it is necessary to estimate CSI, using, for example, a pilot-based training scheme. Imperfect CSI can lead to both inaccurate AS and erroneous decoding of data, increasing the symbol error probability [25].

Quite surprisingly, it has been shown that transmit and receive AS can achieve full diversity order, even in the presence of channel estimation errors [19]. However, most of the past work on AS with imperfect CSI suffers from three drawbacks. First, it assumes that the receiver equally divides the pilots among the available antenna elements during the training phase [23, 25]. However, when the channel is slowly-varying, such an equal allocation is not optimal, as past estimates of the channel and the time-correlation information can be used to re-allot pilots among the antennas in subsequent training periods. Second, link-layer error checks on the received packets provide additional information on the channel, and this is typically not exploited in the literature. Third, a quasi-static block-fading channel is usually assumed [5, 7], which precludes the receiver from fully exploiting the temporal channel correlation. Our work seeks to overcome all these three drawbacks and fully exploit the information available at the receiver in deciding the optimal pilot allocation for channel estimation and AS for data packet reception.

5.3 Contributions

The work presented in this part has been performed in collaboration with Orange Labs (Jean-Marc Kélif) in the framework of the PhD thesis of Dorra Ben Cheikh (co-directed with Ph. Godlewski). The goal of our contributions is to provide easy-to-compute expressions of the outage probability for SISO, MISO (Multiple Input Single Output) and MIMO systems in a multicellular context considering different transmission schemes and different channel models. The very last contribution on antenna selection has been performed in collaboration with Chandra Murthy (Indian Institute of Science, Bangalore) in the framework of the Master thesis of Reuben G. Stephen.

- In order to build a benchmark for MIMO systems, we have first conducted an analysis of the joint impact of path-loss, shadowing and fast fading on SISO cellular networks in [32]. Two analytical methods have been developed to express the outage probability. The first one based on the Fenton-Wilkinson approach (denoted FWBM for Fenton-Wilkinson Based Method), approximates a sum of log-normal RVs by a log-normal RV and approximates fast fading coefficients in interference terms by their average value. The second one (denoted CLCFM for Central Limit Theorem for Causal Functions Method) is based on the central limit theorem for causal functions. It allows to approximate a sum of positive random variables by a Gamma distribution. Each method allows to establish a simple and easily computable outage probability formula, which jointly takes into account path-loss, shadowing and fast fading. We compute the outage probability, for mobile stations located at any distance from their serving BS, by using the fluid model. We validate our approach by comparing all results to extensive Monte Carlo simulations performed in a traditional hexagonal network and we provide the limits of the two methods in terms of system parameters.

- In [24, 39], we have studied the performance of MIMO systems using the Alamouti code at the transmitter side and a MRC at the receiver side (see Section 2.6.2). The channel model includes path-loss, shadowing and fast fading and the system is considered to be interference limited. If the shadowing can be considered as sufficiently slow, closed form expressions of the outage probability can be derived. For a log-normally distributed shadowing, we derive easily computable approximations of the outage probability. Again, we use the fluid model approach to provide simpler outage probability expressions depending only on the distance between the considered user and its serving base station. Then, in [30], we have shown how the above results could be used to derive the user performance in terms of session throughput in a dynamic environment modeled as a processor sharing queue (see Section 2.8.1).

- In [31], we have proposed an analytical expression of the outage probability of the zero forcing precoding technique in a multicellular multiuser context (MU-MIMO), see Section 2.6.3. The channel model includes path-loss shadowing and Rayleigh flat fading. Two cases are examined, the first one considers a slowly varying log-normal shadowing compared to the rapid fluctuation of the fast fading. In this case, a closed form expression of the outage probability is derived. In the second case, we consider a log-normal shadowing and we propose an easily computable integral form expression of the outage probability.

- In [38], we have studied the performance of a multiple antenna cooperative multicellular system in terms of outage probability. We have considered the joint processing multiple antenna CoMP using the MRT technique (see Section 2.6.4). It is a diversity transmission scheme that each BS applies separately to the symbol to transmit intended to a user served in cooperation. A closed form expression of the outage probability is derived for Rayleigh flat fading channel model considering path-loss and constant shadowing. Analytical results are validated using Monte Carlo simulation results. In particular, we bring to the light the influence of the number of cooperating BSs and the number of antennas of each BS.

- Recently, we have studied in [40, 41] AS for packet reception at a receiver equipped with multiple antenna elements but only a single radio frequency chain. The receiver makes its AS decisions based on noisy channel estimates obtained from the training symbols (pilots). The time-correlation of the wireless channel and the results of the link-layer error checks upon data packet reception provide additional information that can be exploited for AS. This information can also be used to optimally distribute pilots among the antenna elements, so that packet loss due to selection errors is minimized. The task of the receiver, then, is to sequentially select (a) the pilot symbol allocation for channel estimation on each of the receive antennas and (b) the antenna to be used for data packet reception. The goal is to maximize the expected throughput, based on the history of allocation and selection decisions, and the corresponding noisy channel estimates and error check observations. This joint problem of pilot allocation and AS is solved as a POMDP (Partially Observable Markov Decision Process) and the solutions yield the optimal policies that maximize the long-term expected throughput. The performance of the POMDP solution is compared with several other schemes and it is illustrated that it outperforms the others.

5.4 Conclusion

In this section, we have shown our contributions in the field of MIMO cellular networks. We have considered the Alamouti scheme, the zero forcing precoding technique for MU-MIMO and a CoMP technique based on MRT. All studies take into account the inter-cell interference and are compared to a classical SISO system. Our studies make a intensive use of the fluid model and of the central limit theorem for causal functions and provide simple formulas for the outage probability of the SINR. Recent studies adopt a different approach and consider the POMDP framework for the design of a pilot allocation and antenna selection scheme when there is a single RF chain at the receiver. Although there are already some contributions in the literature, the relationship between CoMP techniques and traffic still remains to be studied. CoMP indeed consumes radio resources in cooperating BSs so that its advantage turns to be a drawback when the traffic is high. So, when activating CoMP and for which mobile users in an optimal manner is still an open question.

Bibliography

[1] S. M. Alamouti. A Simple Transmit Diversity Technique for Wireless Communications. *IEEE Journal on Selected Areas in Communications*, 16(8):1451–1458, Oct. 1998.

[2] G. J. Foschini and M. J. Gans. On Limits of Wireless Communications in a Fading Environment when using Multiple Antennas. *Wireless Personal Communications*, 6(3):311–335, Mar. 1998.

[3] V. Tarokh, H. Jafarkhani, and A. R. Calderbank. Space-Time Block Codes from Orthogonal Designs. *IEEE Trans. on Information Theory*, 45(5):1456–1467, Jul. 1999.

[4] E. Telatar. Capacity of Multi-antenna Gaussian Channels. *European Transactions on Telecommunications*, 10(6):585–595, 1999.

[5] D. Gore and A. Paulraj. Statistical MIMO Antenna Sub-Set Selection with Space-Time Coding. In *Proc. of IEEE International Conference on Communications (ICC)*, Apr. 2002.

[6] Z. Chen, J. Yuan, B. Vucetic, and Z. Zhou. Performance of Alamouti Scheme with Transmit Antenna Selection. *Electronic Letters*, 39(23):1666–1668, Nov. 2003.

[7] A. Gorokhov, D. Gore, and A. Paulraj. Receive Antenna Selection for MIMO Flat-Fading Channels: Theory and Algorithms. *IEEE Trans. on Information Theory*, 49(10):2687–2696, Oct. 2003.

[8] A.F. Molisch and M.Z. Win. MIMO Systems with Antenna Selection. *IEEE Microwave Magazine*, 5(1):46–56, Mar. 2004.

[9] H. Zhang and H. Dai. Cochannel Interference Mitigation and Cooperative Processing in Downlink Multicell Multiuser MIMO Networks. *EURASIP Journal on Wireless Communications and Networking*, 2004(2):222–235, 2004.

[10] H. Zhang, H. Dai, and Q. Zhou. Base Station Cooperation for Multiuser MIMO: Joint Transmission and BS Selection. In *Proc. of Conference on Information Sciences and Systems (CISS)*, Mar. 2004.

[11] T. Yoo and A. Goldsmith. On the Optimality of Multiantenna Broadcast Scheduling Using Zero-Forcing Beamforming. *IEEE Journal on Selected Areas in Communications*, 24(3):528–541, Mar. 2006.

[12] W. Choi, N. Himayat, S. Talwar, and M. Ho. The Effects of Co-Channel Interference on Spatial Diversity Techniques. In *Proc. of IEEE Wireless Communications and Networking Conference (WCNC)*, Mar. 2007.

[13] W. Jing, L. Zhanli, W. Yan, and Y. Xiaohu. Performance of the Zero Forcing Precoding MIMO Broadcast Systems with Channel Estimation Errors. *Journal of Electronics*, 24(4):490–495, 2007.

[14] M. Rahman, E. de Carvalho, and R. Prasad. Impact of MIMO Co-Channel Interference. In *Proc. of IEEE Personal, Indoor, Mobile Radio Communications Conference (PIMRC)*, Sept. 2007.

[15] C. Schnurr, S. Stanczak, and A. Sezgin. The Impact of Different MIMO Strategies on the Network Outage Performance. *International ITG/IEEE Workshop on Smart Antennas*, Feb. 2007.

[16] X. Shao, J. Yuan, and Y. Shao. Error Performance Analysis of Linear Zero Forcing and MMSE Precoders for MIMO Broadcast Channels. *IET Communications*, 1(5):1067–1074, 2007.

[17] L. Yang. Outage Performance of OSTBC in Double Scattering MIMO Channels. *Wireless Personal Communications*, 45(2):225–230, Oct. 2007.

[18] B. K. Chalise and A. Czylwik. Exact Outage Probability Analysis for a Multiuser MIMO Wireless Communication System With Space-Time Block Coding. *IEEE Trans. on Vehicular Technology*, 57(3):1502–1512, May 2008.

[19] T. Gucluoglu and E. Panayirci. Performance of Transmit and Receive Antenna Selection in the Presence of Channel Estimation Errors. *IEEE Communications Letters*, 12(5):371–373, May 2008.

[20] Y. Li, L. Cimini, and N. Himayat. Performance Analysis of Space Time Block Coding with Co-Channel MIMO Interferers. In *Proc. of IEEE Global Communications Conference (GLOBECOM)*, Nov. 2008.

[21] Y. Xu and T. Le-Nogc. Optimal Power Allocation with Channel Inversion Regularization-based Precoding for MIMO Broadcast Channels. *EURASIP Journal on Advances in Signal Processing*, 2008(Article ID 587243), 2008.

[22] V. Jungnickel et al. Capacity Measurements in a Cooperative MIMO Network. *IEEE Trans. on Vehicular Technology*, 58(5):2392–2405, Jun. 2009.

[23] TR Ramya and S. Bhashyam. Using Delayed Feedback for Antenna Selection in MIMO Systems. *IEEE Trans. on Wireless Communications*, 8(12):6059–6067, Dec. 2009.

[24] D. Ben Cheikh, J.-M. Kélif, M. Coupechoux, and Ph. Godlewski. Outage Probability in a Multi-Cellular Network Using Alamouti Scheme. In *Proc. of IEEE Sarnoff Symposium*, Apr. 2010.

[25] V. Kristem, N.B. Mehta, and A.F. Molisch. Optimal Receive Antenna Selection in Time-Varying Fading Channels with Practical Training Constraints. *IEEE Trans. on Communications*, 58(7):2023–2034, July 2010.

[26] S. Ramanath, M. Debbah, E. Altman, and V. Kumar. Asymptotic Analysis of Precoded Small Cell Networks. *Proc. of IEEE International Conference on Computer Communications (INFOCOM)*, Mar. 2010.

[27] N. Reider and G. Fodor. On Opportunistic Power Control for MIMO-OFDM Systems. In *Proc. of 6th IEEE Broadband Wireless Access (BWA) Workshop*, Miami, FL, USA, Dec. 2010.

[28] M. Sawahashi, Y. Kishiyama, A. Morimoto, D. Nishikawa, and M. Tanno. Coordinated Multipoint Transmission/Reception Technique For LTE-Advanced. *IEEE Wireless Communications*, 17(3):26–34, Jun. 2010.

[29] B.H. Wang, H.T. Hui, and M.S. Leong. Global and Fast Receiver Antenna Selection for MIMO Systems. *IEEE Trans. on Communications*, 58(9):2505–2510, Sept. 2010.

[30] D. Ben Cheikh, J.-M. Kélif, M. Coupechoux, and Ph. Godlewski. Dynamic System Performance of SISO, MISO and MIMO Alamouti Schemes. In *Proc. of IEEE Sarnoff Symposium*, May 2011.

[31] D. Ben Cheikh, J.-M. Kélif, M. Coupechoux, and Ph. Godlewski. Multicellular Zero Forcing Precoding Performance in Rayleigh and Shadow Fading. In *Proc. of IEEE Vehicular Technology Conference (VTC Spring)*, May 2011.

[32] D. Ben Cheikh, J.-M. Kélif, M. Coupechoux, and Ph. Godlewski. SIR Distribution Analysis in Cellular Networks Considering the Joint Impact of Path-loss, Shadowing and Fast Fading. *EURASIP Journal on Wireless Communications and Networking*, 2011(1):137, Oct. 2011.

[33] Virgile Garcia, Nikolai Lebedev, and Jean-Marie Gorce. Capacity Outage Probability for Multi-Cell Processing under Rayleigh Fading. *IEEE Communication Letters*, 15(8), Aug. 2011.

[34] X. Ge, K. Huang, C-X. Wang, X. Hong, and X. Yang. Capacity Analysis of a Multi-Cell Multi-Antenna Cooperative Cellular Network with Co-Channel Interference. *IEEE Trans. on Wireless Communications*, 10(10):3298–3309, Oct. 2011.

[35] S. Ben Halima, M. Helard, and D. T. Phan Huy. New Coordination and Resource Allocation Schemes for Uniform Rate in Femtocell Networks. In *Proc. of IEEE Vehicular Technology Conference (VTC)*, May 2011.

[36] F. J. Lopez-Martinez, E. Martos-Naya, K.-K. Wong, and J. T. Entrambasaguas. Closed-Form BER Analysis of Alamouti-MRC Systems with ICSI in Ricean Fading Channels. *IEEE Communications Letters*, 15(1):46–48, Jan. 2011.

[37] P. Marsch, M. Grieger, and G. Fettweis. Large Scale Field Trial Results on Different Uplink Coordinated Multi-Point (CoMP) Concepts in an Urban Environment. In *Proc. of IEEE Wireless Communications and Networking Conference (WCNC)*, Mar. 2011.

[38] D. Ben Cheikh, J.-M. Kélif, M. Coupechoux, and Ph. Godlewski. Analytical Joint Processing Multi-Point Cooperation Performance in Rayleigh Fading. *IEEE Wireless Communications Letters*, 1(4):272–275, Aug. 2012.

[39] D. Ben Cheikh, J.-M. Kélif, M. Coupechoux, and Ph. Godlewski. Multi-cellular Alamouti Scheme Performance in Rayleigh and Shadow Fading. *Springer Annals of telecommunications*, 68(5-6):345–358, June 2012.

[40] R. G. Stephen, C. R. Murthy, and M. Coupechoux. A Markov Decision Theoretic Approach to Pilot Allocation and Receive Antenna Selection. *IEEE Trans. on Wireless Communications*, 2013. to appear.

[41] R. G. Stephen, C. R. Murthy, and M. Coupechoux. Pilot Allocation and Receive Antenna Selection: A Markov Decision Theoretic Approach. In *Proc. of IEEE International Conference on Communications (ICC)*, June 2013.

[42] D. Tse and P. Viswanath. *Fundamentals of Wireless Communications*. Cambridge University Press, 2006.

6 DYNAMIC SPECTRUM ACCESS

6.1 Introduction

Radio resource management algorithms are the subject of an intense research in the wireless communication scientific community. This effort is motivated by several factors:

1. Several experimental studies have concluded that the radio spectrum is both congested and under-utilized (see e.g. [7, 15], [9] gives an illustration of the current spectrum allocation in the U.S.). The frequency spectrum is indeed not utilized homogeneously: depending on the day time, on the geographical location, some spectrum bands are overloaded (e.g. the ISM band heavily used by WiFi in dense urban areas) while others are almost free of transmissions.

2. SDR (Software Defined Radio), which consists of implementing in software most of the components of a radio communication system, has recently done considerable progress [47]. With SDR, RF (Radio Frequency) front end and analog to digital converter are the only components to be implemented in hardware. This gives potentially a very high flexibility to radio equipments, which could be able ultimately to access any frequency band and to reconfigure its radio protocols in a very flexible way.

3. As a consequence of the above two points, the notion of Cognitive Radio has emerged (introduced by Mitola in 1999 [6]). CR generally refers to a radio system that has the ability to sense its RF environment and modify its spectrum usage based on what it detects [25]. We can see that CR builds upon SDR cognition functions such as spectrum sensing, environment analyses, and decision making.

4. Todays wireless systems are characterized by a high heterogeneity due to the superposition of several communication standards (WiFi, HSPA, LTE, etc), and due to the equipments variety (laptops, tablets, smart phones on the terminal side, macro BS, small cells, femto cells, relays, etc. on the network side). The need arises to jointly manage this diversity in a centralized way when possible, or with distributed algorithms. In a near future, a sharing of the spectrum resource across technologies and possibly across operators is expected.

5. In cellular systems, interference appears as a central bottleneck for the furniture of high data rates and a homogeneous user quality of experience (whatever its location and along its movements). This leads to the development of inter-cell interference coordination or base station cooperation techniques such as the ones described in the previous chapters.

These main factors motivate the design of radio resource management schemes based on flexible radio equipments, taking into account the network heterogeneity and aiming at better utilizing the spectrum and limiting the impact of interference.

6.2 Related Work

6.2.1 *Spectrum Management Models*

There are several spectrum management classifications in the literature. The one proposed by Buddhikot in [16] has the merit of simplicity. We propose in figure 6.1 a slight variation of it. Models can be classified in four main classes:

- Command and control: In this model the regulator assigns the spectrum bands while applying restricted rules. The spectrum owner has no right to resell (or rent) the right of using the spectrum (or a part of it) to another player. The spectrum owner has no right to change the service, for which he originally obtained the license. In addition, the license duration is almost eternal. Examples of bands managed under this model are those bands used by government, military, and radio astronomy operations.

- Exclusive use of the spectrum: In this model, a spectrum band is exclusively used by a single operator. This model is divided into two sub-models. The long term sharing is the current model in use in todays cellular networks. Each operator manages its own spectrum (licensed for several years) thanks to interference management techniques, dynamic spectrum allocation and has to deal with heterogeneous networks. There is no interactions between operators. In a dynamic sharing mode of operation, spectrum can be rent on a secondary market, operators can dynamically access a pool of frequency bands.

- Primary and secondary usage: In this context, the spectrum band is owned by a PU (Primary User), but the band can be opportunistically used by SU (Secondary User) with minimum impact on the primary user. In the ideal case, the primary user is not even aware of the secondary user transmissions. According to the strategy used by the secondary user, sharing is called *spectrum interweave*, *spectrum underlay* or *spectrum overlay* [41]. In the former case, access is opportunistic (in time or space) and is based on the detection of *white spaces*. This approach can be called "opportunistic spectrum access (OSA)", "listen-before-talk" (in relation with the type of MAC protocol that can be used), or simply "cognitive radio". In case of spectrum underlay, secondary users use the same radio resources than the primary user but try to control the amount of interference received at the primary user receivers. In the third model, the secondary user is aware of the primary user message and performs interference cancellation at the receivers. These three sub-models assume an increasing amount of known information at the secondary user.

- Commons: Here, no entity has exclusive license to the spectrum band. The band is a public resource shared by everyone with minimum regulation (i.e. ISM and U-NII bands).

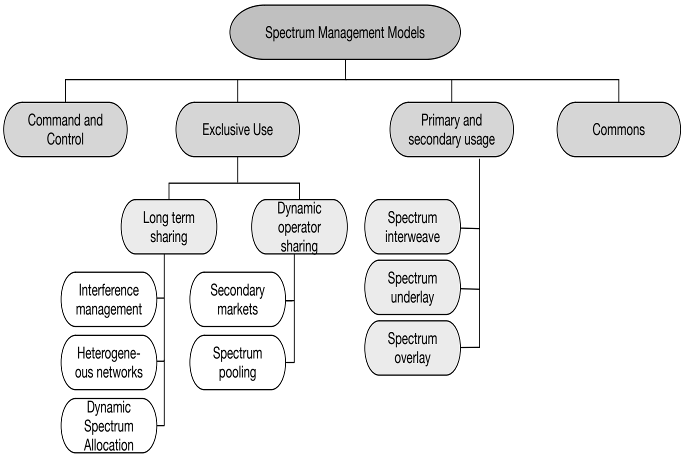

Figure 6.1: Spectrum management models.

6.2.2 *Dynamic Operator Sharing*

In the framework of dynamic operator sharing, we have considered a generic framework for mobile operators able to access to a pool of frequency bands or CAB (Coordinated Access Band). This framework has been introduced by M. Buddhikot et al. in [12]. In the proposed architecture, the access to the spectrum, in a specific region, is controlled by a central entity called spectrum broker or regulator. The spectrum controlled by the regulator is called the CAB and divided in chunks that can be dynamically allocated to operators. Each operator can in turn dynamically allocate these frequency bands to different RAN (Radio Access Network). The same principle has been adopted in the research project DRIVE [5], where spectrum is supposed to be shared between cellular and broadcast services. This model is also consistent with the first use case defined by the IEEE P1900.4 working group on dynamic spectrum management [22, 23]. There are also several papers that are dealing with DSA for cellular networks. Apart from the seminal work [12], we can cite the genetic algorithm proposed by [26], a MAC protocol for SUs in a GSM network [13], or approaches based on pricing mechanisms [18, 24]. The originality of our works lies in the dynamic traffic model we have considered, in the fact that we took into account the effect of interferences on the user quality of service and in our conclusions that showed how one can benefit from the time and spatial variations of the traffic demand to better share the spectrum between two technologies or operator networks.

6.2.3 *Primary and Secondary Spectrum Usage*

6.2.3.1 *Auction Mechanism*

We have also tackled resource allocation problems related to the primary and secondary usage of the spectrum. Specifically, we have proposed distributed mechanisms for the radio resource sharing between SUs. We have first focused on auction mechanisms controlled by the PU. Due to their perceived fairness and allocation efficiency [58], auctions are indeed among the best-known market-based mechanisms to allocate spectrum [14, 17, 27, 36, 37, 46]. In most proposed auctions, the spectrum resource is treated as goods in traditional auctions studied by economists, i.e., one licensed band (or a collection of multiple bands) is awarded to one SU. However, spectrum auction differs from conventional auctions in that it has to address radio interference. Spectrum auction is essentially a problem of interference-constrained resource allocation. Only a few papers have discussed spectrum auctions under interference constraint, among which [17] and [36] studied conflict-free spectrum allocation with high spectrum efficiency. [14] developed an auction-based spectrum sharing framework to allow a single spectrum manager to share its spectrum with a group of users, subject to the interference temperature constraint at the measurement point, a requirement proposed by FCC in [8]. Based on the same model as [14], our work conducts an in-depth analysis on the spectrum auction for multiple PUs to allocate their spectrum to multiple SUs efficiently and fairly. We also investigated the spectrum auction with free spectrum bands and developed a distributed adaptive algorithm based on no-regret learning to converge to a correlated equilibrium of the auction game.

6.2.3.2 *Multi-user MAB*

We have then focused on the generic model of cognitive networks consisting of several frequency channels, each characterized by a channel availability probability determined by the activity of PUs on the channel. In such model, a challenging problem for SUs that opportunistically access the unused spectrum of PUs is to learn the channel availabilities and coordinate with other SUs in order to choose, in a distributed way, the best channels for transmissions without collision. The model (with single SU) is closely related to the MAB (Multi-Armed Bandit) problem [19], a classical reinforcement learning problem where a SU should strike a balance between exploring the environment to find profitable channels and exploiting the best one as often as possible. Gittins developed an index policy in [3] that consists of selecting the arm with the highest index termed as Gittins index. This policy is shown to be optimal in the most general case. Lai and Robbins [1] and then Agrawal [4] studied the MAB problem by proposing policies based on the *upper confidence bounds* with logarithmic regret. Agrawal [2] proposed a block and frame based policy that achieves logarithmic regret for the MAB problem with switching cost, a variant of the original MAB problem. A detailed survey on the single player MAB problem with switching cost can be found in [11].

Despite of the similarity to the MAB problem, the spectrum access problem in cognitive radio networks has several specificities that make it especially challenging to tackle. One major specialty lies in the fact of multiple SUs that can cause collisions if they simultaneously access the same channel. Some recent works have investigated this issue, among which Anandkumar *et al.* proposed two algorithms with logarithmic regret, where the number of SUs is known [38] or unknown and estimated by each SU [39], Liu and Zhao developed a time-division fare share (TDFS) algorithm with convergence and logarithmic regret [32]. In our work, we have investigated the channel access problem by taking into account the channel switching cost due to the change from one frequency band to another. In this approach, the number of primary channels is supposed to be greater than the number of SUs and two SUs accessing at the same time the same channel are in collision.

6.2.3.3 *Imitation*

We have then considered another model, where the number of SUs is large with respect to the number of channels. Time is divided in blocks at the boundary of which SUs decide to change or keep unchanged their strategy (i.e. channel). If several SUs access the same channel during a block, they share the channel according to some MAC protocol. In order to study such a problem, we relied on mechanisms based on imitation (simple and double) and population games.

Due to the success of applying evolutionary [10] and population game theories [60] in the study of biological and economic problems [60], a handful of recent studies have applied these tools to study resource allocation problems arisen from wired and wireless networks (see e.g. [30, 51]), among which Shakkottai *et al.* addressed the problem of non-cooperative multi-homing of users to WLANs access points by modeling it as a population game [20]. Authors however focus on the system dynamics rather than on the distributed algorithms as we do in our work. Niyato *et al.* studied the dynamics of network selection in a heterogeneous wireless network using the theory of evolutionary game [35]. The proposed algorithm leading to the replicator dynamics is however based on a centralized controller able to broadcast to all users the average payoff. Our algorithms are on the contrary fully distributed. Coucheney *et al.* studied the user-network association problem in wireless networks with multi-technology and proposed an algorithm based on trial and error mechanisms to achieve the fair and efficient solution [30].

Several theoretical works focus on imitation dynamics. Ackermann *et al.* investigated the concurrent imitation dynamics in the context of finite population symmetric congestion games by focusing on the convergence properties [28]. Berenbrik *et al.* applied the Proportional Imitation Rule to load-balance system resources by focusing on the convergence speed [48]. Ganesh *et al.* applied the Imitate If Better rule[1] (see [29] for a review on imitation rules) in order to load-balance the service rate of parallel server systems [42]. Contrary to our work, it is assumed in [48] and [42] that a user is able to observe the load of any another resource before taking its decision to switch to this resource.

As it is supposed to model human behavior, imitation is mostly studied in economics. In the context of CRN (Cognitive Radio Networks), specific protocol or hardware constraints may however arise so that imitation dynamics are modified, as we show it in our papers. Two very recent works in the context of CRN are [59] and [52], which have the same goals as ours. In [59], authors propose a distributed learning algorithm for spectrum access. User decisions are based on their accumulated experience and they are using a mixed strategy. In [52], imitation is also used for distributed spectrum access. However, the proposed scheme relies on the existence of a common control channel for the sampling procedure. Double imitation is moreover not considered.

1 Imitate If Better (IIB) is a rule consisting in picking a player and migrating to its strategy if the latter has yielded a higher payoff than the achieved one. IIB is called Random Local Search in [42].

6.3 Contributions

The work presented in this section has been done in the context of the Ph.D. thesis of Hany Kamal (co-directed with Ph. Godlewski) within the SYSTEMATIC URC collaborative project, in the context of the Ph.D. thesis of Stefano Iellamo (co-directed with Ph. Godlewski and L. Chen from University of Paris XI/Orsay), or in collaboration with Orange Labs (Jean-Marc Kelif). Our contributions are in the design of radio resource allocation algorithms either of cellular operators (dynamic spectrum allocation, joint radio resource management) or for cognitive radio networks (based on auctions, MAB techniques or imitation).

- In a series of papers [31, 33, 34, 45], we have proposed DSA algorithms for operators sharing in a dynamic way a common access band, i.e., a pool of radio resources. Our first approach is based on SMDP (Semi-Markov Decision Process). We take into account the spectrum price, and maximizing the operator revenue is our main concern. We then propose a heuristic algorithm and a Q-learning based scheme that overcome the limitations of the optimal policies that necessitate a full knowledge of the model to be effective. In order to show how we can take advantage of the spatial heterogeneity of the traffic, we proposed a distributed Tabu Search based DSA algorithm to be run on clusters of cells [43, 44, 55].
- In [21], we have proposed joint radio resource management algorithms for an operator having deployed two co-localized RAT (Radio Access Technology). In this work, we address this issue by focusing on small cells (typically femto to micro) where two RATs are co-localized, i.e., there is a common access point and geographical cells are overlapping. We concentrate on algorithms fully controlled by the network that take into account not only the current load of each RAT but also the spatial distribution of the MSs in the cell. Numerical applications show that the optimal policy is not an obvious one and can clearly outperform an a priori common sense algorithm.
- In [40, 50], we have proposed auction mechanisms for the primary/secondary usage of the spectrum paradigm. While existing algorithms mainly focus on single-PU scenarios, we extend the approach to multiple PUs. As a distinctive feature of the proposed auction framework, the SU strategy (bid) is two-dimensional and non-continuous, leading to a competition scenario with more complex interactions among players and requiring an original study of the resulting equilibrium. We also investigated the spectrum auction with free spectrum bands and developed a distributed adaptive algorithm based on no-regret learning to converge to a correlated equilibrium of the auction game. To the best of our knowledge, our work is the first to adapt the auction framework to address the spectrum sharing problem in heterogeneous environments with both licensed and free bands.
- In a series of papers [49, 53, 54, 56], we have proposed distributed learning mechanisms when several SUs want to access a set of PU channels with unknown availabilities (multi-user MAB type of problems). For the case, where

the number of SUs is small with respect to the number of channels, we investigated the channel switching cost problem due to the change from one frequency band to another [49]. Such channel switching cost is non-negligible in terms of delay (a radio reconfiguration may be needed), packet loss and protocol overhead (since SU transmitter and SU receiver have to coordinate). In such context, it is crucial to design channel access policies reluctant to switch channels unless necessary. This problem has not been systematically addressed in the literature. Through mathematical analysis, we show that the proposed policy achieves logarithmic regret in spite of the channel switching cost. Extensive simulation studies show that the proposed policy outperforms the solutions in the literature.

- We then considered the case, where the number of SUs is large with respect to the number of channels and SUs accessing the same channel share the bandwidth according to some distributed MAC protocol. It is already known that if a SU can imitate any other SU strategy, the resulting evolution of the system is described by a replicator dynamics [54]. In our analysis, we develop imitation-based spectrum access policies, where a SU can only imitate the other SUs operating on the same channel (due to hardware constraints) [53, 56]. More specifically, we propose two spectrum access policies based on the following two imitation rules: the Proportional Imitation (PI) rule where a SU can sample one other SU; the more advanced adjusted proportional imitation rule with double sampling (Double Imitation, DI) where a SU can sample two other SUs. Under both imitation rules, each SU strives to improve its individual payoff by imitating other SUs with higher payoff. A systematic theoretical analysis is presented for both policies on the induced imitation dynamics and the convergence properties of the proposed policies to the NE (Nash Equilibrium). We have recently extended this work to a new protocol that does not require any information exchange between SUs [57]. With this approach, cognitive radios choose their strategy based only on their past experienced payoffs and strategies. We show that our protocol is guaranteed to converge to an equilibrium state within a bounded delay.

6.4 Conclusion

Dynamic spectrum management is a hot research topic. Our contributions in this domain are twofold: first, we considered an inter-operator spectrum sharing scenario, where operators dynamically access to a pool of resources according to their needs; second, we have studied the paradigm of primary and secondary usage of the spectrum in cognitive radio networks. The algorithms proposed in the former case could be practically implemented if the regulation allows spectrum sharing. The cognitive radio scenario is a more prospective approach, where devices are independent, sense and learn from their environment, and share radio resources in a distributed way using learning algorithms. Assumed models are still very simple and there is still work to be done to fill the gap between theory and realistic implementations.

Bibliography

[1] T. L. Lai and H. Robbins. Asymptotically Efficient Adaptive Allocation Rules. *Advances in Applied Prob.*, 6(1):4–22, Mar. 1985.

[2] R. Agrawal, D. Teneketzis, and V. Anantharam. Asymptotically Efficient Adaptive Allocation Rules for the Multiarmed Bandit Problem with Switching. *IEEE Trans. on Automatic Control*, 33(10):899–906, Oct. 1988.

[3] J. C. Gittins. Multi-armed Bandit Allocation Indices. *Wiley-Interscience Series in Systems and Optimization, John Wiley & Sons*, 1989.

[4] R. Agrawal. Sample Mean Based Index Policies with O(logn) Regret for the Multi-Armed Bandit Problem. *Advances in Applied Prob.*, 27(4):1054–1078, Dec. 1995.

[5] IST DRIVE Project. Deliverable D09. Technical report, 1999.

[6] J. Mitola, and G.Q. Maguire. Cognitive Radio: Making Software Radios More Personal. *IEEE Personal Communications*, 6(4):13–18, Aug. 1999.

[7] FCC Spectrum Policy Task Force. Report of the Spectrum Efficiency Working Group. Technical report, FCC, Nov. 2002.

[8] FCC Spectrum Policy Task Force. Report of the Unlicensed Devices and Experimental Licenses Working Group. Technical report, FCC, Nov. 2002.

[9] FCC. United States Frequency Allocations. http://www.ntia.doc.gov/osmhome/allochrt.PDF, 2003.

[10] J. Hofbauer and K. Sigmund. Evolutionary Game Dynamics. *Bull. Amer. Math. Soc.*, 40(4):479–519, Jul. 2003.

[11] T. Jun. A Survey on the Bandit Problem with Switching Costs. *De Economist*, 152(4):513–541, Dec. 2004.

[12] M.M. Buddhikot, P. Kolodzy, S. Miller, K. Ryan, and J. Evans. DIMSUMnet: New Directions in Wireless Networking using Coordinated Dynamic Spectrum. In *Proc. of IEEE Int. Symp. on a World of Wireless Mobile and Multimedia Networks (WoWMoM)*, June 2005.

[13] A. Mishra S. Hershey S. Sankaranarayanan, P. Papadimitratos. A Bandwidth Sharing Approach to Improve Licensed Spectrum Utilization. In *Proc. of IEEE Int. Symp. on New Frontiers in Dynamic Spectrum Access Networks (DySPAN)*, Nov. 2005.

[14] J. Huang, R. Berry, and M. L. Honig. Auction-Based Spectrum Sharing. *Mobile Networks and Applications*, 11(3):405–418, 2006.

[15] M. A. McHenry, P. A. Tenhula, D. McCloskey, D. A. Roberson, and C. S. Hood. Chicago Spectrum Occupancy Measurements and Analysis and a Long-term Studies Proposal. In *Proc. of ICST Int. Workshop on Technology and Policy for Accessing Spectrum (TAPAS)*, Aug. 2006.

[16] M. M. Buddhikot. Understanding Dynamic Spectrum Allocation: Models, Taxonomy and Challenges. *Proc. IEEE Int. Symp. on New Frontiers in Dynamic Spectrum Access Networks (DySPAN)*, Apr. 2007.

[17] S. Gandhi, C. Buragohain, L. Cao, H. Zheng, and S. Suri. A General Framework for Wireless Spectrum Auctions. In *Proc. IEEE Int. Symp. on New Frontiers in Dynamic Spectrum Access Networks (DySPAN)*, 2007.

[18] J. Acharya, and R.D. Yates. A Price Based Dynamic Spectrum Allocation Scheme. *Proc. of the Asilomar Conf. on Signals, Systems and Computers (ACSSC)*, Nov. 2007.

[19] A. Mahajan and D. Teneketzis. Multi-armed Bandit Problems. *Foundations and Applications of Sensor Management, Springer-Verlag*, 2007.

[20] S. Shakkottai, E. Altman, and A. Kumar. Multihoming of Users to Access Points in WLANs: A Population Game Perspective. *IEEE Journal on Selected Areas in Communications*, 25(6):1207–1215, Aug. 2007.

[21] M. Coupechoux, J. M. Kélif, and Ph. Godlewski. SMDP Approach for JRRM Analysis in Heterogeneous Networks. In *Proc. of IEEE European Wireless Conf. (EW)*, June 2008.

[22] S. Buljore et al. IEEE P1900.4 Standard: Reconfiguration of Multi-Radio Systems. *Proc. of IEEE Int. Conf. on Computational Technologies in Electrical and Electronics Engineering (SIBIRCON)*, July 2008.

[23] S. Filin et al. Dynamic Spectrum Assignment and Access Scenarios, System Architecture, Functional Architecture and Procedures for IEEE P1900.4 Management System. *Proc. of IEEE/ICST Int. Conf. on Cognitive Radio Oriented Wireless Networks and Communications (CrownCom)*, May 2008.

[24] L. Vanbien, L. Yuewei, W. Xiaomeng, F. Zhiyong, and Z. Ping. A Cell Based Dynamic Spectrum Management Scheme with Interference Mitigation for Cognitive Networks. *Proc. of IEEE Vehicular Technology Conf. (VTC Spring)*, May 2008.

[25] M. Sherman and A. N. Mody and R. Martinez and C. Rodriguez and R. Reddy. IEEE Standards Supporting Cognitive Radio and Networks, Dynamic Spectrum Access and Coexistence. *IEEE Communications Magazine*, 46(7):72–29, July 2008.

[26] D. Thilakawardana, K. Moessner, and R. Tafazolli. Darwinian Approach for Dynamic Spectrum Allocation in Next Generation Systems. *IET Communications*, 2(6):827 –836, July 2008.

[27] J. Zhu and K. J. R. Liu. Multi-Stage Pricing Game for Collusion-Resistant Dynamic Spectrum Allocation. *IEEE Journal on Selected Areas in Communications*, 26(1):182–191, Jan. 2008.

[28] H. Ackermann, P. Berenbrink, S. Fischer, and M. Hoefer. Concurrent Imitation Dynamics in Congestion Games. In *Proc. ACM Symposium on Principles of Distributed Computing (PODC)*, Jun. 2009.

[29] C. Alos-Ferrer and K. H. Schlag. Imitation and Learning. In *The Handbook of Rational and Social Choice*. Oxford University Press, 2009.

[30] P. Coucheney, C. Toutati, and B. Gaujal. Fair and Efficient User-Network Association Algorithm for Multi-Technology Wireless Networks. In *Proc. IEEE Int. Conf. on Computer Communication (INFOCOM)*, Apr. 2009.

[31] M. Coupechoux, H. Kamal, P. Godlewski, and J.-M. Kelif. Optimal and Heuristic DSA Policies for Cellular Networks with Coordinated Access Band. In *Proc. of IEEE European Wireless Conf. (EW)*, May 2009.

[32] K. Liu and Q. Zhao. Distributed Learning in Multi-Armed Bandit with Multiple Players. *Arxiv 0910.2065*, 2009.

[33] H. Kamal, M. Coupechoux, and Ph. Godlewski. Inter-Operator Spectrum Sharing for Celullar Networks using Game Theory. In *Proc. of IEEE Personal, Indoor and Mobile Radio Communications Symp. (PIMRC)*, Sept. 2009.

[34] H. Kamal, M. Coupechoux, and Ph. Godlewski. Traffic Studies for DSA Policies in a Simple Cellular Context with Packet Services. In *Proc. of IEEE/ICST Int. Conf. on Cognitive Radio Oriented Wireless Networks and Communications (CrownCom)*, June 2009.

[35] D. Niyato and E. Hossain. Dynamics of Network Selection in Heterogeneous Wireless Networks: An Evolutionary Game Approach. *IEEE Transactions on Vehicular Technology*, 58(4):2008–2017, May. 2009.

[36] Y. Wu, B. Wang, K. J. R. Liu, and T. C. Clancy. A Scalable Collusion-Resistant Multi-Winner Cognitive Spectrum Auction Game. *IEEE Transactions on Communications*, 57(12):3805–3816, Dec. 2009.

[37] X. Zhou and H. Zheng. Trust: A General Framework for Truthful Double Spectrum Auctions. In *Proc. IEEE Int. Conf. on Computer Communication (INFOCOM)*, Apr. 2009.

[38] A. Anandkumar and N. Michael and A. Tang and A. Swami. Distributed Algorithms for Learning and Cognitive Medium Access with Logarithmic Regret. *IEEE Journal on Selected Areas in Communications*, 29(4):731–745, Apr. 2010.

[39] A. Anandkumar, N. Michael, and A. Tang. Opportunistic Spectrum Access with Multiple Users: Learning under Competition. In *Proc. IEEE Int. Conf. on Computer Communication (INFOCOM)*, Apr. 2010.

[40] L. Chen, S. Iellamo, M. Coupechoux, and P. Godlewski. An Auction Framework for Spectrum Allocation with Interference Constraint in Cognitive Radio Networks. In *Proc. IEEE Int. Conf. on Computer Communication (INFOCOM)*, Mar. 2010.

[41] N. Devroye. Chapter 11 - Information Theoretical Limits on Cognitive Radio Networks. In *Cognitive Radio Communications and Networks*, pages 307 – 333. Academic Press, Oxford, 2010.

[42] A. Ganesh, S. Lilienthal, D. Manjunath, A. Proutiere, and F. Simatos. Load Balancing via Random Local Search in Closed and Open Systems. In *Proc. ACM SIGMETRICS International Conference on Measurement and Modeling of Computer Systems*, June 2010.

[43] H. Kamal, M. Coupechoux, and P. Godlewski. A Tabu Search DSA Algorithm for Reward Maximization in Cellular Networks. In *Proc. of IEEE Int. Conf. on Wireless and Mobile Computing, Networking and Communications (WiMob)*, Oct. 2010.

[44] H. Kamal, M. Coupechoux, and P. Godlewski. An Efficient Tabu Search DSA Algorithm for Heterogeneous Traffic in Cellular Networks. In *IFIP Wireless Days Conf. (WD)*, Oct. 2010.

[45] H. Kamal, M. Coupechoux, P. Godlewski, and J.-M. Kelif. Optimal, Heuristic and Q-Learning Based DSA Policies for Cellular Networks with Coordinated Access Band. *European Transactions on Telecommunications*, 21(8):694–703, Dec. 2010.

[46] G. S. Kasbekar and S. Sarkar. Spectrum Auction Framework for Access Allocation in Cognitive Radio Networks. *IEEE/ACM Transactions on Networking*, 18(6):1841–1854, Dec. 2010.

[47] O. Anjum, T. Ahonen, F. Garzia, J. Nurmi, C. Brunello, and H. Berg. State of the Art Baseband DSP Platforms for Software Defined Radio: A Survey. *EURASIP Journal on Wireless Communications and Networking*, 2011(5), June 2011.

[48] P. Berenbrik, T. Friedetzky, L.A. Goldberg, and P. Goldberg. Distributed Selfish Load Balancing. In *Proc. of ACM-SIAM Symp. on Discrete Algorithms (SODA)*, Jan. 2011.

[49] L. Chen, S. Iellamo, and M. Coupechoux. Opportunistic Spectrum Access with Channel Switching Cost for Cognitive Radio Networks. In *Proc. of IEEE Int. Conf. on Communications (ICC)*, June 2011.

[50] L. Chen, S. Iellamo, M. Coupechoux, and Ph. Godlewski. Spectrum Auction with Interference Constraint for Cognitive Radio Networks with Multiple Primary and Secondary Users. *Springer Wireless Networks*, 17(5):1355–1371, July 2011.

[51] H. Tembine, E. Altman, R. El-Azouzi, and Y. Hayel. Bio-inspired Delayed Evolutionary Game Dynamics with Networking Applications. *Telecommunication Systems*, 47(1-2):137–152, June 2011.

[52] X. Chen and J. Huang. Imitative Spectrum Access. In *Proc. of IEEE Int. Symp. on Modeling and Optimization in Mobile, Ad Hoc, and Wireless Networks (WiOpt)*, May 2012.

[53] S. Iellamo, L. Chen, and M. Coupechoux. Imitation-based Spectrum Access Policy for CSMA/CA-based Cognitive Radio Networks. In *Proc. of IEEE Wireless Communications and Networking Conference (WCNC)*, Apr. 2012.

[54] S. Iellamo, L. Chen, M. Coupechoux, and A. V. Vasilakos. Imitation-based Spectrum Access Policy for Cognitive Radio Networks. In *Proc. Int. Symp. on Wireless Communication Systems (ISWCS)*, Aug. 2012.

[55] H. Kamal, M. Coupechoux, and Ph. Godlewski. Tabu Search for Dynamic Spectrum Allocation (DSA) in Cellular Networks. *European Transactions on Telecommunications*, 23(6):508–521, Oct. 2012.

[56] S. Iellamo, L. Chen, and M. Coupechoux. Proportional and Double Imitation Rules for Spectrum Access in Cognitive Radio Networks. *Elsevier Computer Networks*, 57(8):1863–1879, June 2013.

[57] S. Iellamo, L. Chen, and M. Coupechoux. Retrospective Spectrum Access Protocol: A Payoff-based Learning Algorithm for Cognitive Radio Networks. In *IEEE International Conference on Communications (ICC)*, Sydney, Australia, June 2014.

[58] V. Krishna. *Auction Theory*. Academic Press, 2002.

[59] X. Chen and J. Huang. Evolutionarily Stable Spectrum Access. *IEEE Transactions on Mobile Computing*, to appear.

[60] W. H. Sandholm. *Population Games and Evolutionary Dynamics*. The MIT Press, 2010.

7

SPONTANEOUS NETWORKS

7.1 Introduction

Spontaneous networks are characterized by a possible short-lived deployment, the use of unlicensed frequencies, the lack of infrastructure, their distributed mode of operation, their ability to self-organize (autonomous nodes), or their ease of deployment. Contrary to cellular networks, they are usually not operated. The engineering and the performance evaluation of such networks is thus very specific. Protocols should take into account sometimes the absence of a central controller. Among spontaneous networks, we can cite *ad hoc networks*, which are a set of mobile nodes able to communicate on a peer-to-peer basis, possibly over multiple hops, without the need of an infrastructure (used in military or emergency situations). *Mesh networks* have similar properties but are rather intended for bakhauling purposes, so that nodes are not supposed to move. A *WLAN (Wireless Access Network)* shares with cellular networks its organization in cells around an access point. It is however deployed mostly in unlicensed bands, often in a chaotic manner without any central planning, and IEEE 802.11, its underlying MAC protocol, is distributed. *Sensor networks* are supposed to collect informations in a distributed way and to convey them to a central base. They are characterized by low capabilities, especially in terms of battery and processing. Most of my contributions in this domain have been done during my PhD thesis. Only recently, during my sabbatical stay at Indian Institute of Science (Bangalore, India), I have worked with Prof. Anurag Kumar and his students, Abhishek Sinha, Arpan Chattopadhyay and K. P. Naveen on sensor networks. In this chapter, I focus on this field.

7.2 Related Work[1]

We focus in this section on the notion of *impromptu deployment* for sensor networks.

Wireless networks, such as cellular networks or multihop ad hoc networks, would normally be deployed via a planning and design process. There are situations, however, that require the impromptu (or "as-you-go") deployment of a multihop wireless packet network. Such an impromptu approach would be required to deploy a wireless sensor network for situational awareness in emergency situations such as those faced by firemen or commandos (see [1, 27]). For example, as they attack a fire in a building, firemen might wish to place temperature sensors on fire-doors to monitor the spread of fire, and ensure a route for their own retreat. With the above larger motivation in mind, we are concerned with the rigorous formulation and solution of a problem of impromptu deployment of a multi-hop wireless network along a random lattice path, see figure 7.1. The objective is to create a multihop wireless path for packet communication from the end of the path to its beginning.

1 This section is taken from [31].

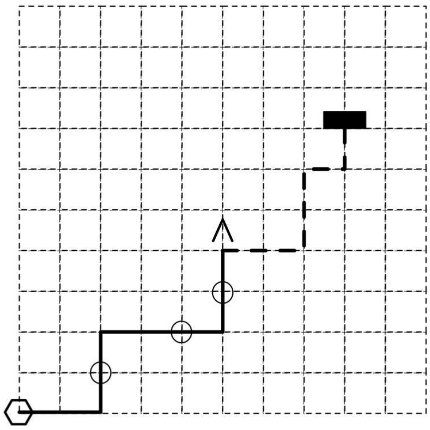

Figure 7.1: A wireless network being deployed as a person steps along a random lattice path. Inverted **V**: location of the deployment person; path drawn with a solid line: path already covered; circles: deployed relays; path drawn with a thick dashed line: a possible evolution of the remaining path. The source to be placed at the end is also shown as the black rectangle.

"As-you-go" deployment of wireless relay networks has, in the past, been motivated by "first responder" networks, a concept that has been around at least since 2001. In [1], Howard et al. provide heuristic algorithms for the problem of incremental deployment of sensors (such as surveillance cameras) with the objective of covering the deployment area. Their problem is related to that of self-deployment of autonomous robot teams. Creation of a communication network that is optimal in some sense is not an objective in [1]. In a somewhat similar vein, the work of Loukas et al. [24] is concerned with the dynamic positioning of robots that, in an emergency situation, can serve as wireless relays between the infrastructure and human-carried wireless devices.

The problem of impromptu deployment of static wireless networks has been considered in [20, 22, 23, 25, 26]. In [22], Naudts et al. provide a methodology in which, after a node is deployed, the next node to be deployed is turned on and begins to measure the signal strength to the last deployed node. When the signal strength drops below a predetermined level, the next node is deployed and so on. Souryal et al. provide a similar approach in [23, 26], where an extensive study of indoor RF link quality variation is provided, and a system is developed and demonstrated. The work reported in [25] is yet another example of the same approach for relay deployment. More recently, Liu et al. [28] describe a "breadcrumbs" system for aiding firefighters inside buildings, and is similar to our work in terms of the class of problems it addresses. In a survey article [27], Fischer et al. describe various localization technologies for assisting emergency responders, thus further motivating the class of problems we consider. Bao and Lee [20] consider the problem of multiple persons, each carrying some relays, exploring an unknown region, and collaboratively placing relays to stay connected to a command center. The objective is to maximize the area they can explore while staying connected, using these relays. They propose a heuristic algorithm based on measurements between the deployed relays and between the mobile individuals.

In the literature referred to above, heuristic algorithms are proposed for relay placement. In an earlier work of Prof. A. Kumar's team (Mondal et al. [30]), authors took the first steps towards rigorously formulating and addressing the problem of impromptu optimal deployment of a multi-hop wireless network along a line at the end of which a source has to be placed. The source (e.g., a sensor) placement location is discovered only as the network is deployed. A probabilistic model is used for the unknown location of the source along the line. Once placed, the sensor sends periodic measurement packets to a control centre near the start of the line. It is assumed that the measurement rate at the sensor is low, so that (with a very high probability) a packet is delivered to the control centre before the next packet is generated at the sensor. This, so called, "lone packet model" is realistic for situations in which the sensor makes a measurement every few seconds, or where the main purpose of the sensor network is to detect sporadic events, and communicate the detection to the sink.

The objective of the sequential decision problem is to minimize a certain expected per packet cost (e.g., end-to-end delay or total energy expended by a node), which can be expressed as the sum of the costs over each hop, subject to a constraint on the number of relays used for the operation. It has been proved in [30] that an optimal placement policy solving the above mentioned problem is a threshold rule, i.e., there is a threshold r^* such that, after placing a relay, if the operative has walked r^* steps without the path ending, then a relay must be placed at r^*.

7.3 Contributions

With Prof. Anurag Kumar and his students, we have done the following contributions to impromptu sensor network deployments:

- We have formulated the problem as a total cost MDP (Markov Decision Process), and characterized the optimal policies in terms of placement sets [31]. We showed that these optimal policies are threshold policies and thus the placement sets are characterized by boundaries in the two-dimensional lattice. Beyond these boundaries, it is optimal to place a relay. Noticing that placement instants are renewal points in the random process, we recognized and proved the OSLA (One Step Look Ahead) characterization of the placement sets. Based on the OSLA characterization, we proposed an iterative algorithm, which converges to the optimal placement set in a finite number of steps. We have observed that this algorithm converges much faster than value iteration. We provided several numerical results that illustrate the theoretical development. The relay placement approach proposed in [22, 23, 25, 26] would suggest a distance threshold based placement rule. We numerically obtained the optimal rule in this class, and found that the cost of this policy is numerically indistinguishable from that of the overall optimal policy provided by our theoretical development. This suggests that it might suffice to utilize a distance threshold policy. However, the distance threshold should be carefully designed taking into account the system parameters and the optimality objective.

- This work has been extended to measurement based policies, where the deployment person takes decision based on its measurements of the radio channel [32]. The lone packet model assumption is difficult to relax. Finding the optimal placement of relay nodes on a line between a source and a destination and assuming information theoretic achievable rates is already an heavy task tackled in [29].

I have other contributions in the field of spontaneous networks. The works presented herafter have been mostly done during my PhD thesis under the supervision of Christian Bonnet (Institut Eurecom) and Vinod Kumar (Alcatel-Lucent Bell Labs). Several papers and patents have been written with Bruno Baynat (UMPC), Marie-Line Alberi-Morel, Luc Brignol, Jérôme Brouet, Véronique Capdevielle, Michel Cohen, Lionel Fiat, Thierry Lestable, Hervé Maillard and Denis Rouffet (all from Alcatel-Lucent Bell Labs at that time).

- The main contribution of my PhD thesis is the design of a distributed MAC protocol for mobile ad hoc networks called CROMA (Collision-free Receiver Oriented Medium Access) [2, 4, 5, 16]. CROMA is a hybrid protocol that employs random access techniques at the initiation of a packet call and ensures collision-free transmission during the whole packet call. It is thus characterized by short access delays (like other random access schemes) and high bandwidth utilization at high load (like collision-free protocols). As interference and collisions should ideally be detected at the receiver, CROMA is receiver oriented, i.e., the receiver nodes controls the transmission during the collision-free phase. The proposal has been analytically studied in a complete graph network using Markov chain theory and in multi-hop and mobile scenarios through simulations. It clearly outperforms IEEE 802.11 in the same conditions.

- Several internal Alcatel-Lucent Bell Labs projects were aiming at evaluating WiFi performance in various contexts. In [6], we have proposed solutions to the near far effect in multi-rate WLANs. In [7], we have evaluated the performance of a multi-hop network based on WiFi and deployed for indoor coverage. In [10], we have proposed an Internet access architecture for rural areas based on satellite communication and WiFi. In [15], we have evaluated the voice over IP capacity of a WLAN cell in terms of number of simultaneous calls. The approach is based on a subjective perception of the voice quality called the E model.

- We have proposed several patents [3, 8, 9, 14, 18, 17, 19, 21] in the field of spontaneous networks.

- We have studied additional mechanisms for capacity enhancements in spontaneous networks [11]. We have proposed a scheduling policy for delay tolerant networks in [2]. We have proposed a closed-form formula for the capacity of the channel aware slotted Aloha protocol over Rayleigh and Nakagami-m channels [12]. In [13], we analyzed the throughput of a multi-hop network, where nodes use slotted Aloha and are able to receive simultaneously several packets in a slot. We have provided a closed-form formula for the throughput assuming a matched filter or a minimum mean-square error (MMSE) multi-user detector (MUD) receiver. Capacity results show the great advantage of multi-packet reception and highlight the near-far resistance of the MUD scheme.

7.4 Conclusion

We have focused in this chapter on a recent contribution in the domain of sensor networks. The network issue raised by Prof. A. Kumar and his students is very original and very practical. Only very few papers had considered the impromptu deployment of nodes although the problem arises in various contexts. Existing literature has only focused so far on practical approaches without looking for optimal solutions. Here again, the gap to be filled between theory and practice is large and there are several directions to be investigated like the joint deployment of sensors by several persons trying to coordinate their actions.

Bibliography

[1] Andrew Howard, Maja J. Matarić, and S. Sukhat Gaurav. An Incremental Self-Deployment Algorithm for Mobile Sensor Networks. *Kluwer Autonomous Robots*, 13(2):113–126, Sept. 2002.

[2] M. Coupechoux and C. Bonnet and V. Kumar. A Scheduling Policy for Dense and Highly Mobile Networks. In *Proc. of Workshop on Mobile Ad Hoc Network (WMAN)*, Mar. 2002.

[3] V. Kumar and M. Coupechoux. Method for Providing Access to a Data-Network for a Vehicle Travelling on a Road. Patent EP1233575A1, Aug. 2002.

[4] M. Coupechoux and B. Baynat and C. Bonnet and V. Kumar. CROMA - A Slotted MAC Protocol with Multi-Slot Communications. In *Proc. of WNCG Wireless Networking Symp. (WNCG)*, Oct. 2003.

[5] M. Coupechoux and B. Baynat and C. Bonnet and V. Kumar. Modeling a Slotted MAC Protocol for MANETs. In *Proc. of Workshop on Mobile Ad Hoc Networking and Computing (MADNET)*, Mar. 2003.

[6] M. Coupechoux and J. Brouet and L. Brignol and V. Kumar. Suggested Solutions for the Near-Far Effect in Multimode WLANs. In *Proc. of Wireless World Research Forum (WWRF10)*, Oct. 2003.

[7] V. Capdevielle and T. Lestable and M. Coupechoux and M.L. Alberi-Morel and L. Brignol. Multi-Hop Coverage Extension of an IEEE 802.11b WLAN in a Corporate Environment. In *Proc. of WNCG Wireless Networking Symp. (WNCG)*, Oct. 2003.

[8] V. Kumar and M. Coupechoux. Mobile Station with Two Communication Interfaces. Patent EP1289320A1 US2003/0045294A1, Mar. 2003.

[9] V. Kumar and M. Coupechoux and H. Maillard. Method for Establishing a Connection between Terminals Having a Short-Range Wireless Communication Interface. Patent EP1333627A1, Aug. 2003.

[10] M. Cohen, D. Rouffet, L. Brignol et M. Coupechoux. Internet rapide en zones peu denses. *Alcatel Telecommunication Review*, 2004.

[11] M. Coupechoux and B. Baynat and T. Lestable and V. Kumar and C. Bonnet. Improving the MAC Layer of Multi-Hop Networks. *Kluwer Wireless Personal Communications*, 29(1-2):71–100, Apr. 2004.

[12] M. Coupechoux and T. Lestable. On the Capacity of the Channel Aware Slotted Aloha over Rayleigh and Nakagami-m Channels. In *Proc. of IEEE Intl. Symp. on Modeling and Optimization in Mobile, Ad Hoc, and Wireless Networks (WiOpt)*, Mar. 2004.

[13] M. Coupechoux and T. Lestable and C. Bonnet and V. Kumar. Throughput of the Multi-hop Slotted Aloha with Multi-Packet Reception. In *Wireless On-demand Network Systems (WONS)*, Lecture Notes in Computer Science, pages 239–243. Springer, 2004.

[14] M. Coupechoux and V. Kumar. A Method of Selecting a Path to Establish a Telecommunication Link. Patent EP1448011A1, Aug. 2004.

[15] M. Coupechoux and V. Kumar and L. Brignol. Voice over IEEE 802.11b Capacity. In *Proc. of ITC Specialist Seminar*, Oct. 2004.

[16] M. Coupechoux, B. Baynat, Ch. Bonnet, and V. Kumar. CROMA: An Enhanced Slotted MAC Protocol for MANETs. *ACM/Kluwer Mobile Networks and Applications*, 10(1-2):183–197, June 2005.

[17] M. Coupechoux and J. Brouet. Wireless Mobile Terminal and Telecommunication System. Patent EP1585283A1 US2005/0243718A1, Oct. 2005.

[18] V. Kumar and M. Coupechoux. Fast Delivery of Multimedia Messages in Cellular Networks. Patent EP1511333A1 US2005/0048980A1, Mar. 2005.

[19] M. Coupechoux and L. Fiat. Method for Improving Handovers in a WLAN. Patent EP1648115A1 US2006/0077933A1, Apr. 2006.

[20] J. Q. Bao and W. C. Lee. Rapid Deployment of Wireless Ad Hoc Backbone Networks for Public Safety Incident Management. In *Proc. of IEEE Global Communications Conference (GLOBECOM)*, pages 1217–1221, Nov. 2007.

[21] M. Coupechoux and V. Kumar. Method of Selecting of a Path to Establish a Telecommunication Link. Patent US 7,302,230B2, Nov. 2007.

[22] D. Naudts, S. Bouckaert, J. Bergs, A. Schouttcet, C. Blondia, I. Moerman, and P. Demeester. A Wireless Mesh Monitoring and Planning Tool for Emergency Services. In *Proc. of IEEE Workshop on End-to-End Monitoring Techniques and Services (E2EMON)*, May 2007.

[23] M. R. Souryal, J. Geissbuehler, L. E. Miller, and N. Moayeri. Real-Time Deployment of Multihop Relays for Range Extension. In *Proc. of ACM International Conference on Mobile Systems, Applications and Services (MobiSys)*, June 2007.

[24] G. Loukas, S. Timotheou, and E. Gelenbe. Robotic Wireless Network Connection of Civilians for Emergency Response Operations. In *Proc. of IEEE Intl. Symp. on Computer and Information Sciences (ISCIS)*, Oct. 2008.

[25] T. Aurisch and J. Tölle. Relay Placement for Ad-hoc Networks in Crisis and Emergency Scenarios. In *Proc. of the Information Systems and Technology Panel (IST) Symp.*, Bucharest, Romania, May 2009. NATO Science and Technology Organization.

[26] M. R. Souryal, A. Wapf, and N. Moayeri. Rapidly-Deployable Mesh Network Testbed. In *Proc. of IEEE Conference on Global Telecommunications (GLOBECOM)*, Nov. 2009.

[27] C. Fischer and H. Gellersen. Location and Navigation Support for Emergency Responders: A Survey. *IEEE Pervasive Computing*, 9(1):38–49, Jan.-Mar. 2010.

[28] H. Liu, J. Li, Z. Xie, S. Lin, K. Whitehouse, J. A. Stankovic, and D. Siu. Automatic and Robust Breadcrumb System Deployment for Indoor Firefighter Applications. In *Proc. of ACM Intl. Conf. on Mobile Systems, Applications and Services (MobiSys)*, June 2010.

[29] A. Chattopadhyay, A. Sinha, M. Coupechoux, and A. Kumar. Optimal Capacity Relay Node Placement in a Multi-hop Network on a Line. In *Proc. of Intl. Workshop on Resource Allocation and Cooperation in Wireless Networks (RAWNET), in conjunction with WiOpt*, May 2012.

[30] P. Mondal, K. P. Naveen, and A. Kumar. Optimal Deployment of Impromptu Wireless Sensor Networks. In *Proc. of IEEE National Conference on Communications (NCC)*, Feb. 2012.

[31] A. Sinha, A. Chattopadhyay, K. P. Naveen, M. Coupechoux, and A. Kumar. Optimal Sequential Wireless Relay Placement on a Random Lattice Path. *CoRR*, abs/1207.6318, 2012.

[32] A. Chattopadhyay, M. Coupechoux, and A. Kumar. Measurement Based Impromptu Deployment of a Multi-Hop Wireless Relay Network. In *Proc. of IEEE Intl. Symp. on Modeling and Optimization in Mobile, Ad Hoc, and Wireless Networks (WiOpt)*, May 2013.

8 RESEARCH PROJECT AND CONCLUSIONS

8.1 Introduction

My research is motivated by several important trends in the field of mobile networks. In my opinion, the three main trends are the following:

- Users want to use their favorite applications (voice, file downloading, video streaming, social networking, etc) on their various terminals (smartphones, tablets) in a seamless way whatever the technology, whatever their location. This implies for radio engineers and researchers to design high data rates networks (maybe towards one or several Gbits/s per cell) able to support existing and coming applications. The seamless experience should be supported by efficient mobility procedures and a careful interference management, so that the quality of experience (or service) is not too variable.

- One of the main obstacles towards high data rate networks is the saturation and fragmentation of the available frequency spectrum. An important challenge for operators and regulators in the coming years will be to make a better usage of this scarce resource. This can be achieved by implementing new radio resource management mechanisms and/or new regulatory rules. The notions of *dynamic spectrum access* and *cognitive radio* and their related algorithms will still be very active research fields in the future.

- Because of the foreseen low extinction of fossil energy sources and their negative impact on environment, there is a clear need for sobriety and alternative power resources. Sobriety actions can be divided in two parts: on the one hand, information technologies are huge consumers of energy; every technological choice should thus be though in the light of energy saving. On the other hand, these technologies can help other domains (like transportation, health, electrical grid, smart cities, etc) to save energy. Defining new performance metrics, new models, new radio resource management schemes for saving energy are important challenges for researchers. The use of alternative power sources like wind or sun in telecom equipments open new research areas, especially in the joint management of energy and radio resources.

8.2 Towards Very High Data Rates

Todays cellular networks (LTE) can reach the peak rate of 300 Mbits/s on the downlink, in a 20 MHz band, in the best radio conditions, i.e., near the base station. We should however keep in mind that this data rate can drop to 1 Mbits/s at cell edge, that the average cell throughput is rather around 50 Mbits/s [16] and that the overall capacity has to be shared among users. On the other hand, there were already 3.2 bn unique mobile subscribers in the world in 2012, almost 4 bn are expected in 2017 (LTE will account for one on five connections) [23]. There is an explosion of mobile data volumes: the growth has been higher in 2012 than in all preceding years (around 900 Petabytes per month) [23]. The phenomenon of growing traffic and limited network capacity, known as the *capacity crunch* of wireless networks, is driven by new demanding applications and terminals, and by an increasing number of devices connected to the Internet through cellular networks (the so called *Internet of things*). In order to answer this growing demand, rates in the order of 1 Gbits/s and then 10 Gbits/s are probably expected in the next ten to twenty years (although optimistic, 2020 is commonly invoked deadline for the definition of the fifth generation 5G).

How to achieve these data rates, how to ensure a seamless quality of experience? I personally see four important means: (1) identifying new frequencies and larger spectrum bands; (2) incorporating new physical layers techniques into cellular network standards; (3) densifying the network, i.e., increasing the number of base stations per square meter; and (4) managing in a more efficient way radio resources and interference.

Identifying new frequencies and larger spectrum bands is mainly a task for regulators and electronic component designers, but their choices will influence the network design. Recent field trials have demonstrated the transmission of 1 Gbits/s over a distance of 2 Km in the millimeter wave band at a frequency of 28 GHz using a 64 element antenna array transmitter [24]. Note that as the frequency band increases, the antenna size decreases so that base stations with tens of antennas become realistic (*massive MIMO*). The millimeter wave band (between 30 and 300 GHz) has also a huge potential in terms of available spectrum. It has however some drawbacks. For example, designing electronics components able to work at these frequencies is a challenge. More important for the network designer, the propagation suffers from very large losses compared to 4G bands (e.g. 2.6 GHz), that can only be compensated by highly directional antennas. Even if regulators can identify large spectrum bands for mobile communications, it is likely that these bands will be fragmented. LTE-A standards have already introduced the *carrier agregation* feature to take into account this drawback. Its impact on the network performance has to be assessed.

Recent advances at the physical layer are mainly related to multiple antenna techniques (MIMO) and their variants (MU-MIMO, network MIMO, massive MIMO, beamforming, vertical sectorization, coordinated multipoint). They allow an increase of the throughputs and/or of the signal robustness without using new frequency or power resources [25]. Cooperative relaying is also a paradigm in information theory, where a source and one or more relays cooperatively and simultaneously transmit to a destination with the result of a capacity increase [2]. Some of these techniques (e.g. variants of MIMO) are now well known for point-to-point transmissions. Their performance need however sometimes to be assessed at the network level (considering e.g. multi-cellular interference, traffic considerations, imperfect information). Some others (e.g. interference alignment [3]) still make unrealistic assumptions to be deployed on a real network. My research objective in this field is to model (when possible) these kinds of techniques at the network level in order to extract the macroscopic essence of these features, and then to assess their performance in a cellular system. This requires expertise mainly in the involved technologies (to be able to model and to understand the related technical issues), in stochastic modeling (for example for the evaluation of the radio quality), traffic modeling (for capacity evaluations) and sometimes in combinatorial optimization (as we have seen for the relay placement problem).

Network densification is a well known technique to increase capacity and user throughputs in cellular networks. It consists in increasing the number of base stations per square meter so as to increase the reuse of radio resources. It has also the side effect of reducing the transmit power of both antennas and mobile terminals [7]. It is however an expensive solution and the deployment of small cells, femto cells, or relays may be preferred to macro base stations. These new network elements impose their own constraints. To give some short examples, the operator has to manage the interference between small cells and the umbrella macro cell; femto cells are potentially deployed in a chaotic manner without a strict control of the operator; in-band relays performance is closely related to the backhaul link capacity. Again, how to assess the performance of these network entities within a traditional macro-cellular network will be part of my research in the coming years.

We see from the previous discussion that future networks are characterized by a high heterogeneity, in terms of frequency bands, of network elements, of user terminals or types of applications (including e.g. machine to machine or device to device communications). In a context of limited radio resources, it is needed to manage this heterogeneity in a efficient way with the goal of offering a seamless experience to the mobile user. There is now a trend to design distributed and adaptive radio resource management schemes, where network elements take their own decisions without the help of a central controller (networks are *self-organized*). This approach is pushed by the development of game theory in the network community and aims at making exchanges of information between entities as small as possible and algorithms scalable. However, centralized solutions have also their advantages, e.g. for mutualizing radio resources. In RoF (Radio over Fiber) systems (also known as *cloud radio access network*) for example, base band units are co-located in a central controller and shared by different cells fed by an optical fiber. Proposing radio resource management schemes (centralized or decentralized) able to account for the heterogeneity of the network will be a major axis of my future research. For this, I intend to develop my expertise on the one hand in the field of Markov Decision Processes for centralized approaches, on the other hand in game theory and decentralized learning approaches.

8.3 A Better Spectrum Usage

On the one hand, the idea that the frequency spectrum is today both congested and inefficiently used is commonplace among regulators, operators and many scientists: although some frequency bands are saturated in the busy hours, in some cities, others remain underutilized [1]. On the other hand, software radio has seen important advances in the past few years: terminals and equipments are already able to communicate on a very large spectrum and will be soon able to reconfigure very rapidly their transceiver parameters or protocols. The conjunction of these two phenomena, i.e., a saturated but underutilized spectrum and the advances of software radio, makes possible and desirable the birth of a *cognitive radio*. This cognitive radio is able to adapt to its environment, to self-reconfigure, and to access to frequencies left free of any transmission, in an opportunistic way. A cognitive radio is thus able to communicate over the *holes* of the spectrum.

One of the paradigms of the cognitive radio consists in the opportunistic access of secondary users to the frequency channels sometimes left free by a licensed primary user. In this domain, the literature has mainly focused on the distributed allocation of radio resources among cognitive radios on the one hand (they indeed cannot rely on central controller), and on the sensing techniques allowing to detect a primary user activity (see e.g. [4] for a combined approach). My research project is to improve the results already obtained by the research community in the former domain. The proposed models are indeed relatively simple and neglect some basic constraints related to wireless networks.

Among the main constraints not taken into account today, I can cite the imperfect medium access control protocol. Many papers (with some notable exceptions like [17]) assume a perfect MAC allowing transmitters and receivers to perfectly use the available bandwidth when it is free. Switching from one channel to another as it is usually assumed without incurring any cost in terms of signaling, delay or packet error rate is unrealistic. We have started to investigate this point in [12] but a lot need still to be done. The usual network topology is a complete graph, where all cognitive radios are within the same transmission range. A more realistic scenario would consider hidden terminals and the possibility to reuse radio resources if the distance between receivers is sufficiently large. A promising tool for studying such topologies is a recent paper on congestion games on graphs [22]. Due to the varying nature of the wireless channel, users payoff can be subject to random perturbations. Is it still possible to converge to a desirable equilibrium in this context assuming various learning algorithms? There are some answers in [20] for the exponential learning, we have also done some simulations in [19] for the proportional imitation rule, but the question is still open for other learning algorithms. The number of cognitive radios is usually supposed to be fixed in the literature, while in a real system, users can arrive in the system at random instants, and leave it when their transmission has ended. So introducing traffic aspects in the resource allocation schemes is an interesting challenge. At last, cognitive radios could have different quality of service requirements and this aspect is also usually ignored.

Improving existing distributed resource allocation schemes and proposing new ones adapted to more realistic models will be one my research goals in the near future. The natural frameworks for these studies are game theory, distributed learning and traffic theory.

8.4 Green communications

Everyone has in mind that ICT (Information and Communication Technologies) represents only 2% of the greenhouse gas emissions, however with an important growth rate (about 20% per year) [18]. By 2020, the mobile industry should represent 50% of the ICT emissions. About 70% of the mobile industry energy consumption is from the network operation. Base stations are by far the most consuming network equipments [6]. On the other hand, ICT is sometimes presented as a potential driver for greenhouse gas emission reductions (the GeSI, an industry funded initiative, expects a 16.5% abatement thanks to ICT by 2020 [18]) in various sectors like the power (smart grids), transportation, buildings, manufacturing sectors, etc. At the same time, there are health, societal, economic and political debates on the need to reduce the human exposure to radiations. Research has two major paths for reducing the energy consumption that are summarized in the two keywords: "green IT" and "IT for green". In the next few years, I will focus on the first aspect.

If we go in more details in the field of green cellular networks, we can highlight three important means to reduce the energy consumption and/or the transmit power [9, 10, 21]: (1) improve the efficiency of electrical components, (2) improve the efficiency of transmission schemes and signal processing algorithms, (3) propose radio resource management schemes that take into account the energetic factor in their decisions.

Although the first two means are not in my research domain, there is a need for models at these levels in order to evaluate the impact of technological choices on network planning. The consumption model of every component in different sleep or switch off modes of the base station has for example a decisive impact for radio planning and can determine if it is worth switching off a base station or not. It is relatively easy to find energy consumption models [5] but it is not clear what is the global footprint of a base station (depending on the technology and taking into account its life duration), if it is better to deploy a lot of small stations or few large base stations, if there is a cost of switching from a sleep mode to another, etc. Another example is related to renewable energy. Alternative energy sources, e.g. from solar or wind origin, are indeed characterized by a high variability and an uncertainty of their availability. There is thus a need to analyze the behavior of a battery loaded by a renewable energy using a probabilistic approach and to jointly manage energy and radio resources. There are already some works in this direction in the field of so called *energy harvesting* sensors [13] that could be extended to cellular networks. A complete new base station architecture could also be investigated thanks to the notion of *radio over fiber* (see e.g. [15]). In this approach, signal processing units of several cells are co-located in a central controller. The radio signal is then transferred over wavelengths to distributed antennas. This kind of architecture almost eliminates the cable losses of a classical base station and save energy by sharing signal processing resources. Concerning the transmission schemes, it is shown in [10] that MIMO systems can improve the energy efficiency in terms of bits/Joule. It is also clear that beamforming techniques that focus the energy in the direction of the receiver can be used to reduce the transmit power without decreasing the quality of service. Whereas todays physical layer advances are used by operators to boost their throughputs and capacities, they should be evaluated in the light of their energy efficiency at the network level.

The third means to save energy is the radio resource management and the network planning. Network dimensioning is usually based on the worst case assumption, for example at the busy hour. Activating the network components in a dynamic way as a function of the needs is a general approach in this domain. A first idea consists in switching off or putting in sleep mode a certain proportion of base stations. Switching off transmitters has a direct impact on the energy consumption but also on the quality of service. The papers that propose this approach usually rely on the effect of cell breathing or cell zooming to ensure a continuous coverage of the cellular service (see e.g. [8]). In dense urban areas, the cell range is indeed limited by the capacity constraint (and not by the radio propagation constraint as it is the case in rural environments). When the traffic is low, it is thus possible to switch off a portion of the transmitters and to extend the cell range of active base stations. In the best case, this can be done without increasing the transmit power. Although the basic idea of this approach is known, there is still work to be done to obtain realistic algorithms. For example, the cost of the transitions from sleep to active modes is not known, or is there an impact on the base station life duration? New models should thus be developed. Scalable solutions are also needed in order to decide which stations should be switched off or put in sleep mode and when. Distributed algorithms may be preferred here. At last, there are protocol issues, for example to handover existing communications when a station goes idle.

Densifying the network, i.e., deploying a lot of small cells (pico-cells, femto-cells, relays, etc forming with macro-cells a *heterogeneous network*) is another classical radio resource management approach (see e.g. [14]). As we have shown in [11], this allows to decrease the transmit power per station and even the power consumed per unit area (W/m^2). The radio quality is indeed measured thanks to the SINR, which is close to the Signal to Interference Ratio (S/I) in a dense network. In such a situation, decreasing the transmit power of all stations, decreases the useful signal power S but also the interference power I. As a consequence, transmit power can be decreased with a small impact of the radio quality... until the point where the thermal noise has again a decisive impact. Although densifying the network may appear as an attractive path, the global ecological footprint of such a solution is unknown because more cells mean more components, more operational costs, etc.

At last, cognitive radio algorithms that aim at better utilizing the radio spectrum can be seen as an enabling technology for green cellular networks [9]. A gain in spectrum efficiency or in interference management can indeed be often converted into a decrease of the transmit power. The possibility for a terminal to analyze its environment can lead to a better radio access technology selection based on energy efficiency criteria.

Although my existing contributions in green cellular networks are still small, I intend to increase my activities significantly in this field in the near future. I have indeed a good expertise in the performance evaluation of cellular networks, a good knowledge in the involved trade-offs between energy consumption on the one hand and coverage and capacity of cellular networks on the other hand. This expertise represents a solid foundation to explore this relatively new area of research.

8.5 Conclusion

As a conclusion, I summarize the different axis I want to investigate in the coming years. Towards very high data rates: I intend to model and assess the performance of physical layer advances at the network level; evaluate the performance of heterogeneous networks; propose radio resource management algorithms for high data rates cellular networks. A better spectrum usage: I want to improve the models assumed for the paradigm involving a primary and a secondary usage of the spectrum, propose new distributed algorithms and evaluate their performance in terms of convergence speed and achieved equilibrium. Green communications: I intend to evaluate the performance of physical layer and components advances at the network level in terms of energy efficiency, propose realistic cell planning algorithms, use cognitive radio as an enabling technology for green communications and propose algorithms to jointly manage renewable energy and radio resource.

As we have seen, these research axes require various competencies that go beyond my initial expertise in cellular networks and network dimensioning. I have developed several collaborations in light of these expertise needs. For example, the theory of Markov Decision Processes is a central tool in my collaborations with the Indian Institute of Science (Bangalore). Distributed learning and game theory are the subject of my collaborations with University of Paris XI (via a PhD co-direction), the University of Versailles Saint-Quentin and INRIA Grenoble (via the ANR project NETLEARN). I use combinatorial optimization techniques with the Novosibirsk State University (PhD student exchange), University of Paris VI (Master student co-direction) or the TSI department of Telecom ParisTech (Marc Sigelle). Concerning traffic theory, I had in the past collaborations with UPMC/LIP6 (Bruno Baynat) that deserve to be reactivated. My research in the field of green cellular networks is driven by a collaboration with Orange Labs and a SYSTEMATIC competitivity cluster project.

Bibliography

[1] FCC Spectrum Policy Task Force. Report of the Spectrum Efficiency Working Group. Technical report, FCC, Nov. 2002.

[2] A. Reznik, S.R. Kulkarni, and S. Verdú. Degraded Gaussian Multirelay Channel: Capacity and Optimal Power Allocation. *IEEE Transactions on Information Theory*, 50(12):3037–3046, Dec. 2004.

[3] V. R. Cadambe and S. A. Jafar. Interference Alignment and the Degrees of Freedom for the K User Interference Channel. *CoRR*, abs/0707.0323, 2007.

[4] Y. Chen, Q. Zhao, and A. Swami. Joint Design and Separation Principle for Opportunistic Spectrum Access in the Presence of Sensing Errors. *IEEE Transactions on Information Theory*, 54(5):2053–2071, May 2008.

[5] G. Miao, N. Himayat, Y. Li, and A. Swami. Cross-Layer Optimization for Energy-Efficient Wireless Communications: a Survey. *Wireless Communications and Mobile Computing*, 9(4):529–542, Apr. 2008.

[6] GSMA and The Climate Group. Mobile's Green Manifesto. Technical report, GSMA, 2009.

[7] J. M. Kélif and M. Coupechoux. Cell Breathing, Sectorization and Densification in Cellular Networks. In *Proc. of International Symposium on Modeling and Optimization in Mobile, Ad Hoc, and Wireless Networks (WiOpt)*, June 2009.

[8] M. A. Marsan, L. Chiaraviglio, D. Ciullo, and M. Meo. Optimal Energy Savings in Cellular Access Networks. In *Proc. of IEEE Int. Conf. on Communications (ICC), ICC Communications Workshops*, June 2009.

[9] J. Palicot. Cognitive Radio: an Enabling Technology for the Green Radio Communications Concept. In *Proc. of ACM Int. Conf. on Wireless Communications and Mobile Computing (IWCMC)*, June 2009.

[10] E. V. Blemega, S. Lasaulce, and M. Debbah. A Survey on Energy Efficiency Communications. In *Proc. of IEEE Int. Symp. on Personal, Indoor and Mobile Communications (PIMRC), PIMRC Workshops*, Sept. 2010.

[11] J.-M. Kélif, M. Coupechoux, and F. Marache. Limiting Power Transmission of Green Cellular Networks: Impact on Coverage and Capacity. In *Proc. of IEEE International Conference on Communications (ICC)*, May 2010.

[12] L. Chen, S. Iellamo, and M. Coupechoux. Opportunistic Spectrum Access with Channel Switching Cost for Cognitive Radio Networks. In *Proc. of IEEE Int. Conf. on Communications (ICC)*, June 2011.

[13] S. Sudevalayam and P. Kulkarni. Energy harvesting Sensor Nodes: Survey and Implications. *IEEE Communications Surveys and Tutorials*, 13(3):443–461, 2011.

[14] X. Weng, D. Cao, and Z. Niu. Energy-Efficient Cellular Network Planning under Insufficient Cell Zooming. In *Proc. of IEEE Vehicular Technology Conference (VTC Spring)*, May 2011.

[15] J. Zhang and N. Ansari. On OFDMA Resource Allocation and Wavelength Assignment in OFDMA-Based WDM Radio-Over-Fiber Picocellular Networks. *IEEE Journal on Selected Areas in Communications*, 29(6):1273–1283, June 2011.

[16] 3GPP TR 36.912. Feasibility study for Further Advancements for E-UTRA (LTE-Advanced). *Release 11 V11.0.0*, Sept. 2012.

[17] X. Chen and J. Huang. Spatial Spectrum Access Game: Nash Equilibria and Distributed Learning. In *Proc. ACM SIGMOBILE International Symposium on Mobile Ad Hoc Networking and Computing (MobiHoc)*, Hilton Head Island, South Carolina USA, June 2012.

[18] Global e Sustainability Initiative and the Boston Consulting Group. GeSI SMARTer 2020: The Role of ICT in Driving a Sustainable Future. Technical report, GeSi, 2012.

[19] S. Iellamo, L. Chen, and M. Coupechoux. Imitation-based Spectrum Access Policy for CSMA/CA-based Cognitive Radio Networks. In *Proc. of IEEE Wireless Communications and Networking Conference (WCNC)*, Apr. 2012.

[20] P. Mertikopoulos and A. L. Moustakas. The Emergence of Rational Behavior in the Presence of Stochastic Perturbations. *The Annals of Applied Probability*, 20(4):1359–1388, 2012.

[21] L. Suarez, L. Nuaymi, and J.-M. Bonnin. An Overview and Classification of Research Approaches in Green Wireless Networks. *EURASIP Journal on Wireless Communications and Networking*, 2012(142), Apr. 2012.

[22] C. Tekin, M. Liu, R. Southwell, J. Huang, and S. H. Ali Ahmad. Atomic Congestion Games on Graphs and Their Applications in Networking. *IEEE/ACM Trans. on Networking*, 20(5):1541–1552, Oct. 2012.

[23] GSMA and ATKearney. The Mobile Economy. Technical report, 2013.

[24] Samsung. Samsung Announces World's First 5G mmWave Mobile Technology. Press Release, May 2013.

[25] D. Tse and P. Viswanath. *Fundamentals of Wireless Communications*. Cambridge University Press, 2006.

Résumé

Ce mémoire d'habilitation présente l'ensemble de mes travaux et recherches dans le domaine de l'ingénierie des réseaux sans fil ainsi que mes projets de recherche pour les années à venir. Le premier chapitre est un cours sur le dimensionnement des réseaux cellulaires qui introduit les principaux modèles utilisés pour l'évaluation de performances. Un accent particulier est mis sur la probabilité de dépassement du rapport signal à interférence plus bruit (SINR), qui apparaît comme un élément central tant pour l'estimation de la couverture que pour les études de trafic. Les trois chapitres suivants résument l'ensemble de mes contributions dans le domaine de l'évaluation des performances des réseaux cellulaires. Les réseaux à accès multiple par répartition en code (CDMA), dont font partie les réseaux de troisième génération, se caractérisent par un certain nombre de fonctionnalités absentes des réseaux précédents, notamment le contrôle de puissance rapide, l'interférence intra-cellulaire ou un taux de réutilisation fréquenciel 1. Notre apport a consisté principalement à caractériser l'interférence et à fournir des formules approximatives mais simples du SINR permettant d'analyser ce type de réseaux. L'accès multiple par répartition en fréquences orthogonales (OFDMA) domine la quatrième génération. Nous avons étendu nos recherches à ces réseaux et montré notamment les avantages et inconvénients d'une réutilisation fractionnelle des fréquences. Nous avons également proposé une méthodologie de dimensionnement de ces réseaux allant des aspects radio aux aspects trafic. Nous avons proposé une méthode de placement optimal des relais dans un réseau cellulaire. Enfin, nous avons analysé les performances de différents schémas de transmission et de réception multi-antennes dans un environnement cellulaire et montré comment les interférences co-canal dégradaient sensiblement les gains apportés par ces techniques. Le chapitre suivant est dédié à la radio cognitive et à l'accès dynamique au spectre. Ce dernier étant réputé mal utilisé (certaines portions sont engorgées alors que d'autres sont sous-utilisées), une littérature scientifique s'est développée pour proposer des algorithmes de gestion des ressources plus efficaces. Nous avons proposé des algorithmes d'allocation dans le cadre d'un partage de spectre dynamique entre opérateurs ou entre technologies. Nous avons également proposé plusieurs algorithmes distribués (ou en partie) permettant à des radios dites cognitives d'accéder au spectre de manière opportuniste. L'avant dernier chapitre rassemble l'ensemble de mes contributions dans le domaine des réseaux spontanés, c'est-à-dire les réseaux ad hoc, maillés, de capteurs et les réseaux locaux sans fil. Mes travaux se sont concentrés en grande partie sur l'évaluation de performances et sur la conception de mécanismes d'accès distribués. Une récente étude se concentre sur le déploiement optimal *à la volée* de nœuds relais ou de capteurs. Ce mémoire se termine par mon projet de recherche pour les prochaines années. On peut distinguer trois grands axes : « vers de très hauts débits », axe qui inclut l'évaluation des performances des réseaux cellulaires du futur, « une meilleure utilisation spectrale », qui approfondit mes recherches dans le domaine de la radio cognitive et « communications vertes », axe qui se donne comme objectif de réduire la consommation d'énergie et les puissances d'émission dans les réseaux sans fil. Les compétences dont j'aurai besoin ainsi que les collaborations que j'entends développer ou approfondir pour atteindre ces objectifs sont détaillés en fin de mémoire.

Abstract

This thesis presents my work and contributions in the field of the radio engineering of wireless networks as well as my research project for the next few years. The first chapter is a short lecture on the dimensioning of cellular networks that introduces the main models used for performance evaluation. A special focus lies on the outage probability of the Signal to Interference plus Noise Ratio (SINR), which appears as a central parameter for coverage and capacity studies. The three next chapters are a summary of my contributions in the domain of the performance evaluation of cellular networks. Code Division Multiple Access (CDMA) is the basis of third generation networks. Such networks are in particular characterized by a fast power control, intra-cell interference and a frequency reuse 1, features that were not part of previous networks. Our contribution consists in providing simple formulas for the average SINR or for the SINR distribution that can easily be used to analyze this kind of networks. OFDMA is the dominant access scheme in fourth generation networks. We have extended our researches to these networks by showing in particular the advantages and drawbacks of fractional frequency reuse. We have also proposed a complete dimensioning methodology for OFDMA networks going from radio to traffic aspects. We have proposed a optimization approach for the placement of relays in a cellular network. At last, we have analyzed several Multiple Inputs Multiple Outputs (MIMO) schemes in a cellular context and shown how co-channel interference degrades significantly the gain brought by these techniques. The next chapter is dedicated to cognitive radio and dynamic spectrum access. Spectrum is indeed supposed to be inefficiently used: some portions are congested while others are underutilized. There is thus a new scientific literature that aims to propose new radio resource management schemes. We have proposed several allocation algorithms in the context of a dynamic spectrum sharing between operators or radio access technologies. We have also studied cognitive radios, that are devices able to sense and analyze their environment and to adapt to it in a distributed and dynamic way. We have proposed for such radios distributed algorithms for an opportunistic access to the spectrum. A chapter focuses on spontaneous networks, i.e., ad hoc, mesh, sensor and local area networks. We have performed several performance evaluation studies and designed distributed medium access schemes. A very recent study is on optimal *on-the-fly* (or *impromptu*) deployment of relays or sensor networks in a unknown environment. The thesis ends with my research projects for the next few years. They are organized into three main axes: "towards very high data rates", which includes the performance evaluation of future cellular networks, "a better spectrum usage", which is related to cognitive radio, and "green communications, which aims at reducing the energy consumption and the transmit powers in wireless networks. The competencies and collaborations I intend to develop or strengthen to achieve these objectives are detailed at the end of the thesis.

Performance Evaluation 67 (2010) 318–337

Contents lists available at ScienceDirect

Performance Evaluation

journal homepage: www.elsevier.com/locate/peva

Analytical performance evaluation of various frequency reuse and scheduling schemes in cellular OFDMA networks

Masood Maqbool [a,*], Philippe Godlewski [a], Marceau Coupechoux [a], Jean-Marc Kélif [b]

[a] *TELECOM ParisTech & CNRS LTCI, 46 rue Barrault, 75013 Paris, France*

[b] *France Telecom R&D, Issy-les-Moulineaux, France*

ARTICLE INFO

Article history:
Received 1 December 2008
Received in revised form 10 May 2009
Accepted 1 August 2009
Available online 5 August 2009

Keywords:
OFDMA
Fluid model
SINR
Frequency reuse
IFR
FFR
TLPC
Scheduling
Equal data rate scheduling
Equal bandwidth scheduling
Opportunist

ABSTRACT

In this paper, we present an analytical solution to carry out performance analysis of various frequency reuse schemes in an OFDMA based cellular network. We study the performance in downlink in terms of signal to interference (SIR) ratio and total cell data rate. The latter is analyzed while keeping in view three different scheduling schemes: equal data rate, equal bandwidth and opportunist. Analytical models are proposed for integer frequency reuse (IFR), fractional frequency reuse (FFR) and two level power control (TLPC) schemes. These models are based on a fluid model that was originally being proposed for CDMA networks. The modeling key of this approach is to consider the discrete base station entities as a continuum. To validate our approach, Monte Carlo simulations are carried out. Validation study shows that results obtained through our analytical method are in conformity with those obtained through simulations. A comparison between the above-mentioned frequency reuse schemes and scheduling policies is also presented. We also propose an optimal tuning of involved parameters (inner cell radius and power ratios).

1. Introduction

Orthogonal frequency division multiple access (OFDMA) is a promising multiple access technique being proposed for next generation mobile networks. The underlying technology for OFDMA based systems is orthogonal frequency division multiplexing (OFDM). With OFDM, available spectrum is split into a number of parallel orthogonal narrowband subcarriers. These subcarriers can be independently assigned to different users in a cell. Resources of an OFDMA system occupy place both in time (OFDM symbols) and frequency (subcarriers) domains thus introducing both the time and frequency multiple access [1].

Co-channel interference (CCI) limits the spectral efficiency of an integer frequency reuse 1 (IFR1) cellular network (cf. Section 3 for an introduction on IFR). The CCI becomes more critical for the users present in the border area of a cell. To combat this problem, in an OFDMA based system, fractional frequency reuse (FFR) has been proposed in [2]. In FFR, cell is divided into inner (close to base station) and outer (border area) regions. Available bandwidth is divided among inner and outer regions in such a way that former employs reuse 1 while the latter applies frequency reuse 3. Hence, users located in border area of the cell mitigate CCI owing to frequency reuse 3. By properly adjusting the sizes of inner and outer regions, spectral efficiency can be improved.

* Corresponding author. Tel.: +33 145817148.
E-mail addresses: masood.maqbool@telecom-paristech.fr (M. Maqbool), philippe.godlewski@telecom-paristech.fr (P. Godlewski), marceau.coupechoux@telecom-paristech.fr (M. Coupechoux), jeanmarc.kelif@orange-ftgroup.fr (J.-M. Kélif).

0166-5316/$ – see front matter
doi:10.1016/j.peva.2009.08.001

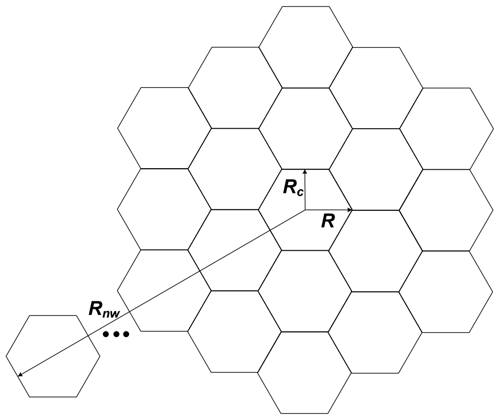

Fig. 1. Hexagonal network and main parameters of the study.

Authors of [3] studied the performance of FFR for 3GPP/3GPP2 OFDMA systems and term it soft frequency reuse. Authors have used system level simulations (SLS) in their analysis. In [4,5], author has studied the FFR in a IEEE 802.16 based system. Author has proposed an interference coordination system, which focuses on the scheduling of users. Proposed algorithm is implemented in SLS to present results. Two new algorithms, fractional time reuse (FTR) and fractional time and frequency reuse (FTFR), are proposed in [6] to cater for reduced capacity in the border area of cell because of FFR. In [7], authors have studied the capacity of a WiMAX system in the presence of FFR. In [8] also, performance of a FFR system is analyzed through simulations.

In contrast to the existing work, in this paper we present approximate analytical models for IFR, FFR and TLPC schemes of an OFDMA based cellular network. We derive expressions to calculate SIR at a given distance from base station (BS) and compute spectral efficiency using Shannon's classical formula. We also determine total cell data rate while considering three different scheduling schemes: equal data rate, equal bandwidth and opportunist.

This paper extends the framework, based on a fluid model, proposed in [9,10]. The model provides a simple closed-form formula for the other-cell interference factor f in downlink of CDMA networks as a function of distance to BS, path-loss exponent, distance between two BS and network size. The modeling key of this approach is to consider the discrete BS entities of a cellular network as a continuum.

Rest of the paper is organized as follows: Section 2 introduces notations used throughout the paper and recalls the main result of the fluid model. Section 3 focuses on IFR and derives SIR and spectral efficiency expressions for both reuse 1 and reuse K. The case of FFR is studied in Section 4. A two level power control scheme is considered in Section 5. In Section 6, three frequency reuse schemes (IFR, FFR and TLPC) are compared in terms of SINR and total cell data rate. Finally, Section 7 discusses the conclusion of this analysis.

2. Fluid model and notations

In this section, we explain the application of fluid model to an OFDMA system. We focus on downlink and consider a single subcarrier. BS have omni-directional antennas, such that one BS covers a single cell. If a user u is attached to a station b (or serving BS), we write $b = \psi(u)$.

The propagation path-gain $g_{b,u}$ designates the inverse of the path-loss pl between station b and user u, $g_{b,u} = 1/pl_{b,u}$. In the rest of this paper, we assume that $g_{b,u} = Ar_{b,u}^{-\eta}$, where A is a constant, $r_{b,u}$ is the distance between BS b and user u and η (>2) is the path-loss exponent.

Before presenting the expression of fluid model, we establish the following terms:

- P_{Tx} is the transmitted power per subcarrier. We assume that the output power per subcarrier is constant. Only in Section 5, we consider two possible values of output power per subcarrier: P_i for the inner region of the cell and P_o for the outer region. In this paper, we do not consider dynamic power allocation per subcarrier since in current OFDMA systems (WiMAX, Long Term Evolution), output power per subcarrier is constant;
- $S_{b,u} = P_{Tx} g_{b,u}$ is the useful power received by user u from station b;
- W is the total system bandwidth and W_u is the bandwidth dedicated to user u;
- R, R_c and R_{nw} are respectively the cell radius, half distance between neighboring base stations and network range (see Fig. 1);
- R_e is the radius of a circular region whose area is equal to that of the hexagon with length of each side equal to R. Based on definitions of R_e, R and R_c, it can be deduced that $R_e = aR_c = a\frac{\sqrt{3}}{2}R$, where $a = \sqrt{\frac{2\sqrt{3}}{\pi}}$.
- ρ_u, ρ_{BS} and N_u are respectively the user density, BS density and number of users per cell;
- D_u is the data rate allocated to a user and D_T is the total cell data rate;
- N_{BS} represents the total number of base stations in the network.

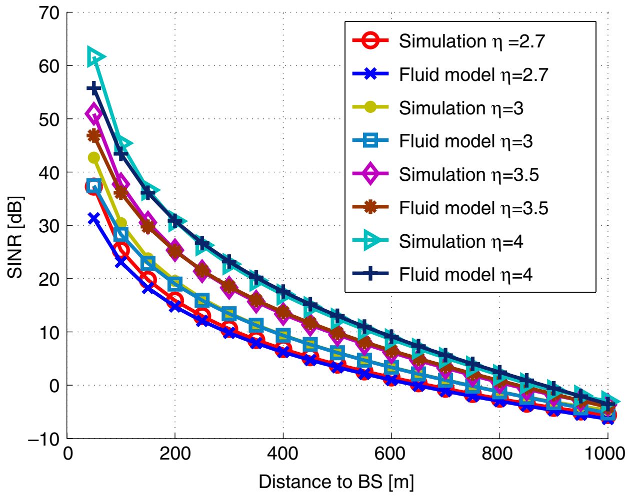

Fig. 2. SINR versus distance to the BS; comparison of the fluid model with simulations on a hexagonal network with $\eta = 2.7$, 3, 3.5, and 4 (reuse 1).

The total amount of power received by a user u in a cellular system can always be split up into three parts: useful signal ($S_{b,u}$), interference and noise (N_{th}). It is common to split the system power into two parts: $I_u = I_{int,u} + I_{ext,u}$, where $I_{int,u}$ is the *internal* (or own-cell) received power and $I_{ext,u}$ is the *external* (or other-cell) interference. We consider that useful signal $S_{b,u}$ is included in $I_{int,u}$. It should be noted that this useful signal power has to be distinguished from the commonly considered own-cell interference. In a CDMA network, the lack of orthogonality induces own-cell interference. In a OFDMA network, there is a perfect orthogonality between users and thus $I_{int,u} = S_{b,u}$.

With the above notations, the signal to interference plus noise ratio (SINR) is given by:

$$\gamma_u = \frac{P_{Tx} g_{b,u}}{\sum\limits_{j \neq b} P_{Tx} g_{j,u} + N_{th}}, \tag{1}$$

where $g_{j,u}$ is the path-gain between BS j and user u.

Ref. [9] has defined the interference factor for user u as the ratio of total power received from other BS to the total power received from the serving BS $\psi(u)$: $f_u = I_{ext,u}/I_{int,u}$. The quantities f_u, $I_{ext,u}$, and $I_{int,u}$ are location dependent and can thus be defined for any location x as long as the serving BS is known. In an OFDMA network, $I_{ext,u}$ is the total interference, and thus f_u is the inverse of the signal to interference ratio (SIR) per subcarrier. Throughout this paper, we shall neglect noise in our analytical calculations. This is a common assumption for macro-cells in dense urban areas. In this case, the SINR, γ_u can be approximated by the SIR:

$$\gamma_u \approx \frac{S_{b,u}}{I_{ext,u}} = 1/f_u.$$

As a consequence, it is clear that the approach developed in [9] can be adapted to OFDMA networks, till the time the orthogonality factor α considered in CDMA networks is zero (details on fluid model are given in Appendix. In this case, SIR per subcarrier is simply the inverse of the interference factor considered in [9].

$$\gamma_u = \frac{r_u^{-\eta}(\eta - 2)}{2\pi \rho_{BS} (2R_c - r_u)^{2-\eta}}. \tag{2}$$

Note that the shadowing effect is neglected in this paper. An extension of the fluid model has been proposed in [11] to take into account the shadowing factor. The results presented in this paper can thus be extended accordingly.

We now compare the results obtained with Eq. (2) with those obtained numerically through Monte Carlo simulations. The simulator assumes a homogeneous hexagonal network made of several rings around a central cell. Fig. 1 shows an example of such a network with the main parameters involved in this study.

Fig. 2 shows the simulated SINR (using Monte Carlo simulations) as a function of the distance from the base station. Following are the simulation parameters: $R = 1$ km, η between 2.7 and 4, $\rho_{BS} = (3\sqrt{3}R^2/2)^{-1}$, the number of rings around central BS is 15, and the number of snapshots is 3000. To include the effect of path-loss, Erceg model [12] is used: $g_{b,u} = Ar_{b,u}^{-\eta}$, such that $A = \left(\frac{4\pi d_0 f}{c d_0^{\eta/2}}\right)^2$, $d_0 = 100$ m, $f = 2.5$ GHz and c is the speed of light. Thermal noise density has been taken as -174 dB m/Hz and a subcarrier spacing of 11 kHz is considered [13]. Eq. (2) is also plotted for comparison.

In all cases, the fluid model matches very well the simulation results in a hexagonal network for various values of path-loss exponent. Only in a short area around the BS, the fluid model is a little bit pessimistic, but this is not a region of prime

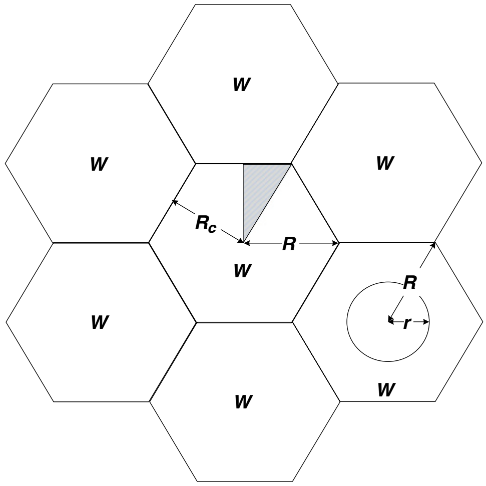

Fig. 3. Integer Frequency Reuse (IFR) case (reuse 1). Shaded triangular region shows the basic integration area.

interest for operators. It is to be noted that thermal noise was not considered in the fluid model while simulator does include its effect. However, the results of the two (fluid model and simulator) still match. It indicates that value of interference is much more pronounced as compared to that of thermal noise. Hence, neglecting thermal noise in the fluid model is a reasonable assumption.

For the rest of the paper, all the above parameters are used for simulations. However, instead of different values of η, a fixed value of 3 is used in the rest of the simulations, except mentioned otherwise. The closed-form formula (2) will allow us to quickly compute performance parameters of an OFDMA network and in particular to compare different frequency reuse schemes with different scheduling algorithms.

3. Integer frequency reuse (IFR)

In this section, we consider the application of fluid model to IFR scheme. In integer frequency reuse, all subcarriers allocated to a cell can be used anywhere in the cell without any specification of user's location. However, reutilization of subcarriers in network cells may be one or greater. An example of IFR with frequency reuse 1 is shown in Fig. 3, where W represents the available network bandwidth. For frequency reuse 1, cell bandwidth equals network bandwidth.

Two cases, frequency reuse 1 and K, have been considered in this paper. We first derive SINR and spectral efficiency expressions as functions of the distance from the BS using the fluid model. Next we take into account the three scheduling schemes (equal data rate, equal bandwidth and opportunist) and derive the total cell data rate expression for each of them. Results of analytical expressions are also compared with those of Monte Carlo simulations.

3.1. IFR with reuse 1

Consider Eq. (2) that gives expression for SINR of a subcarrier for a user at distance r_u. A user at distance r from BS has a specific value of SINR and spectral efficiency. Hence, in rest of the paper, subscript u is omitted for r, SINR and spectral efficiency. With $\rho_{BS} = 1/(2\sqrt{3}R_c^2)$ and introducing the normalized distance x such that $x = r/R_c$, the expression for SINR can be rewritten as:

$$\gamma_{IFR1}(x) = \frac{\sqrt{3}}{\pi}(\eta - 2)(2 - x)^{-2}(2/x - 1)^{\eta}. \tag{3}$$

For comparison between simulation and fluid model, Fig. 2 can be consulted in which all curves for fluid model have been drawn using Eq. (3).

By using Shannon's formula, spectral efficiency (in bps/Hz) as a function of variable x is given as:

$$C_{IFR1}(x) = \log_2[1 + \gamma_{IFR1}(x)], \tag{4}$$

where $\gamma_{IFR1}(x)$ is furnished by Eq. (3).

In the following sections, we use this expression of spectral efficiency to calculate total cell data rate for the three scheduling schemes.

3.1.1. Equal data rate

While considering equal data rate, users are assigned the bandwidth in a way that resultant data rate for every user, D_u, is the same. As SINR and spectral efficiency depend on r, higher the distance of a user from BS, lower is the available spectral efficiency and thus higher is the bandwidth (or number of subcarriers) allocated to it. Let $W_u(r)$ be the bandwidth allocated

Table 1
Total cell data rate ($D_{T,IFR1}$) versus η (IFR reuse 1, bandwidth = 10 MHz, equal data rate).

η	$D_{T,IFR1}$ (Mbps)		Difference (%)
	Fluid model	Simulation	
2.5	6.62	7.43	10.9
2.6	7.83	8.26	5.21
2.7	9.01	9.08	0.77
2.8	10.16	9.89	2.73
3	12.4	11.6	6.9
3.2	14.5	13.2	9.85
3.3	15.5	13.9	11.51

by the scheduler to a user at distance r from the BS. User data rate, D_u, can now be written for any r as:

$$D_u = W_u(r)C(r), \tag{5}$$

under the constraint that total cell bandwidth W cannot be exceeded. Total bandwidth used in a cell is thus given as:

$$W = 12\int_0^{\pi/6}\int_0^{R_c/\cos\theta} W_u(r)\rho_u\, r\, \mathrm{d}r\, \mathrm{d}\theta. \tag{6}$$

Integration is done over the shaded triangular region in Fig. 3 and multiplied by twelve to obtain the result over the entire hexagonal cell.

If N_u is the number of users in a cell, user density is $\rho_u = N_u/(2\sqrt{3}R_c^2)$. Using Eqs. (6) and (5), value of ρ_u and variable transformation r to x, user data rate is given as:

$$D_u = \frac{\sqrt{3}W/6}{N_u\int_0^{\pi/6}\int_0^{1/\cos\theta}\frac{x}{C_{IFR1}(x)}\,\mathrm{d}x\,\mathrm{d}\theta},$$

where $C_{IFR1}(x)$ is given by Eq. (4).

Since all users receive same data rate and there are N_u users in the cell, total cell data rate is $D_{T,IFR1} = N_uD_u$ and can be written using previous result as:

$$D_{T,IFR1} = \frac{\sqrt{3}W/6}{\int_0^{\pi/6}\int_0^{1/\cos\theta}\frac{x}{C_{IFR1}(x)}\,\mathrm{d}x\,\mathrm{d}\theta}. \tag{7}$$

A worth noting observation regarding Eq. (7) is that the total cell data rate neither depends upon the number of users in the cell nor upon the value of R_c.

The change of variables $\theta = z$ and $x = \frac{y}{\cos z}$, whose Jacobian is $\left|\frac{\partial(\theta,x)}{\partial(z,y)}\right| = \left|\frac{1}{\cos z}\right|$, provides the equivalent equation:

$$D_{T,IFR1} = \frac{\sqrt{3}W/6}{\int_0^{\pi/6}\int_0^{1}\frac{y/\cos z}{\cos z C_{IFR1}(y/\cos z)}\,\mathrm{d}y\,\mathrm{d}z}.$$

To compare the above results with those of simulations, parameters of Section 2 are used. We set the available network bandwidth to $W = 10$ MHz and the number of users per cell to $N_u = 30$ in simulations. In Table 1, total cell data rate $D_{T,IFR1}$ with both the fluid model (Eq. (7)) and simulations, for various values of η, are given. The best agreement is for $\eta = 2.7$, while the difference remains below 10% for η between 2.6 and 3.2. The user data rate (D_u) can be easily obtained by dividing the total cell data rate (i.e., $D_{T,IFR1}$ in this case) by number of users (N_u) in the cell. To avoid the complexity of calculating double integral, it is also possible to integrate $W_u(r)$ over a disk, whose area equals the hexagon area. Such a disk has a radius $R_e = aR_c$, where $a = \frac{\sqrt{2\sqrt{3}}}{\pi}$. Using this approach, total cell data rate can be approximated as:

$$D_{T,IFR1} \approx \frac{\sqrt{3}W/\pi}{\int_0^{a}\frac{x}{C(x)}\,\mathrm{d}x}. \tag{8}$$

For value of $\eta = 3$ and $W = 10$ MHz, data rates obtained with Eqs. (7) and (8) are found to be 12.4 Mbps and 12.6 Mbps respectively with a difference of only 1.6%.

3.1.2. Equal bandwidth

Equal bandwidth means that all users are assigned the same bandwidth whatever the spectral efficiency is available to them. Since users close to BS benefit from higher spectral efficiency, they will attain a higher data rate as compared to users at cell edge. Let W_u denote the bandwidth allocated to each user such that $W = N_uW_u$. Data rate of a user at a distance r is

Table 2
Total cell data rate ($D_{T,IFR1}$) versus η (IFR reuse 1, bandwidth = 10 MHz, equal bandwidth).

η	$D_{T,IFR1}$ (Mbps)		Difference (%)
	Fluid model	Simulation	
2.5	12.2	13	5.92
2.6	14.2	14.3	0.76
2.7	16.1	15.8	1.86
2.8	18	17.3	4.28
3	21.6	20.1	7.3
3.2	25.1	22.7	10.33
3.3	26.8	24.5	9.43

then given as:

$$D_u(r) = W_u C(r), \tag{9}$$

total data rate can then be obtained by integrating the user data rates over cell surface:

$$D_{T,IFR1} = 12 \int_0^{\pi/6} \int_0^{R_c/\cos\theta} D_u(r) \rho_u \, r \, \mathrm{d}r \, \mathrm{d}\theta, \tag{10}$$

using Eq. (9), user density $\rho_u = N_u/(2\sqrt{3}R_c^2)$, user bandwidth $W_u = N_u/W$ and transformation of variable r to x, we get:

$$D_{T,IFR1} = \frac{6W}{\sqrt{3}} \int_0^{\pi/6} \int_0^{1/\cos\theta} x C_{IFR1}(x) \, \mathrm{d}x \, \mathrm{d}\theta. \tag{11}$$

The simulation and fluid model results are compared in Table 2.

3.1.3. Opportunist

In opportunist scheduling, user experiencing the greatest SINR is assigned all the resources and the rest of the users receive no resources at all. In light of assumptions considered in this paper, user closest to the BS will have the maximum SINR value. To calculate the total cell data rate for opportunist scheduling, we require PDF (probability density function) of the distance, X, of the user nearest to the BS. For N_u users in the cell, the CDF (cumulative distribution function) of X is given by:

$$F_X(r) = p[X \le r] = 1 - p[X > r] = 1 - (1 - \pi r^2/2\sqrt{3}R_c^2)^{N_u},$$

and its PDF can be obtained by differentiating the CDF:

$$p_{X,IFR}(r) = \frac{\pi N_u r}{\sqrt{3}R_c^2} \left(1 - \frac{\pi r^2}{2\sqrt{3}R_c^2}\right)^{N_u - 1},$$

with change of variable r to x, the PDF for IFR over small distance dx can be rewritten as:

$$p_{X,IFR}(x)\mathrm{d}x = \frac{\pi N_u x}{\sqrt{3}} \left(1 - \frac{\pi x^2}{2\sqrt{3}}\right)^{N_u - 1} \mathrm{d}x, \tag{12}$$

taking into account the circular disk of radius $R_e = aR_c$ with $a = \frac{\sqrt{2\sqrt{3}}}{\pi}$ (refer Section 2) the average cellular spectral efficiency for opportunist scheduling can be calculated using the following equation:

$$\bar{C}_{IFR1} = \int_0^a C_{IFR1}(x) p_{X,IFR}(x) \, \mathrm{d}x.$$

Finally total cell data rate is written as:

$$D_{T,IFR1} = W \bar{C}_{IFR1}.$$

To verify this approach, simulations are carried out with $N_u = 30$. The results of simulation and model are given in Table 3 with maximum difference equal to 5.9%.

3.2. IFR with reuse K

For IFR with reuse higher than one, analytical study is very similar to the previous one. The difference lies in the fact that only co-channel BS are considered in interference calculation and thus the half distance between base stations and BS density have to be modified. As a consequence, previous analysis results are still valid provided that R_c is replaced by $\sqrt{K}R_c$ and BS density is divided by K, i.e., ρ_{BS} is replaced by ρ_{BS}/K. Hence, using Eq. (2) and this new half distance between BS, SINR is given as:

$$\gamma(r) = \frac{r^{-\eta}(\eta - 2)}{2\pi \cdot \frac{\rho_{BS}}{K}(2\sqrt{K}R_c - r)^{2-\eta}}. \tag{13}$$

Table 3
Total cell data rate ($D_{T,IFR1}$) versus η (IFR reuse 1, bandwidth = 10 MHz, opportunist).

η	$D_{T,IFR1}$ (Mbps)		Difference (%)
	Fluid model	Simulation	
2.5	56.6	56.9	0.48
2.6	62.8	61.6	1.95
2.7	68.5	66.5	3
2.8	74	71.5	3.6
3	84.5	80.3	5.2
3.2	94.4	89.2	5.9
3.3	99.3	93.8	5.8

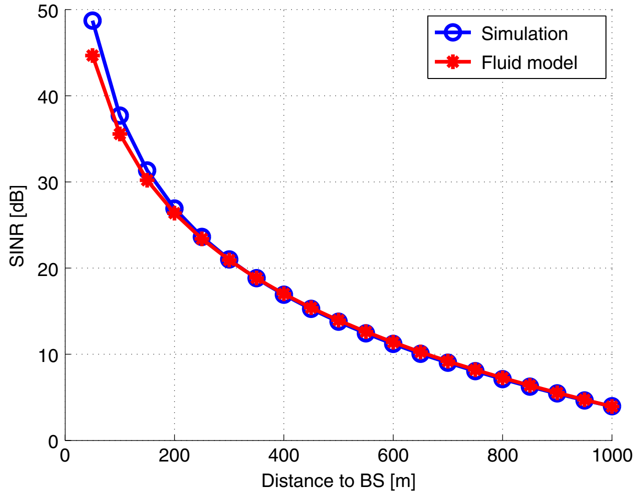

Fig. 4. SINR versus distance to BS for IFR with reuse 3.

Using the same distance normalization as before (leading to the transformation of variable r to x) and after few manipulations, SINR can be written as:

$$\gamma_{IFRK}(x) = \frac{K\sqrt{3}}{\pi}(\eta - 2)(2\sqrt{K} - x)^{-2}(2\sqrt{K}/x - 1)^{\eta}. \tag{14}$$

Hence, spectral efficiency (in bps/Hz) for IFR reuse K can be given as:

$$C_{IFRK}(x) = \log_2[1 + \gamma_{IFRK}(x)]. \tag{15}$$

To validate the above approach, reuse 3 is considered as an example. Plot of SINR versus distance to BS for reuse 3 case, for both fluid model and simulation, is shown in Fig. 4. As expected SINR is higher than for reuse 1. However, bandwidth per cell equals one third the network bandwidth. Again, both analysis and simulation provide similar results. The fluid model is thus accurate not only for reuse 1 networks but also for higher reuse factors provided the parameters are adjusted.

As far as total cell data rate for three scheduling schemes is concerned, method used for IFR reuse 1 is still valid provided that $C_{IFR1}(x)$ is replaced by C_{IFR3} (Eq. (15)) and cell bandwidth is divided by 3, in all calculations. Values of total cell data rate for fluid model and simulations are shown in Tables 4–6. In all cases, the difference between simulation and fluid model remains below 10% for η between 2.6 and 3.5.

4. Fractional frequency reuse (FFR)

An example of FFR scenario is depicted in Fig. 5. As can be seen in the figure, cell space is divided into two regions, inner and outer. Inner region is a circular disk with radius $R_0 \leq R_c$ and the rest of the hexagon forms the outer region. Bandwidth is allocated to inner and outer in such a way that former incorporates frequency reuse 1 while the latter applies frequency reuse 3. As can be seen in Fig. 5, the network bandwidth W is equal to $W_0 + W_1 + W_2 + W_3$. It is also considered that $W_1 = W_2 = W_3$.

SINR versus distance with $R_0 = 0.7R_c$ for fluid model and simulation is given in Fig. 6. As expected FFR scheme improves radio quality at cell edge. Moreover, the results follow the previous positive trend, i.e., fluid model and simulations are in conformity.

Now we derive the expressions for total cell data rate assuming equal data rate, equal bandwidth and opportunist scheduling schemes. We also estimate the optimized inner region radius.

Table 4
Total cell data rate ($D_{T,IFR3}$) versus η (IFR reuse 3, BW = 10/3 MHz, equal data rate).

η	$D_{T,IFR3}$ (Mbps)		Difference (%)
	Fluid model	Simulation	
2.5	6.4	7.2	11.11
2.6	7.55	7.95	5.03
2.7	8.66	8.73	0.8
2.8	9.74	9.55	1.99
3	11.8	11.2	5.36
3.1	12.8	12.0	6.67
3.2	13.8	12.8	7.81
3.5	16.7	15.2	9.87

Table 5
Total cell data rate ($D_{T,IFR3}$) versus η (IFR reuse 3, bandwidth = 10/3 MHz, equal bandwidth).

η	$D_{T,IFR3}$ (Mbps)		Difference (%)
	Fluid model	Simulation	
2.5	8.38	9.04	7.38
2.6	9.63	9.91	2.81
2.7	10.8	10.76	0.71
2.8	12.	11.7	3.04
3	14.2	13.4	5.9
3.1	15.3	14.4	6.55
3.2	16.4	15.2	7.46
3.5	19.4	17.8	8.8

Table 6
Total cell data rate ($D_{T,IFR3}$) versus η (IFR reuse 3, bandwidth = 10/3 MHz, opportunist).

η	$D_{T,IFR3}$ (Mbps)		Difference (%)
	Fluid model	Simulation	
2.5	25.4	26	2.2
2.6	27.8	28.0	0.7
2.7	30	29.6	1.3
2.8	32.2	31.5	2
3	36.2	34.7	4.3
3.1	38.2	36.6	4.4
3.2	40.1	38.2	5.1
3.5	45.7	43.4	5.4

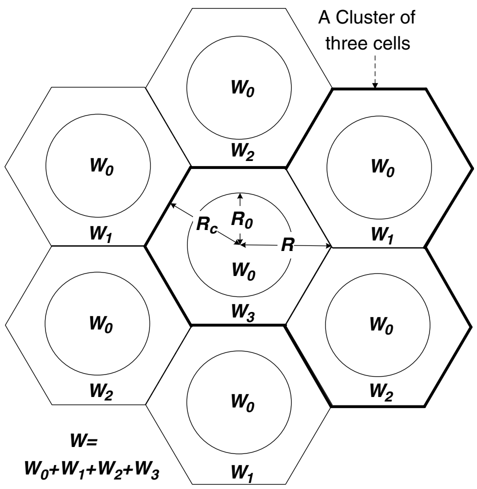

Fig. 5. Fractional Frequency Reuse (FFR) case. Bandwidth W_0 is deployed with reuse 1 in the inner regions, while W_1, W_2 and W_3 are deployed with reuse 3 in outer regions.

4.1. Equal data rate

To carry out total cell data rate, we first consider the inner circular region. Since for this region, frequency reuse is 1, the expression of SINR is given by Eq. (2) or equivalently by Eq. (3). Once again, it is considered that users are uniformly

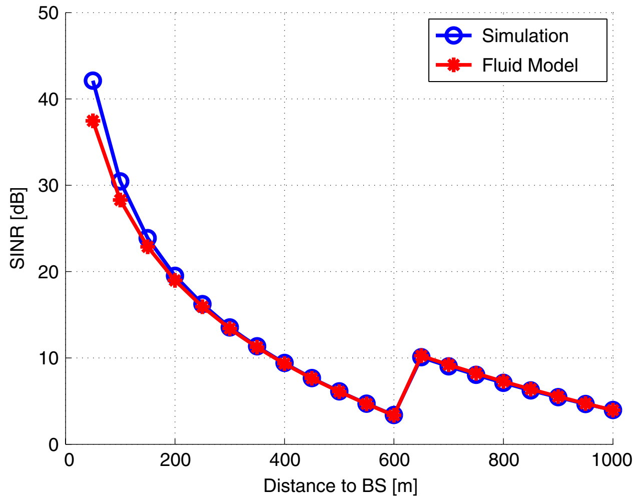

Fig. 6. SINR versus distance to BS for FFR with $R_0 = 0.7R_c$.

distributed in the cell space with $\rho_u = N_u/2\sqrt{3}R_c^2$. Since it is a circular region, the bandwidth of inner region is given as:

$$W_0 = \int_0^{R_0} W_u(r)\rho_u\, 2\pi r\, \mathrm{d}r. \tag{16}$$

After replacing ρ_u by its value, transformation of variable r to x and using Eq. (5), we get

$$W_0 = \frac{\pi}{\sqrt{3}} D_u N_u \int_0^{R_0/R_c} \frac{x}{C_{IFR1}(x)}\, \mathrm{d}x,$$

where $C_{IFR1}(x)$ is given by Eq. (4). Let I_0 be the integral in the previous expression, so that $W_0 = \pi/\sqrt{3} I_0 D_u N_u$.

Let us now consider the outer area, which applies reuse 3. SINR for reuse 3 is given by Eq. (13) or equivalently by Eq. (14). In order to calculate the total bandwidth used in the outer region, double integral used in Eq. (6) is applied. With change of limits and replacing $W_u(r)$ by $W_{1,u}(r)$ we get:

$$W_1 = 12 \int_0^{\pi/6} \int_{R_0}^{R_c/\cos\theta} W_{1,u}(r)\rho_u\, r\, \mathrm{d}r\, \mathrm{d}\theta,$$

where $W_{1,u}(r)$, assuming equal data rate scheduling, is given as: $W_{1,u}(r) = D_u C_{IFR3}(r)$. After replacing ρ_u by its value and transformation of variable r to x, we get

$$W_1 = \frac{6}{\sqrt{3}} D_u N_u \int_0^{\pi/6} \int_{R_0/R_c}^{1/\cos\theta} \frac{x}{C_{IFR3}(x)}\, \mathrm{d}x\, \mathrm{d}\theta. \tag{17}$$

Let I_1 be the double integral in the previous expression, so that $W_1 = \frac{6}{\sqrt{3}} I_1 D_u N_u$.

Considering the fact that total network bandwidth is W with $W = W_0 + W_1 + W_2 + W_3$ and $W_1 = W_2 = W_3$ we can write: $W = W_0 + 3 \times W_1$. Finally using Eqs. (16) and (17) and keeping in view that $D_T = D_u N_u$, we get expression of the total cell data rate $D_{T,FFR}$ for FFR case:

$$D_{T,FFR} = \frac{\sqrt{3}W}{\pi I_0 + 18 I_1}. \tag{18}$$

Total cell data rate calculation shows that fluid model and simulation differ by 5.6% with values of 13.2 Mbps and 12.5 Mbps respectively for 10 MHz of network bandwidth. Fig. 7 shows the total cell data rate as a function of the inner cell radius R_0. Both fluid model and simulations provide an optimum value of approximately 757 m.

4.2. Equal bandwidth

To calculate cell data rate in this case, we adopt the same approach as was used in Section 3.1.2 while considering $N_u W_u = W_0 + W_1$. By integrating the user data rate over inner circular region (using frequency reuse 1), total data rate of inner region is given as:

$$D_{T,Inner} = \frac{\pi(W_0 + W_1)}{\sqrt{3}} \int_0^{R_0/R_c} x C_{IFR1}(x)\, \mathrm{d}x. \tag{19}$$

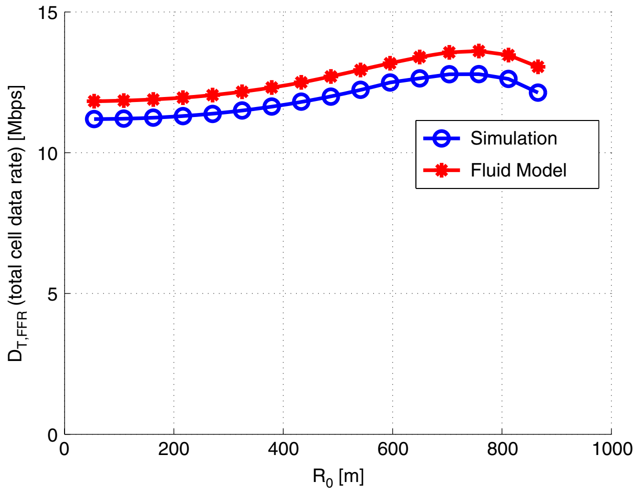

Fig. 7. $D_{T,FFR}$ (total cell data rate) versus radius of inner region with equal data rate scheduling for FFR scheme. Maximum value occurs at $R_0 = 757$ m approx.

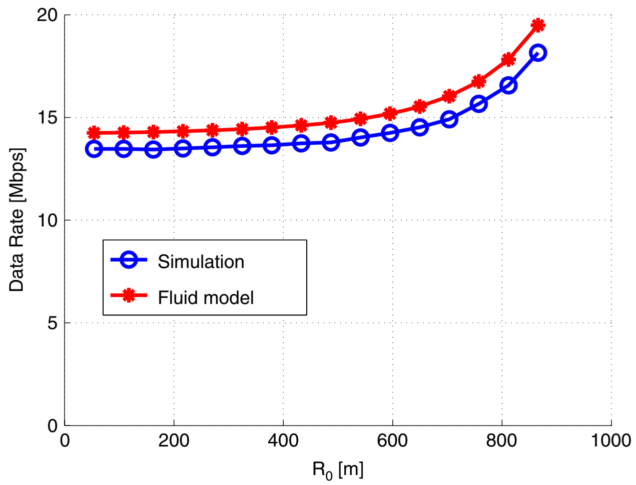

Fig. 8. $D_{T,FFR}$ (total cell data rate) versus radius of inner region with equal bandwidth scheduling for FFR scheme. Maximum value occurs at $R_0 = R_c$.

Similarly, assuming frequency reuse 3 for the outer region, total data rate of outer region is:

$$D_{T,Outer} = \frac{6(W_0 + W_1)}{\sqrt{3}} \int_0^{\pi/6} \int_{R_0/R_c}^{1/\cos\theta} xC_{IFR3}(x)\, \mathrm{d}x\, \mathrm{d}\theta, \tag{20}$$

and total cell data rate is the sum of inner and outer region data rates:

$$D_{T,FFR} = D_{T,Inner} + D_{T,Outer}. \tag{21}$$

Since this scheduling scheme assigns equal resources to all users (whether located in inner or outer region), the ratio of W_0 to W_1 should be proportional to number of users in two regions. But as we have assumed that users are uniformly distributed in cell space, this ratio should be equal to ratio of inner region area to outer region area:

$$\frac{W_1}{W_0} = \frac{2\sqrt{3}R_c^2}{\pi R_0} - 1, \tag{22}$$

and since $W_0 + 3W_1 = W$, it can be shown that:

$$W_1 = \frac{2\sqrt{3}R_c^2 - \pi R_0^2}{6\sqrt{3}R_c^2 - 2\pi R_0^2} W. \tag{23}$$

It can be made out from Eq. (23) that for every value of R_0, there is a specific value of W_1 and hence W_0. For different values of R_0, total cell data rate has been plotted in Fig. 8. It can be seen that maximum value of total cell data rate is for $R_0 = R_c$.

Tables 2 and 5 have shown that IFR1 provides higher data rates than IFR3. In FFR, increasing R_0 and thus the bandwidth W_0 used with reuse 1, makes FFR closer to IFR1. On the contrary, decreasing R_0 makes FFR closer to IFR3. As a consequence, total cell data rate is maximum for the highest value of R_0.

4.3. Opportunist

For opportunist scheduling in FFR case, we assume that two users are simultaneously scheduled in a cell such that one user having the greatest SINR among inner region users and other one having the highest SINR among outer region users. If there is no user in any of the regions, bandwidth of that region goes unallocated. Following the methodology of Section 3.1.3, for the inner region, PDF of the user's (nearest to the BS) distance, knowing there are $N_{u,i}$ users located in the inner region is given as:

$$p_{X,inner|N_{u,i}}(r) = \frac{2rN_{u,i}}{R_0^2}\left(1-\frac{r^2}{R_0^2}\right)^{N_{u,i}-1},$$

or with substitution of r by x, the same PDF over small distance dx can be written as:

$$p_{X,inner|N_{u,i}}(x)\,\mathrm{d}x = \frac{2xN_{u,i}}{(R_0/R_c)^2}\left(1-\frac{x^2}{(R_0/R_c)^2}\right)^{N_{u,i}-1}\mathrm{d}x.$$

Hence, the average spectral efficiency of inner region, given that there are $N_{u,i}$ located inside it, can be expressed by the following integral:

$$\bar{C}_{FFR,inner|N_{u,i}} = \int_0^{R_0/R_c} C_{IFR1}(x)p_{X,inner|N_{u,i}}(x)\,\mathrm{d}x.$$

Similarly for the outer region, PDF of the user's (nearest to the BS) distance, knowing there are $N_{u,i}$ users located in the inner region is given as:

$$p_{X,outer|N_{u,i}}(r) = \frac{2\pi(N_u-N_{u,i})r}{2\sqrt{3}R_c^2-\pi R_0^2}\left(1-\frac{\pi r^2-\pi R_0^2}{2\sqrt{3}R_c^2-\pi R_0^2}\right)^{N_u-N_{u,i}-1},$$

where $(N_u - N_{u,i})$ is the number of users in the outer region.

Once again with change of variable r to x, the PDF over small distance dx for outer region can be expressed as:

$$p_{X,outer|N_{u,i}}(x)\,\mathrm{d}x = \frac{2\pi(N_u-N_{u,i})x}{2\sqrt{3}-\pi(R_0/R_c)^2}\left(1-\frac{\pi x^2-\pi(R_0/R_c)^2}{2\sqrt{3}-\pi(R_0/R_c)^2}\right)^{N_u-N_{u,i}-1}\mathrm{d}x,$$

and the average spectral efficiency for the outer region such that there are $N_{u,i}$ users in the inner region is given by the following equation:

$$\bar{C}_{FFR,outer|N_{u,i}} = \int_{R_0/R_c}^{a} C_{IFR3}(x)p_{X,outer|N_{u,i}}(x)\,\mathrm{d}x.$$

Note that in this latter equation, we approximate the hexagon by a disk of radius R_e. Finally, averaging the sum of data rates (of inner and outer regions) for all possible values of $N_{u,i}$ results in total cell data rate for FFR case:

$$D_{T,FFR} = \sum_{N_{u,i}=0}^{N_u}(W_0\bar{C}_{FFR,inner|N_{u,i}} + W_1\bar{C}_{FFR,outer|N_{u,i}})P[N_{u,i}],$$

where $P[N_{u,i}]$ is the probability that there are $N_{u,i}$ out of N_u users in the inner region:

$$P[N_{u,i}] = \left(\frac{\pi R_0^2}{2\sqrt{3}R_c^2}\right)^{N_{u,i}}\left(1-\frac{\pi R_0^2}{2\sqrt{3}R_c^2}\right)^{N_u-N_{u,i}}\binom{N_u}{N_{u,i}}.$$

The total cell data rate (for FFR scheme) as a function of different values of W_1 and R_0 is shown in Fig. 9. Maximum value of total cell data rate can be observed for a value of $W_1 = 11$ kHz (i.e., one subcarrier) and $R_0 = 487$ m for both the simulation and fluid model. The maximum difference between simulation and analytical model results for all values of W_1 and R_0 is found to be 6.7%.

5. Two level power control (TLPC)

In previous section, we discussed the concept of FFR in OFDMA and we have shown that SINR could be improved by using a reuse 3 pattern in cell outer regions. With FFR, it is however not possible to use full network bandwidth in a cell, which reduces the overall cell bandwidth.

To overcome this drawback, it is possible to adopt a reuse 1 pattern while using a two level power control (TLCP) mechanism to improve the radio quality in the outer region. The TLPC scheme is shown in Fig. 10. Total bandwidth in a

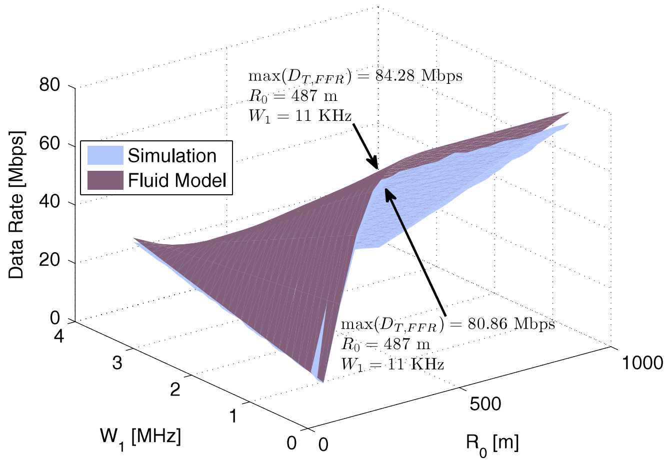

Fig. 9. $D_{T,FFR}$ (total cell data rate) versus radius of inner region and versus bandwidth allocated in the outer region with opportunist scheduling for FFR scheme. Maximum value occurs at $R_0 = 487$ m and $W_1 = 11$ kHz.

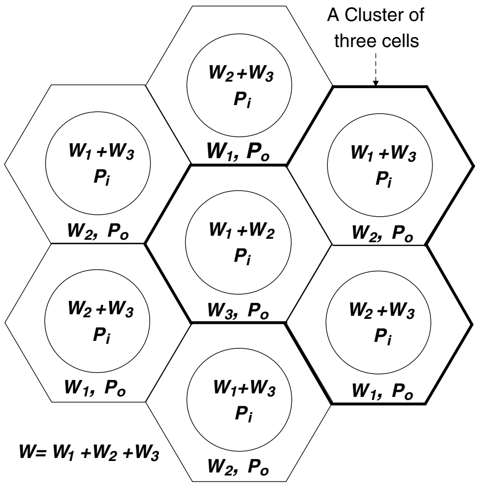

Fig. 10. Two level power control case. Bandwidth W is partitioned into three equal parts, i.e., $W_1 = W_2 = W_3$.

cell (equal to network bandwidth) is divided into three equal parts: two parts allocated to inner region and one to the outer region. The output power per subcarrier in the inner region is P_i and that in the outer region is P_o. These two values of power are related as: $P_o = \delta P_i$, such that $\delta \geq 1$. The three spectrum parts W_1, W_2 and W_3 alternate from cell to cell in such a way that there is a pseudo-reuse 3 scheme in outer regions. Neighboring cells contribute to interference in the outer region but with a reduced power P_i. As a consequence, the total network bandwidth is used in every cell but interference is expected to be reduced in outer regions.

Let us calculate SINR for inner and outer region of this two level power control network. For a user in the outer region (using e.g. W_3 in the center cell in Fig. 10), we divide the interference into two categories. One is from the cells using same subcarriers in the outer region and we represent it by I_{outer}. Other is from cells using same subcarriers in the inner region (neighboring cells) and is represented by I_{inner}. Then, SINR for a subcarrier in the outer region can be written as:

$$\frac{1}{\gamma_{TLPC,outer}} = \frac{I_{inner}}{P_o A r^{-\eta}} + \frac{I_{outer}}{P_o A r^{-\eta}}. \tag{24}$$

In order to find the values of I_{inner} and I_{outer}, consider that $\mathcal{B}_{outer}$ represents the set of BS causing I_{outer}. For a user u in outer region of a cell b, I_{outer} is given as:

$$I_{outer} = P_o A \sum_{j=1, j\in\mathcal{B}_{outer}}^{N_{BS}} r_{j,u}^{-\eta}. \tag{25}$$

As outer regions of BS in $\mathcal{B}_{outer}$ form together a reuse 3 scheme, the second term of right-hand side of Eq. (24) is simply $1/\gamma_{IFR3}$.

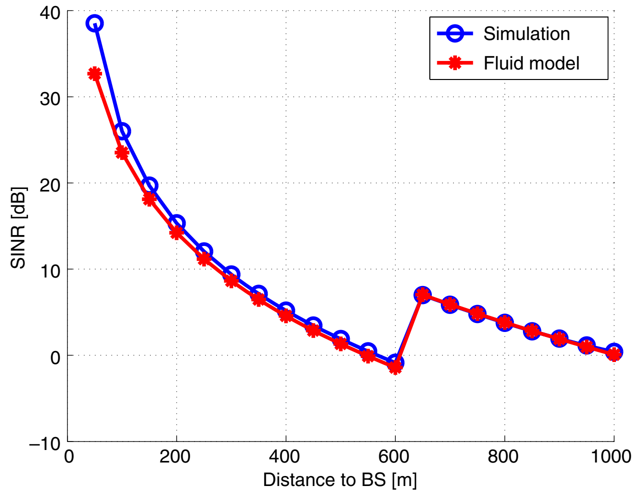

Fig. 11. SINR versus distance to BS for TLPC scheme with $R_0 = 0.7R_c$ and $\delta = 5$.

Adding up the interference from all network cells, I_{inner} can be written as:

$$I_{inner} = P_i A \sum_{j=1, j\neq b}^{N_{BS}} r_{j,u}^{-\eta} - P_i A \sum_{j=1, j\in \mathcal{B}_{outer}}^{N_{BS}} r_{j,u}^{-\eta}. \tag{26}$$

Thus, considering $\delta = P_o/P_i$:

$$\frac{I_{inner}}{P_o A r^{-\eta}} = \frac{1}{\delta}\frac{1}{\gamma_{IFR1}} - \frac{1}{\delta}\frac{1}{\gamma_{IFR3}}. \tag{27}$$

Combining previous results, we can rewrite Eq. (24) as:

$$\frac{1}{\gamma_{TLPC,outer}} = \frac{1}{\delta}\frac{1}{\gamma_{IFR1}} + \left(1 - \frac{1}{\delta}\right)\frac{1}{\gamma_{IFR3}}. \tag{28}$$

Now we find out SINR expression for inner region. Consider the central cell of Fig. 10, in which W_1 and W_2 are allocated to inner region and W_3 is used in the outer region. A user in inner region will be allocated a subcarrier that will either belong to W_1 or W_2. If we look at the bandwidth utilized in the six neighboring cells of center cell, we notice that out of six, three are transmitting on the same subcarrier with power P_o, while the other three with P_i. Hence, SINR for this inner region subcarrier can be approximated while considering that neighboring cells transmit with average power $(P_i + P_o)/2$.

$$\gamma_{TLPC,inner}(r) \approx \frac{P_i A r_{b,u}^{-\eta}}{\frac{P_o+P_i}{2} A \sum_{j=1,j\neq b}^{N_{BS}} r_{j,u}^{-\eta}} = \frac{2}{1+\delta}\gamma_{IFR1}. \tag{29}$$

Using the values of SINR for outer and inner regions, spectral efficiencies for two regions are given in Eqs. (30) and (31).

$$C_{TLPC,inner} = \log_2(1 + \gamma_{TLPC,inner}), \tag{30}$$

$$C_{TLPC,outer} = \log_2(1 + \gamma_{TLPC,outer}). \tag{31}$$

To verify the above results, SINR versus distance to BS (with $R_0 = 0.7R_c$ and $\delta = 5$) is given in Fig. 11. As expected, radio quality is improved in outer region with TLPC compared to the IFR1 case in a similar way does the FFR. Let us now compare total cell data rates.

In order to calculate data rate for inner and outer regions for three scheduling schemes, we assume that in Fig. 10, $W_1 = W_2 = W_3$. We start with equal data rate scheduling scheme.

5.1. Equal data rate

Using the similar approach of Section 4, we can write:

$$W_1 + W_2 = \frac{2W}{3} = \frac{\pi}{\sqrt{3}} D_{u,inner} N_u \int_0^{R_0/R_c} \frac{x dx}{C_{TLPC,inner}(x)},$$

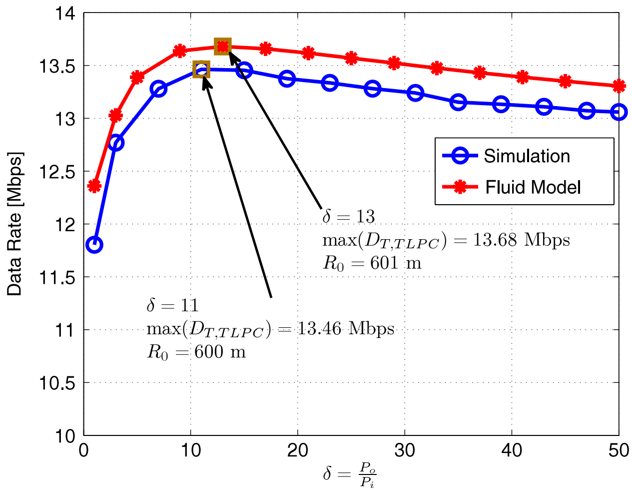

Fig. 12. Total cell data rate versus different values of δ with equal data rate scheduling for TLPC scheme.

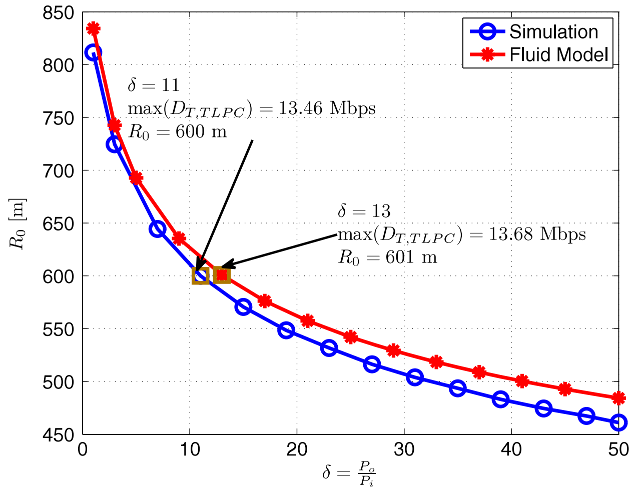

Fig. 13. R_0 (radius of inner region that guarantees equal data rate among users) versus different values of δ for TLPC scheme.

and

$$W_3 = \frac{W}{3} = \frac{6}{\sqrt{3}} D_{u,outer} N_u \int_0^{\pi/6} \int_{R_0/R_c}^{1/\cos\theta} \frac{x}{C_{TLPC,outer}(x)} \,\mathrm{d}x\,\mathrm{d}\theta.$$

Using the above two equations, we can write the ratio between data per user for inner and outer regions as:

$$\frac{D_{u,inner}}{D_{u,outer}} = \frac{12}{\pi} \frac{\int_0^{\pi/6} \int_{R_0/R_c}^{1/\cos\theta} \frac{x}{C_{TLPC,outer}(x)} \,\mathrm{d}x\,\mathrm{d}\theta}{\int_0^{R_0/R_c} \frac{x}{C_{TLPC,inner}(x)} \,\mathrm{d}x}.$$

Now, if we assume an equal data rate scheduler, $\frac{D_{u,inner}}{D_{u,outer}}$ should be equal to one. For a given value of δ, there exists a unique value of R_0 for which the above condition is satisfied. In Fig. 12, total cell data rate satisfying equal data rate scheme has been plotted for various values of δ. It is clear that for small values of δ, total cell data rate increases with increasing values of δ. The total cell data rate attains its maximum value of 13.68 Mbps for $\delta = 13.2$. Beyond $\delta = 13.2$ (or 11.2 dB), the total cell data rate starts decreasing. The corresponding values of R_0 for these total cell data rates are given in Fig. 13. The figure shows that R_0 is a decreasing function of δ. The value of R_0 corresponding to maximum value of cell data rate is approximately 600 m.

5.2. Equal bandwidth

With equal bandwidth allocation, the bandwidth of inner and outer regions should be proportional to areas of the two regions (cf. Section 4.2) and since for TLPC schemes bandwidth of inner and outer regions are fixed, there exists a unique

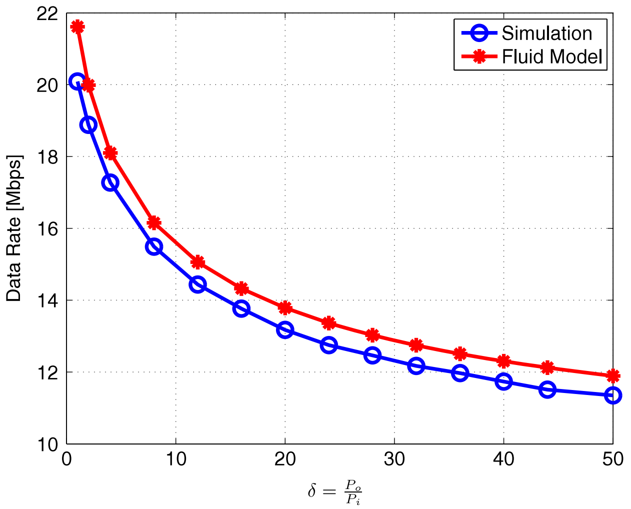

Fig. 14. Total cell data rate versus different values of δ with equal bandwidth scheduling for TLPC scheme.

value of R_0 satisfying the two conditions.

$$\frac{W_3}{W_1+W_2} = \frac{2\sqrt{3}R_c^2}{\pi R_0^2} - 1,$$

with $W_1 = W_2 = W_3 = W/3$,

$$R_0 = \frac{2}{\sqrt{\pi\sqrt{3}}}R_c.$$

Now the total data rate of inner region is given by Eq. (32):

$$D_{T,Inner} = \frac{\pi W}{\sqrt{3}} \int_0^{R_0/R_c} xC_{TLPC,inner}(x)\,\mathrm{d}x. \tag{32}$$

Similarly total data rate for outer region is given as:

$$D_{T,Outer} = \frac{6W}{\sqrt{3}} \int_0^{\pi/6} \int_{R_0/R_c}^{1/\cos\theta} xC_{TLPC,outer}(x)\,\mathrm{d}x\,\mathrm{d}\theta. \tag{33}$$

Total cell data rate is the sum of total data rates of two regions:

$$D_{T,TLPC} = D_{T,Inner} + D_{T,Outer}. \tag{34}$$

A comparison of simulation and fluid model $D_{T,TLPC}$ values, as function of δ values, is shown in Fig. 14 which shows a close proximity between the two curves.

5.3. Opportunist

The computation of cell data rate is similar to the method used in Section 4.3. However, in this case, inner bandwidth is $2W/3$, outer bandwidth is $W/3$ and average spectral efficiency for TLPC is used:

$$D_{T,TLPC} = \sum_{N_{u,i}=0}^{N_u} \left(\frac{2W}{3}\bar{C}_{TLPC,inner|N_{u,i}} + \frac{W}{3}\bar{C}_{TLPC,outer|N_{u,i}} \right) P[N_{u,i}].$$

The results of simulation and fluid model are compared in Fig. 15. Total cell data rates are plotted as functions of R_0 and δ. The maximum cell data rate is found to be for $R_0 = 270$ m and $\delta = 1$ for both the simulation and fluid model. The maximum difference between the values of total cell data rates with simulation and fluid model is 7.23%.

6. Comparison of reuse schemes and scheduling policies

In previous sections, we have established through validation that analytical approach based on the fluid model can be used for IFR, FFR and TLPC schemes while considering three different scheduling types: equal data rate, equal bandwidth and opportunist. In this section, we present a comparison between these three reuse schemes and the three scheduling policies by applying fluid model.

If we look at Fig. 16, it can be deduced that IFR with reuse 3 shows the best performance in terms of SINR values. IFR reuse 1 is much lower than IFR reuse 3 in terms of radio quality. FFR exactly follows IFR reuse 1 curve until R_0 and IFR reuse

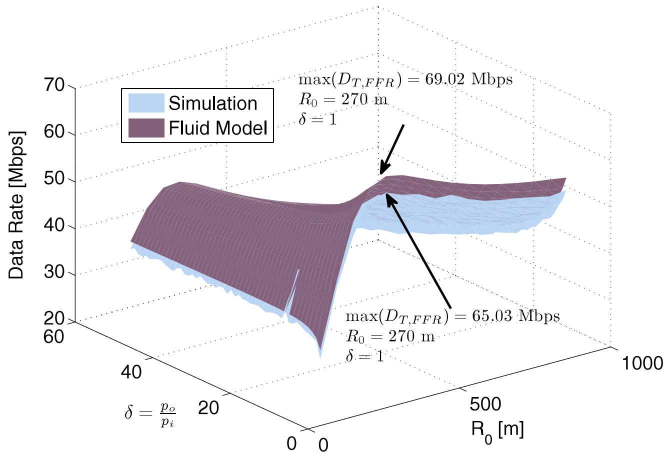

Fig. 15. $D_{T,TLPC}$ (total cell data rate) versus radius of inner region and δ with opportunist scheduling for TLPC scheme. Maximum value occurs at $R_0 = 270$ m and $\delta = 1$.

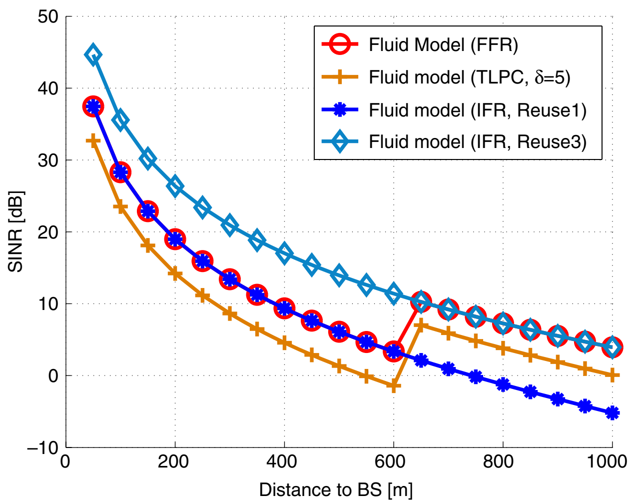

Fig. 16. SINR versus distance to BS for three reuse schemes.

Table 7
Total cell data rate (D_T) comparison of three reuse schemes and three scheduling policies.

Frequency reuse scheme	D_T (Mbps)		
	Equal data rate	Equal bandwidth	Opportunist ($N_u = 30$)
FFR	13.61 ($R_0 = 757$ m)	19.5 ($R_0 = R_c$)	84.28 ($W_1 = 11$ kHz, $R_0 = 487$ m)
TLPC	13.68 ($\delta = 13.2$, $R_0 = 600$ m)	21.6 ($\delta = 1$, $R_0 = 742$ m)	69.02 ($\delta = 1$, $R_0 = 270$ m)
IFR, Reuse 1	12.4	21.6	84.5
IFR, Reuse 3	11.8	14.2	36.2

3 onwards. Compared to IFR reuse 1, TLPC improves SINR in outer region at the expense of a degraded radio quality in inner region.

We now compare total cell data rates for all frequency reuse schemes in the presence of three scheduling algorithms. Total cell data rates in FFR may depend upon value of R_0 and W_1. The same applies to TLPC w.r.t. parameters R_0 and δ. For these two schemes, maximum possible value of total cell data rate, based on optimal values of their parameters, has been considered in the comparison. These optimal values are presented aside with values of data rates (see Table 7).

The value of network bandwidth is 10 MHz. The number of users per cell N_u is considered to be thirty in all cases. Path-loss constant η is taken as three. Results of cell data rate are listed in Table 7.

With equal data rate, IFR3 touches the lowest performance although SINR values are greater. This is due to the fact that utilization of network bandwidth per cell is lower as compared to other schemes. TLPC has the maximum value with $\delta = 13.2$ and has a comparable performance w.r.t. FFR (with $R_0 = 757$ m). Hence, by applying TLPC and FFR schemes, we

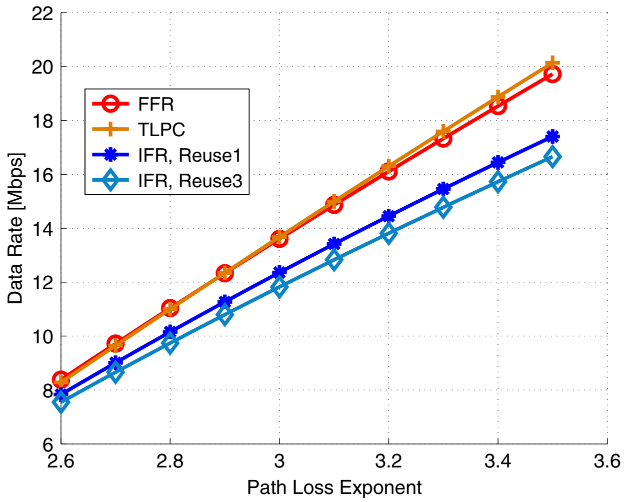

Fig. 17. Data rate versus path-loss exponent with equal data rate scheduling for three reuse schemes.

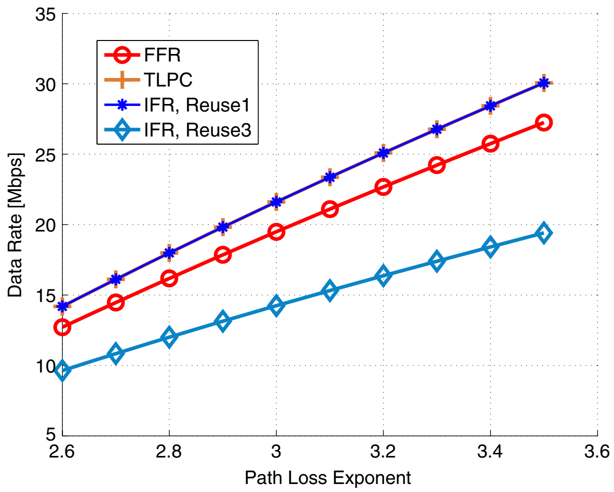

Fig. 18. Data rate versus path-loss exponent with equal bandwidth scheduling for three reuse schemes.

can diminish the problem of reduced radio quality (SINR) for the case of IFR1 in the border region of the cell. At the same time, bandwidth is more efficiently utilized than with IFR3. Due to its simplicity, FFR could be preferred to TLPC with equal data rate scheduling.

An equal bandwidth scheduling aims at improving resource utilization (compared to equal data rate scheduling) while ensuring resource allocation to every user (on the contrary to opportunist scheduling). So, for all reuse schemes, total cell data rate is in between two other schemes. With equal bandwidth, IFR1 achieves the highest cell capacity because it benefits from the usage of total network bandwidth in every cell. Although SINR values are higher with IFR3, this scheme allocates only one third of the total network bandwidth to each cell, this explains again the lower achieved performance.

FFR and TLPC cannot do better than IFR1 and reach their maximum value for a set of parameters that makes them very close to IFR1. With FFR, setting $R_0 = R_c$ makes most of the bandwidth to be used with reuse 1. A higher radio quality at cell border is obtained at the price of a small reduction of the total cell data rate compared to IFR1. With TLPC, setting $\delta = 1$ reduces almost this scheme to IFR1.

Total cell data rate obtained with opportunist scheduling provides an upper bound (for a given number of users) on the cell performance at the price of fairness. Except in TLPC, only the best user is served and gets the whole bandwidth. IFR1 achieves once again the highest cell data rate. FFR tends towards IFR1 with very small bandwidth being allocated to the outer region. The choice of scheduling two users (one in the inner region, one in the outer) reduces the performance of TLPC compared to IFR1 since part of the bandwidth is allocated to a user a bit far from the BS.

Figs. 17–19 show the total cell data rate as a function of the path-loss exponent for the three frequency reuse schemes and the three scheduling policies. It can be noticed that the hierarchy between frequency reuse schemes observed with $\eta = 3$ still holds for η between 2.6 and 3.6. For equal data rate scheduling, the advantage of TLPC over FFR is a bit more

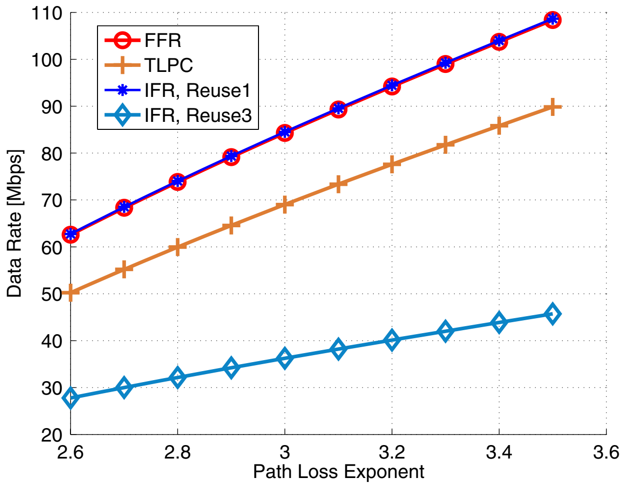

Fig. 19. Data rate versus path-loss exponent with opportunist scheduling for three reuse schemes.

pronounced when η increases. However, the main result is that in all cases, the total cell data rate increases linearly as a function of path-loss exponent.

7. Conclusions

In this paper, we have presented an analytical approach, based on the fluid model, for analyzing OFDMA based networks. We have shown that our proposed technique is very flexible and can be used in different frequency reuse scenarios. We have introduced expressions of SINR and cell data rate for IFR, FFR and TLPC schemes and taking into account equal data rate, equal bandwidth and opportunist scheduling types. We have also validated our technique by comparing its results with those obtained from Monte Carlo simulations. Time required to obtain results with our analytical technique is however much shorter. We have shown that our proposed technique gives a fairly good performance for η values between 2.6 and 3.5 which is a range found in most of the practical scenarios. A comparison of the above three schemes is also provided. For each scheduling type, we have established the frequency reuse scheme which provides the maximum cell data rate.

Acknowledgments

This work was prepared through collaborative participation in the URC: Urban Planning for Radio Communications project, sponsored by the System@tic Paris-Région Cluster.

The authors would also like to thank Trung Dung Nguyen, student at ENST, whose project [14] under the supervision of Philippe Godlewski formed the first step in carrying out this work.

Appendix. Fluid model in OFDMA networks

In this section, we recall the main results of the fluid model and derive the closed-form formula for SIR per subcarrier.

The key modeling step of the fluid model is replacing a given fixed finite number of BS by an equivalent continuum of transmitters which are spatially distributed in the network. This means that the transmitting power is now considered as a continuum field all over the network. In this context, the network is characterized by a user density ρ_u and a base station density ρ_{BS} [9]. We assume that users and BS are uniformly distributed in the network, so that ρ_u and ρ_{BS} are constant. We also assume that all base stations have the same output power per subcarrier P_{Tx}.

We focus on a given cell, a generic subcarrier and consider a round shaped network around this central cell with radius R_{nw}. The half distance between two base stations is R_c (see Fig. A.1 in case of reuse 1).

Let us consider a user u at a distance r_u from its serving base station b. Each elementary surface $z\mathrm{d}z\mathrm{d}\theta$ at a distance z from u contains $\rho_{BS}z\mathrm{d}z\mathrm{d}\theta$ base stations which contribute to $I_{ext,u}$. Their contribution to the external interference is thus $\rho_{BS}z\mathrm{d}z\mathrm{d}\theta P_{Tx}Az^{-\eta}$. We approximate the integration surface by a ring with center u, inner radius $2R_c - r_u$, and outer radius $R_{nw} - r_u$ (see Fig. A.2).

$$I_{ext,u} = \int_0^{2\pi}\int_{2R_c-r_u}^{R_{nw}-r_u} \rho_{BS}P_{Tx}Az^{-\eta}z\mathrm{d}z\mathrm{d}\theta$$
$$= \frac{2\pi\rho_{BS}P_{Tx}A}{\eta-2}\left[(2R_c-r_u)^{2-\eta}-(R_{nw}-r_u)^{2-\eta}\right]. \quad \text{(A.1)}$$

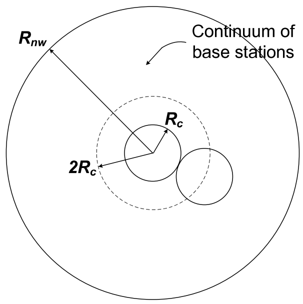

Fig. A.1. Network and cell of interest in the fluid model; the distance between two BS is $2R_c$ and the network is made of a continuum of base stations.

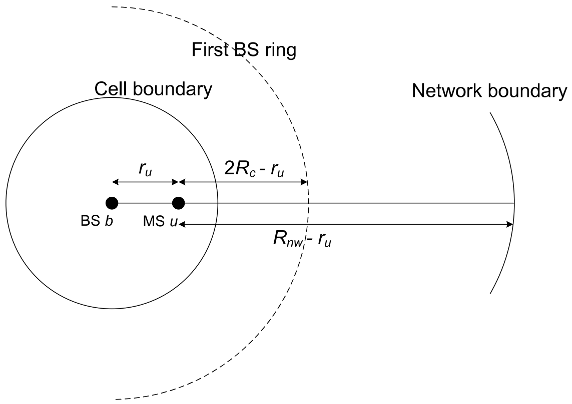

Fig. A.2. Integration limits for interference computation.

So, the SINR $\gamma_u \approx S_{b,u}/I_{ext,u} = P_{Tx}Ar_u^{-\eta}/I_{ext,u}$ can be expressed by:

$$\gamma_u = \frac{r_u^{-\eta}(\eta - 2)}{2\pi \rho_{BS}\left[(2R_c - r_u)^{2-\eta} - (R_{nw} - r_u)^{2-\eta}\right]}. \tag{A.2}$$

Note that γ_u does not depend on the BS output power. This is due to the fact that we assumed a homogeneous network and so all base stations emit the same power on a given subcarrier. In this model, γ only depends on the distance r from the BS and can be defined for each location, so that we can write γ as a function of r i.e., $\gamma(r)$. If the network is large, i.e., R_{nw} is big as compared to R_c, γ_u can be further approximated by:

$$\gamma_u = \frac{r_u^{-\eta}(\eta - 2)}{2\pi \rho_{BS}(2R_c - r_u)^{2-\eta}}. \tag{A.3}$$

The fluid model and the traditional hexagonal model are two simplifications of the reality. None is a priori better than the other but the latter is widely used, especially for dimensioning purposes. That is the reason why comparisons are performed throughout this paper.

Ref. [10] has shown that the considered network size can be finite and can be chosen to characterize each specific local network's environment. This model thus allows us to do the analysis adapted to each zone while taking into account considered zone's specific parameters. Moreover, it can be noticed that the fluid model can be used even for great distances between the base stations.

References

[1] G. Kulkarni, S. Adlakha, M. Srivastava, Subcarrier allocation and bit loading algorithms for OFDMA-based wireless networks, IEEE Transactions on Mobile Computing (2005).
[2] Mobile WiMAX-Part II: A comparative analysis, Tech. Rep., WiMAX Forum, May 2006.
[3] G. Liu, J. Zhu, F. Jiang, B. Zhou, Y. Wang, P. Zhang, Initial performance evaluation on TD-SCDMA long term evolution system, in: Proc. of IEEE VTC Spring, 2006.
[4] M.C. Necker, Local interference coordination in cellular 802.16e networks, in: Proc. of IEEE VTC Fall, 2007.
[5] M.C. Necker, Coordinated fractional frequency reuse, in: Proc. of ACM MSWiM, 2007.
[6] C. He, F. Liu, H. Yang, C. Chen, H. Sun, W. May, J. Zhang, Co-channel interference mitigation in MIMO–OFDM system, in: Proc. of IEEE WiCom, 2007.
[7] C. Tarhini, T. Chahed, On capacity of OFDMA-based IEEE802.16 WiMAX including adaptive modulation and coding (AMC) and inter-cell interference, in: Proc. of IEEE Workshop on LANMAN, 2007.

[8] H. Jia, Z. Zhang, G. Yu, P. Cheng, S. Li, On the performance of IEEE 802.16 OFDMA system under different frequency reuse and subcarrier permutation patterns, in: Proc. of IEEE ICC, 2007.
[9] J.-M. Kelif, E. Altman, Downlink fluid model of CDMA networks, in: Proc. of IEEE VTC Spring, 2005.
[10] J.-M. Kelif, M. Coupechoux, P. Godlewski, Spatial outage probability for cellular networks, in: Proc. of IEEE GLOBECOM, 2007.
[11] J.-M. Kelif, M. Coupechoux, P. Godlewski, Effect of shadowing on outage probability in fluid cellular networks, in: Proc. of WiOpt, 2008.
[12] V. Erceg, L.J. Greenstein, et al., An empirically based path loss model for wireless channels in suburban environments, IEEE Journal on Selected Areas in Communications (1999).
[13] K. Ramadas, R. Jain, WiMAX system evaluation methodology, Tech. Rep., WiMAX Forum, Jan. 2007.
[14] T.D. Nguyen, P. Godlewski, Capacité OFDMA, Technical Report, ENST (Télécom ParisTech), 2006.

Masood Maqbool was born in Multan, Pakistan. He received the B.E. Avionics degree from College of Aeronautical Engineering (a campus of National University of Sciences and Technology), Risalpur, Pakistan, in 1999. From 1999 to 2005, he was with Pakistan International Airlines, where he worked on communication and navigation systems of aircraft. In 2006, he received the M.S. degree in wireless communication from Supélec, France and is currently working toward the Ph.D. degree at Ecole Nationale Supérieure des Télécommunications (ENST, TELECOM ParisTech), Paris, France. His Ph.D. thesis is a joint venture of TELECOM ParisTech and AlcatelLucent Bell Labs, France. His research interests include dimensioning of wireless networks and performance evaluation of cellular networks.

Philippe Godlewski was born in Paris, France in November 29, 1949. He received the Engineer's degree from Télécom Paris (ENST) in 1973 and the Ph.D. in 1976 from the University Paris 6. He is professor at ENST (or presently Telecom ParisTech). His fields of interest include Cellular Networks, Air Interface Protocols, Multiple Access Techniques, Error Correcting Codes, Communication and Information Theory.

Marceau Coupechoux is Associate Professor at Ecole Nationale Supérieure des Télécommunications in Paris (ENST, TELECOM ParisTech) since 2005. He obtained his master from ENST in 1999 and from the University of Stuttgart, Germany in 2000, and his Ph.D. from Institut Eurecom, SophiaAntipolis, France, in 2004. From 2000 to 2005, he was with AlcatelLucent (Research & Innovation and then in the Network Design department). In the Computer and Network Science department of ENST, he is working on cellular networks, wireless networks and ad hoc networks, focusing mainly on layer 2 protocols, scheduling and resource management.

Jean-Marc Kélif received the "Licence" degree of Fundamental Physics Sciences from the Louis Pasteur University of Strasbourg (France), and the Engineer degree in Materials and Solid State Physics Sciences from the University of Paris XIII (VilletaneuseFrance) in 1984. After a few years in different enterprises as engineer in materials, he specialised in the field of telecommunications. Since 1993, he has been with France Telecom R&D (Research Centre of France Telecom) in Issy les Moulineaux, France. He obtained his Ph.D. from Ecole Nationale Supérieure des Télécommunications in Paris (ENST, TELECOM ParisTech), France. His current research interests include the performance evaluation, modeling, dimensioning and optimization of wireless telecommunication networks.

This article has been accepted for inclusion in a future issue of this journal. Content is final as presented, with the exception of pagination.

Optimal Relay Placement in Cellular Networks

Mattia Minelli, Maode Ma, Marceau Coupechoux, Jean-Marc Kelif, Marc Sigelle, and Philippe Godlewski

***Abstract*—In this paper, we address the problem of optimally placing relay nodes in a cellular network with the aim of maximizing cell capacity. In order to accurately model interference, we use a dynamic framework, in which users arrive at random time instants and locations, download a file and leave the system. A fixed point equation is solved to account for the interactions between stations. We also propose an extension of a fluid model to relay based cellular networks. This allows us to obtain quick approximations of the Signal to Interference plus Noise Ratio (SINR) that are very close to 3GPP LTE-A guideline results in terms of SINR distribution. We then use these formulas to develop a dedicated Simulated Annealing (SA) algorithm, which adapts dynamically the temperature to energy variations and uses a combination of coarse and fine grids to accelerate the search for an optimized solution. Simulations results are provided for both in-band and out-of-band relays. They show how relays should be placed in a cell in order to increase the capacity in case of uniform and non-uniform traffic. The crucial impact of the backhaul link is analyzed for in-band relays. Insights are given on the influence of shadowing.**

***Index Terms*—Cellular network; relay; optimal placement; fluid model; simulated annealing; processor sharing.**

I. Introduction

RELAYING is a promising feature of future cellular networks. The scenarios envisioned by the two standards IEEE 802.16j (for WiMAX networks) and 3GPP Release 10 and 11 (LTE-A) are the following: (a) coverage extension: relays should increase user experience in indoor or allow connection in shadowed zones; (b) group mobility: relays can aggregate the traffic related to a group of users within a train or a bus; (c) capacity boost: by deploying low-cost relay stations, a cellular operator can densify its network and increase its capacity. In this paper, we tackle the problem of optimal relay placement for capacity increase in an LTE-A-like cellular network.

A. Related Work

The relay placement problem arises in various contexts: wireless sensor networks (see e.g. [1] and references therein), Wireless Local Area Networks (WLAN), WiMAX networks and cellular networks (like LTE-A); relays represent also a paradigm in information theory (see e.g. [2] and references therein). In this short literature review, we focus on the three first cases characterized by a hierarchical structure made of Relay Nodes (RN) served by Base Stations (BS) or access points. The RNs location problem can be seen as a sub-case of the well studied facility location problem, which has been proved to be NP-hard [3]. It deserves however some attention because the objective functions and the interdependence between transmitting stations through interference make it very specific.

Several papers in the literature focus on a single BS controlling several RNs [4]–[8]. In [4], authors consider the problem of optimal relay placement in a single WLAN cell. The problem consists in minimizing the average packet transmission time. The method is based on a discretization of the possible relay locations, a Lagrangian relaxation and an iterative algorithm. In [5], RNs are constrained to be on a circle around the BS, so that authors come up with a single variable optimization problem. The same approach is taken in [6] except that cooperative strategies (Decode and Forward, DF and Amplify and Forward, AF) are assumed. In [7], a region controlled by a BS is divided into sub-regions characterized by their traffic requirements. The goal of the authors is to place relays such that capacity is maximized and user minimum bandwidth requirements are satisfied. Although useful, for example in rural areas, these approaches cannot be directly applied in a cellular network made of a dense network of BSs and RNs.

References [9]–[15] consider several BSs and several RNs per BS. A hierarchical optimization problem is formulated in [9] for WiMAX networks: authors first focus on short term call admission control decisions (they use here the Markov Decision Process framework) and then, on the long term, on network planning (a binary integer linear problem, ILP, is solved with standard methods). Authors of [10] consider the joint deployment of BSs and RNs and try to maximize network capacity with a fixed budget. They formulate the problem as an ILP and propose a two stage RN and BS deployment algorithm to obtain sub-optimal strategies. A similar idea is used in [11]. Wang et al. [15] try to minimize the installation cost for serving a given demand or to maximize the served demand for a fixed budget. Approximate algorithms are proposed and related approximation ratios are computed or bounded. Recently, [12] has also tackled the joint problem of BSs and RNs placement, user allocation and transmit power setting. The goal is to maximize the network sum capacity while minimizing the installation cost. Sub-optimal solutions to the resulting mixed integer non linear program are obtained thanks to an iterative algorithm. These papers suffer from two main drawbacks. First, interference is never accurately modeled. It

Manuscript received May 6, 2013; revised September 18, 2013; accepted October 27, 2013. The associate editor coordinating the review of this paper and approving it for publication was Y. Jing.

M. Minelli and M. Ma are with the Nanyang Technological University, Nanyang Avenue, Singapore (e-mail: mattia1@e.ntu.edu.sg, emdma@ntu.edu.sg). M. Minelli is also with Télécom ParisTech and CNRS LTCI, 46, rue Barrault, Paris, France.

M. Coupechoux, M. Sigelle, and P. Godlewski are with Télécom ParisTech and CNRS LTCI, 46, rue Barrault, Paris, France (e-mail: {marceau.coupechoux, marc.sigelle, philippe.godlewski}@telecom-paristech.fr.).

J.-M. Kelif is with Orange Labs, Issy-Les-Moulineaux, France (e-mail: jeanmarc.kelif@orange.com).

Digital Object Identifier 10.1109/TWC.2013.010214.130814

is out of the scope of [9], [12], [15]; [10] considers only noise for the calculation of data rates; [11] tries to minimize the sum of path-losses, whereas data rate is related to the Signal to Interference plus Noise Ratio (SINR); [13] assumes a single-interferer model. Second, user locations are often supposed to be known from the network planner (see e.g. [15]). This assumption is realistic in a WiMAX network but cannot be considered for a cellular network.

Three recent papers take into account co-channel interference in their problem formulation. In [16], authors propose a fixed point algorithm for the RN placement problem. RNs are however constrained to be on a circle around their serving BS. [17] relies on extensive system level simulations and constraints also RNs to be placed according to a predefined pattern. Sambale and Walke [18] propose a Simulated Annealing (SA) algorithm based on Monte Carlo simulations compliant with 3GPP LTE-A guidelines (although shadowing is ignored in the optimization). [19] deals with RN positioning for network planning and optimization. Authors set up an analytic performance evaluation model, based on simple path-loss based SINR one-dimensional calculations with a single interferer. [14], which is an extension of [18], also copes with the problem of RN placement, taking into account physical and MAC layer in their model (shadowing is taken into account), and optimizing RNs placement in terms of cell spectral efficiency. However, this paper, as well as [16]–[19] and other works, assumes that RNs and BSs transmit at every time instant (*full buffer* traffic). Hence, it does not model buffers loads and is equivalent to a *static* approach. This often results in misleading performance evaluation, as this model tends to overestimate interference.

B. Contributions

The contributions of this paper are the following:

- We introduce a "dynamic" framework for relays placement performance evaluation based on traffic analysis. This model overcomes the limits of widely used static models by considering users arriving in the system at random time instants and locations, downloading a file and leaving the system, rather than a fixed set of known user locations. RNs and BSs are modeled as M/G/1/PS queue and a fixed point iteration captures the interactions between transmitting nodes. Contrary to most of the literature, our framework takes into account non uniform traffic patterns.
- We propose an extension of the fluid model, developed in [20] for interference modeling, to relay-based cellular networks in order to obtain quick calculations of the SINR. We thus take into account co-channel interference of the whole network in our optimization. Numerical results show that we are very close to 3GPP LTE-A guidelines results in terms of SINR distribution.
- Based on these quick SINR calculations, we develop a dedicated SA algorithm for the relay placement problem. Our algorithm enjoys some enhancements with respect to the standard SA. These enhancements have been already investigated in the field of image processing but have not been yet considered for wireless network optimization, to the best of authors' knowledge. More specifically, we propose a method to dynamically adapt temperature to energy variations and a combination of coarse and fine grids to accelerate the search for an optimal solution.

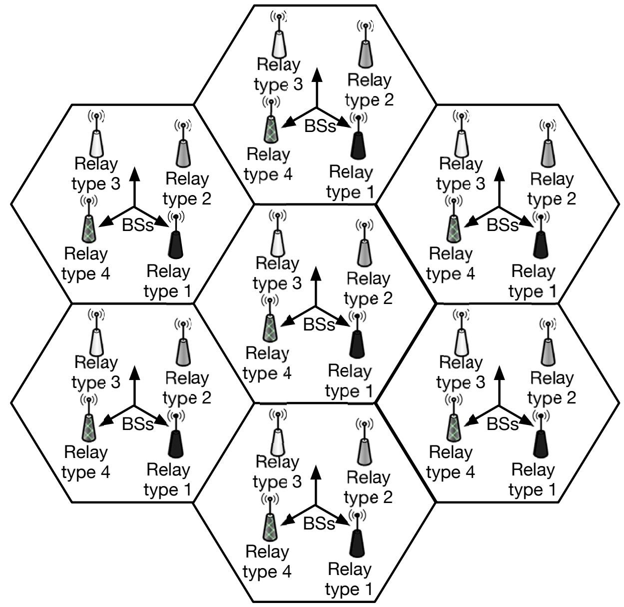

Fig. 1. Example of relay deployment with $n = 4$ relays. The cell range is R. Sites are tri-sectorized and boresight directions of sector BSs are shown with arrows.

The paper is organized as follows. In Section II, we present the system model, while in Section III, we deal with the performance of RNs placement, by formulating cell capacity. The SA algorithm is presented in Section IV and simulation results in Section V. Section VI concludes the paper.

II. System Model

A. Network Topology and Serving Station Assignment

We consider a single frequency cellular network (all stations use the same frequency) consisting of tri-sectorized hexagonal cells. Every sector is controlled by a sector BS. In every hexagonal cell, n non-cooperative DF RNs [19] are deployed. Every *station* (sector BS or RN) can be either *active* (i.e., transmitting) or *idle* (i.e., not transmitting), at any given time instant. We denote with P the transmit power of an active sector BS, and with P_R the transmit power of an active RN. Let $\mathcal{B}$ and $\mathcal{R}$ be respectively the set of sector BSs and the set of RNs. We focus on capacity evaluation for the downlink.

The generic relay deployment is illustrated in Fig. 1. The deployment pattern is identical in all cells[1] (the relative locations of the relays w.r.t. the cell center are constant across the cells). We label RNs of each cell with indices $1 \cdots n$, and define as *type* i relays those RNs labeled with i. The set of type i relays forms a regular stations pattern.

Each User Equipment (UE) is connected to its *best server*, i.e., the station which provides the highest signal power. We define $\mathcal{S}_i$ as the region, of surface S_i, where station i is the best server. Moreover, denoting with $\mathcal{K}_c$ the set of

[1]The possibility to change the deployment pattern from cell to cell could improve performance. This aspect is left for further studies.

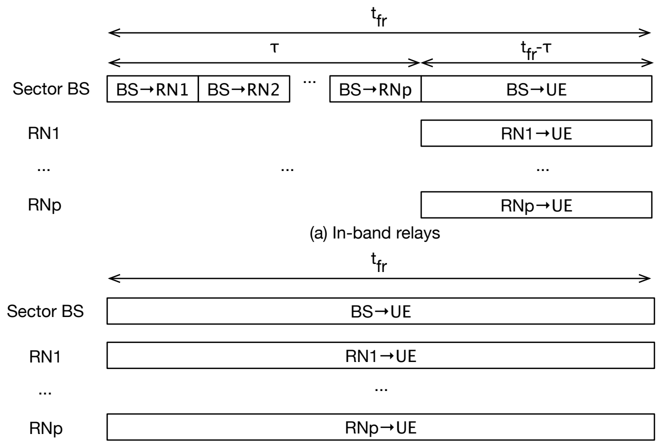

Fig. 2. Frame structure on the downlink for (a) in-band relays and (b) out-of-band relays when BS sector controls $p \leq n$ relays.

stations belonging to a given hexagonal cell c, we define $\mathcal{A}_c \triangleq \bigcup_{i \in \mathcal{K}_c} \mathcal{S}_i$ as the region, of surface A_c, where users are served by a station of c.

B. Resource Organization

We consider in-band and out-of-band half-duplex relays. We assume a time division access between sector BSs and RNs illustrated in Fig. 2. Without loss of generality, the frame duration and the overall band are set to 1 time unit. When in-band relays are considered, a sector BS transmits data to the RNs it controls over the Backhaul Link (BL) during a time τ. Then, during $1 - \tau$ and simultaneously, the BS transmits over the Direct Link (DL, BS-UE link) and RNs transmit over the Relay Link (RL, RN-UE link) to their respective attached UEs (Fig. 3). When out-of-band relays are considered, the BL is using another frequency band (e.g. over a microwave link) or a dedicated narrow beam, so that BL radio resources are not subject to the cellular network planning. In this case, $\tau = 0$. These definitions of in-band and out-of-band relays are in accordance with the definitions of the 3GPP [21].

C. Propagation Model

Let consider a transmitting station j (RN on the RL, sector BS on the DL or BL) and a receiver u (UE on the DL or RL, RN on the BL) located in (r_j, θ_j), where r_j is the receiver-station distance and θ_j is defined as the angle between the receiver-station direction and the station antenna boresight direction ($\theta_j = 0$ for omnidirectional antennas). We denote with superscripts L and N the propagation parameters referred to Line of Sight (LOS) and Non Line of Sight (NLOS) propagation respectively, and with subscripts B, R and D the propagation parameters referred to BL, RL and DL respectively. According to the 3GPP guidelines for relay performance evaluation [22], the path-gain g_l between a station and a receiver location can be written as follows:

$$
\begin{aligned}
g_l(r_j, \theta_j) &= \delta_l(r_j) h_l^L(r_j, \theta_j) + (1 - \delta_l(r_j)) h_l^N(r_j, \theta_j), \quad (1)\\
&= \delta_l(r_j) A_l(\theta_j) \frac{K_l^L}{r_j^{\eta_l^L}} + (1 - \delta_l(r_j)) A_l(\theta_j) \frac{K_l^N}{r^{\eta_l^N}} X_l^{(u,j)},
\end{aligned}
$$

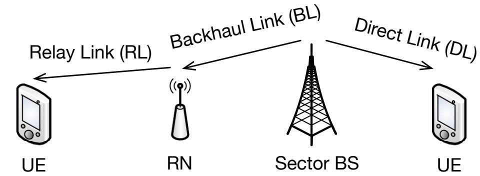

Fig. 3. Relay Link (RL), Backhaul Link (BL), and Direct Link (DL).

where $l \in \{B, R, D\}$ depends on the link type, K_l^L and K_l^N are propagation constants, η_l^L and η_l^N are path-loss exponents, $\delta_l(r_j)$ is a Bernoulli random variable (RV), which is equal to 1 when the considered link is LOS. The probability for a given link to be LOS depends on l and r_j (for details see [22]). Antenna pattern is given by $A_l(\theta)$. RNs are equipped with omnidirectional antennas, hence $A_R(\theta_j) = 1 \; \forall \theta_j$. A sector BS uses the same antenna for BL and DL, so that $A_B = A_D \triangleq A$. Shadowing is modeled by a log-normal RV $X_l^{(u,j)}$ with standard deviation σ_l. Note that the LOS or NLOS condition is supposed to be constant in time. Shadowing is assumed to change *slowly* in time, this notion will be detailed later in the paper.

D. Traffic Model

In this paper, we assume that each station is equivalent to an M/G/1/PS queue [23], [24]. This corresponds to a fair radio resource scheduling policy. Flow calls from users arrive according to a Poisson process of intensity $\lambda(s)ds$ $[flows/s]$ in the location s of surface ds and flow calls sizes are i.i.d. with mean π $[bit/flow]$. We suppose for simplicity that the function $\lambda(s)$ follows the same pattern in every cell. Now, let decompose $\lambda(s) \triangleq \bar{\lambda}\phi(s)$, where the constant $\bar{\lambda} = \int_{\mathcal{A}_c} \lambda(s)ds/A_c$ $[flows/s/m^2]$ is the average flow call intensity in $\mathcal{A}_c$, and $\phi(s) = \lambda(s)/\bar{\lambda}$ is named *normalized flow intensity*. The term $\phi(s)$ allows us to consider spatially non-uniform traffic and can be seen as a traffic profile. Moreover, we define $\omega(s) = \lambda(s)\pi$ $[bit/s/m^2]$ as the *traffic density* in s. Finally, $\bar{\omega} = \bar{\lambda}\pi$ $[bit/s/m^2]$ denotes the average traffic density in $\mathcal{A}_c$. The latter can be decomposed according to the surface controlled by each station: $\bar{\omega} = \sum_{i=1}^{n+3} \bar{\omega}_i \frac{S_i}{A_c}$, where $\bar{\omega}_i$ is the average traffic density on the surface S_i controlled by device i: $\bar{\omega}_i \triangleq \frac{\pi}{S_i} \int_{\mathcal{S}_i} \lambda(s)ds$.

We denote with $C(s) > 0$ the *user spectral efficiency* (in bits/s/Hz) in location s, and with $\bar{\rho}_i$ the *load* of the M/G/1/PS associated to station i. If $\bar{\rho}_i > 1$, station i is said to be *saturated*. According to the M/G/1/PS results, when $\bar{\rho}_i < 1$, $\bar{\rho}_i$ is also the probability that station i is active (and thus interfere). By extension, if a station is saturated, it is always active. If α_i is the Bernoulli RV, which is equal to 1 when station i is active and 0 otherwise, we have $\mathbb{P}[\alpha_i = 1] = \mathbb{E}[\alpha_i] = \min\{\bar{\rho}_i, 1\}$. By symmetry, all stations of the same type (sector BSs with the same antenna boresight direction or type i RNs) have the same load. At a given time instant t, the spectral efficiency in s, which depends on the SINR, is an explicit function of the α_j, $j \neq i$, where i is the serving station, because of the interference term. We thus write $C(s, \boldsymbol{\alpha}_{-i}(t))$, where $\boldsymbol{\alpha}_{-i}(t)$ is the vector of the activity variables of all stations in the network at time t, except i.

This article has been accepted for inclusion in a future issue of this journal. Content is final as presented, with the exception of pagination.

III. Relays Placement Performance

Performance of RNs placement is measured with the corresponding cell capacity. This section is devoted to the assessment of the capacity of a cell made of three sectors and n RNs. Cell capacity (derived in III-C) depends on the BL capacity (III-A), on the spectral efficiency (III-D) and on the maximum traffic intensity stations can sustain, which is obtained by deriving stations loads (III-B). Subsection III-E introduces a method to speed up capacity evaluation, by approximating interference from *far* stations.

A. Backhaul Link Dimensioning

We derive here the proportion τ of radio resources dedicated to the BL, based on average RN throughputs, supposing that stations are not saturated. Let us consider a sector BS b and the set of p_b RNs controlled by b (see Fig. 2). Denote $\tau_{i,b}$ the proportion of resources needed by b to serve RN i and $\tau_b = \sum_{i=1}^{p_b} \tau_{i,b}$. The average throughput of RN i is given by $\int_{\mathcal{S}_i} \omega(s)ds = \bar{\omega}_i S_i$. Let $C_{BL}(i,b)$ be the average throughput on the BL between b and i. The link between b and RN i is not overloaded if $C_{BL}(i,b)\tau_{i,b} > \bar{\omega}_i S_i$. Hence, a lower bound on τ_b is given by: $\tau_b > \sum_{i=1}^{p_b} \frac{\bar{\omega}_i S_i}{C_{BL}(i,b)}$. Note that τ_b is the load of the backhaul link between b and its corresponding RNs. In order to ensure a time synchronization between all sectors of a cell, we impose $\tau = \max_b\{\tau_b\}$, so that in the best case:

$$\tau \triangleq \max_b \sum_{i=1}^{p_b} \frac{\bar{\omega}_i S_i}{C_{BL}(i,b)}. \quad (2)$$

Suppose that the flow call intensity is uniform, i.e., $\omega(s) = \bar{\omega}\ \forall s$. In this case (2) simplifies to:

$$\tau(\bar{\omega}) \triangleq \bar{\omega} \max_b \sum_{i=1}^{p_b} \frac{S_i}{C_{BL}(i,b)}. \quad (3)$$

In the following, we write $\tau(\bar{\omega})$ to designate (2) or (3) in order to show the dependency of τ on the input traffic. The value of τ is set to zero when out-of-band relaying is adopted.

B. Stations Loads

The stations loads, which are related to their probability to be active, are coupled through the spectral efficiency function, which in turn is a function of the stations activities. We solve this problem using a fixed point iteration.

Lemma 1. *The load of a station i is expressed by:*

$$\bar{\rho}_i = \frac{\bar{\omega}}{1-\tau(\bar{\omega})} \int_{\mathcal{S}_i} \phi(s) \mathbb{E}_{\boldsymbol{\alpha}} \left[\frac{1}{C(s,\boldsymbol{\alpha}_{-i})} \middle| \alpha_i = 1 \right] ds. \quad (4)$$

Proof:

$$\begin{aligned}
\bar{\rho}_i &\overset{(1)}{=} \lim_{T\to\infty} \frac{1}{1-\tau(\bar{\omega})} \frac{\displaystyle\int_0^T \int_{\mathcal{S}_i} \frac{\omega(s)}{C(s,\boldsymbol{\alpha}_{-i}(t))}\ \mathbb{1}_{\alpha_i(t)=1} ds\ dt}{\displaystyle\int_0^T \mathbb{1}_{\alpha_i(t)=1}\ \ dt}, \\
&\overset{(2)}{=} \lim_{T\to\infty} \frac{\bar{\omega}}{1-\tau(\bar{\omega})} \frac{\displaystyle\frac{1}{T}\int_0^T \int_{\mathcal{S}_i} \frac{\phi(s)}{C(s,\boldsymbol{\alpha}_{-i}(t))}\ \mathbb{1}_{\alpha_i(t)=1} ds\ dt}{\displaystyle\frac{1}{T}\int_0^T \mathbb{1}_{\alpha_i(t)=1}\ \ dt}, \\
&\overset{(3)}{=} \frac{\bar{\omega}}{1-\tau(\bar{\omega})} \frac{\mathrm{E}_{\boldsymbol{\alpha}}\left[\displaystyle\int_{\mathcal{S}_i} \frac{\phi(s)}{C(s,\boldsymbol{\alpha}_{-i})}\ \mathbb{1}_{\alpha_i=1}\ ds\right]}{\mathrm{P}_{\boldsymbol{\alpha}}(\alpha_i = 1)}, \\
&\overset{(4)}{=} \frac{\bar{\omega}}{1-\tau(\bar{\omega})} \mathrm{E}_{\boldsymbol{\alpha}}\left[\int_{\mathcal{S}_i} \frac{\phi(s)}{C(s,\boldsymbol{\alpha}_{-i})}\ ds \middle| \alpha_i = 1\right], \\
&\overset{(5)}{=} \frac{\bar{\omega}}{1-\tau(\bar{\omega})} \int_{\mathcal{S}_i} \mathrm{E}_{\boldsymbol{\alpha}}\left[\frac{\phi(s)}{C(s,\boldsymbol{\alpha}_{-i})} \middle| \alpha_i = 1\right]\ ds.
\end{aligned}$$

(1) comes from the fact that at a given instant t, the load generated in a small area ds in s is $\frac{\omega(s)}{C(s,\boldsymbol{\alpha}_{-i}(t))}ds$ when the serving station i is active. Averaging is done on the time activity of station i. (2) comes from $\omega(s) = \bar{\omega}\phi(s)$. (3) comes from the assumption that the process $\boldsymbol{\alpha}(t)$ has a time-stationary limit $\boldsymbol{\alpha}$. (4) is by definition of the conditional expectation. (5) comes from the assumption that the shadowing changes *slowly* in time (and hence with respect to the realizations of $\boldsymbol{\alpha}(t)$)[2]. Hence, we assume that the expectation is taken over a period of time large enough for the steady-state of the M/G/1/PS queues to be reached, but sufficiently small to keep the channel constant at each location. Recall moreover that the LOS and NLOS conditions are fixed in time. As a consequence, $\mathcal{S}_i$ is fixed with respect to the realizations of $\boldsymbol{\alpha}(t)$. ∎

We denote $\boldsymbol{\rho} \triangleq (\bar{\rho}_1, ..., \bar{\rho}_{n+3})$ the vector of loads corresponding to the $n+3$ stations (n relays and three sector BSs) in the central hexagonal cell. For a given normalized flow intensity ϕ, let define the operator $F(\boldsymbol{\rho}, \bar{\omega}) = (F_1(\boldsymbol{\rho}, \bar{\omega}), ..., F_{n+3}(\boldsymbol{\rho}, \bar{\omega}))$ as follows:

$$F_i(\boldsymbol{\rho}, \bar{\omega}) = \frac{\bar{\omega}}{1-\tau(\bar{\omega})} \int_{\mathcal{S}_i} \phi(s) \mathbb{E}_{\boldsymbol{\alpha}} \left[\frac{1}{C(s,\boldsymbol{\alpha}_{-i})} \middle| \alpha_i = 1 \right] ds, \quad (5)$$

where $\forall i,\ \mathbb{P}_{\boldsymbol{\alpha}}[\alpha_i = 1] = \mathbb{E}_{\boldsymbol{\alpha}}[\alpha_i] = \min\{\bar{\rho}_i, 1\}$. Let also define $\bar{\omega}_i^{max} \triangleq \frac{\bar{\omega}}{1-\tau(\bar{\omega})} \int_{\mathcal{S}_i} \frac{\phi(s)ds}{C(s,\mathbf{1})}$.

Theorem 1. *If $\boldsymbol{\alpha} \mapsto C(s,\boldsymbol{\alpha})$ is a continuous mapping and $1/C(s,\boldsymbol{\alpha})$ is non-decreasing in $\boldsymbol{\alpha}$, $F : \prod_{i=1}^{n+3}[0; \bar{\omega}_i^{max}] \to \prod_{i=1}^{n+3}[0; \bar{\omega}_i^{max}]$ has at least one fixed point.*

Proof: We have for any $\boldsymbol{\rho} \in \prod_{i=1}^{n+3}[0; \bar{\omega}_i^{max}]$ and any station i, $0 \leq F_i(\boldsymbol{\rho}, \bar{\omega})$ and:

$$\begin{aligned}
F_i(\boldsymbol{\rho}, \bar{\omega}) &\overset{(1)}{=} \frac{\bar{\omega}}{1-\tau(\bar{\omega})} \int_{\mathcal{S}_i} \phi(s) \lim_{N\to\infty} \frac{1}{N} \sum_{h=1}^{N} \frac{1}{C(s,\boldsymbol{\alpha}_{-i}(h))} ds, \\
&\overset{(2)}{\leq} \frac{\bar{\omega}}{1-\tau(\bar{\omega})} \int_{\mathcal{S}_i} \phi(s) \lim_{N\to\infty} \frac{1}{N} \sum_{h=1}^{N} \frac{1}{C(s,\mathbf{1})} ds, \\
&\overset{(3)}{=} \frac{\bar{\omega}}{1-\tau(\bar{\omega})} \int_{\mathcal{S}_i} \frac{\phi(s)}{C(s,\mathbf{1})} ds, \\
&\overset{(4)}{=} \bar{\omega}_i^{max},
\end{aligned}$$

where $\boldsymbol{\alpha}_{-i}(h)$ indicates the h-th realization of RV $\boldsymbol{\alpha}_{-i}$. (1) comes from the definition of average. (2) results from the fact that, for each realization h of $\boldsymbol{\alpha}_{-i}$, we have $1/C(s,\boldsymbol{\alpha}_{-i}(h)) \leq 1/C(s,\mathbf{1})$. (3) follows from the consideration that all terms $(1/C(s,\mathbf{1}))$ in the summation have the same value. Finally, (4) is by definition of $\bar{\omega}_i^{max}$. Now, using the Brouwer's fixed point theorem, we conclude the proof. ∎

[2]Measurements for outdoor static scenarios reported in [25] justify our hypothesis, explaining this result with the fact that most of physical elements causing shadowing outdoor are fixed.

A similar approach is considered in [26] (Corollary 1) for a cellular network without relays. We extend here the result to relay-based sectorized networks and we adopt a different mapping F that guarantees the existence of a fixed point (which is possibly outside the $[0,1)^{n+3}$ interval). As in [26], we cannot conclude on the uniqueness of the fixed point. Starting from a central isolated cell (i.e., without interference) in the fixed point iteration makes however sense in a context of increasing traffic.

The fixed point of (5) yields the loads $\bar{\rho}_i$ of all stations $i = 1 \cdots n+3$, for a given RN placement, a given normalized flow call intensity $\phi(s)$, and a given traffic density $\bar{\omega}$.

C. Cell Capacity

The *capacity* of the cell is defined as

$$C_{cell} \triangleq \bar{\omega}^{max} A_c \; [bit/sec/Hz/cell], \tag{6}$$

where $\bar{\omega}^{max}$ is the maximum average traffic density that can be supported by a RN placement (without any station being saturated):

$$\bar{\omega}^{max} = \max\{\bar{\omega} \in \mathbb{R}_+ : F(\boldsymbol{\rho}, \bar{\omega}) = \boldsymbol{\rho} \text{ and } \boldsymbol{\rho} \in [0,1)^{n+3}\} \tag{7}$$

The value of $\bar{\omega}^{max}$ can be found for any given normalized flow call intensity $\phi(s)$, by solving the fixed point of (5) for several values of $\bar{\omega}$ and choosing the highest $\bar{\omega}$, for which no station is saturated, according to the desired accuracy. This can be done e.g. with a dichotomic search over $\bar{\omega}$.

D. Spectral Efficiency and SINR

We will now assume that the spectral efficiency in s is derived by means of a saturated Shannon formula:

$$C(s, \boldsymbol{\alpha}_{-i}) = \min\left\{\log_2(1+\gamma_s(\boldsymbol{\alpha}_{-i})), \tilde{C}\right\}, \tag{8}$$

where $\tilde{C}$ is the maximum achievable spectral efficiency and $\gamma_s(\boldsymbol{\alpha}_{-i})$ is the SINR in s. Note that this function fulfills the conditions of Theorem 1.

Now, consider a UE u located in s and receiving from its serving station i a useful signal power $P_i(s) = \max_{j \in \mathcal{B} \cup \mathcal{R}} P_j(s)$. The SINR $\gamma_s(\boldsymbol{\alpha}_{-i})$ experienced by u is:

$$\gamma_s(\boldsymbol{\alpha}_{-i}) = \frac{P_i(s)}{I_s(\boldsymbol{\alpha}_{-i}) + N_{th}}, \tag{9}$$

where N_{th} is the thermal noise power and $I_s(\boldsymbol{\alpha}_{-i}) = \sum_{j \in \mathcal{B} \cup \mathcal{R},\, j \neq i} \alpha_j P_j(s)$.

E. Interference Computation with Fluid Model of Far Network Stations

Relays placements performance assessment through (6) and (8) involves intensive use of SINR evaluation: interference sum and SINR must be evaluated on the whole cell surface for each realization of $\boldsymbol{\alpha}$, at each iteration of the fixed point and for each proposed $\bar{\omega}$.

In this subsection, we propose a fast methodology for the computation of SINR, which should be simplified as much as possible in order to reduce the computation time of the optimization, while remaining accurate. Our approach decomposes the interference into two parts: the contribution of the near stations and that of the far stations. Far interference is approximated thanks to a fluid model [27] adapted to relay-based cellular networks, while interference from near stations is exactly computed.

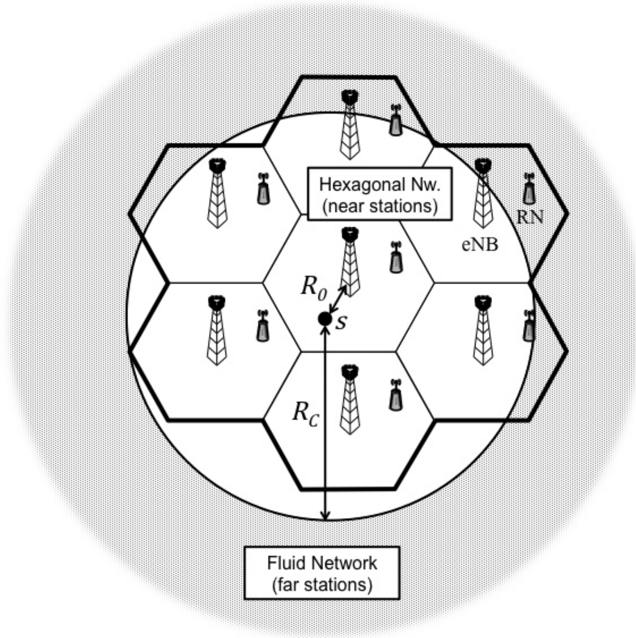

Fig. 4. Interference is exactly computed for near stations, while it is approximated for far stations by means of a fluid model of far stations network.

Let define the *near BSs* as the set $\mathcal{B}_c$ of BSs in the central cell and in the first cells ring around the central cell, and *far BSs* as the set $\mathcal{B}_f$ of BSs which are not near, so that $\mathcal{B} = \mathcal{B}_c \cup \mathcal{B}_f$ and $\mathcal{B}_c \cap \mathcal{B}_f = \varnothing$. Sets $\mathcal{R}_c$ and $\mathcal{R}_f$ are similarly defined for RNs (see Figure 4).

Now, the overall interference $I_s(\boldsymbol{\alpha}_{-i})$ can be decomposed into two contributions: $I_s(\boldsymbol{\alpha}_{-i}) = I_{s,c}(\boldsymbol{\alpha}_{-i}) + I_{s,f}(\boldsymbol{\alpha}_{-i})$, where

$$I_{s,c}(\boldsymbol{\alpha}_{-i}) = \sum_{j \in \mathcal{B}_c \cup \mathcal{R}_c,\, j \neq i} \alpha_j P_j(s) \tag{10}$$

is the power received from near stations, while

$$I_{s,f}(\boldsymbol{\alpha}_{-i}) = \sum_{j \in \mathcal{B}_f \cup \mathcal{R}_f,\, j \neq i} \alpha_j P_j(s) \tag{11}$$

is the power received from far stations.

In our study, we compute $I_{s,c}(\boldsymbol{\alpha}_{-i})$ explicitly, while $I_{s,f}(\boldsymbol{\alpha}_{-i})$ is approximated with its average value over activity (cf. $\boldsymbol{\alpha}$) and shadowing (cf. X) variations:

$$\begin{aligned} I_{s,f}(\boldsymbol{\alpha}_{-i}) &\approx \mathbb{E}_{\boldsymbol{\alpha},X}\left[I_{s,f}(\boldsymbol{\alpha}_{-i})\right], \\ &= \sum_{j \in \mathcal{B}_f} \mathbb{E}_{\boldsymbol{\alpha},X}\left[\alpha_j P_j(s)\right] + \sum_{k \in \mathcal{R}_f} \mathbb{E}_{\boldsymbol{\alpha},X}\left[\alpha_k P_k(s)\right]. \end{aligned} \tag{12}$$

In the above equation, expectations should be taken *knowing* $\alpha_i = 1$. However, we make the approximation that the activities of the far stations are independent on α_i.

It is reasonable to assume that a UE u in the central cell be always served by a near station, and that the propagation on all links between u and far stations be NLOS. This is valid considering commonly used shadowing standard deviations and LOS probability expressions (see e.g. [21], [22]). Our simulations, based on the assumptions suggested in [22], confirm these hypothesis, showing that less than 1% of users are connected to far stations, and LOS probability between u and a far station is close to zero. Hence, we assume $I_{s,f}(\boldsymbol{\alpha}_{-i})$ to be composed by NLOS interferers, and express it as

$$\begin{aligned} I_{s,f}(\boldsymbol{\alpha}_{-i}) & \\ \approx & \sum_{j\in\mathcal{B}_f} e^{a\sigma_D^2/2}\mathbb{E}_{\boldsymbol{\alpha}}\left[\alpha_j P K_D^N r_{s,j}^{-\eta_D^N} A(\theta)\right] \\ & + \sum_{k\in\mathcal{R}_f} e^{a\sigma_R^2/2}\mathbb{E}_{\boldsymbol{\alpha}}\left[\alpha_k P_R K_R^N r_{s,k}^{-\eta_R^N}\right] \\ = & \; e^{a\sigma_D^2/2}\sum_{k=1}^{3}\min\{1,\bar{\rho}_k\}\sum_{j\in\mathcal{B}_{f,k}} P K_D^N r_{s,j}^{-\eta_D^N} A(\theta) \\ & + e^{a\sigma_R^2/2}\sum_{h=1}^{n}\min\{1,\bar{\rho}_h\}\sum_{k\in\mathcal{R}_{f,h}} P_R K_R^N r_{s,k}^{-\eta_R^N}, \quad (13) \end{aligned}$$

where $r_{s,j}$ is the distance between station j and s, $\mathcal{B}_{f,k}$ is the set of far BSs of type k, $\mathcal{R}_{f,h}$ is the set of RNs of type h and $a = \ln(10)/10$. Note that parameters K_D^N, η_D^N, K_R^N and η_R^N in (13) are referred to NLOS propagation.

Sums $\sum_{j\in\mathcal{B}_{f,k}} P K_D^N r_{s,j}^{-\eta_D^N} A(\theta)$ and $\sum_{k\in\mathcal{R}_{f,h}} P_R K_R^N r_{s,k}^{-\eta_R^N}$ can be approximated by adopting a fluid model [20] for the far stations networks $\mathcal{B}_{f,k}, k\in\{1\cdots 3\}$ and $\mathcal{R}_{f,h}, h\in\{1\cdots n\}$. The fluid model is a powerful tool to simplify interference computation in hexagonal [27] and dense Poisson [28] cellular networks. It is based on approximating a discrete set of network stations, lying on a given region, with a continuum of stations. The *density* (measured in $[stations/m^2]$) of the continuum is set to be equal to the density of discrete stations in the original network. Interference sum is then approximated by integrating received power from the continuum of stations, over the considered area. The main advantage of this approach is that it allows us to obtain approximate closed-form interference expressions, which solely depend on the distance between s and the network center. We refer the reader to [27] for a detailed explanation and validation through Monte Carlo simulations.

Let now focus on $\sum_{j\in\mathcal{B}_{f,k}} P K_D^N r_{s,j}^{-\eta_D^N} A(\theta), k\in\{1\cdots 3\}$. We adopt the fluid model, substituting the hexagonal network of type-k far BSs with a continuum of BSs of the same type, lying on a ring centered at s. Following the approach presented in [29], interference sum can be approximated as

$$\begin{aligned} & \sum_{j\in\mathcal{B}_{f,k}} P K_D^N r_{s,j}^{-\eta_D^N} A(\theta) \\ \approx & \; \rho_{BS}\int_{R_c-r_0}^{\infty}\int_0^{2\pi}\left(P K_D^N r^{-\eta_D^N} A(\theta)\right) r dr d\theta, \\ = & \; \rho_{BS} b \frac{P K_D^N}{\eta_D^N - 2}(R_c - r_0)^{2-\eta_D^N}, \quad (14) \end{aligned}$$

where ρ_{BS} is the BS sites density, $b = \int_0^{2\pi} A(\theta)d\theta$, r_0 is the distance between the location s and the cell center and R_c is the distance between the closest far BS and the cell center.

Terms $\sum_{k\in\mathcal{R}_{f,h}} P_R K_R^N r_{s,k}^{-\eta_R^N}, h \in \{1\cdots n\}$ can also be approximated adopting a fluid network model, obtaining

$$\begin{aligned} & \sum_{k\in\mathcal{R}_{f,h}} P_R K_R^N r_{s,k}^{-\eta_R^N} \\ \approx & \; \rho_{BS}\int_{R_c-r_h}^{\infty}\int_0^{2\pi}\left(P_R K_R^N r^{-\eta_R^N}\right) r dr d\theta, \\ = & \; 2\pi\rho_{BS}\frac{P_R K_R^N}{\eta_R^N - 2}(R_c - r_h)^{2-\eta_R^N}, \quad (15) \end{aligned}$$

where r_h is the distance between s and the RN of type h in the central cell.

Using (14) and (15), $I_s(\boldsymbol{\alpha}_{-i})$ is finally approximated as

$$\begin{aligned} I_s(\boldsymbol{\alpha}_{-i}) \approx & \sum_{j\in\mathcal{B}_c\cup\mathcal{R}_c,\, j\neq i} \alpha_j P_j(s) \quad (16) \\ & + e^{a\sigma_D^2/2}\sum_{k=1}^{3}\min\{1,\bar{\rho}_k\}\rho_{BS} b\frac{P K_D^N}{\eta_D^N - 2}(R_c - r_0)^{2-\eta_D^N} \\ & + e^{a\sigma_R^2/2}\sum_{h=1}^{n}\min\{1,\bar{\rho}_h\} 2\pi\rho_{BS}\frac{P_R K_R^N}{\eta_R^N - 2}(R_c - r_h)^{2-\eta_R^N}. \end{aligned}$$

The use of a fluid model allows to approximate the sum of interference from all far stations, at each considered cell point, by only computing $n+1$ closed-form formulae, while the hexagonal model requires to calculate the sum of $(n+3)\sum_{i=N_f}^{N_R} 6i$ far stations received powers, where N_R denotes the number of cells rings around the central cell and N_f the first ring of far cells. This considerably reduces computational burden, considering that interference calculation is inserted in multiple nested computation cycles, as mentioned above.

IV. Optimal Placement

In this section, we study the optimization of relays placement, by means of a dedicated Metropolis-Hastings Simulated Annealing (SA) optimization algorithm, with the target of maximizing cell capacity C_{cell}, defined in Section III (see (6)). We first detail the configuration space, i.e., the set of variables to be sought, and then describe the used SA algorithm, with several enhancements which have been implemented.

In this work, a configuration is given by the positions of all relays in a cell, which we assume to lay on an hexagonal grid, due to the symmetry of the problem (see Fig. IV-1). As the RN location problem includes the capacitated facility location problem as a special case, it is NP-hard [3]. For a typical grid of size $N = 1024$ measurements points per cell and $n = 6$ relays, the cardinality of the configuration space Ω is: $|\Omega| = C_n^N = C_6^{1024} > (1000)^6/6! > 10^{15}$. Hence, exhaustive search is infeasible in practice and we have to address other optimization techniques. Simulated Annealing (SA) is a well-known stochastic technique for solving such large combinatorial optimization problems endowed with fairly non-trivial energy landscapes. It originates to [30] but was rediscovered later [31], and with great success in network optimization up to now [32], [33]. It leads to efficient optimization if its parameters (especially the *temperature schedule*) are well set-up [34]. Recall that Ω is a finite configuration space and that we consider a cost energy function $U(x) : \Omega \mapsto \mathbb{R}$ to be minimized. In this work, the energy of a candidate configuration x is the inverse of its related cell capacity (see

This article has been accepted for inclusion in a future issue of this journal. Content is final as presented, with the exception of pagination.

(6)):

$$U(x) = -C_{cell}(x). \tag{17}$$

The principle of SA lays in assigning the following exponential probability to any configuration:

$$\mathbb{P}(x) = \frac{e^{-U(x)}}{Z} \quad \forall x \in \Omega \quad (\text{with } Z = \sum_{x \in \Omega} e^{-U(x)}). \tag{18}$$

A minimizer of $U(.)$ possesses thus maximal probability $\mathbb{P}(.)$ and can be found as follows (using Metropolis-Hastings variant [35]):

• Initialization: assign an arbitrary initial configuration $x_0 \in \Omega$.

• At step $m \geq 0$: let $x = x_m$ be the current configuration. Apply the following procedure: pick up a candidate configuration $x' \in \Omega$ according to a *user-specified* proposal law $r(x \to x')$ and compute then the following acceptance rate:

$$\begin{aligned}\Xi(x \to x') &= \min\left(1, \left(\frac{\mathbb{P}(x')}{\mathbb{P}(x)}\right)^{\frac{1}{T_m}} \cdot \frac{r(x' \to x)}{r(x \to x')}\right), \\ &= \min\left(1, \; e^{-\frac{U(x')-U(x)}{T_m}} \cdot \frac{r(x' \to x)}{r(x \to x')}\right). \end{aligned} \tag{19}$$

Assign $x_{m+1} = x'$ with probability $p = \Xi(x \to x')$ (and $x_{m+1} = x$ with probability $1 - p$).

Here, T_m is a *positive temperature* parameter depending on step m required to slowly decrease to 0 as $m \to +\infty$ (and rigorously to satisfy $T_m \geq \frac{T_0}{1+\log(m+1)}$). Usually a *geometric* law is adopted $T_m = T_0 \;.\; \beta^m$ with $\beta < 1$ but close to 1. Hereafter an adaptive temperature schedule is investigated. Notice also that when the proposal law is uniform or more generally symmetric, i.e., $r(x' \to x) = r(x \to x')$, the acceptance rate boils down to the usual Metropolis form:

$$\Xi(x \to x') = \min\left(1, \; e^{-\frac{U(x')-U(x)}{T_m}}\right). \tag{20}$$

This generic method enjoys a number of extensions and variants that are implemented here:

1) "Restricted Image Spaces" [34]: It is indeed preferable to draw at each step a configuration x' which is close to x, for instance by varying one variable only (say, the position ξ_i of the relay of type i) and in a restricted range around its current value. This is known to increase the global algorithm search speed [34]. To this aim we adopt a *continuous* framework, with symmetric gaussian proposal probability distribution function (PDF) given by:

$$r(\xi_i, \; \xi_i') = \frac{1}{2\pi} \, \frac{1}{\zeta^2} \, \mathcal{N}(\parallel \xi_i' - \xi_i \parallel \; ; \; \zeta^2). \tag{21}$$

Here, ζ controls the average distance between sites ξ_i and ξ_i' (Fig. IV-1). Finally the closest discrete grid site to ξ_i' is selected. This is justified (mostly at fine resolution) for reasonable values of ζ w.r.t. the lattice step: first, there is low probability to reject proposed grid node, i.e., to find an already busy site. Then, the overall periodicity of RN lattice is injected by periodizing the proposed site itself into the whole lattice (Fig. IV-1). Thus, with this approximation the proposal laws cancels down in Hastings-Metropolis, and we obtain the usual Metropolis acceptance ratio.

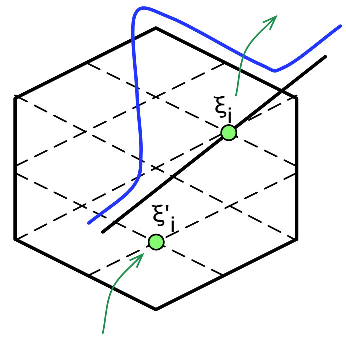

Fig. 5. Typical hexagonal cell with a hexagonal grid of possible relay locations. The current location is ξ_i and the acceptance law is Gaussian along a random direction. If the candidate ξ_i' falls outside the hexagon, it is "periodized" inside the cell.

2) Adaptive temperature scheme: In this work, we try to automatically (and adaptively) estimate both initial temperature T_0 and the cooling coefficient β. This has been previously done in the literature [34] provided that one knows the energy landscape (which is not the case here). This is done in two steps:

- Initial temperature setting: it is adjusted by imposing that the initial average acceptance ratio $\Xi_0 = \lessdot\Xi(x \to x')\gtrdot \in [a, b]$ (in practice, we select $[a, b] = [0.5, 0.8]$). To do this, T_0 is first kept constant during some number of steps (depending on the size of Ω). Then, a dichotomic-type update process is applied:

$$T_0 \leftarrow \beta \; T_0 \;\; \text{if} \;\; \Xi_0 > b \;\; \text{and} \;\; T_0 \leftarrow \frac{0.5}{\beta} \; T_0 \;\; \text{if} \;\; \Xi_0 < a.$$

- Cooling schedule: after the previous initialization phase, a fixed number of simulated annealing steps M^l and a final temperature ${T_M}^l$ [34] are assigned at each scale $l = 1, 2$ (see below), with related temperature schedule:

$${T_m}^l = {T_0}^l \;\times\; ({T_M}^l / {T_0}^l)^{m/M^l}. \tag{22}$$

3) Multiscale implementation: Multiscale algorithms have been employed long ago in various branches of Applied Mathematics. In image processing several multiscale strategies have been outlined in [36], and fast algorithms for movement detection/segmentation of video sequences can be found in [37]. For instance a hand movement can be decomposed first in a large range displacement (translation-rotation) of the hand, followed by detection of fingers moves at a finer scale. Similarly here we use a two-step setup with a first optimization on a coarse grid, then refinement of this solution at a finer level. Both steps employ SA with their own adapted parameters (initial temperature, temperature step and spatial grid resolution). The advantage of such a multiscale strategy seems twofold here. First, it allows, at lower level, to avoid spurious transitions between (high level) symmetry-invariant configurations, which can arise due to the complexity of the global energy landscape. Then, it enables to check the robustness at both coarse and fine level of the placement solution to shadowing, LOS and NLOS conditions.

V. Results

A. Simulation Assumptions

1) Spectral Efficiency Computation: Simulation assumptions related to network layout and propagation (see (1)) follow the setup described in [22, Appendix: Simulation Assumptions] (case 3) for LTE-Advanced. In particular, the sector BS and RN transmit powers are resp. 46 dBm and 30 dBm and the cell range is 1 km. The shadowing standard deviations are 10, 8 and 6 dB on the RL, DL, and BL resp. for NLOS propagation. Shadowing RVs between cell sites and between sector BSs are correlated (see [13]). The correlation distance is 50 m (we use the Cholesky decomposition as in [38]).

The SINR is computed on a regular hexagonal grid of Measurement Points (MP) in the cell (with 25 m spacing), in order to adapt to the problem geometry. For a given realization of the propagation random variables, a given value of $\bar{\omega}$, a given vector of station loads $\boldsymbol{\rho}$ and a given realization of the activity vector $\boldsymbol{\alpha}$, the SINR is computed according to (9).

Instead of computing spectral efficiency using (8), we rely on the Modulation and Coding Schemes (MCS) indicated in [39] in order to have more realistic results. According to [39], below a certain SINR threshold, a MP is in *outage*, i.e., this position cannot be served by any station. In this case, the contribution of such MP to stations loads is zero. Any placement with an outage probability greater than 1% is rejected by the optimization process (see [40], [41]).

2) Fixed Point Iteration: The expectation of the spectral efficiency is computed on every MP over hundred realizations of $\boldsymbol{\alpha}$ and a new vector $\boldsymbol{\rho}$ is deduced from (4). We iteratively solve the fixed point equation $F(\boldsymbol{\rho}, \bar{\omega}) = \boldsymbol{\rho}$ (about six iterations ensures convergence in our context). If $\exists i$, s.t. $\bar{\rho}_i \geq 1$, this means that $\bar{\omega} > \bar{\omega}^{max}$, otherwise $\bar{\omega} < \bar{\omega}^{max}$, see (7). The values of $\bar{\omega}$ to be used in the fixed point iteration are selected based on a dychotomous update process, which ensures a maximum error for C_{cell} equal to $\pm 2.3 \times 10^{-3}$ $[bit/s]$ (this corresponds to ± 23 $[kbit/(s \times cell)]$ for a system bandwidth of 10 MHz).

3) Simulated Annealing: Optimization of RN positioning is performed by evaluating the energy of a number of candidate RN placements during the execution of the SA. Each RN is allowed to be located on a hexagonal grid spanning the whole cell. Two RNs are not allowed to be located on the same spot, or in the cell center. During the first optimization phase, RNs can be located on a coarse hexagonal grid (see Section IV), where the spacing between 2 neighboring MPs is 200 m. During the second phase, the spacing becomes 50 m. In this phase, candidate RN locations cannot be farther than 300 m from the location found at the end of the first phase. The number of states analyzed during each phase varies according to n. For example, if $n = 3$, the first phase of the SA is composed of $M^1 = 30$ temperatures steps. During each temperature step, the energy of 250 candidate placements are evaluated. The second phase of the SA is characterized by $M^2 = 20$ and 150 placements for each step. The SA is stopped if the acceptance rate Ξ is zero for two consecutive temperature steps. In this case, we assume that the algorithm has already reached a 'stable' solution, and we elect as final placement the one with the lowest energy among those analyzed up to the algorithm stop. Note that the implemented SA provides *optimized* solutions and not necessarily *optimal* solutions that can be obtained theoretically after an infinite number of iterations.

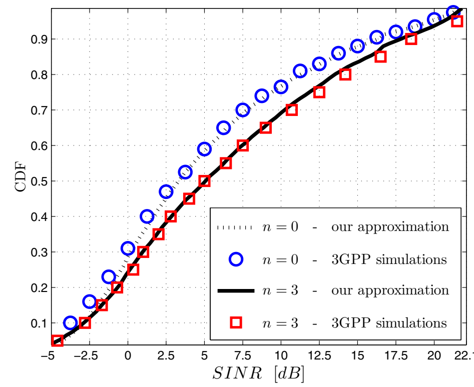

Fig. 6. SINR distribution, our SINR approximation vs. 3GPP results [22] (static case, $n = 0$ or 3 relays).

B. Model Validation

We first show the accuracy of SINR approximation introduced in Section III-E. Fig. 6 plots the Cumulative Distribution Function (CDF) of the SINR for the static case ($\boldsymbol{\alpha}(t) = \mathbf{1}, \forall t$) with $n = 3$ relays and without relays. We have compared the curves obtained in [22] with those derived by means of our SINR approximation under the same assumptions. The results show that there is a good match between our fluid model approach and the results obtained by 3GPP. This can be explained by the shadowing model (the standard deviation is relatively low and RVs are correlated) and the resulting low probability for a UE to be attached to a far station.

C. Simulation Results

Unless specified, simulation assumptions are taken from [22] (case 3). In Fig. 7, we first show the influence of the number of RNs and of their transmit power on their distance to the cell center. Let us first consider out-of-band RNs. The absence of backhaul constraints allows the RNs to cover the most interfered regions of the cell, i.e., the cell edge. Increasing n tends to decrease the average distance to the cell center because of a repulsion effect: RNs interfere more and tends to move away from each other. While a set of RNs is remaining close to cell edge, another set moves closer to the BS site so that several rings of RNs may appear. Increasing P_R induces a similar but smaller repulsion effect for $n \geq 5$. When n is small, P_R has however less influence because the inter-RN distances are bigger and thus their mutual influence is lower. The in-band case is characterized by a trade-off between the advantage of covering the cell edge and the price to be paid on the backhaul in terms of capacity. When P_R is increased, a RN controls a bigger region (especially when n is small) and thus require a higher data rate on the backhaul. Consequently, RNs have to be placed closer to the sector BSs.

This article has been accepted for inclusion in a future issue of this journal. Content is final as presented, with the exception of pagination.

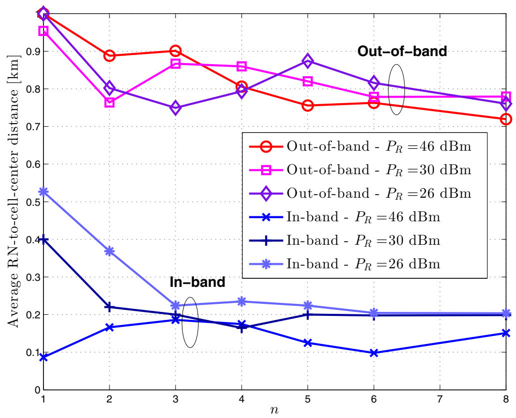

Fig. 7. Average RN to cell center distance vs. n, the number of RNs per cell (in-band and out-of-band, $P_R = 26$, 30 and 46 dBm).

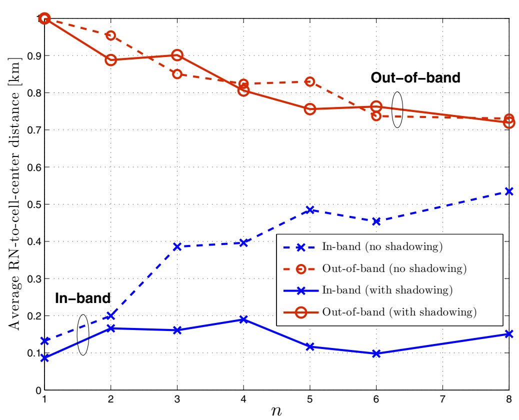

Fig. 8. Average RN to cell center distance vs. n (in-band and out-of-band, $P_R = 46$ dBm, with and without shadowing).

In Fig. 8, we can observe that the shadowing has a negligible effect on the location of out-of-band RNs. The best server mechanism assumed on the DL and the RL indeed compensates the effect of the channel variations. The impact is however decisive for in-band RNs. The best server policy is indeed not assumed on the BL[3]. This means that the BL is possibly highly interfered and its capacity is degraded. This explains that RNs have to move closer to the sector BS in order to benefit from higher MCSs and LOS propagation.

Fig. 9 and 10 show some examples of optimized RN placements. In the out-of-band case, we see how RNs are preferably placed on the cell edge. With one or two RNs (not shown on the figure), the RNs cover corners of the hexagon. When the number of RNs increases, e.g. with 6 RNs, we see how three of them move closer to the cell center. If n still increases a second ring of RNs around the BS site appears. It is also noticeable from these figures that the RN placement in a given cell is coherent with the RN placement in neighboring cells. With four RNs for example, RNs attached to different cell sites form a regular pattern around the edge of the central cell. In the in-band case, RNs are much closer to the BS site because of the BL influence. The boresight direction of the sector BSs, which has almost no influence on the out-of-band case, plays now an important role. On the one hand, RNs tends to be in the boresight direction in order to benefit from a better backhaul. On the other hand, most interfered regions lies on the frontier between two sectors. For two RNs for example, the first effect is preponderant.

Fig. 11 shows the cell capacity as a function of n. In the out-of-band case, increasing n or P_R leads to a capacity increase. When there is no backhaul constraint, relaying is indeed equivalent to a classical *network densification*, which clearly increases the network capacity [42]. Higher is P_R, higher is the offload of the sector BSs towards RNs. As they control bigger regions, sector BSs are indeed the limiting stations: their load reaches 1 well before the RN loads do. According to (7), this limits in turn the cell capacity. Increasing P_R consequently balances the traffic among RNs and BSs, which results in a higher capacity. For in-band RNs, there are two contradictory effects: increasing P_R offloads the sector BSs but increases also the proportion of resources dedicated to the BL (RNs control bigger regions). Numerical results show that the first effect is slightly preponderant. The increase of capacity observed for out-of-band as well as in-band RNs contradicts the effect observed in [19], which suggests a capacity decrease after 3 to 7 RNs (depending on P_R). This can be explained by the fact that [19] assumes a full buffer traffic model (stations are always active) and supposes that RNs are placed on a circle around the BS. Fig. 12 confirms the influence of shadowing: it has a relative small impact on out-of-band RNs but greatly degrades the in-band RNs performance.

These results clearly show the advantage of deploying out-of-band relays, especially in terms of cell capacity. The benefit of in-band relays in a scenario similar to the one defined by the 3GPP is less obvious. First, the increase of capacity is small. Second, RNs are placed close to the BS because of the backhaul constraints, so that the capacity increase benefits mainly to UEs having already good radio conditions without relays. The deployment of in-band RNs can thus be interesting only if the BL benefits from a much higher capacity either because of a good radio propagation (as in [43]) or because RN cell selection is adopted (as in [13]).

Finally, Fig. 13 shows an example of non-uniform traffic pattern inside the cell. The normalized traffic intensity $\phi(s)$ follows a bivariate normal distribution centered in $(0.3,\ 0.4)$ km and with standard deviation 0.3 km. Iso-flow intensity levels are shown with concentric circles. As expected, the relays are placed closed to the hot spot. In the out-of-band case, the relays are also close to the cell border in order to cover the most interfered region. On the contrary, in-band relays are between the BS site and the hot spot in order to benefit from a good BL.

Now the question arises of the accuracy of the solutions obtained by SA. There are few results on this problem in the literature and they are generally based on some consideration over the energy surface. For example, the work of Catoni (see e.g. [44]) is based on large deviations theory, and deals with the evaluation (in a *probabilistic* framework) of the distance of the final attained configuration to the optimal one. However,

[3]Reference [13] proposes to attach a RN to the best BS, it is however not an option offered by the standard so far.

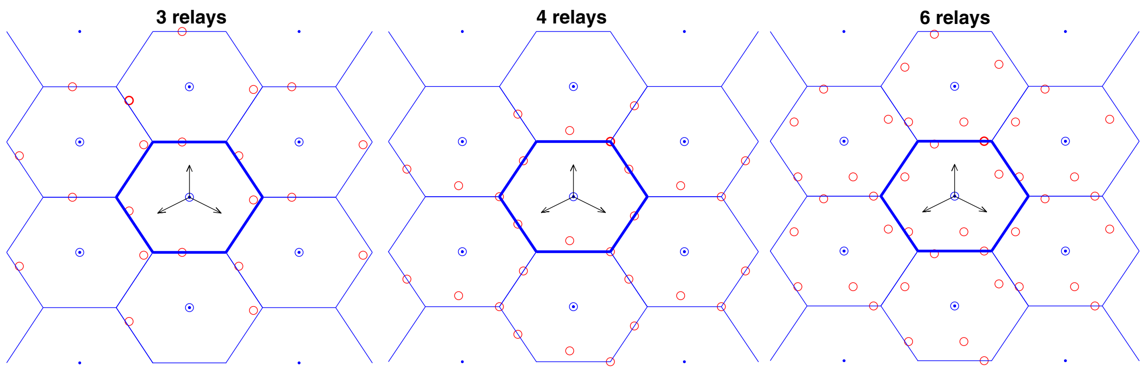

Fig. 9. Optimized out-of-band relay locations ($P_R = 30$ dBm, $n = 2$, 4 and 6, RNs are empty circles, BS sites are filled circles).

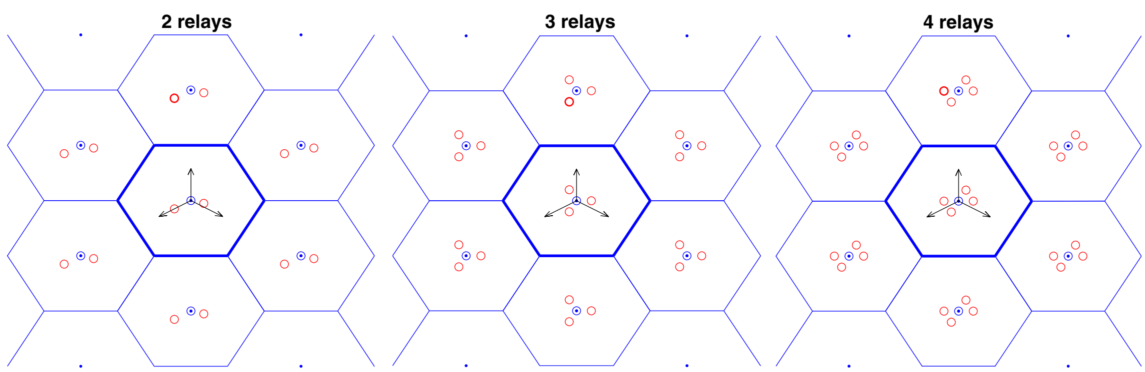

Fig. 10. Optimized in-band relay locations ($P_R = 30$ dBm, $n = 2$, 3 and 4, RNs are empty circles, BS sites are filled circles).

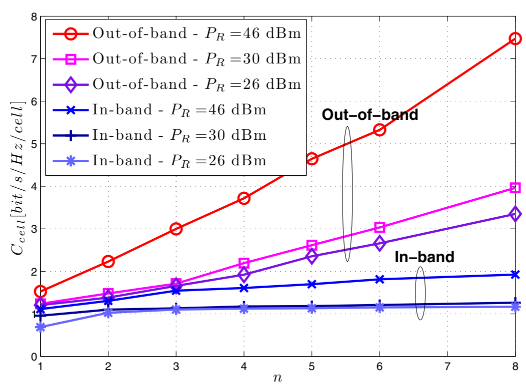

Fig. 11. Cell capacity vs. n (in-band and out-of-band, $P_R = 26$, 30 and 46 dBm).

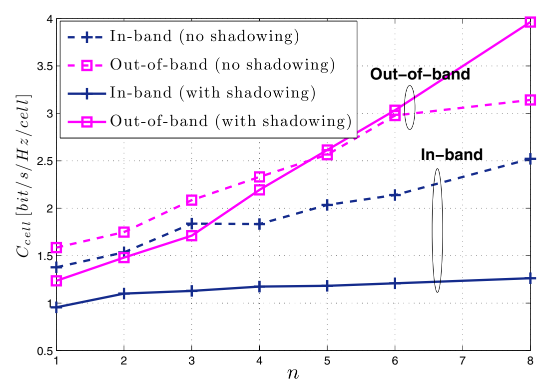

Fig. 12. Cell capacity vs. n (in-band and out-of-band, $P_R = 30$ dBm, with and without shadowing).

the performed analysis seems not to be applicable in our case, since we have a very weak knowledge of the energy landscape of this complex problem.

VI. Conclusion

In this paper, we have addressed the problem of the optimal placement of relays in a cellular network with the aim of increasing the downlink cell capacity. Compared to other works on this subject, traffic and SINR computation models are more realistic: we have set up a dynamic traffic model, where each station is equivalent to a M/G/1/PS queue. The interaction between stations is captured by a fixed point equation. The system is stable if none of the stations is overloaded. This approach accurately models the activity of the stations and the relative weight of most interfered regions. Uniform and non-uniform traffic can be analyzed. The optimization of the placement is done using a dedicated Simulated Annealing algorithm. In order to speed up the search for an optimized solution, we have developed an extension of a fluid model to relay based cellular networks. This approach yields very good approximations of the SINR at every location. Our SA algorithm adapts dynamically the temperature to the energy variations and uses a combination of coarse and fine grids. Simulation results shows that out-of-band relays are preferably

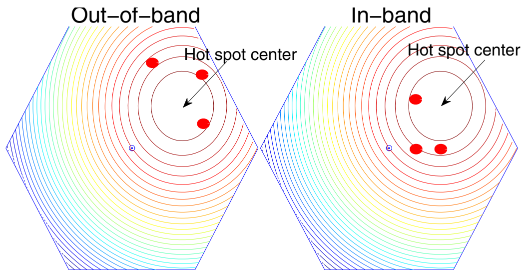

Fig. 13. Optimized out-of-band and in-band relay locations with a non-uniform traffic pattern ($P_R = 30$ dBm, $n = 3$, the BS site is in the center of the hexagons, RNs are filled circles).

placed on the cell edge and are arranged in rings around the BS, when their number increases. In-band relays suffer from the poor quality of the backhaul link, especially in presence of shadowing and tends to be much closer to the BS. In both cases, cell capacity increases with the number of relays. The benefit is however small with in-band relays.

Acknowledgment

The authors would like to thank the anonymous reviewers for their comments and suggestions that helped improve the quality of this paper. M. Minelli is supported by the A-STAR Singapore International Graduate Award. This work is also supported by the french ANR project NETLEARN (ANR-13-INFR-004).

References

[1] K. Akkaya, M. Younis, and W. Youssef, "Positioning of base stations in wireless sensor networks," *IEEE Commun. Mag.*, vol. 45, no. 4, pp. 96–102, Apr. 2007.
[2] A. Chattopadhyay, A. Sinha, M. Coupechoux, and A. Kumar, "Optimal capacity relay node placement in a multi-hop network on a line," in *Proc. 2012 Int. Symp. Modeling Optimization Mobile, Ad Hoc, Wireless Netw.*
[3] Z. Drezner and H. W. Hamacher, *Facility Location: Applications and Theory*. Springer-Verlag, 2004.
[4] A. So and B. Liang, "Enhancing WLAN capacity by strategic placement of tetherless relay points," *IEEE Trans. Mobile Comput.*, vol. 6, no. 5, pp. 487–500, May 2007.
[5] L.-C. Wang, W.-S. Su, J.-H. Huang, A. Chen, and C.-J. Chang, "Optimal relay location in multi-hop cellular systems," in *Proc. 2008 IEEE Wireless Commun. Netw. Conf.*
[6] Y. Dong, Y. Zhang, M. Song, Y. Teng, and Y. Man, "Optimal relay location in OFDMA based cooperative networks," in *Proc. 2009 IEEE Int. Conf. Wireless Commun., Netw. Mobile Comput.*
[7] C.-Y. Chang, C.-T. Chang, M.-H. Li, and C.-H. Chang, "A novel relay placement mechanism for capacity enhancement in IEEE 802.16j WiMAX networks," in *Proc. 2009 IEEE Int. Conf. Commun.*
[8] D. Yang, X. Fang, G. Xue, and J. Tang, "Relay station placement for cooperative communications in WiMAX networks," in *Proc. 2010 IEEE Global Conf. Commun.*
[9] D. Niyato, E. Hossain, D. I. Kim, and Z. Han, "Relay-centric radio resource management and network planning in IEEE 802.16j mobile multihop relay networks," *IEEE Trans. Wireless Commun.*, vol. 8, no. 12, pp. 6115–6125, Dec. 2009.
[10] H.-C. Lu and W. Liao, "Joint base station and relay station placement for IEEE 802.16j Networks," in *Proc. 2009 IEEE Global Conf. Commun.*
[11] Y. Yu, S. Murphy, and L. Murphy, "Planning Base station and relay station locations for IEEE 802.16j network with capacity constraints," in *Proc. 2010 IEEE Consumer Commun. Netw. Conf.*
[12] M. H. Islam, Z. Dziong, K. Sohraby, M. F. Daneshmand, and R. Jana, "Capacity-optimal relay and base station placement in wireless networks," in *Proc. 2012 IEEE Int. Conf. Inf. Netw.*
[13] A. B. Saleh, O. Bulakci, J. Hämäläinen, S. Redana, and B. Raaf, "Analysis of the impact of site planning on the performance of relay deployments," *IEEE Trans. Veh. Technol.*, vol. 61, no. 7, pp. 3139–3150, Sept. 2012.
[14] K. Sambale and B. Walke, "Cell spectral efficiency optimization in relay enhanced cells," in *2012 IEEE Int. Symp. Personal, Indoor, Mobile Radio Commun.*
[15] S. Wang, W. Zhao, and C. Wang, "Approximation algorithms for cellular networks planning with relay nodes," in *Proc. 2013 IEEE Wireless Commun. Netw. Conf.*
[16] S. Khakurel, M. Mehta, and A. Karandikar, "Optimal relay placement for coverage extension in LTE-A cellular systems," in *Proc. 2012 IEEE National Conf. Commun.*
[17] A. Hamdi, M. El-Khamy, and M. El-Sharkawy, "Optimized dual relay deployment for LTE-advanced cellular systems," in *Proc. 2012 IEEE Wireless Commun. Netw. Conf.*
[18] K. Sambale and B. Walke, "Decode-and-forward relay placement for maximum cell spectral efficiency," in *Proc. 2012 IEEE European Wireless.*
[19] W. Guo and T. O'Farrell, "Relay deployment in cellular networks: planning and optimization," *IEEE J. Sel. Areas Commun.*, 2013, to appear.
[20] J.-M. Kelif and E. Altman, "Downlink fluid model of CDMA networks," in *Proc. 2005 IEEE Veh. Technol. Conf. – Spring.*
[21] 3GPP, "TR 36.814 v9.0.0 - Technical Specification Group Radio Access Network; Evolved Universal Terrestrial Radio Access (E-UTRA); Further advancements for E-UTRA physical layer aspects (Release 9) - (2010-03)," Mar. 2010.
[22] 3GPP TSG-RAN WG1 Meeting N63, "Type-1 Relay Performance for Downlink," Nokia Siemens Networks, Nokia, Tech. Rep., Nov. 2010.
[23] F. P. Kelly, *Reversibility and Stochastic Networks*. Cambridge University Press, 2011.
[24] T. Bonald and A. Proutière, "Wireless downlink data channels: User performance and cell dimensioning," in *Proc. 2003 ACM Int. Conf. Mobile Comput., Netw.*
[25] A. Seetharam, J. Kurose, D. Goeckel, and G. Bhanage, "A Markov chain model for coarse timescale channel variation in an 802.16e wireless network," in *Proc. 2012 IEEE Int. Conf. Comput. Commun.*
[26] L. Rong, S. E. Elayoubi, and O. B. Haddada, "Performance evaluation of cellular networks offering TV services," *IEEE Trans. Veh. Technol.*, vol. 60, no. 2, pp. 644–655, Feb. 2011.
[27] J.-M. Kelif, M. Coupechoux, and P. Godlewski, "A fluid model for performance analysis in cellular networks," *EURASIP J. Wireless Commun. Netw.*, vol. 2010, no. 435189, Aug. 2010.
[28] R. Combes and J.-M. Kelif, "A justification of the fluid network model using stochastic geometry," in *2013 IEEE Int. Conf. Commun.*
[29] J.-M. Kelif, M. Coupechoux, and P. Godlewski, "Fluid model of the outage probability in sectored wireless networks," in *Proc. 2008 IEEE Wireless Commun. Netw. Conf.*
[30] N. Metropolis, A. Rosenbluth, M. Rosenbluth, A. Teller, E. Teller, *et al.*, "Equation of state calculations by fast computing machines," *J. Chemical Physics*, vol. 21, no. 6, pp. 1087–1092, Mar. 1953.
[31] P. Laarhoven and E. Aarts, *Simulated Annealing: Theory and Applications*, ser. Mathematics. Springer, 1987.
[32] G. Keung, Q. Zhang, and B. Li, "The base station placement for delay-constrained information coverage in mobile wireless networks," in *Proc. 2010 IEEE Int. Conf. Commun.*
[33] C. Chen and F. Baccelli, "Gibbsian method for the self-optimization of cellular networks," *EURASIP J. Wireless Commun. Netw.*, vol. 2012, no. 273, Aug. 2012.
[34] M. Robini, T. Rastello, and I. Magnin, "Simulated annealing, acceleration techniques, and image restoration," *IEEE Trans. Image Process.*, vol. 8, no. 10, pp. 1374–1387, Oct. 1999.
[35] W. K. Hastings, "Monte Carlo sampling methods using Markov Chains and their applications," *Biometrika*, vol. 57, no. 1, pp. 97–109, Apr. 1970.
[36] C. Graffigne, F. Heitz, P. Pérez, F. Prêteux, M. Sigelle, and J. Zerubia, "Hierarchical Markov random field analysis models applied to image analysis: A review," in *Proc. 1995 SPIE Conf. Neural, Morphological, Stochastic Methods Image Process.*
[37] P. Pérez and F. Heitz, "Restriction of a Markov random field on a graph and multiresolution statistical image modeling," *IEEE Trans. Inf. Theory*, vol. 42, no. 1, pp. 180–190, Jan. 1996.
[38] T. Klingenbrunn and P. Mogensen, "Modelling cross-correlated shadowing in network simulations," in *Proc. 1999 IEEE Veh. Technol. Conf. – Fall.*

[39] 3GPP, "TR 36.942 v11.0.0 - Technical Specification Group Radio Access Network; Evolved Universal Terrestrial Radio Access (E-UTRA); Radio Frequency (RF) system scenarios (Release 11) - (2012-09)," Sept. 2012.

[40] C. Fischione, M. Butussi, K. H. Johansson, K. T. Hgskolan, C. Fischione, M. Butussi, and K. H. Johansson, "Power and rate control with outage constraints in CDMA wireless networks," *IEEE Trans. Commun.*, vol. 57, no. 8, pp. 225–229, Aug. 2007.

[41] A. Alsawah and I. Fijalkow, "Base-station and subcarrier assignment in two-cell OFDMA downlink under QoS fairness," in *Proc. 2008 IEEE Int. Symp. Personal, Indoor, Mobile Radio Commun.*

[42] J.-M. Kelif and M. Coupechoux, "Cell breathing, sectorization and densification in cellular networks," in *Proc. 2009 IEEE Int. Symp. Modeling Optimization Mobile, Ad Hoc, Wireless Netw.*

[43] R. Combes, Z. Altman, and E. Altman, "Self-organizing relays: dimensioning, self-optimization, and learning," *IEEE Trans. Netw. Service Management*, vol. 9, no. 4, pp. 487–500, Dec. 2012.

[44] O. Catoni, "Sharp large deviations estimates for simulated annealing algorithms," in *Annales de l'institut Henri Poincaré (B) Probabilités et Statistiques*, vol. 27, no. 3. Gauthier-Villars, 1991, pp. 291–383.

Mattia Minelli received his Master degree in telecommunications engineering from Politecnico di Milano in Italy, in 2009. He is currently participating in a Joint PhD Program between the School of Electrical and Electronic Engineering at Nanyang Technological University in Singapore and the Computer and Network Science Department of Telecom ParisTech in Paris. His research interests include wireless networks, propagation and radio resource management issues, and relaying in OFDMA networks.

Ma Maode received his PhD degree in computer science from Hong Kong University of Science and Technology in 1999. Now, Dr. Ma is an Associate Professor in the School of Electrical and Electronic Engineering at Nanyang Technological University in Singapore. He has extensive research interests including wireless networking and network security. Dr. Ma has more than 250 international academic publications including over 100 journal papers and more than 130 conference papers. He currently serves as the Editor-in-Chief of *International Journal of Electronic Transport*. He also serves as an Associate Editor for other five international academic journals. Dr. Ma is an IET Fellow and a senior member of the IEEE Communication Society and the IEEE Education Society. He is the vice Chair of the IEEE Education Society, Singapore Chapter. He is also an IEEE Communications Society Distinguished Lecturer.

Marceau Coupechoux has been working as an Associate Professor at Telecom ParisTech since 2005. He obtained his Masters' degree from Telecom ParisTech in 1999 and from University of Stuttgart, Germany, in 2000, and his Ph.D. from Institut Eurecom, Sophia-Antipolis, France, in 2004. From 2000 to 2005, he was with Alcatel-Lucent. He was a Visiting Scientist at the Indian Institute of Science, Bangalore, India, during 2011–2012. Currently, at the Computer and Network Science department of Telecom ParisTech, he is working on cellular networks, wireless networks, ad hoc networks, cognitive networks, focusing mainly on radio resource management and performance evaluation.

Jean-Marc Kelif received the Licence of Fundamental Physics Sciences from the Louis Pasteur University of Strasbourg (France), and the Engineer degree in Materials and Solid State Physics Sciences from the University of Paris XIII in 1984. He worked as engineer in materials, and specialized in telecommunications. Since 1993, he has been with Orange Labs in Issy-les-Moulineaux, France. His current research interests include the performance evaluation, modeling, dimensioning and optimization of wireless telecommunication networks.

Marc Sigelle graduated as an Engineer from Ecole Polytechnique in 1975 and from Telecom ParisTech in 1977. He obtained a PhD from Telecom ParisTech in 1993. He worked first at Centre National d'Etudes des Télécommunications in physics and computer algorithms. Since 1989 he has been working at Telecom ParisTech in image processing, his main topics of interests being the restoration and segmentation of images using stochastic/statistical models and methods (Markov Random Fields, Bayesian networks, Graph Cuts in relationships with Statistical Physics). In the past few years he has been involved in the transfer of this knowledge to the modeling and optimization (namely, stochastic) of wireless networks.

Philippe Godlewski received the Engineers degree from Telecom ParisTech (formerly ENST) in 1973 and the PhD in 1976 from University Paris 6. He is Professor at Telecom ParisTech in the Computer and Network Science department. His fields of interest include Cellular Networks, Air Interface Protocols, Multiple Access Techniques, Error Correcting Codes, Communication and Information Theory.

Analytical Joint Processing Multi-Point Cooperation Performance in Rayleigh Fading

Dorra Ben Cheikh, Jean-Marc Kelif, Marceau Coupechoux, and Philippe Godlewski

***Abstract*—Coordinated multi-point (CoMP) is a very promising transmission scheme since it permits interference reduction and cell-edge throughput improvement. In this work, we study the performance of the joint processing multiple antenna multi-point cooperation using the maximum ratio transmission (MRT) technique. A closed form expression of the outage probability is derived for Rayleigh flat fading channel model considering path-loss and constant shadowing. Analytical and simulation results are compared.**

***Index Terms*—CoMP, MRT, outage probability, multiple antenna, Rayleigh fading.**

I. Introduction

Coordinated multi-point transmission is a new technique targeted to the LTE-Advanced (LTE-A) standard and promising better cellular performance. In the 3rd Generation Partnership Project (3GPP) LTE-A two main schemes were highlighted [1]: coordinated beamforming/scheduling (CoMP-CBF) and joint processing (CoMP-JP). In the CoMP-CBF strategy, a user is served by only one base station (the master cell) and the surrounding BSs schedule users so as to generate the least interference possible to the user of the master cell. In the CoMP-JP strategy, coordinated BSs share information data to serve a user cooperatively. The CoMP-JP generates higher backhaul load since the cooperating BSs need to share user data, channel state information (CSI) and synchronization signals, while the CoMP-CBF needs to share only CSI and scheduling decisions. However, the JP strategy offers larger performance gain than the CBF [2], [3]. In this paper, we focus on CoMP-JP transmission. In [4], a measurement study showed that multicell cooperation attain larger mean capacity than an isolated cell when considering a sufficiently high capacity and low latency backbone. In [5], field trial was performed to confirm the throughput enhancement introduced by CoMP-JP strategy. In [6], a numerical study of different joint processing schemes showed the potential of this technique to enhance the overall system performance. In [7], the performance of the femtocell coordination strategy was studied for zero forcing (ZF) and maximum ratio transmission (MRT) schemes. Two power allocation algorithms were proposed and compared. In [4], [5], [6], [7], authors performed simulation, measurement or field study but no theoretical studies were conducted. In [8], an analytical expression of the capacity outage probability was derived for an open-loop Alamouti-like CoMP downlink transmission in Rayleigh fading. The proposed SINR expression can only be achieved when using a distributed Alamouti for two cooperating BSs. In [9], an analytical study of a multicell multi-antenna cooperative MRT/MRC scheme was conducted. An analytical expression of the probability density function (PDF) of the signal-to-interference ratio (SIR) was derived considering path-loss, shadowing and Rayleigh fading. However, the authors resorted to many assumptions: a cell-edge user served in cooperation is at equal distances from the cooperative BSs, a Gamma distributed shadowing and a Poisson spatial distribution of interfering transmitters. Furthermore, there is a significant difference between simulation and theoretical results.

In this work, our main contribution is to perform an analytical study of a downlink multicell cooperation system using the MRT precoding technique. The MRT [10] is a transmission technique achieving maximum transmit diversity and maximizing the SNR. We propose an approximate outage probability expression of the downlink multiple antenna CoMP-JP using the MRT precoding considering path-loss, constant shadowing and Rayleigh fading. Our analytical approach consolidates the numerical performance studies provided in the literature.

This paper is outlined as follows. In the next section, we introduce the system model. In section III, the outage probability expression is derived. In section IV, simulation results are presented and discussed. Concluding remarks are proposed in section V.

The following notations are used: $(.)^T$ denotes the transpose conjugate operator, E[.] the expectation value and var(.) the variance.

II. System Model

Consider a downlink multicellular (B base stations) multiuser system (K active users) and consider multiple antenna BSs (M antennas) and single antenna user equipments. Let a *cluster* be a subset of BSs cooperating to serve a user. The clusters are disjoint. The selection algorithm of the BSs in a cluster is beyond the scope of this work, a possible simple criterion is the minimization of the distance depending path-loss. A cluster of BSs transmits to a single user per transmit time interval (TTI). BSs use the MRT to transmit their data. We assume coherent multicell transmission which needs a tight synchronization across transmitting BSs (like in [11]) that can be ensured using low-latency and high-capacity backhaul communication. The information data intended to a user are shared by all BSs in its cooperation cluster. CSI between

Manuscript received December 23, 2011. The associate editor coordinating the review of this letter and approving it for publication was H. Nguyen.

D. Ben Cheikh is with Orange Labs Issy-les-moulineaux, France, and with TELECOM ParisTech & CNRS LTCI, Paris, France (e-mail: dorra_ibn_cheikh@yahoo.com).

Jean-Marc Kelif is with Orange Labs Issy-les-moulineaux, France (e-mail: jeanmarc.kelif@orange.com).

M. Coupechoux and P. Godlewski are with TELECOM ParisTech & CNRS LTCI, Paris, France (e-mail: {coupecho, godlewski}@enst.fr).

Digital Object Identifier 10.1109/WCL.2012.041612.110273

the considered user and the cooperating BSs are estimated using feedback for the frequency division duplex (FDD) mode or uplink-downlink channel reciprocity for the time division duplex (TDD) mode. The cluster of BSs serving a user k is denoted B_k. The signal received by a user k is given by [12]:

$$y_k = \sum_{b \in B_k} \sqrt{p_{b,k}} \mathbf{h}_{b,k} \mathbf{x}_{b,k} + \sum_{i=1, i \neq k}^{K} \sum_{j \in B_i} \sqrt{p_{j,k}} \mathbf{h}_{j,k} \mathbf{x}_{j,i} + n, \quad (1)$$

where $p_{b,k}$ is the power received by user k from BS b, $\mathbf{h}_{b,k} \in \mathbb{C}^{1 \times M}$ is the complex Gaussian channel between user k and BS b, n is the AWGN and $\mathbf{x}_{b,k} \in \mathbb{C}^{M \times 1}$ is the MRT data vector transmitted from BS b to the user k and is given by:

$$\mathbf{x}_{b,k} = \frac{\mathbf{h}_{b,k}^T}{\|\mathbf{h}_{b,k}\|} s_k, \quad (2)$$

$s_k \in \mathbb{C}$ is the normalized information symbol intended to user k from BS b. The received power $p_{b,k}$ includes path-loss and shadowing:

$$p_{b,k} = P_T C d_{b,k}^{-\eta} 10^{\frac{\xi_{b,k}}{10}}, \quad (3)$$

where P_T is the total transmit power of BS b, C is a constant, $d_{b,k}$ is the distance between the considered user and BS b, η is the path-loss exponent and $\xi_{b,k}$ is a Normal random variable with zero mean and standard deviation σ.

The output SINR perceived by a user k is given by:

$$\begin{aligned} \gamma_k &= \frac{\left(\sum_{b \in B_k} \sqrt{p_{b,k}} \mathbf{h}_{b,k} \frac{\mathbf{h}_{b,k}^T}{\|\mathbf{h}_{b,k}\|}\right)^2}{\sum_{i=1, i \neq k}^{K} \left| \sum_{j \in B_i} \sqrt{p_{j,k}} \mathbf{h}_{j,k} \frac{\mathbf{h}_{j,i}^T}{\|\mathbf{h}_{j,i}\|} \right|^2 + \sigma_n^2}, \quad (4) \\ &= \frac{\left(\sum_{b \in B_k} \sqrt{p_{b,k}} \|\mathbf{h}_{b,k}\|\right)^2}{\sum_{i=1, i \neq k}^{K} \left| \sum_{j \in B_i} \sqrt{p_{j,k}} \mathbf{h}_{j,k} \frac{\mathbf{h}_{j,i}^T}{\|\mathbf{h}_{j,i}\|} \right|^2 + \sigma_n^2}. \quad (5) \end{aligned}$$

In dense urban interference limited system, the noise power can be neglected compared to the interference power, thus the SINR can be approximated as:

$$\gamma_k \approx \frac{X}{Y}, \quad (6)$$

where

$$\begin{aligned} X &= \left(\sum_{b \in B_k} \sqrt{p_{b,k}} \|\mathbf{h}_{b,k}\| \right)^2, \quad (7) \\ Y &= \sum_{i=1, i \neq k}^{K} \left| \sum_{j \in B_i} \sqrt{p_{j,k}} \mathbf{h}_{j,k} \frac{\mathbf{h}_{j,i}^T}{\|\mathbf{h}_{j,i}\|} \right|^2. \quad (8) \end{aligned}$$

III. Outage Probability

The outage probability is an important QoS performance metric since it measures the probability of failure to satisfy a required threshold for a given service. It is defined as:

$$P_{out} = P[\gamma_k < \gamma_{th}] \approx P[\frac{X}{Y} < \gamma_{th}], \quad (9)$$

where γ_{th} is the SINR threshold value characterizing the considered service.

Let us derive the PDF of X. X can be written as:

$$X = U^2, \quad U = \sum_{b \in B_k} \sqrt{p_{b,k}} \|\mathbf{h}_{b,k}\|. \quad (10)$$

U can also be written as:

$$U = \sum_{b \in B_k} \sqrt{p_{b,k}} \sqrt{\sum_{i=1}^{M} |h_{b,k,i}|^2}. \quad (11)$$

To the best of our knowledge, there is no possible closed form expression for the PDF of U. We will hence use the central limit approximation for causal functions [13]. It permits to approximate the sum of positive independent and not necessarily identically distributed random variables by a Gamma distribution given by:

$$f_U(u) = \frac{u^{\nu-1} e^{-\frac{u}{\theta}}}{\Gamma(\nu)\theta^\nu}. \quad (12)$$

where $\nu = \frac{\mathrm{E}[U]^2}{\mathrm{var}(U)}$ and $\theta = \frac{\mathrm{var}(U)}{\mathrm{E}[U]}$.

To derive ν and θ, let us calculate the mean and the variance of U, $\mathrm{E}[U]$ can be derived as follows:

$$\mathrm{E}[U] = \sum_{b \in B_k} \sqrt{p_{b,k}} \mathrm{E}\left[\sqrt{\sum_{i=1}^{M} |h_{b,k,i}|^2} \right]. \quad (13)$$

Denoting $V = \sqrt{\sum_{i=1}^{M} |h_{b,k,i}|^2}$, it can be noticed, that V is a square root of a Gamma distributed random variable and thus we can write the PDF of V as:

$$f_V(v) = \frac{2}{(M-1)!} v^{2M-1} e^{-v^2}, \quad (14)$$

$\mathrm{E}[V]$ can be derived using (14) and is given by:

$$\mathrm{E}[V] = \int_0^\infty \frac{2}{(M-1)!} v^{2M} e^{-v^2} dv = \frac{(2M-1)!!}{2^M (M-1)!} \sqrt{\pi}, \quad (15)$$

where $(2N+1)!! = 1 \times 3 \times 5 ... \times (2N+1)$ and $(2N)!! = 2 \times 4 \times ...(2N)$. From (13), $\mathrm{E}[U]$ is given by:

$$\mathrm{E}[U] = \frac{(2M-1)!!}{2^M (M-1)!} \sqrt{\pi} \sum_{b \in B_k} \sqrt{p_{b,k}}. \quad (16)$$

The variance of U can be derived as follows:

$$\begin{aligned} \mathrm{var}(U) &= \mathrm{E}[\sum_{b \in B_k} \sqrt{p_{b,k}} \|\mathbf{h}_{b,k}\| \sum_{n \in B_k} \sqrt{p_{n,k}} \|\mathbf{h}_{n,k}\|] \\ &- (\mathrm{E}[\sum_{b \in B_k} \sqrt{p_{b,k}} \|\mathbf{h}_{b,k}\|])^2, \\ &= \sum_{b \in B_k} p_{b,k} \mathrm{E}[\|\mathbf{h}_{b,k}\|^2] - \sum_{b \in B_k} p_{b,k} \mathrm{E}[\|\mathbf{h}_{b,k}\|]^2 \\ &= (M - \pi(\frac{(2M-1)!!}{2^M (M-1)!})^2) \sum_{b \in B_k} p_{b,k}. \quad (17) \end{aligned}$$

The parameters ν and θ are thus given by:

$$\nu = \frac{(2M-1)!!^2}{M 2^{2M} (M-1)!^2 - \pi (2M-1)!!^2} \frac{(\sum_{b \in B_k} \sqrt{p_{b,k}})^2}{\sum_{b \in B_k} p_{b,k}}, \quad (18)$$

$$\theta = \frac{M 2^{2M} (M-1)!^2 - \pi (2M-1)!!^2}{2^M (M-1)! (2M-1)!! \sqrt{\pi}} \frac{\sum_{b \in B_k} p_{b,k}}{\sum_{b \in B_k} \sqrt{p_{b,k}}} \quad (19)$$

Using the Gamma approximation of the PDF of U, we can derive the CDF of X as follows:

$$F_X(v) = \int_0^{\sqrt{v}} \frac{u^{\nu-1}e^{-\frac{u}{\theta}}}{\Gamma(\nu)\theta^\nu}du, \quad (20)$$

$$= \frac{\gamma(\nu, \frac{\sqrt{v}}{\theta})}{\Gamma(\nu)}, \quad (21)$$

where $\gamma(.,.)$ is the lower incomplete Gamma function and $\Gamma(.)$ is the Gamma function.

It is clear from (16) and (17) that adding new cooperating BSs improves the mean useful signal power but increases also its variability. We can also show that the mean and the variance are increasing with M.

Let us derive, now, the PDF of Y. We can write the expression (8) as:

$$Y = \sum_{i=1, i\neq k}^{K} \left| \sum_{j\in B_i} \sqrt{p_{j,k}} g_{j,k,i} \right|^2, \quad (22)$$

where $g_{j,k,i} = \mathbf{h}_{j,k}\frac{\mathbf{h}^T_{j,i}}{\|\mathbf{h}_{j,i}\|}$. It was proven in [14], that, since the elements of $\mathbf{h}_{j,k}$ and $\mathbf{h}_{j,i}$ are zero-mean complex Gaussian random variables, $g_{j,k,i}$ is also complex Gaussian independent of $\mathbf{h}_{j,i}$. Let $c_{k,i} = \sum_{j\in B_i}\sqrt{p_{j,k}}g_{j,k,i}$, it is the sum of independent complex Gaussian random variables. Y can be written as:

$$Y = \sum_{i=1, i\neq k}^{K} |c_{k,i}|^2, \quad (23)$$

$\{c_{k,i}\}_{(i=1\ldots K, i\neq k)}$ being independent zero-mean complex Gaussian elements with variances:

$$\lambda_{i,k} = \text{var}(c_{k,i}) = \sum_{j\in B_i} p_{j,k}. \quad (24)$$

The PDF of Y is, hence, given by [15]:

$$f_Y(y) = \sum_{i=1, i\neq k}^{K} \frac{\Pi_i}{\lambda_{i,k}} \exp(-\frac{y}{\lambda_{i,k}}), \quad (25)$$

where $\Pi_i = \prod_{p=1..K, p\neq k, p\neq i} \frac{\lambda_{p,k}}{\lambda_{p,k}-\lambda_{i,k}}$.
Some $\{\lambda_{p,k}\}_{p=1..K, p\neq k}$ may be equal. In this case, a very small number can be added to differentiate equal terms [15] and hence the distribution (25) is still valid and yields good results.

Having the PDF of X and the PDF of Y, and since they are independent random variables, we derive the outage probability as follows:

$$P(\gamma_k < \gamma_{th}) = \int_0^\infty F_X(\gamma_{th}y)f_Y(y)dy, \quad (26)$$

$$= \sum_{i=1, i\neq k}^{K} \frac{\Pi_i}{\lambda_{i,k}\Gamma(\nu)} \times \int_0^\infty \exp(-\frac{y}{\lambda_i})\gamma(\nu, \frac{\sqrt{\gamma_{th}y}}{\theta})dy. \quad (27)$$

The outage probability is given by [16]:

$$P(\gamma_k < \gamma_{th}) = \sum_{i=1, i\neq k}^{K} \Pi_i \left(\frac{\sqrt{\gamma_{th}\lambda_{i,k}}}{2\theta}\right)^\nu U\left(\frac{\nu}{2}, \frac{1}{2}, \frac{\gamma_{th}\lambda_{i,k}}{4\theta^2}\right) \quad (28)$$

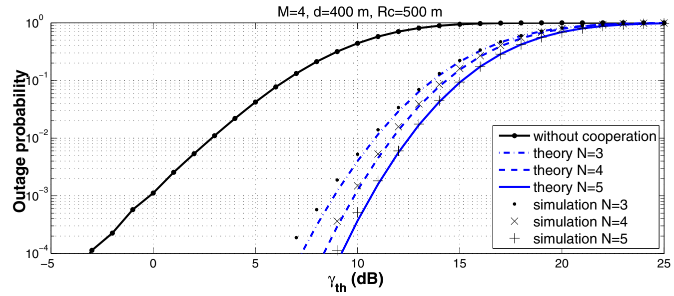

Fig. 1. Comparison between simulated and analytical results of the outage probability without CoMP and with CoMP MRT strategy for 3, 4 or 5 cooperating BSs.

where $U(.,.,.)$ is the confluent hypergeometric function of second kind. Expression (28) is a closed form approximation of the outage probability. It is a finite sum over the number of the active users in the network of easily computable elements allowing for rapid evaluation of the cooperative MISO system performance.

IV. Simulation Results

Fig. 1 presents a comparison between simulated and theoretical outage probability. We consider a network of 19 BSs equipped with 4 antennas (the central cell and two surrounding rings of BSs). We consider $N = 3$, 4 or 5 cooperating BSs and 5 interfering clusters of BSs so that $K = 6$. A user is served by the N BSs with smallest path-loss degradation. We first generate 19 realizations of the shadowing using a lognormal random variable with $\sigma = 6$ dB standard deviation. In each iteration of our Monte Carlo simulation, the SINR is calculated using these same realizations. All BSs emit a power of 20 W. The cell radius is $R_c = 500$ m and the considered mobile station is at a distance $d = 400$ m from the central BS (cell-edge user). The path-loss exponent is $\eta = 3.41$. In an urban environment and considering a frequency carrier $f_0 = 2$ GHz, the path-loss constant $C = 4.95\times10^{-4}$ [17]. The figure shows that there is a good match between simulations and analytical results. We can see that the approximation is all the more precise when the number of BSs is larger; however, it still holds even for a small number of cooperating BSs (3 or 4 BSs). We can also notice the considerable gain of performance of the CoMP strategy over the non cooperative one.

In Fig. 2 we plot the outage probability of the SIR and of the SINR for $R_c = 500$ m and $R_c = 1$ Km. Thermal noise power is computed as $\sigma_n^2 = N_0W$ where $N_0 = -174$ dBm/Hz is the noise density power and W is the system bandwidth. Considering the same system parameters as for Fig. 1, it can be seen that for a dense urban environment where $R_c \leq 500$ m and for a bandwidth of $W = 20$ MHz, the two curves are superposed, thus the influence of the noise power is negligible compared to the interference power. In this case the system is said *interference limited*. The difference between SIR and SINR outage probability becomes significant only for large cell ranges ($R_c \geq 1$ Km), large system bandwidths ($W \geq 10$ MHz) and high SINR. On Fig. 2, we can note however that even for $R_c = 1$ Km, $W = 20$ MHz, our formula can be

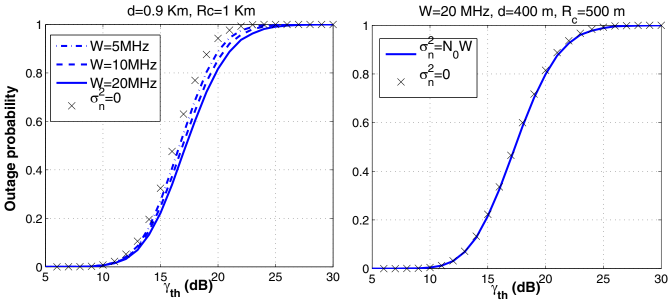

Fig. 2. Impact of the noise power on the outage probability.

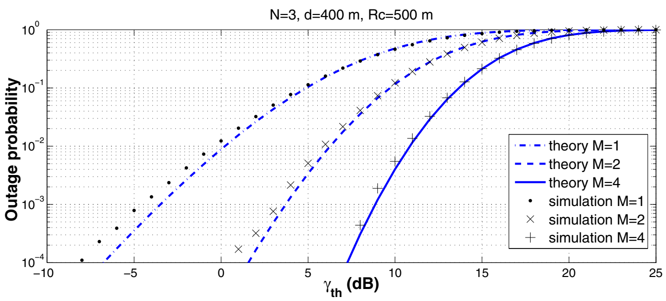

Fig. 3. Outage probability versus SINR threshold for a downlink multicellular system using CoMP and $M = 1$, 2, 4 antennas per BS.

efficiently used in the low SINR region (for coverage studies for example).

In Fig. 3 we fix $N = 3$ and varies $M = 1$, 2 or 4. Again, we notice that our formula provides a good approximation of the outage probability. As an expected result, we can observe that increasing the number of antenna per BS enhances the system performance and that the improvement is decreasing with M. This is a classical result related to the diversity gain brought by multiple antenna at the BSs.

V. Conclusion

In this paper, the performance of the joint processing maximum ratio transmission technique was studied in terms of outage probability. A closed-form expression has been derived using a Gamma approximation of useful power PDF and an exact interference power PDF. Simulation validates the derived outage probability expression. Our model is definitely optimistic since we assume perfect CSI at the transmitter. A more realistic approach should take into consideration the imperfectness of the CSI or consider open loop diversity achieving techniques, e.g., space time coding.

References

[1] 3GPP TR 36.814, "Evolved Universal Terrestrial Radio Access (E-UTRA); further advancements for E-UTRA physical layer aspects," R9 V9.0.0, Mar. 2009.

[2] J. Li, E. Lu, and I.-T. Lu, "Performance benchmark for network MIMO systems: a unified approach for MMSE transceiver design and performance analysis," in *Proc. 2010 IEEE GLOBECOM*, pp. 1–6.

[3] Y. Rui, M. Li, P. Chengo, Y. Luo, and A. Guo, "Achievable rates of coordinated multi-point transmission schemes under imperfect CSI," in *Proc. 2011 IEEE ICC*, pp. 1–6.

[4] V. Jungnickel, *et al.*, "Capacity measurements in a cooperative MIMO network," *IEEE Trans. Veh. Technol.*, vol. 58, pp. 2392–2405, June 2009.

[5] P. Marsch, M. Grieger, and G. Fettweis, "Large scale field trial results on different uplink coordinated multi-point (CoMP) concepts in an urban environment," in *Proc. 2011 IEEE WCNC*, pp. 1858–1863.

[6] H. Zhang, H. Dai, and Q. Zhou, "Base station cooperation for multiuser MIMO: joint transmission and BS selection," in *Proc. 2004 Conf. Inform. Sciences and Sys.*

[7] S. Ben Halima, M. Helard, and D. Phan-Huy, "New coordination and resource allocation schemes for uniform rate in femtocell networks," in *Proc. 2011 IEEE VTC – Spring*, pp. 1–5.

[8] V. Garcia, N. Lebedev, and J.-M. Gorce, "Capacity outage probability for multi-cell processing under Rayleigh fading," *IEEE Commun. Lett.*, vol. 15, pp. 801–803, Aug. 2011.

[9] X. Ge, K. Huang, C.-X. Wang, X. Hong, and X. Yang, "Capacity analysis of a multi-cell multi-antenna cooperative cellular network with co-channel interference," *IEEE Trans. Wireless Commun.*, vol. 10, pp. 3298–3309, Oct. 2011.

[10] T. K. Y. Lo, "Maximum ratio transmission," *IEEE Trans. Commun.*, vol. 47, pp. 1458–1461, Oct. 1999.

[11] E. Bjornson, R. Zakhour, D. Gesbert, and B. Ottersten, "Cooperative multicell precoding: rate region characterization and distributed strategies with instantaneous and statistical CSI," *IEEE Trans. Wireless Commun.*, vol. 58, pp. 4298–4310, Aug. 2010.

[12] A. Tolli, H. Pennanen, and P. Komulainen, "On the value of coherent and coordinated multi-cell transmission," in *Proc. 2009 IEEE ICC Workshops*.

[13] A. Papoulis, *The Fourier Integral and Its Applications*. McGraw-Hill, 1962.

[14] A. Shah and A. Haimovich, "Performance analysis of maximum ratio combining and comparison with optimum combining for mobile radio communications with cochannel interference," *IEEE Trans. Veh. Technol.*, vol. 49, pp. 1454–1463, July 2000.

[15] R. Visoz and E. Bejjani, "Matched filter bound for multichannel diversity over frequency-selective Rayleigh-fading mobile channels," *IEEE Trans. Veh. Technol.*, vol. 49, pp. 1832–1844, Sep. 2000.

[16] I. Gradshteyn and I. Ryzhik, *Table of Integrals, Series and Products*. Academic Press, 1963.

[17] J.-M. Kelif, M. Coupechoux, and F. Marache, "Limiting power transmission of green cellular networks: impact on coverage and capacity," in *Proc. 2010 IEEE ICC*, pp. 1–6.

This full text paper was peer reviewed at the direction of IEEE Communications Society subject matter experts for publication in the IEEE INFOCOM 2010 proceedings
This paper was presented as part of the main Technical Program at IEEE INFOCOM 2010.

An Auction Framework for Spectrum Allocation with Interference Constraint in Cognitive Radio Networks

Lin Chen* Stefano Iellamo† Marceau Coupechoux‡ Philippe Godlewski‡

*Laboratoire de Recherche en Informatique (LRI)
CNRS, University of Paris-Sud XI and INRIA
91405 Orsay, France
Lin.Chen@lri.fr

†Dpt. Electronics and Information
Politecnico di Milano
Piazza L. da Vinci 32, Milan, Italy
dajelvento@gmail.com

‡Dpt. Computer Science and Networking
Telecom ParisTech - LTCI CNRS 5141
46 Rue Barrault, Paris 75013, France
{coupecho, godlewsk}@enst.fr

***Abstract*—Extensive research in recent years has shown the benefits of *cognitive radio* technologies to improve the flexibility and efficiency of spectrum utilization. This new communication paradigm, however, requires a well-designed spectrum allocation mechanism. In this paper, we propose an auction framework for cognitive radio networks to allow unlicensed secondary users (SUs) to share the available spectrum of licensed primary users (PUs) fairly and efficiently, subject to the interference temperature constraint at each PU. To study the competition among SUs, we formulate a non-cooperative multiple-PU multiple-SU auction game and study the structure of the resulting equilibrium by solving a non-continuous two-dimensional optimization problem. A distributed algorithm is developed in which each SU updates its strategy based on local information to converge to the equilibrium. We then extend the proposed auction framework to the more challenging scenario with free spectrum bands. We develop an algorithm based on the no-regret learning to reach a correlated equilibrium of the auction game. The proposed algorithm, which can be implemented distributedly based on local observation, is especially suited in decentralized adaptive learning environments as cognitive radio networks. Finally, through numerical experiments, we demonstrate the effectiveness of the proposed auction framework in achieving high efficiency and fairness in spectrum allocation.**

I. Introduction

Cognitive radio [1] has emerged in recent years as a promising paradigm to enable more efficient and spectrum utilization. Apart from the conventional command and control model, three more flexible spectrum management models are presented in [2], namely, exclusive use (or operator sharing), commons and shared use of primary licensed spectrum. In the last model, unlicensed secondary users (SUs) are allowed to access the spectrum of licensed primary users (PUs) in an opportunistic way. In such a model, a well-designed spectrum allocation mechanism is crucial to achieve efficient spectrum usage and harmonious coexistence of PUs and SUs. On one hand, the radio resource allocation mechanism should ensure that the spectrum resource (unused by PUs) is allocated efficiently and fairly among SUs. On the other hand, the communication of PUs should not be disturbed by the SUs.

In this paper, we tackle the challenging research problem of designing efficient spectrum allocation mechanism for cognitive radio networks. We consider a generic network scenario in which multiple PUs and SUs coexist. To use the spectrum resource efficiently, the SUs share the available spectrum of the PUs under the condition that the *interference temperature* constraint [3] is always satisfied at each PU, i.e. the total received power of the SUs at each PU should be kept under some threshold in order to protect the PU's traffic. The considered scenario can represent various network scenarios, e.g. the PUs are the access points of a mesh network and the SUs are the mobile devices.

In our work, we develop an auction framework to allow SUs to share the available spectrum of PUs. Under the proposed auction framework, each PU acts as a resource provider by (1) announcing a price and a reserve bid (2) allocating the received power as a function of the bids submitted by SUs. Each SU acts as a customer by (1) submitting a two-dimensional bid indicating which PU to bid for resource and how much to bid (2) paying the chosen PU an amount of payment proportional to the allocated resource and the announced price. To study the competition among SUs, we formulate a non-cooperative auction game and study the structure of the resulting Nash equilibrium (NE) by solving a non-continuous two-dimensional optimization problem. A distributed algorithm is developed in which each SU updates its strategy based on local information to converge to the NE. Our analysis can serve as a decision and control framework for the SUs to exploit the underutilized spectrum resource.

We then extend the proposed auction framework to the more challenging scenario with free spectrum bands. In this context, a SU should strike a balance between accessing a free spectrum band with more interference if the competitors take the same strategy, and paying more for communication gains by staying with a licensed band. We show that the *ping-pong effect* may occur under the best-response update, i.e., a SU keeps switching between the free band and a licensed band. To eliminate the ping-pong effect, we develop an algorithm based on the no-regret learning [4] to reach a correlated equilibrium (CE) [5] of the auction game. The proposed algorithm, which can be implemented distributedly and requires only local observation, is especially suited in decentralized adaptive learning environments as cognitive radio networks.

Due to their perceived fairness and allocation efficiency [6], auctions are among the best-known market-based mechanisms to allocate spectrum [7], [8], [9], [10], [11], [12]. In most proposed auctions, the spectrum resource is treated as goods in traditional auctions studied by economists, i.e., one licensed band (or a collection of multiple bands) is awarded to one SU. However, spectrum auction differs from conventional

*This work is supported by the project TEROPP (technologies for TERminal in OPPortunistic radio applications) funded by the French National Research Agency (ANR).

This full text paper was peer reviewed at the direction of IEEE Communications Society subject matter experts for publication in the IEEE INFOCOM 2010 proceedings
This paper was presented as part of the main Technical Program at IEEE INFOCOM 2010.

auctions in that it has to address radio interference. Spectrum auction is essentially a problem of interference-constrained resource allocation. Only a few papers have discussed spectrum auctions under interference constraint, among which [11] and [12] studied conflict-free spectrum allocation with high spectrum efficiency. [10] developed an auction-based spectrum sharing framework to allow a single spectrum manager to share its spectrum with a group of users, subject to the interference temperature constraint at the measurement point, a requirement proposed by FCC in [3]. Based on the same model as [10], our work is among the relative few that investigate the interference-constraint radio resource allocation problem under the auction framework. Compared with previous work, we make the following key contributions:

- Existing auction mechanisms mainly focus on single-PU scenario with very limited analytical and numerical studies on multiple-PU case. Our work, however, conduct an in-depth analysis on the spectrum auction for multiple PUs to allocate their spectrum to multiple SUs efficiently and fairly. As a distinctive feature of the proposed auction framework, the SUs' strategy (bid) is two-dimensional and non-continuous, leading to a competition scenario with more complex interactions among players and requiring an original study of the resulting equilibrium.
- We investigate the spectrum auction with free spectrum bands and develop a distributed adaptive algorithm based on no-regret learning to converge to a CE of the auction game. To the best of our knowledge, our work is the first to adapt the auction framework to address the spectrum sharing problem in heterogeneous environments with both licensed and free bands.

The rest of this paper is structured as follows. Section II presents our system model and auction framework followed by the formulation of the non-cooperative auction game. Section III solves the auction game and analyzes the structural properties of the resulting NE. Section IV extends our auction framework to the more challenging scenario with free spectrum bands. Simulation results are presented in Section V. Section VI concludes the paper.

II. System Model and Spectrum Auctions

This section introduces the notation and the system model of our work, followed by the presentation of the proposed spectrum auction framework and the formulation of the auction game under the framework.

A. Cognitive radio network model

We consider a cognitive radio network consisting of a set of primary users referred to as PUs and a set of secondary transmitter-receiver pairs referred to as secondary users or SUs. We use $\mathcal{N} = \{1, 2, \cdots, N\}$ and $\mathcal{M} = \{1, 2, \cdots, M\}$ to denote the PU set and the SU set, respectively. We use S_i and D_i to denote the transmitter and the receiver of SU $i \in \mathcal{M}$. Each PU $n \in \mathcal{N}$ operates on a spectrum band n with bandwidth B_n that is non-overlapped with the spectrum bands of other PUs, i.e. $n_1 \bigcap n_2 = \Phi, \forall n_1, n_2 \in \mathcal{N}$.[1]

[1]The extension of our analysis to the more competitive scenario where the PUs' bands are overlapped with each other is left for future work.

SU i's valuation of the spectrum is defined by a utility function $U_i(\gamma_i)$, where γ_i is the received signal-to-interference-plus-noise ratio (SINR) at SU i's receiver D_i. $U_i(\gamma_i)$ characterizes the application payoff (e.g. satisfaction level) of SU i from SINR γ_i. We assume $U_i(\gamma_i)$ is continuously differentiable, strictly increasing and concave in γ_i with $U_i(0) = 0$. For each SU i, the received SINR using PU n's band is given by

$$\gamma_i = \frac{p_i h_{ii}}{n_0 B_n + \sum_{j \neq i} p_j h_{ji}}, \tag{1}$$

where p_i denotes SU i's transmission power, h_{ji} denotes the channel gain from SU j's transmitter S_j to SU i's receiver D_i, n_0 denotes the background noise power spectral density.

In the considered scenario, to ensure that the transmissions of PUs are not significantly degraded by the SUs, an interference temperature constraint is imposed such that the total received power of SUs at PU n must satisfy

$$\sum_{i=1}^{M} p_i g_{in} \leq P_n \quad \forall n \in \mathcal{N},$$

where g_{in} is the channel gain from S_i to PU n, P_n is the tolerable interference threshold at PU n.

B. Spectrum auction framework

We apply auction mechanisms to tackle the spectrum allocation problem. By definition, an auction is a decentralized market mechanism for allocating resources and can be formulated as a non-cooperative game, where players are bidders, strategies are bids, both allocations and payments are functions of bids. A well-known auction is the Vickrey-Clarke-Groves (VCG) auction [6], which is shown to have social optimal outcome. However, the VCG auction requires global information to perform centralized computations. To overcome this limitation, two one-dimensional share auction mechanisms, namely the SINR auction and the power auction are proposed in [10] to study the spectrum allocation problem in single-PU networks. In the following, we extend the work of [10] to the multiple-PU scenario by proposing the two-dimensional SINR and power auction, as shown in Algorithm 1.[2]

Algorithm 1 Two-dimensional spectrum auction algorithm

Price announcing: Each PU n announces a reserve bid β_n and a price $\pi_n > 0$.

Bidding: Based on β_n and π_n, each SU i submits a bid (a_i, b_i) where $a_i \in \mathcal{N}$ and $b_i \geq 0$.

Spectrum allocation: Each SU i is allocated a transmission power p_i from PU a_i as follows:

$$p_i = \frac{P_{a_i}}{g_{ia_i}} \frac{b_i}{\sum_{j \in \mathcal{M}, a_j = a_i} b_j + \beta_{a_i}}. \tag{2}$$

Payment collection: Each SU i pays PU a_i a payment $C_i = \pi_{a_i} \gamma_i g_{ia_i}$ in the SINR auction and $C_i = \pi_{a_i} p_i g_{ia_i}$ in the power auction.

[2]In our study, we assume that SUs are honest, and indeed make the payments. We do not consider the issue of *payment enforcement*, which may require a separate mechanism and is beyond the scope of the paper.

This full text paper was peer reviewed at the direction of IEEE Communications Society subject matter experts for publication in the IEEE INFOCOM 2010 proceedings
This paper was presented as part of the main Technical Program at IEEE INFOCOM 2010.

Under the above auction framework, the received SINR of SU i is

$$\gamma_i = \frac{P_{a_i}\frac{h_{ii}}{g_{ia_i}}b_i}{n_0 B_{a_i}\left(\sum_{j\in\mathcal{M},a_j=a_i} b_j + \beta_{a_i}\right) + \sum_{j\in\mathcal{M},a_j=a_i,j\neq i} P_{a_i}\frac{h_{ji}}{g_{ja_i}}b_j}. \quad (3)$$

In contrast to [10] where SUs are charged the same price per unit SINR, we apply the economic concept of *price discrimination* in the proposed SINR auction by imposing g_{ia_i} as a user-dependent pricing factor on SU i. The design rationale is that for two SUs choosing the same PU, the SU causing more interference at the PU should be charged more per unit SINR than the SU causing less interference. As we will show via numerical experiments, this feature is especially suited in multi-PU case by resulting a more balanced equilibrium. For the power auction, noticing that the received power of SU i at PU a_i is $p_i g_{ia_i}$, the auction scheme actually implements a pricing policy under which a price π_n per unit received power is imposed by PU n to the SUs connecting to it.

C. Non-cooperative spectrum auction game formulation

Under the proposed auction framework, we model the interaction among SUs as a non-cooperative spectrum auction game, denoted as G_{NSA} and G_{NPA} for the SINR and power auction, respectively.[3] Let $s_i = (a_i, b_i)$ denote the strategy of SU i and s_{-i} denote the strategy of the SUs except i, given the price vector $\pi = (\pi_n, n \in \mathcal{N})$, each SU i chooses its strategy s_i to maximize his *surplus function* defined as follows:

$$S_i(s_i, s_{-i}) = U_i(\gamma_i(s_i, s_{-i})) - C_i(s_i, s_{-i}).$$

The resulting non-cooperative SINR (power) auction game can then be defined formally as:

$$G_{NSA}(G_{NPA}): \max_{s_i=(a_i,b_i),a_i\in\mathcal{N},b_i\geq 0} S_i(s_i, s_{-i}),\ \forall i \in \mathcal{M}.$$

The solution of the auction game is characterized by a Nash Equilibrium (NE), a strategy profile $\mathbf{s}^* = (s_i^*, s_{-i}^*)$ from which no player has incentive to deviate unilaterally [13], i.e.,

$$S_i(s_i^*, s_{-i}^*) \geq S_i(s_i, s_{-i}^*), \quad \forall i \in \mathcal{M}, \forall a_i \in \mathcal{N}, \forall b_i \geq 0.$$

As a distinguished feature from the single-PU auction, the auction framework proposed in our work is two-dimensional and involves both PU selection and bid adjustment, which leads to a competition scenario with more complex interactions among players. Consequently, characterizing structural properties of the auction game in our context requires an original study of the game equilibria that cannot draw on existing well-known results, as will be shown in later analysis.

III. Solving the Auction Game: NE Analysis

In this section, we solve the auction game by deriving the NE of the game and study the structure properties of the NE. To this end, we focus on the following optimization problem faced by each SU i in the spectrum auction game, given the price of PUs $\pi = \{\pi_n, n \in \mathcal{N}\}$ and strategies of others s_{-i}:

$$s_i^* = (a_i^*, b_i^*) = \operatorname*{argmax}_{s_i} S_i(s_i, s_{-i}), \quad (4)$$

which, according to the following lemma, can be written as

$$s_i^* = (a_i^*, b_i^*) = \operatorname*{argmax}_{a_i\in\mathcal{N}} \operatorname*{argmax}_{b_i\geq 0} S_i(s_i, s_{-i}).$$

Lemma 1. $\max_{(a_i,b_i)} S_i(s_i, s_{-i}) = \max_{a_i\in\mathcal{N}} \max_{b_i\geq 0} S_i(s_i, s_{-i})$.

Proof: On one hand, it follows from (4) that

$$S_i((a_i^*, b_i^*), s_{-i}) \geq \max_{a_i\in\mathcal{N}} \max_{b_i\geq 0} S_i((a_i, b_i), s_{-i}).^4$$

On the other hand, we have

$$\begin{aligned}\max_{a_i\in\mathcal{N}} \max_{b_i\geq 0} S_i((a_i, b_i), s_{-i}) &\geq \max_{b_i\geq 0} S_i((a_i^*, b_i), s_{-i}) \\ &\geq S_i((a_i^*, b_i^*), s_{-i}).\end{aligned}$$

Combining the above results completes our proof. ■

A. SINR auction

We start with the SINR auction game. Unlike the single-PU auction studied in [10], where each SU maximizes its surplus function over its bid only, the SU optimization problem in the multiple-PU case is a joint two-dimensional problem over the submitted bid and the PU to whom the SU bids for spectrum. To solve the SUs' optimization problem, a straightforward way to find (a_i^*, b_i^*) is to search over all possible PU settings and perform optimization over bid for every setting, which is computationally intensive and makes the resulting NE intractable. In our analysis, we overcome this technical difficulty by decomposing the two-dimensional optimization problem based on the structural properties of the surplus function, detailed in Lemma 2.

Lemma 2. *For each SU i, given* π *and* s_{-i}*, it holds that*

$$a_i^* = \operatorname*{argmax}_{n\in\mathcal{N}} S_i(\gamma_{in}^*) = \operatorname*{argmax}_{n\in\mathcal{N}} U_i(\gamma_{in}^*) - \pi_n g_{in}\gamma_{in}^*,$$

where $\gamma_{in}^* = \min\{U_i'^{-1}(\pi_n g_{in}), P_n h_{ii}/(n_0 B_n g_{in})\}, \forall n \in \mathcal{N}$.

Proof: Let γ_{in} denote the SINR of SU i when connecting to PU n, recall (3), we can show that:

1) γ_{in} is upper-bounded by $P_n h_{ii}/(n_0 B_n g_{in})$;
2) For $\gamma_{in} \leq P_n h_{ii}/(n_0 B_n g_{in})$, there is an one-to-one mapping between γ_{in} and b_i.

From Lemma 1, the optimization problem of SU i is thus equivalent to the following one:

$$\max_{n\in\mathcal{N}} \max_{\gamma_{in}\leq\frac{P_n h_{ii}}{n_0 B_n g_{in}}} S_i(n, \gamma_{in}).$$

Moreover, when choosing PU n, S_i can be written as a function of γ_{in} as

$$S_i(\gamma_{in}) = U_i(\gamma_{in}) - \pi_n g_{in}\gamma_{in},$$

whose derivative is

$$\frac{\partial S_i}{\partial \gamma_{in}} = U_i'(\gamma_{in}) - \pi_n g_{in}.$$

Following the concavity of U_i, U_i' is monotonously decreasing in γ_{in}. Hence S_i is a quasi-concave function of γ_{in}, thus has a unique global maximizer $\gamma_{in}^* =$

[3] In this work, we do not consider the PUs as players. A significant extension of our work presented in this paper is to model the spectrum auction as a *Stackelberg game*, in which the PUs are the leaders that choose their strategy (price) first, and the SUs are the followers that respond by choosing their strategies (bids) accordingly, knowing the leaders' strategies [13]. We leave this extension of exploring the Stackelberg game for future work.

[4] For the sake of simplicity, in case of non-ambiguity, we note $S_i((a_i^*, b_i^*), s_{-i})$ as a function of s_i, i.e. $S_i(s_i)$ or $S_i(a_i^*, b_i^*)$.

$\min\{U_i'^{-1}(\pi_n g_{in}), P_n h_{ii}/(n_0 B_n g_{in})\}$. The maximum of S_i under PU n is given by $S_i(\gamma_{in}^*)$. It then follows that

$$a_i^* = \operatorname*{argmax}_{n\in\mathcal{N}} \ S_i(\gamma_{in}^*) = \operatorname*{argmax}_{n\in\mathcal{N}} \ U_i(\gamma_{in}^*) - \pi_n g_{in}\gamma_{in}^*,$$

where $\gamma_{in}^* = \min\{U_i'^{-1}(\pi_n g_{in}), P_n h_{ii}/(n_0 B_n g_{in})\}$. ■

Specifically, when π_n is significantly large, more precisely, $\pi_n g_{in} \geq U_i'(P_n h_{ii}/n_0 B_n g_{in}), \forall n \in \mathcal{N}, \forall i \in \mathcal{M}$, Lemma 2 can be simplified to Corollary 1.

Corollary 1. *If $\pi_n g_{in} \geq U_i'(P_n h_{ii}/n_0 B_n g_{in}), \forall n \in \mathcal{N}, \forall i \in \mathcal{M}$, it holds that $a_i^* = \operatorname{argmin}_{n\in\mathcal{N}} \pi_n g_{in}$.*

Proof: Recall that $U_i(\gamma_i)$ is concave in γ_i, $\pi_n g_{in} \geq U_i'(P_n h_{ii}/n_0 B_n g_{in})$ leads to $U_i'^{-1}(\pi_n g_{in}) \leq P_n h_{ii}/(n_0 B_n g_{in})$. It then follows from Lemma 2 that $\gamma_{in}^* = U_i'^{-1}(\pi_n g_{in})$ and

$$\begin{aligned} a_i^* &= \operatorname*{argmax}_{n\in\mathcal{N}} S_i(U_i'^{-1}(\pi_n g_{in})) \\ &= \operatorname*{argmax}_{n\in\mathcal{N}} U_i(U_i'^{-1}(\pi_n g_{in})) - \pi_n g_{in} U_i'^{-1}(\pi_n g_{in}). \end{aligned}$$

Let $x = \pi_n g_{in}$, regard $S_i = U_i(U_i'^{-1}(x)) - xU_i'^{-1}(x)$ as a function of x, after some mathematical operations, we have

$$\frac{\partial S_i}{\partial x} = -U_i'^{-1}(x),$$

which, following the concavity of U_i, is non-positive. $S_i(x)$ is thus non-increasing in x. Hence

$$a_i^* = \operatorname*{argmax}_{n\in\mathcal{N}} \ S_i(U_i'^{-1}(\pi_n g_{in})) = \operatorname*{argmin}_{n\in\mathcal{N}} \ \pi_n g_{in},$$

which concludes our proof. ■

If we denote $\pi_n g_{in}$ as the effective price for SU i when choosing PU n, Corollary 1 states that SU i always chooses the PU with the minimum effective price.

As the key results of this subsection, we have demonstrated that in the SINR auction game, the choice of PU only depends on the effective price set by PUs. Consequently, the optimization problem of each SU i can be decomposed into two sub-problems, which can be performed sequentially:

1) i chooses PU a_i^* based on the effective price of PUs and stay with PU a_i^*;
2) i performs bid optimization by adjusting its bid submitted to PU a_i^*, which is degenerated into single-PU case.

The following theorem on the NE of the SINR auction game is then immediate whose proof follows straightforwardly from that of Theorem 1 and Proposition 6 in [10].

Theorem 1. *For the SINR auction with $\beta_n > 0, \forall n \in \mathcal{N}$, there exists a threshold price vector $\pi_{th}^s = \{\pi_{th,n}^s, n \in \mathcal{N}\}$ such that if the price vector $\pi > \pi_{th}^s$,[5] a NE exists to which the best response update converges. The NE is unique if a_i^* is singleton for every SU i. On the other hand, if there exists some $n_0 \in \mathcal{N}$ such that $\pi_{n_0} \leq \pi_{th,n_0}^s$, there is no NE.*

B. Power auction

In this subsection, we turn to the power auction game. As the payment function C_i in the power auction has a different structure to that in the SINR auction (i.e. C_i is a function of p_i instead of γ_i), the decomposition in the previous analysis on the SINR auction is no more applicable here. To characterize the equilibrium of the power auction game, we make the following approximation in the subsequent analysis:

$$\sum_{a_j=a_i, j\neq i} b_j \gg b_i, \forall i \in \mathcal{M}, \text{ or equivalently, } \sum_{s_j=a_i, j\neq i} b_j \sim \sum_{s_j=a_i} b_j. \quad (5)$$

The approximation (5) is accurate in large systems where the bid variation of any individual player has neglectable influence on the system state. More specifically, under (5), the impact of b_i on the interference at the receiver D_i, denoted as I_i, can be neglected, in other words, I_i can be regarded independent w.r.t. b_i. The utility function of SU i can then be written as:

$$S_i = U_i(\gamma_i) - \frac{\pi_{a_i} g_{ia_i} I_i}{h_{ii}} \gamma_i.$$

where $I_i = n_0 B_{a_i} + \sum_{j\in\mathcal{M}, j\neq i, a_j=a_i} p_j h_{ji}$.

To solve the power auction game, we transform the original game G_{NPA} into another game G'_{NPA} in which the strategy of SU i is (a_i, γ_i) instead of (a_i, b_i) in G_{NPA}. Under the approximation (5), γ_i can be regarded as a linear function of b_i. As I_i is independent w.r.t. b_i, any unilateral change in b_i can be transformed into related change in γ_i without any influence on γ_{-i}. Thus the original game G_{NPA} is equivalent to the transformed game G'_{NPA}, formally expressed as

$$G'_{NPA}: \quad \max_{s_i=(a_i,\gamma_i)} \quad S_i(s_i, s_{-i}), \ i \in \mathcal{M}.$$

We now concentrate on the new game G'_{NPA}. Performing the same analysis as Lemma 1 and Corollary 1 by noticing that $I_i \geq n_0 B_{a_i}$, we have the following result that decouples the PU selection and the adjustment of γ_i in G'_{NPA}.

Lemma 3. *If $\pi_n g_{in} n_0 B_n/h_{ii} \geq U_i'(P_n h_{ii}/n_0 g_{in}), \forall n \in \mathcal{N}, \forall i \in \mathcal{M}$, it holds that $a_i^* = \operatorname{argmin}_{n\in\mathcal{N}} \pi_n g_{in} I_i/h_{ii}$.*

Compared with the SINR auction game where the effective price imposed by PU n to SU i is $\pi_n g_{in}$, in the power auction game, the corresponding effective price becomes $\pi_n g_{in} I_i/h_{ii}$. Lemma 3 states that SU i always chooses the PU with the minimum effective price. Armed with Lemma 3, we can then establish the existence of NE in G'_{NPA} under the condition that the prices set by PUs are sufficiently high.

Theorem 2. *Under the approximation* (5) *and the condition in Lemma 3, G'_{NPA} admits a NE.*

Proof: For any SU i, under the strategy of others $s_{-i} = (a_{-i}, \gamma_{-i})$, it follows from Lemma 3 that i chooses PU $a_i^* = \min_{n\in\mathcal{N}} \pi_n g_{in} I_i/h_{ii}$, i.e., for any $a_i' \neq a_i^*$, it holds that

$$\frac{\pi_{a_i^*} h_{ia_i^*} I_i(a_i^*)}{h_{ii}} \leq \frac{\pi_{a_i'} h_{ia_i'} I_i(a_i')}{h_{ii}}.$$

It then follows that for any $\gamma_i \geq 0$

$$S_i(a_i^*, \gamma_i) = U_i(\gamma_i) - \frac{\pi_{a_i^*} h_{ia_i^*} I_i(a_i^*)}{h_{ii}} \gamma_i \geq U_i(\gamma_i) - \frac{\pi_{a_i'} h_{ia_i'} I_i(a_i')}{h_{ii}} \gamma_i = S_i(a_i', \gamma_i),$$

which implies that given the opponents' strategy, choosing PU a_i^* is always the dominating strategy for any γ_i.

On the other hand, performing the same analysis as Lemma 1, we can show that in G'_{NPA},

$$\max_{(a_i,\gamma_i)} \quad S_i(s_i, s_{-i}) = \max_{\gamma_i} \ \max_{a_i} S_i(s_i, s_{-i}).$$

The optimization problem for SU i thus becomes

$$\max_{(a_i,\gamma_i)} S_i(s_i, s_{-i}) = \max_{\gamma_i} \ S_i(a_i^*, \gamma_i),$$

[5] Throughout the paper, the inequality between two vectors is defined as the inequality in all components of the vectors.

This full text paper was peer reviewed at the direction of IEEE Communications Society subject matter experts for publication in the IEEE INFOCOM 2010 proceedings
This paper was presented as part of the main Technical Program at IEEE INFOCOM 2010.

in which the utility function of SU i is $S_i(a_i^*, \gamma_i)$, which is concave in γ_i. Furthermore, it follows from $I_i \geq n_0 B_n$ and $p_i \leq P_n/g_{ia_i}$ when SU i chooses PU n that $\gamma_i \leq \max_{n\in\mathcal{N}} h_{ii}P_n/(g_{ia_i}n_0B_n)$. Thus the strategy space $\gamma = (\gamma_i, i \in \mathcal{M})$ is a nonempty, convex, and compact set. It then follows from Theorem 1 in [14] that G'_{NPA} admits a NE. ■

Due to the complexity of the power auction game in which each SU has to solve a two-dimensional, non-continuous and non-decomposable optimization problem, we do not have a formal proof of the uniqueness of the NE and the convergence under the best response update. However, our experiment results show that the convergence is achieved in the vast majority of cases (cf. Section V-C).

C. The two-level game model

To get more insight on the structure of the auction game, we introduce and analyze in this subsection the following two-level game model: the lower level bidding game under fixed PU setting (Definition 1) and the higher level PU selection game (Definition 2).

Definition 1. *Given a fixed PU setting $\mathbf{a} = \{a_i, i \in \mathcal{M}\}$, the bidding game, denoted as $G^B_{NSA}(\mathbf{a})$ and $G^B_{NPA}(\mathbf{a})$ for the SINR and power auction respectively, is a tuple $(\mathcal{M}, \mathcal{A}, \{S_i, i \in \mathcal{M}\})$, where the SU set $\mathcal{M}$ is the player set, $\mathcal{A} = [0, +\infty)^M$ is the strategy set, $\{S_i\}$ is the utility function set with S_i being the surplus function. Each player (SU) i selects its strategy (bid) $b_i \geq 0$ to maximize its utility S_i.*

The above defined bidding game can be analyzed in the same way as the single-PU bidding game presented in [10] with the following result on the NE.

Lemma 4. *For the SINR auction (for the power auction under the approximation (5)) with $\beta_n > 0, \forall n \in \mathcal{N}$, there exists a threshold price vector $\pi^{sb}_{th}(\mathbf{a})$ ($\pi^{pb}_{th}(\mathbf{a})$) such that there exists a NE to which the best response update converges if the price vector $\pi > \pi^{sb}_{th}(\mathbf{a})$ ($\pi > \pi^{pb}_{th}(\mathbf{a})$), there is no NE otherwise.*

Proof: The proof for the SINR auction follows immediately from Theorem 1 and Proposition 6 in [10]. For the power auction, we show that under the condition in the lemma, the best response function has the same structure as that in the SINR auction in [10] whose convergence to NE is proven (Theorem 1 in [10]). To this end, recall that under (5), the utility function can be written as

$$S_i = U_i(\gamma_i) - \frac{\pi g_{i0} I_i}{h_{ii}}\gamma_i,$$

where I_i is independent of b_i. For each SU i, we can solve the best response $b_i = B(b_{-i})$ as follows:

$$\begin{cases} b_i = +\infty & \text{if } \pi \leq \frac{h_{ii}}{I_i g_{i0}} U_i'(\frac{P_{a_i}h_{ii}}{n_0 B_{a_i} g_{ia_i}}) \\ \pi = \frac{h_{ii}U_i'(\gamma_i)}{I_i g_{i0}} & \text{if } \frac{h_{ii}}{I_i g_{i0}} U_i'(\frac{P_{a_i}h_{ii}}{n_0 B_{a_i} g_{ia_i}}) < \pi < \frac{h_{ii}}{I_i g_{i0}} U_i'(0) \\ b_i = 0 & \text{if } \pi \geq \frac{h_{ii}}{I_i g_{i0}} U_i'(0) \end{cases} \quad (6)$$

Noticing the structural similarity between (6) and (22) in [10], we can establish the existence of NE and the convergence to the NE under the best response update (6). ■

Definition 2. *The PU selection game, denoted as G^{PU}_{NSA} and G^{PU}_{NPA} for the SINR and power auction respectively, is a tuple $(\mathcal{M}, \mathcal{A} = \{A_i\}, \{\widehat{S}_i, i \in \mathcal{M}\})$, where $\mathcal{M}$ is the player set, $A_i = \mathcal{N}$ is the strategy set of SU i, the utility function of SU i is defined as $\widehat{S}_i(a_i, a_{-i}) \triangleq S_i(\mathbf{a}, \mathbf{b}^*)$ where $\mathbf{b}^*(\mathbf{a}) = \{b_i^*(\mathbf{a}), i \in \mathcal{M}\}$ denotes the NE of the bidding game under the PU setting $\mathbf{a}$. Each player (SU) i selects its strategy (PU) $a_i \in \mathcal{N}$ to maximize its utility $\widehat{S}_i$.*

To analyze the PU selection game, we write the optimization problem of each SU i as

$$\max_{a_i} \ \widehat{S}_i(a_i, a_{-i}) = \max_{a_i} \ S_i(\mathbf{a}, \mathbf{b}^*(\mathbf{a})).$$

Noticing that in the bidding game under PU setting $\mathbf{a}$, it holds that $S_i(\mathbf{a}, \mathbf{b}^*(\mathbf{a})) = \max_{b_i} S_i(a_i, b_i)$, we thus have

$$\max_{a_i} \ \widehat{S}_i(a_i, a_{-i}) = \max_{a_i}\max_{b_i} \ S_i(a_i, b_i),$$

which, according to Lemma 1, is the same optimization problem as for the global auction game analyzed previously. Hence, we can map the NE of the PU selection game and the corresponding bidding game to the NE of the global auction game, as stated in the following theorem.

Theorem 3. *Any (pure) NE of the auction game can be mapped to a (pure) NE of the PU selection game $\mathbf{a}^*$ and the corresponding NE of the bid game $\mathbf{b}^*(\mathbf{a}^*)$ under the PU setting $\mathbf{a}^*$, i.e., any pure NE of the power auction game can be expressed as $\mathbf{s}^* = (a_i^*, b_i^*(\mathbf{a}^*), i \in \mathcal{M})$.*

By decomposing the global auction game into the PU selection game and the bidding game, we introduce a two-level architecture into the spectrum auction problem, in which the higher level PU selection game is a finite strategy game. This hierarchicalization can help us analyze the spectrum auction in more complex scenarios, as explored in the next section.

IV. Spectrum auction with free spectrum bands

Until now, we have analyzed the spectrum auction game in which the unlicensed SUs purchase spectrum resource from licensed PUs. In this section, we extend our auction framework to the more challenging scenario with free spectrum bands. In such context, the SUs have the choice between accessing the licensed spectrum bands owned by PUs which is charged as a function of the enjoyed SINR or received power at PUs, and switching to the unlicensed spectrum bands which are free of charge but become more crowded when more SUs operate in these spectrum bands. Consequently, the SUs should strike a balance between accessing the free spectrum bands with probably more interference and paying for communication gains by staying with the licensed bands. In the subsequent study, we assume that there is one free spectrum band available for all SUs. The extension to multiple free band case is straightforward.

We start with the SINR auction. In the new scenario with a free band, we define the spectrum band set $\mathcal{N} = \{1, \cdots, N, N+1\}$ where band 1 to N are the licensed bands processed by PU 1 to N, band $N+1$ denotes the free band with bandwidth B_{N+1}. Compared with the previous analysis without free spectrum band, each SU i has an additional choice of switching to band $N+1$ and the corresponding utility is

$$S_i(N+1) = U_i(\gamma_i), \quad (7)$$

where γ_i is the SINR of SU i. It is obvious to see that all SUs operating at B_{N+1} transmits at its maximum power, denoted as $p_j^{max}, j \in \mathcal{M}$, to maximize their utility. Hence

$$\gamma_i = \frac{p_i^{max} h_{ii}}{n_0 B_{N+1} + \sum_{j \neq i, a_j = N+1} p_j^{max} h_{ji}}.$$

From Corollary 1, each SU i faces the choice of accessing the licensed band with minimum effective price and the free band $N+1$. As in Definition 1 and 2, we can define the corresponding PU selection game and bidding game in the new context[6]. The PU selection game is a finite strategy game and hence has at least one pure or mixed NE. By performing the same analysis as that in Section III-C, we can establish a mapping between a NE of the auction game and a NE of the PU selection game in the new context.

We then address the problem of how to reach a NE of the PU selection game, which is also a NE of the global auction game. We first notice that the myopic best response update in the PU selection game is not guaranteed to converge to a NE. In fact, during the course of PU selection, the SUs may notice that the utility of accessing a licensed spectrum is higher than staying in the free spectrum, and thus switch to the licensed spectrum accordingly. Since the SUs do this simultaneously, the free spectrum becomes under-loaded and the SUs will switch back to the free spectrum in the next iteration. This phenomenon, in which a player keeps switching between two strategies, is known as ping-pong effect.

To eliminate the ping-pong effect, we develop an algorithm based on the no-regret learning to converge to a correlated equilibrium (CE) of the PU selection game, which is shown to be a CE of the global auction game, too. Before presenting the proposed algorithm, we first provide a brief introduction on CE and no-regret learning.

A. Overview of correlated equilibrium

The concept of CE was proposed by Nobel Prize winner, Robert J. Aumann [5], in 1974. It is more general than NE. The idea is that a strategy profile is chosen randomly according to a certain distribution. Given the recommended strategy, it is to the players' best interests to conform with this strategy. The distribution is called CE, formally defined as follows.

Definition 3. *Let $G = (\mathcal{N}, (\Sigma_i, i \in \mathcal{N}), (S_i, i \in \mathcal{N}))$ be a finite strategy game, where $\mathcal{N}$ is the player set, Σ_i is the strategy set of player i and S_i is the utility function of i, a probability distribution p is a correlated equilibrium of G if and only if $\forall i \in \mathcal{N}$, $r_i \in \Sigma_i$, it holds that*

$$\sum_{r_{-i} \in \Sigma_{-i}} p(r_i, r_{-i})[S_i(r_i', r_{-i}) - S_i(r_i, r_{-i})] \leq 0, \ \forall r_i' \in \Sigma_i,$$

or equivalently,

$$\sum_{r_{-i} \in \Sigma_{-i}} p(r_{-i}|r_i)[S_i(r_i', r_{-i}) - S_i(r_i, r_{-i})] \leq 0, \ \forall r_i' \in \Sigma_i.$$

The second formula means that when the recommendation to player i is to choose strategy r_i, then choosing strategy $r_i' \neq r_i$ cannot lead to a higher expected payoff to i.

The CE set is nonempty, closed and convex in every finite strategy game. Moreover, every NE is a CE and corresponds to the special case where $p(r_i, r_{-i})$ is a product of each individual player's probability for different strategies, i.e., the play of the different players is independent.

B. Overview of no-regret learning

The no-regret learning algorithm [4] is also termed regret-matching algorithm. The stationary solution of the no-regret learning algorithm exhibits no regret and the probability of choosing a strategy is proportional to the "regret" for not having chosen other strategies. For any two strategies $r_i \neq r_i'$ at any time T, the regret of player i for not playing r_i' is

$$R_i^T(r_i, r_i') \triangleq \max(D_i^T(r_i, r_i'), 0), \tag{8}$$

where

$$D_i^T(r_i, r_i') \triangleq \frac{1}{T} \sum_{t \leq T} (S_i^t(r_i', r_{-i}) - S_i^t(r_i, r_{-i})). \tag{9}$$

$D_i^T(r_i, r_i')$ has the interpretation of average payoff that player i would have obtainned, if it had played r_i' every time in the past instead of r_i. $R_i^T(r_i, r_i')$ is thus a measure of the average regret. The probability that player i chooses r_i is a linear function of the regret. For every period T, define the relative frequency of players' strategy $\mathbf{r}$ played till T periods of time as follow:

$$z_T(\mathbf{r}) \triangleq \frac{1}{T} N(T, \mathbf{r}),$$

where $N(T, \mathbf{r})$ denotes the number of periods before T that the players' strategy is $\mathbf{r}$. *As an important property, z_T is guaranteed to converge almost surely (with probability one) to a set of CE in no-regret learning algorithm.*

C. Proposed algorithm based on no-regret learning

In this subsection, we develop an algorithm (Algorithm 2) based on no-regret learning and prove its convergence to a CE of the SINR auction game.

Algorithm 2 No-regret learning algorithm: SINR auction

Initialization: For each SU i, let p denote a random number between 0 and 1 and $a_i^* = \min_{n \in \mathcal{N}} \pi_n g_{in}$ (if a_i is not a singleton, randomly choose one), set $p^0_{a_i = a_i^*} = p$ and $p^0_{a_i = N+1} = 1 - p_{a_i}$. Let T_0 be a sufficient iteration duration.
for $t = kT_0$, $k = 1, 2, 3, \cdots$ **do**
  Select spectrum a_i with probability $p_i^t(a_i)$ and use best-response update to converge to the NE of the bidding game.
  When the NE is achieved after sufficient time, update the average regret R_i^t.
  Let a_i^t denote the spectrum which SU i selects for iteration t, let μ be a large constant, calculate p_i^{t+1} as:

$$\begin{cases} p_i^{t+1}(a_i) &= \frac{1}{\mu} R_i^t, \quad \forall a_i \in \mathcal{N}, \ a_i \neq a_i^t \\ p_i^{t+1}(a_i) &= 1 - \sum_{n \in \mathcal{N}, n \neq a_i^t} p_i^{t+1}(n), \quad a_i = a_i^t \end{cases}$$

end for

Theorem 4. *There exists a threshold price vector π^{th} such that if the price vector $\pi > \pi^{th}$, the proposed algorithm converges surely to a CE of the SINR auction game.*

Proof: It follows from the structure of the bidding game that a threshold price vector π^{th} exists such that if the

[6] For the free band, there is no bidding game, or alternatively, we can define a dumb bidding game for the free band, at the NE of which each SU choosing the free band submits 0 as bid and the utility is given by (7)

price vector $\pi > \pi^{th}$, the convergence to the NE of the bidding game is guaranteed under the given spectrum setting. It then follows from the convergence property of the no-regret learning that the proposed algorithm converges surely to a CE of the PU selection game, denoted as $\mathbf{p}$, i.e.,

$$\sum_{a_j \in \mathcal{N}, j \in \mathcal{M}, j \neq i} p(a_{-i}|a_i)[S_i((a_i', b_i'^*), (a_{-i}, b_{-i}'^*)) - S_i((a_i, b_i^*), (a_{-i}, b_{-i}^*))] \leq 0, \quad \forall a_i' \in \mathcal{N},$$

where b_i^* and $b_i'^*$ is the strategy of SU i at the NE of the bidding game under the spectrum setting (a_i, a_{-i}) and (a_i', a_{-i}), respectively. It follows from the NE definition of the bidding game that

$$S_i((a_i', b_i'^*), (a_{-i}, b_{-i}'^*)) = \max_{\gamma_i} U_i(\gamma_i) - \pi_{a_i'} g_{ia_i'} \gamma_i.$$

On the other hand, we have

$$S_i((a_i', b_i'), (a_{-i}, b_{-i}^*)) \leq \max_{\gamma_i} U_i(\gamma_i) - \pi_{a_i'} g_{ia_i'} \gamma_i, \ \forall b_i' \geq 0.$$

Hence, it holds that

$$\sum_{a_j \in \mathcal{N}, j \in \mathcal{M}, j \neq i} p(a_{-i}|a_i)[S_i((a_i', b_i'), (a_{-i}, b_{-i}^*)) - S_i((a_i, b_i^*), (a_{-i}, b_{-i}^*))] \leq 0, \quad \forall a_i' \in \mathcal{N}, \ \forall b_i \geq 0,$$

indicating that $\mathbf{p}$ is also a CE of the SINR auction game. ■

As a desirable property, Algorithm 2 can be implemented distributedly such that each SU i only needs to know the price vector π, its own channel gain h_{ii} and that between S_i and each PU n g_{in}. The best response update of the bidding game can be implemented distributedly at each SU i based on the knowledge of h_{ii} and g_{in}, the measurement of n_0 and the SINR γ_i, as detailed in [10]. We then show that the average regret can be calculated at each SU without any other information. Noticing (9) and recall the utility function of the PU selection game in Definition 2, it suffices to show that at each iteration t, $\Gamma_i^t(a_i^t, a_{-i}^t) \triangleq \sum_{k \leq t} \widehat{S}_i(a_i^t, a_{-i}^k), \forall a_i^t \in \mathcal{N}$ can be calculated distributedly.

In fact, at each iteration k, $\widehat{S}_i$ can be calculated as

$$S_i^k = \begin{cases} U_i(\frac{h_{ii} p_i^{max}}{I_i^{N+1}}) & a_i^t = N+1 \\ U_i(\gamma_{ia_i^t}^*) - \pi_{a_i^t} g_{ia_i^t} \gamma_{ia_i^t}^* & a_i^t \neq N+1 \end{cases},$$

where $\gamma_{ia_i^t}^* = U_i'^{-1}(\pi_{a_i^t} g_{ia_i^t})$, I_i^{N+1} is the interference experienced by SU i when choosing the free band, which can be measured locally. Γ_i^t can then be calculated by induction as

$$\Gamma_i^t = \begin{cases} U_i^t(a_i^t, a_{-i}^t) & t = 1 \\ \Gamma_i^{t-1}(a_i^t, a_{-i}^{t-1}) + U_i^t(a_i^t, a_{-i}^t) & t > 1 \end{cases}.$$

Consequently, the average regret can then be calculated based on only local measurement, which leads to the entirely distributed implementation of the proposed algorithm.

For the power auction, a similar distributed algorithm based on no-regret learning can be derived with convergence to a CE.

V. Simulation analysis

In this section, we conduct simulations to evaluate the performance of the proposed auction framework and demonstrate some intrinsic properties of the proposed auction framework, especially the fairness and efficiency, which are not explicitly addressed in the analytical part of the paper. After presenting the simulation setting, we introduce a reference power allocation scheme, called NAIVE, to which our proposed auction mechanisms are compared. In the first set of simulations, we consider an illustrative scenario to compare the SINR, power auctions with the NAIVE scheme. In the second set of simulations, we focus on the power auction in realistic network configurations with and without free spectrum band.

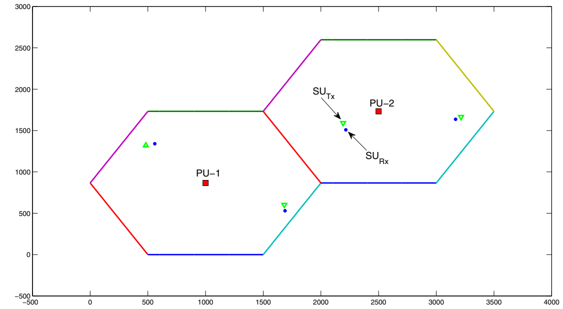

Fig. 1. Simulation setting

A. Simulation parameters and reference scheme

In our simulations, we consider a network of two PUs and multiple SUs (transmitter-receiver pairs). PUs can be seen as two access points or base stations covering two hexagonal cells, as shown in Figure 1. They can accept a certain amount of interference while allowing SUs to communicate during uplink PU transmissions.

In all simulations, we set $B_n = 5$ MHz and $P_n = 2n_0 B_n$ $\forall n$. We adopt a typical urban path-loss model (C2 NLOS WINNER model [15] for WiMAX) with carrier frequency $f_c = 3.5$ GHz and path-loss exponent $\alpha = 3.5$. Shadowing effect is neglected.

In order to show the performance gain brought by our solutions, we introduce a reference power allocation scheme termed NAIVE. In NAIVE, SUs choose the furthest PU based on the knowledge of channel gains g_{in}[7]. Each PU n then allocates power $p_i = P_n/(M_n g_{in})$ to SU i choosing it, where M_n is the number of SU choosing PU n. In the scenario with a free band, the SUs in the NAIVE scheme switch to the free band with certain probability p_{free} (we analyze the cases $p_{free} = 1/2$ and $p_{free} = 1/3$). This simple scheme serves as the reference scheme for performance comparison.

B. Illustrative example: SINR and power auctions

We start with an illustrative example to compare the SINR, power auctions and the NAIVE scheme. We consider the fixed network configuration illustrated in Figure 1 with two PUs and four SUs with $\theta_i \in [1, 20], \forall i$. There is no free band in this example. The prices $\pi_1 = \pi_2$ are optimized by dichotomy[8].

We study the dynamics of the spectrum acution game under the best-response update. In the SINR auction, each SU chooses the PU with the minimum effective price (cf. Corollary 1) and then iteratively adjust its bid. Figure 2 (left) shows the convergence of allocated power to SUs. After about 40 iterations, convergence is reached. Compared with the

[7] The rationale of the choice is that choosing the furthest PU causes the least interference at the PU.

[8] Recall that the more competitive scenario where the PUs set their prices to maximize their revenue consists of a significant extension of the current work and is left for future studies.

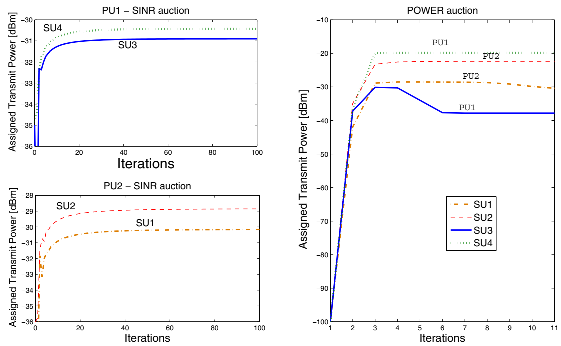

Fig. 2. Convergence of allocated power in the SINR auction (left) and power auction (right); final PU choice is shown for each SU with power auction.

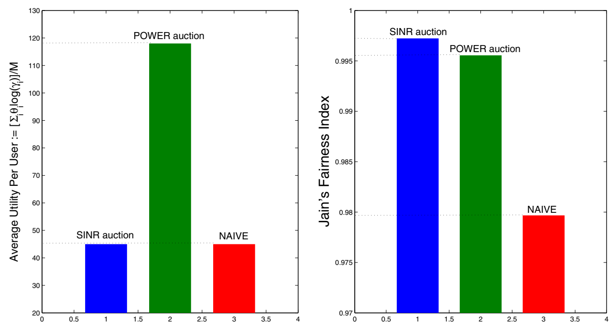

Fig. 3. Average utility per SU (left) and Jain's fairness index calculated based on U_i/θ_i (right) for SINR, power auctions and NAIVE

SINR auction where the choice of PU is done at the very first iteration and is not modified afterwards, in the power auction, the effective price is given by Lemma 3. As one part of the effective price, I_i changes from one iteration to another depending on the strategy of other SUs s_{-i}, thus the choice of PU may also vary from one iteration to another. However, as shown in Figure 2 (right), the final allocated power of each SU converges after about 10 iterations and the choice of PU is stablized. Compared with the SINR auction, the power auction converges in a faster but less smooth way.

In Figure 3, we focus on the efficiency and fairness of the considered schemes by studying the average utility per SU and the Jain's fairness index [16]. The Jain's index is computed based on the normalized utility U_i/θ_i. From the results, we observe that the SINR auction and the NAIVE scheme have almost the same average utility, but the SINR auction outperforms significantly the NAIVE scheme in terms of fairness. The power auction, on the other hand, has a very good performance in terms of both efficiency and fairness.

C. Realistic experiment: power auction

We now turn to more realistic scenarios. We focus on the power auction as it achieves the best performance in the above illustrative example. The power auction is also more natural and realistic in that SUs pay for the interference they create to PUs instead of the SINR they get as in the SINR auction. In our simulation, the transmitters of SUs are randomly located in each of the two cells. the receivers are randomly drawn in a disk with radius 100m whose center is the corresponding transmitter. We run Monte Carlo simulations with 1000 snapshots. At each snapshot, SU locations are randomly drawn with θ_i randomly drawn in $[1, 20]$.

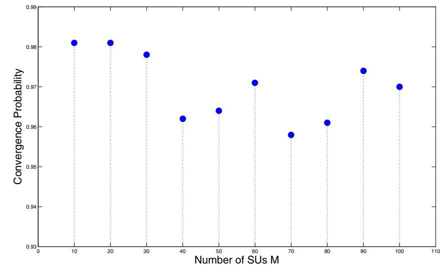

Fig. 4. Convergence probability of power auction

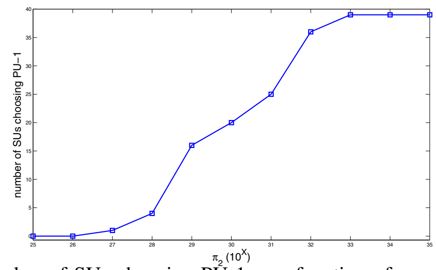

Fig. 5. Number of SUs choosing PU 1 as a function of π_2

1) Convergence: As explained in Section III-B, the best-response update is not guaranteed to converge. We thus study the convergence probability. We consider that the convergence is achieved if the best-response update in the power auction converges within 100 iterations, otherwise we consider that the auction does not converge. Figure 4 shows the probability of convergence as a function of the number of SU under this criterion: in the vast majority cases (more precisely, in more than 95% cases), convergence is achieved. In the subsequent simulations, in case of non-convergence, the results are based on the allocated power values after 100 iterations.

2) Load balancing: Figure 5 shows a scenario in which PU 1 fixes its price $\pi_1 = 10^{30}$ and PU 2 varies its price π_2 in the range $[10^{25}, 10^{35}]$. The total number of SUs M is set to 40. As shown in the figure, the number of SUs choosing PU 1 increases with π_2. The results demonstrate the benefit of the proposed power auction framework in load balancing by adjusting the prices of PUs. This feature is obviously not possible in NAIVE.

3) Efficiency and fairness: We now focus on two key performance metrics: efficiency and fairness. To this end, we compare the power auction and the NAIVE scheme in terms of average utility per SU and the Jain fairness index in two configurations. In the first configuration *M/2 system*, half of SUs are geographically located in cell 1 and the other half in cell 2. In the second configuration *M-2 system*, the number of SUs in cell 2 is constant ($M_2 = 2$), while the number of SU in cell 1 is variable in cell 1 ($M_1 = M - 2$). The two configurations represent two typical network scenarios, the balanced one with a homogeneous distribution of SUs and the unbalanced one with a heterogeneous distribution of SUs. As for the illustrative example, we set $\pi_1 = \pi_2$ and choose the price by dichotomy for the given number of SUs.

Figure 6 (left) shows that the average utility per SU is almost the same in the two configurations in the power auction (see the M/2=M-2 MultiPU Power curve in the figure) and is always higher than that in the NAIVE scheme. Figure 7 shows that the Jain fairness index (calculated in the same way as in the illustrative example) of power auction is always above that

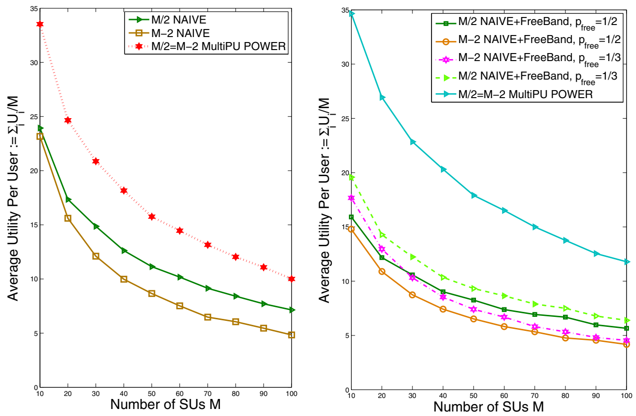

Fig. 6. Utility comparison in balanced (*M/2*) and unbalanced (*M-2*) scenarios between power auction and NAIVE with (left) and without (right) free band

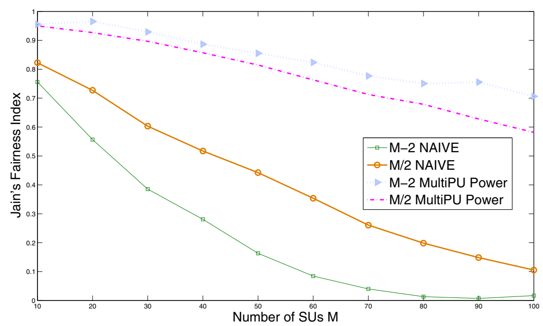

Fig. 7. Fairness comparison in balanced (*M/2*) and unbalanced (*M-2*) scenario between power auction and NAIVE

of NAIVE. In particular, in the unbalanced scenario, the power auction outperforms significantly the NAIVE scheme.

4) Power auction with a free band: We now study the power auction and the proposed no-regret learning algorithm (Section IV-C) by introducing a free band of 5 MHz. $p_i^{max} = 20$ dBm, $\forall i \in \mathcal{M}$. In the simulation, SUs in the NAIVE scheme choose the free band with probability $p_{free} = 1/2$ or $p_{free} = 1/3$ and emit at the maximum power p_i^{max}. The power allocation of SUs staying in licensed bands follows the same way as in the scenario without free band.

Figure 6 (right) shows the average utility of the power auction and NAIVE. As can be observed, compared with the scenario without free band, the average utility in NAIVE is slightly degraded even a new band is introduced. In contrast, the no-regret learning algorithm results a higher utility when the free band is added. Consequently, the utility gap between the power auction and NAIVE is more significant in the scenario with free band. Furthermore, we observe the convergence of the no-regret learning algorithm. Figure 8 shows the evolution of the number of SUs choosing PU1, PU2 and the free band for $M = 50$. The results demonstrate the benefit of the proposed no-regret learning algorithm to converge to an equilibrium with reasonable network efficiency in a distributed fashion.

VI. Conclusion

In this paper, we proposed an auction framework for cognitive radio networks to allow unlicensed SUs to share the available spectrum of licensed PUs, subject to the interference temperature constraint at each PU. We provided an in-

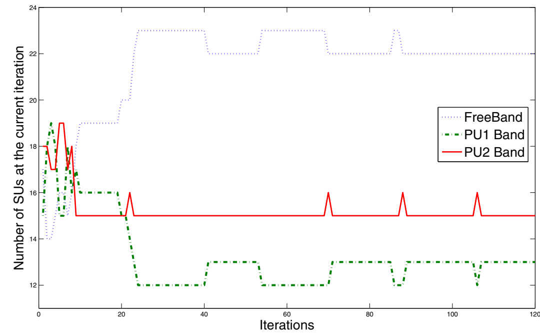

Fig. 8. Evolution of number of SUs choosing PU1, PU2 and the free band

depth analysis on the resulting multiple-PU multiple-SU non-cooperative auction game. We then extended the proposed auction framework to the more challenging scenario with free spectrum bands by developing an algorithm based on no-regret learning to reach a CE of the auction game. The proposed algorithm, which can be implemented distributedly based on local observation, is especially suited in decentralized adaptive learning environments as cognitive radio networks. The simulation results demonstrate the effectiveness of the proposed auction framework in achieving high efficiency and fairness in spectrum allocation.

As stated in the paper, a significant extension of our work is to study the more competitive Stackelberg game in which PUs choose their prices to maximize their revenue. Studying the efficiency of the spectrum auction in that scenario is the subject of our on-going work.

References

[1] S. Haykin. Cognitive radio: brain-empowered wireless communications. *IEEE Journal on Selected Areas in Communications*, 23(2):201–220, 2005.
[2] M. Buddhikot. Understanding dynamic spectrum access: models, taxonomy and challenges. In *Proc. IEEE DySPAN*, April 2007.
[3] Spectrum policy task force report. *Federal Communications Commission*, Nov., 2002.
[4] S. Hart and A. Mas-Colell. A simple adaptive procedure leading to correlated equilibrium. *Econometrica*, 68(5):1127–1150, 2000.
[5] R. J. Aumann. Subjectivity and correlation in randomized strategy. *Journal of Mathematical Economics*, 1(1):67–96, 1972.
[6] V. Krishna. *Auction Theory*. Academic Press, 2002.
[7] X. Zhou and H. Zheng. Trust: A general framework for truthful double spectrum auctions. In *Proc. IEEE Infocom*, 2009.
[8] J. Zhu and K. J. R. Liu. Multi-stage pricing game for collision-resistant dynamic spectrum allocation. *IEEE Journal on Selected Areas in Communications*, 26(1):182–191, Jan 2008.
[9] Gaurav S. Kasbekar and S. Sarkar. Spectrum auction framework for access allocation in cognitive radio networks. In *Proc. ACM Mobihoc*, 2009.
[10] J. Huang, R. Berry, and M. L. Honig. Auction-based spectrum sharing. *Mobile Networks and Applications (MONET)*, 11:405–418, 2006.
[11] S. Gandhi, C. Buragohain, L. Cao, H. Zheng, and S. Suri. A general framework for wireless spectrum auctions. In *Proc. IEEE DySPAN*, April 2007.
[12] Y. Wu, B. Wang, K. J. R. Liu, and T. Charles Clancy. A scalable collision-resistant multi-winner cognitive spectrum auction game. *IEEE Transactions on Communications, to appear*.
[13] R.B. Myerson. *Game Theory: Analysis of Conflict*. Harvard University Press, Cambridge, MA, 1991.
[14] J. B. Rosen. Existence and uniqueness of equilibrium points for concave n-person games. *Econometrica*, 33(3):520–534, Jul 1965.
[15] Roshni Srinivasan. *IEEE 802.16m Evaluation Methodology Document (EMD)*. IEEE, 2008.
[16] R. Jain, D. Chiu, and W. Hawe. A quantitative measure of fairness and discrimination for resource allocation in shared computer systems. *DEC Research Report TR-301, 1984*.

Computer Networks 57 (2013) 1863–1879

Contents lists available at SciVerse ScienceDirect

Computer Networks

journal homepage: www.elsevier.com/locate/comnet

Proportional and double imitation rules for spectrum access in cognitive radio networks ☆

Stefano Iellamo [a], Lin Chen [b], Marceau Coupechoux [a,*]

[a] Telecom ParisTech, CNRS LTCI, 46 Rue Barrault, Paris 75013, France
[b] University Paris-Sud XI, CNRS, LRI, 91405 Orsay, France

ARTICLE INFO

Article history:
Received 29 June 2012
Received in revised form 7 March 2013
Accepted 8 March 2013
Available online 26 March 2013

Keywords:
Cognitive radio networks
Resource allocation
Population game
Learning

ABSTRACT

In this paper, we tackle the problem of opportunistic spectrum access in large-scale cognitive radio networks, where the unlicensed Secondary Users (SUs) access the frequency channels partially occupied by the licensed Primary Users (PUs). Each channel is characterized by an availability probability unknown to the SUs. We apply population game theory to model the spectrum access problem and develop distributed spectrum access policies based on imitation, a behavior rule widely applied in human societies consisting of imitating successful behaviors. We develop two imitation-based spectrum access policies based on the basic Proportional Imitation (PI) rule and the more advanced Double Imitation (DI) rule given that a SU can only imitate the other SUs operating on the same channel. A systematic theoretical analysis is presented for both policies on the induced imitation dynamics and the convergence properties of the proposed policies to the Nash equilibrium. Simple and natural, the proposed imitation-based spectrum access policies can be implemented distributedly based on solely local interactions and thus is especially suited in decentralized adaptive learning environments as cognitive radio networks.

1. Introduction

Cognitive radio [1], with its capability to flexibly configure its transmission parameters, has emerged in recent years as a promising paradigm to enable more efficient spectrum utilization. Spectrum access models in cognitive radio networks can be classified into three categories, namely exclusive use (or operator sharing), commons and shared use of primary licensed spectrum [2]. In the last model, unlicensed Secondary Users (SUs) are allowed to access the spectrum of licensed Primary Users (PUs) in an opportunistic way. In this case, a well-designed spectrum access mechanism is crucial to achieve efficient spectrum usage.

In this paper, we focus on the generic model of cognitive networks consisting of multiple frequency channels, each characterized by a channel availability probability determined by the activity of PUs on it. In such a model, from the SUs perspective, a challenging problem is to coordinate with other SUs in order to opportunistically access the unused spectrum of PUs to maximize its own payoff (e.g., throughput); at the system level, a crucial research issue is to design efficient spectrum access protocols achieving optimal spectrum usage and load balancing on the available channels.

We tackle the spectrum access problem in large-scale cognitive radio networks from an evolutionary game theoretic angle. We formulate the spectrum access problem, show the existence of a Nash Equilibrium (NE) and develop distributed spectrum access policies based on imitation, a behavior rule widely applied in human societies consisting of imitating successful behavior. We study the system

☆ This work is supported by the project TEROPP (technologies for TERminal in OPPortunistic radio applications) funded by the French National Research Agency (ANR).

* Corresponding author. Tel.: +33 1 45 81 75 88; fax: +33 1 45 81 31 19.
E-mail addresses: stefano.iellamo@telecom-paristech.fr (S. Iellamo), chen@lri.fr (L. Chen), marceau.coupechoux@telecom-paristech.fr (M. Coupechoux).

1389-1286/$ - see front matter
http://dx.doi.org/10.1016/j.comnet.2013.03.008

dynamics and the convergence of the proposed policies to the NE when the SU population is large. Simple and natural, the proposed spectrum access policies can be implemented distributedly based on solely local interactions and thus is especially suited in decentralized adaptive learning environments as cognitive radio networks.

In our analysis, we develop imitation-based spectrum access policies where a SU can only imitate the other SUs operating on the same channel. More specifically, we propose two spectrum access policies based on the following two imitation rules: the Proportional Imitation (PI) rule where a SU can sample one other SU; the more advanced adjusted proportional imitation rule with double sampling (Double Imitation, DI) where a SU can sample two other SUs. Under both imitation rules, each SU strives to improve its individual payoff by imitating other SUs with higher payoff. A systematic theoretical analysis is presented for both policies on the induced imitation dynamics and the convergence properties of the proposed policies to the NE.

The key contribution of our work in this paper lies in the systematical application of the natural imitation behavior to address the spectrum access problem in cognitive radio networks, the design of distributed imitation-based channel access policies, and the theoretic analysis on the induced imitation dynamics and the convergence to an efficient and stable system equilibrium. In this paper, we extend the results of [3], where it is assumed that SUs are able to immediately and uniformly imitate any other SU. This assumption makes the theoretical analysis straightforward from the literature on imitation. We assume here that SUs can only imitate SUs on the same channel and obtain a delayed information, as a result of which significant changes should be done in terms of policy design and theoretical analysis.

The rest of the paper is structured as follows. Section 2 discusses related work in the literature. Section 3 presents the system model and Section 4 presents the formulation of the spectrum access game. Section 5 describes the proposed imitation-based spectrum access policies and motivates the choices of proportional and double imitation rules as basis of our policies. In Section 6, we study the system dynamics and the convergence of our algorithms. Section 7 discusses the assumptions of our network model. Section 8 presents simulation based performance evaluation, where our schemes are compared to another decentralized approach called Trial and Error. Section 9 concludes the paper.

2. Related Work

The problem of distributed spectrum access in cognitive radio networks (CRN) has been widely addressed in the literature. A first set of papers assumes that the number of SUs is smaller than the number of channels. In this case, the problem is closely related to the classical Multi-Armed Bandit (MAB) problem [4]. Some recent work has investigated the issue of adapting traditional MAB approaches to the CRN context, among which Anandkumar et al. proposed two algorithms with logarithmic regret, where the number of SUs is known or estimated by each SU [5]. Contrary to this literature, we assume in our paper a large population of SUs, able to share the available bandwidth when settling on the same channel.

Another important thrust consists of applying game theory to model the competition and cooperation among SUs and the interactions between SUs and PUs (see [6] for a review). Several papers propose for example algorithms based on no-regret learning (e.g. [7,8]), which are not guaranteed to converge to the NE. Besides, due to the perceived fairness and allocation efficiency, auction techniques have also attracted considerable research attention and resulted in a number of auction-based spectrum allocation mechanisms (cf. [9] and references therein). The solution proposed in this paper differs from the existing approaches in that it requires only local interactions among SUs and is thus naturally adapted in the distributed environments as CRNs.

Due to the success of applying evolutionary [10] and population game theories [11] in the study of biological and economic problems [11], a handful of recent studies have applied these tools to study resource allocation problems arisen from wired and wireless networks (see e.g. [12,13]), among which Shakkottai et al. addressed the problem of non-cooperative multi-homing of users to WLANs access points by modeling it as a population game [14]. Authors however focus on the system dynamics rather than on the distributed algorithms as we do in this paper. Niyato et al. studied the dynamics of network selection in a heterogeneous wireless network using the theory of evolutionary game [15]. The proposed algorithm leading to the replicator dynamics is however based on a centralized controller able to broadcast to all users the average payoff. Our algorithms are on the contrary fully distributed. Coucheney et al. studied the user-network association problem in wireless networks with multi-technology and proposed an algorithm based on Trial and Error mechanisms to achieve the fair and efficient solution [13].

Several theoretical works focus on imitation dynamics. Ackermann et al. investigated the concurrent imitation dynamics in the context of finite population symmetric congestion games by focusing on the convergence properties [16]. Berenbrik et al. applied the Proportional Imitation Rule to load-balance system resources by focusing on the convergence speed [17]. Ganesh et al. applied the Imitate If Better rule[1] (see [19] for a review on imitation rules) in order to load-balance the service rate of parallel server systems [18]. Contrary to our work, it is assumed in [17,18] that a user is able to observe the load of another resource before taking its decision to switch to this resource.

As it is supposed to model human behavior, imitation is mostly studied in economics. In the context of CRN, specific protocol or hardware constraints may however arise so that imitation dynamics are modified, as we show it in this paper. Two very recent works in the context of CRN are [20,21], which have the same goals as ours. In [20], authors propose a distributed learning algorithm for spectrum access. User decisions are based on their accumulated experience and they are using a mixed strategy. In [21], imitation is also used for distributed spectrum access. However, the proposed scheme relies on the existence of

[1] Imitate If Better (IIB) is a rule consisting in picking a player and migrating to its strategy if the latter has yielded a higher payoff than the achieved one. IIB is called Random Local Search in [18].

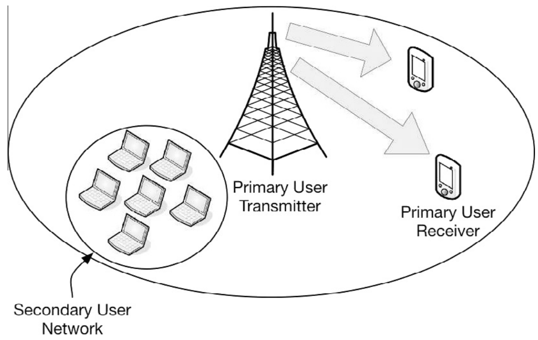

Fig. 1. Network model: N SUs try to opportunistically access the spectrum left free by a PU. The spectrum is made of C slotted frequency channels.

a common control channel for the sampling procedure. Double imitation is moreover not considered.

3. System model

In this section, we present the system model of our work with the notations used.

3.1. System model and PU operation

We consider the network model shown in Fig. 1 made of a primary network and a secondary network. In the former, a primary transmitter is using on the downlink a set $\mathcal{C}$ of C frequency channels, each with bandwidth B. The primary receivers are operated in a synchronous time-slotted fashion. The secondary network is made of a set $\mathcal{N}$ of N SUs, which try to opportunistically access the channels when they are left free by the PU. We assume that SUs can perform a perfect sensing of PU transmissions, i.e., no collision can occur between the PU and SUs. This assumption is adopted in the literature focusing on resource allocation (see e.g. [22,23,5]). The secondary network is also supposed to be sufficiently small so that every SU can receive and decode packets sent on the same channel.

Let $Z_i(k)$ be the random variable equal to 1 when of channel i is unoccupied by any PU at slot k and 0 otherwise. We assume that the process $\{Z_i(k)\}$ is stationary and independent for each i and k, i.e., the $Z_i(k)$ are i.i.d. random variables for all (i, k). We also assume that at each time slot, channel i is free with probability μ_i, i.e., $\mathbb{E}[Z_i(k)] = \mu_i$. Without loss of generality, we assume $\mu_1 \geqslant \mu_2 \geqslant \cdots \geqslant \mu_C$. The channel availability probabilities $\mu \triangleq \{\mu_i\}$ are *a priori* not known by SUs.

3.2. SU operation

We describe in this section the SU operation and capabilities. As shown in Fig. 2 for a given frequency channel j, time-slots of the primary network are organized into blocks of N_b slots. All SUs are assumed to be synchronized, stay on the same channel during a block and may change their channel at block boundary. Let n_i be the number of SUs operating on channel i.

Assuming perfect sensing of the cognitive users, there is no secondary transmission during slots occupied by the PU (gray slots on the figure). When the PU is idle, SUs share the available bandwidth using a decentralized random access MAC protocol (hatched slots on the figure). The way this MAC protocol is implemented is out of the scope of the paper. Mini-slots can for example be used at the beginning of each slot in order to perform CSMA, as assumed in [20], or CSMA/CA can be used, as assumed in [24]. For mathematical convenience, we will assume in Sections 5 and 6 that the MAC protocol is perfect and operates like TDMA. Our motivation of such an assumption is to concentrate the analysis on the interactions between SUs and the resulting structural properties of the system equilibria. The results give an upper-bound on the performance of the developed policies. A similar asymptotic analysis has been carried on in [25].

In our work, each SU j is modeled as a rational decision maker, striking to maximize the throughput it can achieve, denoted as T_j^i when j operates on channel i. Assuming a fair MAC protocol and invoking symmetry reasons, all SUs on channel i obtain the same expected throughput, which can be expressed as a function of n_i as $\pi_i(n_i) = \mathbb{E}[T_j^i]$ for all j operating on channel i. It should be noted that $\pi_i(n_i)$ depends on the MAC protocol implemented at the cognitive users. An example is $\pi_i(n_i) = B\mu_i/n_i$ in the case of a perfect MAC protocol operating like TDMA, where B is a constant standing for the channel bandwidth. Generically, $\pi_i(n_i)$ can be rewritten as $\pi_i(n_i) = B\mu_i S(n_i)$ where $S(n_i)$ denotes the throughput of a channel of unit bandwidth without PU. Without loss of generality, we will now assume that $B = 1$. The assumption that SUs on the same channel obtain the same expected throughput can be found in the literature using evolutionary game theory to study spectrum access, see e.g. [15,26,20].

Channel availabilities, μ_i, are estimated in the long term by SUs, while the expected throughput π_i and the number of SUs n_i are estimated at the end of each block. In all their transmissions in block b, SUs include in the header of their packets the throughput $\pi_i(n_i)$ obtained in block $b-1$ and

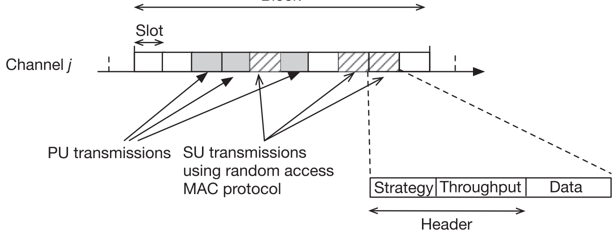

Fig. 2. SU operation: N_b slots of a frequency channel form a block, SUs use a MAC protocol for their transmissions and include in the header of their packets a throughput and strategy indication.

the corresponding channel (or strategy) i. We further assume that every SU can overhear at random one or two packets transmitted by SUs on the same channel and decode the throughput and strategy indications. The overhearing of packets is called a *sampling procedure* and we write $i \rightsquigarrow j$ when SU i samples SU j. Sampling is supposed to be symmetric, i.e., the probabilities $P(i \rightsquigarrow j)$ and $P(j \rightsquigarrow i)$ are identical. After the sampling, SU transmitters communicate to their receiver a channel change order to be executed at the next block boundary.

4. Spectrum access game formulation

To study the interactions among autonomous SUs and to derive distributed channel access policies, we formulate in this section the channel selection problem as a spectrum access game where the players are the SUs and we show the uniqueness of the Nash Equilibrium (NE) when the number of SUs is large. The game is defined formally as follows:

Definition 1. The spectrum access game G is a 3-tuple $(\mathcal{N}, \mathcal{C}, \{\mathcal{U}_|\})$, where $\mathcal{N}$ is the player set, $\mathcal{C}$ is the strategy set of each player. Each player j chooses its strategy $s_j \in \mathcal{C}$ to maximize its payoff function U_j defined as $U_j = \pi_{s_j}(n_{s_j}) = \mathbb{E}[T_j^{s_j}]$.

The solution of the spectrum access game G is characterized by a Nash equilibrium [27], a strategy profile from which no player has incentive to deviate unilaterally.

Lemma 1. *For the spectrum access game G, there exists at least one Nash equilibrium.*

Proof. Given the form of the SU payoff function, it follows from [28] that the spectrum access game is a congestion game and a potential game with potential function: $P(n_1, \ldots, n_C) = \sum_{i \in \mathcal{C}} \sum_{k=1}^{n_i} \pi_i(n_i)$, where n_i is the number of SUs on channel i and $\sum_i n_i = N$. This function takes only a finite set of values and thus achieves a maximum value. □

We now consider the *population* game G, where (1) the number of SUs is large, (2) SUs are small, (3) SUs interact anonymously and (4) payoffs are continuous (see [11] for the discussion on these assumptions). In this model, we focus on the system state $\mathbf{x} \triangleq \{x_i, i \in \mathcal{C}\}$ where x_i denotes the proportion of SUs choosing channel i. In such context, by regarding x_i as a continuous variable, we make the following assumption on the throughput function $S(x_i N)$.

Assumption 1. $S(x_i N)$ is strictly monotonously decreasing and it holds that $S(x_i N) \leqslant 1/(N x_i)$.

We can now establish the uniqueness of the NE in the spectrum access game G for the asymptotic case in the following lemma and theorem.

Lemma 2. *For N sufficiently large, there is no empty channel at NE.*

Proof. Assume, by contradiction, that at a NE, there are no SUs on channel i. Since there are C channels, at a NE, there exists at least one channel where there are at least N/C SUs. Assume that this channel is channel j, i.e., $n_j \geqslant N/C$. Consider a SU on channel j, its payoff is $\pi_j(n_j) = \mu_j S(N/C)$. From Assumption 1, $\pi_j(n_j) \leqslant \mu_j C/N$. Now let a SU in channel j switch to channel i, its payoff becomes $\pi_i(1) = \mu_i S(1)$. It holds straightforwardly that $\pi_j(n_j) < \pi_i(1)$ when $N > \frac{\mu_j C}{\mu_i S(1)}$. Hence there is no empty channel at NE. □

Theorem 1. *For N sufficiently large, G admits a unique NE, where all SUs get the same payoff. Let y denote the root of* $\sum_{i \in \mathcal{C}} S^{-1}\left(\frac{y}{\mu_i}\right) = N$, *at the NE, there are* $S^{-1}\left(\frac{y}{\mu_i}\right)$ *SUs operating on channel i.*

Proof. This theorem is a classical result of population games. See Appendix A for more details. □

We can observe two desirable properties of the unique NE derived in Theorem 1: (1) the NE is optimal from the system perspective as the total throughput of the network achieves its optimum at the NE and (2) at NE, all SUs obtain exactly the same throughput. Note that any state such that $x_i > 0$ for all $i \in \mathcal{C}$ is also system optimal, the NE is one of them. Note also that when N grows indefinitely and as players are symmetric, the NE approaches the Wardrop equilibrium of the system [29].

One critical challenge in the analyzed spectrum access game is the design of distributed spectrum access strategies for rational SUs to converge to the NE. In response to this challenge, we develop in the sequel sections of this paper an efficient spectrum access policy.

5. Imitation-based spectrum access policies

The spectrum access policy we develop is based on *imitation*. As a behavior rule widely observed in human societies, imitation captures the behavior of a bounded rational player that mimics the actions of other players with higher payoff in order to improve its own payoff from one block to the next, while ignoring the effect of its strategy on the future evolutions of the system and forgetting its past experience. The induced imitation dynamics model the spreading of successful strategies under imitation [30]. In this section, we develop two spectrum access policies based on the proportional imitation rule and the double imitation rule. For tractability reasons, we assume in the next sections that $\pi_i(n_i) = \mu_i/n_i$ on a channel i, i.e., a perfect MAC protocol for SUs.

5.1. Motivation

In this first part, we recall some useful definitions given in [30], we introduce new notations and we provide our motivations.

Definition 2. A *behavioral rule with single sampling* (resp. *with double sampling*) is a function $F : \mathcal{C}^2 \to \Delta(\mathcal{C})$ (resp. $F : \mathcal{C}^3 \to \Delta(\mathcal{C})$), where $\Delta(\mathcal{C})$ is the set of probability distributions on $\mathcal{C}$ and $F_{i,j}^k, \forall i,j,k \in \mathcal{C}$ (resp. $F_{i,j,l}^k, \forall i,j,k,l \in \mathcal{C}$) is the probability of choosing channel k in the next iteration (block) after operating on channel i and sampling a SU with strategy j (resp. sampling two SUs with strategies j and l).

Definition 3. A behavioral rule with single sampling is *imitating* if $F^k_{i,j} = 0$ when $k \notin \{i, j\}$. A behavioral rule with double sampling is *imitating* if $F^k_{i,j,l} = 0$ when $k \notin \{i, j, l\}$.

In this paper, we assume that all SUs adopt the same behavioral rule, i.e., the population is *monomorphic* in the sense of Schlag [30] (see e.g. [31–33] for other papers using this notion).

Schlag has shown in [30] that the Proportional Imitation Rule (PIR) is an *improving* rule, i.e., in any state of the system the expected average payoff is increasing after an iteration of the rule. He has also shown that it is a *dominant* rule, i.e., it always achieves a higher expected payoff improvement than any other improving rule. PIR is moreover the unique dominant rule that never imitates a strategy that achieved a lower payoff and that minimizes the probability of switching among the set of dominant rules.

Schlag has also shown in [34] that the Double Imitation (DI) rule is the rule that causes less SUs to change their strategy after each iteration among the set of improving behavioral rules with double sampling. As switching may represent a significant cost for today's wireless devices in terms of delay, packet loss and protocol overhead, this property makes PIR and DI particularly attractive. These properties motivate the design of spectrum access policies based on PIR and DI.

5.2. Spectrum access policy based on proportional imitation

Algorithm 1 presents our proposed spectrum access policy based on the proportional imitation rule, termed as PISAP. The core idea is: At each iteration t, each SU (say j) randomly selects another SU (say j') on the same channel; if the payoff at $t-1$ of the selected SU (denoted $U_{j'}(t-1)$) is higher than its own payoff at $t-1$ (denoted $U_j(t-1)$), the SU imitates the strategy of the selected SU at the next iteration with a probability proportional to the payoff difference, with coefficient the imitation factor σ.[2] The payoff and the strategy at $t-1$ of the sampled SU are read from the packet header.

Algorithm 1. PISAP: Executed at each SU j

Initialization: Set the imitation factor σ
At $t = 0$, randomly choose a channel to stay and store the payoff $U_j(0)$.
while at each iteration $t \geqslant 1$ **do**
Randomly select a SU j'
if $U_j(t-1) < U_{j'}(t-1)$ **then**
Migrate to the channel $s_{j'}(t-1)$ with probability $p = \sigma(U_{j'}(t-1) - U_j(t-1))$
endif
endwhile

[2] One way of setting σ is to set $\sigma = 1/(\omega - \alpha)$, where ω and α are two exogenous parameters such that $U_j \in [\alpha, \omega], \forall j \in \mathcal{C}$. In our case, $\omega = 1$ and $\alpha = 0$ can be chosen.

5.3. Spectrum access policy based on double imitation

In this subsection, we turn to a more advanced imitation rule, the double imitation rule [34] and propose the DI-based spectrum access policy, termed as DISAP. Under DISAP, each SU randomly samples two SUs on the same channel by decoding two packet headers. It then imitates them with a certain probability determined by the payoff differences. The spectrum access policy based on the double imitation is detailed in Algorithm 2, in which each SU j (with payoff U_j and strategy i at $t-1$) randomly samples two other SUs j_1 and j_2 (operating at $t-1$ on channel i_1 and i_2 respectively and, without loss of generality, with utilities $U_{j_1} \leqslant U_{j_2}$) and updates the probabilities of switching to channels i_1 and i_2, denoted as p_{j_1} and p_{j_2} respectively.

Algorithm 2. DISAP: Executed at each SU j.

Initialization: Set the parameters ω, α and $\sigma = 1/(\omega - \alpha)$.
Define $[A]^+ \triangleq \max\{0, A\}$ and $Q(U) \triangleq 2 - \frac{U-\alpha}{\omega-\alpha}$.
At $t = 0$ and $t = 1$, randomly choose a channel and store the payoff $U_j(0)$.
while at each iteration $t \geqslant 2$ **do**
Let i and U_j be resp. the channel and the payoff of j at $t-1$.
Randomly sample two SUs j_1 and j_2 (with channels i_1 and i_2 and with payoffs U_{j_1} and U_{j_2} resp. at $t-1$). Suppose w.l.o.g. that $U_{j_1} \leqslant U_{j_2}$
if $|\{i, i_1, i_2\}| = 1$, i.e., $i = i_1 = i_2$ **then**
Go to channel i.
else if $|\{i, i_1, i_2\}| = 2$ **then**
if $i = i_1$, $i \neq i_2$ and $U_j \leqslant U_{j_2}$ **then**
$p_{j_2} = \frac{\sigma}{2} Q(U_j)(U_{j_2} - U_j)$.
Switch to channel i_2 w.p. p_{j_2} and go to channel i w.p. $1 - p_{j_2}$.
else if $i_1 = i_2$, $i \neq i_1$ and $U_j \leqslant U_{j_1} = U_{j_2}$ **then**
$p_{j_1} = \frac{\sigma}{2}(Q(U_{j_1}) + Q(U_j))(U_{j_1} - U_j)$.
Switch to channel i_1 w.p. p_{j_1} and go to channel i w.p. $1 - p_{j_1}$.
end if
else if $|\{i, i_1, i_2\}| = 3$ **then**
if $U_j \leqslant U_{j_1} \leqslant U_{j_2}$ **then**
$p_{j_1} = \frac{\sigma}{2}[Q(U_j)(U_{j_1} - U_{j_2}) + Q(U_{j_2})(U_{j_1} - U_j)]^+$.
$p_{j_2} = \frac{\sigma}{2}[Q(U_{j_1})(U_{j_2} - U_j) + Q(U_{j_2})(U_{j_1} - U_j)] - p_{j_1}$.
Switch to channel i_1 w.p. p_{j_1}, to channel i_2 w.p. p_{j_2} and go to channel i w.p. $1 - p_{j_1} - p_{j_2}$.
else if $U_{j_1} \leqslant U_j \leqslant U_{j_2}$ **then**
$p_{j_2} = \frac{\sigma}{2}[Q(U_{j_1})(U_{j_2} - U_j) + Q(U_{j_2})(U_{j_1} - U_j)]^+$.
Switch to channel i_2 w.p. p_{j_2} and go to channel i w.p. $1 - p_{j_2}$.
end if
else
Go to channel i.
end if
end while

5.4. Discussion

As pointed in [34], double imitation may seem complicated compared to the proportional imitation rule. We can however extract the following properties [34]: DI is an imitating rule, i.e., a SU never chooses a channel that is not in his sample; switching probabilities are continuous in the sampled payoffs and increase with payoff differences; for a joint sample with three different channels, the most successful channel is chosen more likely; a SU never imitates another SU that obtains a lower payoff.

Note that PISAP is clearly different from the proportional imitation rule presented in [30] in the sense that a SU is not able to uniformly sample another SU across the network. The radio constraint indeed forces it to sample a SU on the same channel. As in this case, current strategies are identical, imitation is based on the previous iteration.

If every SU is able to uniformly sample another SU in the network and to imitate the current strategy, the system dynamics is straightforward to obtain. It is indeed shown e.g. in [35] that in the asymptotic case (assuming continuous time for simplicity), the proportional imitation rule generates a population dynamics described by the following set of differential equations:

$$\dot{x}_i(t) = \sigma x_i(t)[\pi_i(t) - \overline{\pi}(t)], \quad \forall i \in \mathcal{C}, \tag{1}$$

where $\bar{\pi} \triangleq \sum_{i \in \mathcal{C}} x_i \pi_i$ denotes the expected payoff of all SUs in the network. This equation can be easily solved as:

$$x_i(t) = \left(x_i(0) - \frac{\mu_i}{\sum_{l \in \mathcal{C}} \mu_l}\right) e^{-\left(\sum_{l \in \mathcal{C}} \mu_l\right)\sigma t} + \frac{\mu_i}{\sum_{l \in \mathcal{C}} \mu_l}, \quad \forall i \in \mathcal{C}. \tag{2}$$

The imitation dynamics induced by PIR thus converges exponentially in time to an evolutionary equilibrium, which is also the NE of G.

With the same assumption, the double imitation rule generates in the asymptotic case an aggregate monotone dynamics [34,36], which is defined as follows:

$$\dot{x}_i = \frac{x_i}{\omega - \alpha}\left[1 + \frac{\omega - \bar{\pi}}{\omega - \alpha}\right](\pi_i - \bar{\pi}), \quad \forall i \in \mathcal{C}, \tag{3}$$

whose solution is

$$x_i(t) = \left(x_i(0) - \frac{\mu_i}{\sum_{l \in \mathcal{C}} \mu_l}\right) e^{-\frac{\pi}{\omega - \alpha}\left(1 + \frac{\omega - \bar{\pi}}{\omega - \alpha}\right)t} + \frac{\mu_i}{\sum_{l \in \mathcal{C}} \mu_l}, \quad \forall i \in \mathcal{C}. \tag{4}$$

As a consequence, DI converges exponentially in time to the NE of the spectrum access game G, however at a higher rate than PIR because by definition $\sigma = \frac{1}{\omega - \alpha}$ and ω and α being upper and lower bounds on payoffs, $\frac{\omega - \bar{\pi}}{\omega - \alpha} \geqslant 0$. From (2) and (4), it turns out that the aggregate monotone dynamics is a time-rescaled version of the replicator dynamics, as pointed in [10]. We will see in the next section that both dynamics continue to play an important role in our model.

As desirable properties, the proposed imitation-based spectrum access policies (both PISAP and DISAP) are stateless, incentive-compatible for selfish autonomous SUs and requires no central computational unit. The spectrum assignment is achieved by local interactions among autonomous SUs. The autonomous behavior and decentralized implementation make the proposed policies especially suitable for large scale cognitive radio networks. The imitation factor σ controls the tradeoff between the convergence speed and the channel switching frequency in that larger σ represents more aggressiveness in imitation and thus leads to fast convergence, at the price of more frequent channel switching for the SUs.

6. Imitation dynamics and convergence

We have seen that proportional imitation and double imitation rules generate a replicator dynamics and an aggregate monotone dynamics. In the sequel analysis, we study the induced imitation dynamics and the convergence of the proposed spectrum access policies PISAP and DISAP, which take into account the constraint imposed by SU radios.

6.1. System dynamics

In this subsection, we first derive in Theorem 2 the dynamics for a generic imitation rule F with large population. We then derive in Lemma 3, Theorems 3 and 4 the dynamics of the proposed proportional imitation policy PISAP and study its convergence. The counterpart analysis for the double imitation policy DISAP is explored in Lemma 4, Theorems 5 and 6.

We start by introducing the notation used in our analysis. At an iteration, we label all SUs performing strategy i (channel i in our case) as SUs of type i and we refer to the SUs on s_j as neighbors of SU j. We denote $n_i^l(t)$ the number of SUs on channel i at iteration t and operating on channel l at $t-1$. It holds that $\sum_{l \in \mathcal{C}} n_i^l(t) = n_i(t)$ and $\sum_{i \in \mathcal{C}} n_i^l(t) = n_l(t-1)$. For a given state $s(t) \triangleq \{s_j(t), j \in \mathcal{N}\}$ of the system at iteration t and for a finite population of size N, we denote $p_i(t) \triangleq n_i(t)/N$ the proportion of SUs of type i and $p_i^l(t) \triangleq n_i^l(t)/N$ the proportion of SUs migrating from channel l to i. We use x instead of p to denote these proportions when N is large. It holds that $p \to x$ when $N \to +\infty$.

Denote by F a generic imitation rule under the channel constraint. In the case of a simple imitation rule (e.g. PISAP), F is characterized by the probability set $\{F_{j,k}^i\}$, where $F_{j,k}^i$ denotes the probability that a SU choosing strategy j at the precedent iteration imitates another SU choosing strategy k at the precedent iteration and then switches to channel i at next iteration after imitation. Instead, by applying a double imitation rule (e.g. DISAP), we can characterize F by the probability set $\{F_{j,k,l}^i\}$, where $F_{j,k,l}^i$ denotes the probability that a SU choosing strategy j at the precedent iteration imitates two neighbors choosing respectively strategy k and strategy l at the precedent iteration and then switches to channel i at the next iteration after imitation. In both cases the only way to switch to a channel i is to imitate a SU that was on channel i. That means $F_{j,k}^i = 0, \forall k \neq i$ (PISAP) and $F_{j,k,l}^i = 0$, $\forall k, l \neq i$ (DISAP).

At the initialization phase (iterations 0 and 1), each SU randomly chooses its strategy with uniform distribution. In the asymptotic case, we thus have $\forall i \in \mathcal{C}, x_i(0) > 0$ and $x_i(1) > 0$ a.s. After that, the system state at iteration $t+1$, denoted as $\mathbf{p}(\mathbf{t+1})$ ($\mathbf{x}(\mathbf{t+1})$ in the asymptotic case), depends on the states at iteration t and $t-1$.

We have now the following theorem that relates the finite and asymptotic cases.

Theorem 2. *For any imitation rule F, if the imitation among SUs of the same type occurs randomly and independently, then $\forall\delta > 0$, $\epsilon > 0$ and any initial state $\{\tilde{x}_i(0)\}, \{\tilde{x}_i(1)\}$ such that $\forall i \in \mathcal{C}, \tilde{x}_i(0) > 0$ and $\tilde{x}_i(1) > 0$, there exists $N_0 \in \mathbb{N}$ such that if $N > N_0, \forall i \in \mathcal{C}$, the event $|p_i(t) - x_i(t)| > \delta$ occurs with probability less than ϵ for all t, where $p_i(0) = x_i(0) = \tilde{x}_i(0), p_i(1) = x_i(1) = \tilde{x}_i(1)$. In the case of a simple imitation policy it holds that*

$$x_i(t+1) = \sum_{j,l,k\in\mathcal{C}} \frac{x_j^l(t)x_j^k(t)}{x_j(t)} F_{l,k}^i \quad \forall i \in \mathcal{C}.$$

Differently, a double imitation policy yields:

$$x_i(t+1) = \sum_{j,l,k,z\in\mathcal{C}} \frac{x_j^l(t)x_j^k(t)x_j^z(t)}{[x_j(t)]^2} F_{l,\{k,z\}}^i \quad \forall i \in \mathcal{C}.$$

Proof. The proof consists of first showing the theorem holds for iteration $t = 2$ and then proving the case $t \geqslant 3$ by induction. The detail is in Appendix B. □

Theorem 2 is a result on the short run adjustments of large populations under any generic imitation rule *F*: the probability that the behavior of a large population differs from the one of an infinite population is arbitrarily small when *N* is sufficiently large. In what follows, we study the convergence of PISAP and DISAP specifically.

6.2. PISAP dynamics and convergence

In this section, we now focus on PISAP and derive the induced imitation dynamics in the following analysis.

Lemma 3. *On the proportional imitation policy PISAP under channel constraint, it holds that*

$$x_i^j(t+1) = \sum_{l,k\in\mathcal{C}} \frac{x_j^l(t)x_j^k(t)}{x_j(t)} F_{l,k}^i \quad \forall i,j \in \mathcal{C}. \tag{5}$$

Proof. The proof is straightforward from the analysis in the proof of Theorem 2. □

Theorem 3. *The proportional imitation policy PISAP under channel constraint generates the following dynamics in the asymptotic case:*

$$x_i(t+1) = x_i(t-1) + \sigma\pi_i(t-1)x_i(t-1) - \sigma\sum_{j,l\in\mathcal{C}} \pi_l(t-1)\frac{x_j^i(t)x_j^l(t)}{x_j(t)}, \tag{6}$$

where $\pi_i(t)$ denotes the expected payoff of an individual SU on channel i at iteration t.

Proof. See Appendix C. □

Although we are not able to prove it theoretically, we observe via extensive numerical experiments that (6) converges to the NE. The formal proof is left for future work. To get more in-depth insight on the dynamics (6), we notice that under the following approximation:

$$\sum_{l\in\mathcal{C}} \pi_l(t-1)\frac{x_j^l(t)}{x_j(t)} \approx \bar{\pi}(t-1), \tag{7}$$

where $\bar{\pi}(t-1)$ is the average individual payoff for the whole system at iteration $t-1$, noticing $\sum_j x_j^i(t) = x_i(t-1)$, (6) can be written as:

$$x_i(t+1) = x_i(t-1) + \sigma x_i(t-1)[\pi_i(t-1) - \bar{\pi}(t-1)]. \tag{8}$$

Note that the approximation (7) states that in any channel *j* at iteration *t*, the proportions of SUs coming from any channel *l* are representative of the whole population.

Under the approximation (7), given the initial state $\{x_i(0)\}$, $\{x_i(1)\}$, we can decompose (8) into the following two independent discrete-time replicator dynamics:

$$\begin{cases} x_i(u) = x_i(u-1) + \sigma x_i(u-1)[\pi_i(u-1) - \bar{\pi}(u-1)], \\ x_i(v) = x_i(v-1) + \sigma x_i(v-1)[\pi_i(v-1) - \bar{\pi}(v-1)], \end{cases} \tag{9}$$

where $u = 2t$, $v = 2t + 1$. The two equations in (9) illustrate the underlying system dynamics hinged behind PISAP under the approximation (7): it can be decomposed into two

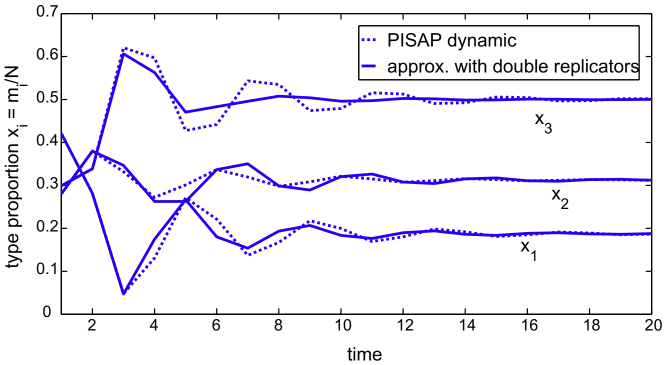

Fig. 3. PISAP dynamics and its approximation by double replicator dynamics.

independent delayed replicator dynamics that alternatively occur at the odd and even iterations, respectively. The following theorem establishes the convergence of (9) to a unique fixed point, which is also the NE of the spectrum access game G.

Theorem 4. *Starting from any initial point, the system described by (9) converges to a unique fixed point which is also the NE of the spectrum access game G.*

Proof. The proof, of which the detail is provided in Appendix D, consists of showing that the mapping described by (9) is a contraction mapping. □

As an illustrative example, Fig. 3 shows that the double replicator dynamics provides an accurate approximation of the system dynamics induced by PISAP.

6.3. DISAP dynamics and convergence

We now focus on DISAP and derive the induced imitation dynamics.

Lemma 4. *On the double imitation policy DISAP under channel constraint, it holds that*

$$x_i^j(t+1) = \sum_{l,k,z \in \mathcal{C}} \frac{x_j^l(t) x_j^k(t) x_j^z(t)}{[x_j(t)]^2} F_{l,k,z}^i \quad \forall i,j \in \mathcal{C}. \tag{10}$$

Proof. The proof is straightforward from the analysis in the proof of Theorem 2. □

Theorem 5. *The double imitation policy DISAP under channel constraint generates the following dynamics in the asymptotic case:*

$$x_i(t+1) = x_i(t-1) + \sum_j x_j^i(t) Q(\bar{\pi}_j(t-1))(\pi_i(t-1) - \bar{\pi}_j(t-1)), \tag{11}$$

where $\bar{\pi}_j(t-1) = \sum_k \frac{x_j^k(t)}{x_j(t)} \pi_k(t-1)$ and $Q(U) \triangleq 2 - \frac{U-\alpha}{\omega-\alpha}$.

Proof. See Appendix E. □

Again, we are not able to prove it analytically and leave the formal proof as future work. However, we observe via extensive numerical experiments that (11) converges to the NE and, as shown in Fig. 5, is also characterized by a smoother and faster convergence with respect to the proportional imitation dynamics (Eq. (6)).

By performing the approximation $\bar{\pi}_j(t-1) \approx \bar{\pi}(t-1)$ for all j, (11) can be written as:

$$x_i(t+1) = x_i(t-1) + x_i(t-1)Q(\bar{\pi}(t-1))(\pi_i(t-1) - \bar{\pi}(t-1)). \tag{12}$$

Given the initial state $\{x_i(0)\}$, $\{x_i(1)\}$, we can now decompose (12) into the following two independent discrete-time aggregate monotone dynamics:

$$\begin{cases} x_i(u) = x_i(u-1) + x_i(u-1)[2 - \bar{\pi}(u-1)][\pi_i(u-1) - \bar{\pi}(u-1)], \\ x_i(v) = x_i(v-1) + x_i(v-1)[2 - \bar{\pi}(v-1)][\pi_i(v-1) - \bar{\pi}(v-1)], \end{cases} \tag{13}$$

where $u = 2t$, $v = 2t+1$. The underlying system dynamics can thus be decomposed into two independent delayed aggregate monotone dynamics that alternatively occur at the odd and even iterations, respectively. The following theorem establishes the convergence of (13) to a unique fixed point which is also the NE of the spectrum access game G. The proof follows exactly the same analysis as that of Theorem 4.

Theorem 6. *Starting from any initial point, the system described by (13) converges to a unique fixed point which is also the NE of the spectrum access game G.*

As an illustrative example, Fig. 4 shows that the double aggregate dynamics provides an accurate approximation of the system dynamics induced by DISAP.

7. Discussion

This paper is a first step to systematically apply imitation rules to cognitive radio networks. There are several points to be tackled in order to make the model more realistic.

- It is assumed in this paper that a SU can capture another SU packet for sampling with probability 1. Assuming a capture probability less than 1 would have the same

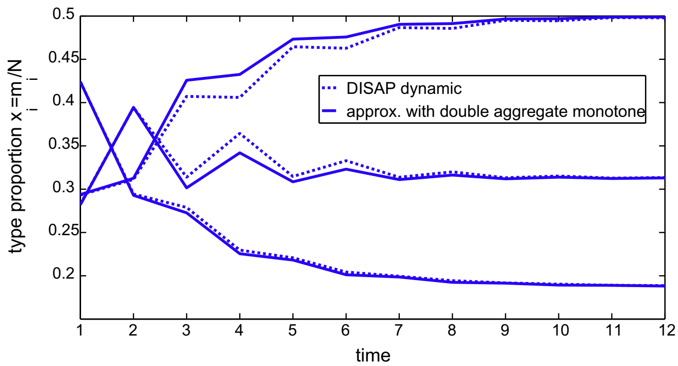

Fig. 4. DISAP dynamics and its approximation by double aggregate monotone dynamics.

effect as decreasing the value of σ in PISAP, i.e., it would slow down the convergence speed of the proposed algorithms.

- It is assumed that all SUs can all hear each other on the same channel. A more realistic setting would consider a graph of possible communications between SUs. In this case, our algorithms are not any more ensured to converge. This point is left for further work. A promising approach is to use the results of the literature on 'learning from neighbors', which studies the conditions under which efficient actions are adopted by a population if agents receive information only from their neighbors (see e.g. [37]).
- In this paper, SUs are supposed to provide in their packet header the exact average throughput that can be obtained on a given channel. We have investigated in [24] the effect of providing only an estimate of the average throughput. Assuming the use of CSMA/CA as SU MAC protocol, we have shown by simulations that our algorithms continue to converge in this more realistic context.
- For mathematical convenience, we have assumed in this paper that the SU MAC protocol was perfect and could act as TDMA. Although unrealistic, this approach gives an upper bound on the performance of our policies. Also, the analysis can be extended with other more realistic MAC protocols by adapting the utility functions. Particularly, we have investigated in [24] the use of CSMA/CA and shown by simulations the convergence of our policies.
- It is assumed that a generic PU transmits with a certain probability in TDMA-like mode. If there are multiple PU transmitters it is possible to distinguish two cases:
  1. The transmission of each PU covers the totality of SU receivers. This scenario boils down to the case of a unique generic PU transmitter.
  2. The transmission of one or more PUs covers a subset of the SU receivers. In this case, different SUs may have different perceptions of the environment and a further analysis, based on the fact that the channel availability probabilities are now dependent on both channel i and SU j, should be carried on. This point is left for future work.

8. Performance evaluation

In this section, we conduct simulations to evaluate the performance of the proposed imitation-based channel access policies (PISAP and DISAP) and demonstrate some intrinsic properties of the policies, which are not explicitly addressed in the analytical part of the paper.

For performance comparison, we also show the results obtained by simulating Trial and Error [38] (shortened into T&E in the following). The latter has been chosen as it is, to the best of our knowledge, one of the best existing mechanisms that (1) applies to our model and (2) is guaranteed to converge to a NE. In T&E, players locally implement a state machine, so that at each iteration each player is characterized by a state, which is defined by the triplet {*current_mood*, *benchmark_mood*, *benchmark_strategy*}. Players current mood (the four possible moods are: *content*, *watchful*, *hopeful* and *discontent*) reflects the machine reaction to its experience of the environment. A NE is reached when everybody is in state *content*.

8.1. Simulation settings

We simulate two cognitive radio networks, termed Network 1 and Network 2. We study the performance of our algorithms on Network 1, and compare their convergence behaviors and fairness to the ones obtained by T&E on Network 2.

- *Network 1*: We consider $N = 50$ SUs, $C = 3$ channels characterized by the availability probabilities $\mu = [0.3, 0.5, 0.8]$.
- *Network 2*: We set $N = 10$, $C = 2$ and $\mu = [0.2, 0.8]$.

Note that the introduction of Network 2 has been necessary as the dynamics induced by T&E turns out to be very slow to converge on the bigger Network 1 (after 10^5 iterations convergence is still not achieved).

We assume that the block duration is long enough, so that the SUs, regardless of the occupied channel, can evaluate their payoff without errors. T&E learning parameters (i.e., experimentation probability and benchmark mood acceptance ratio) are set at each iteration according to [39].

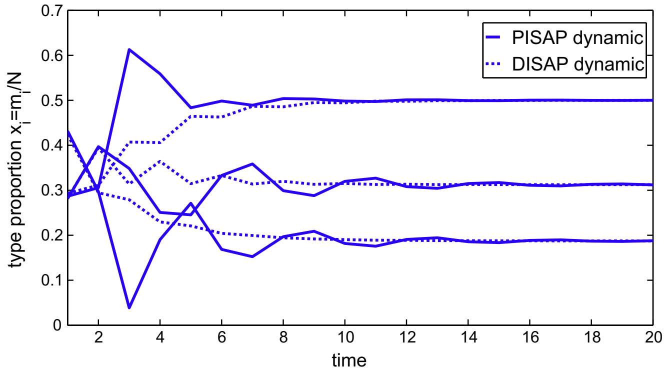

Fig. 5. PISAP and DISAP system dynamics in the asymptotic case.

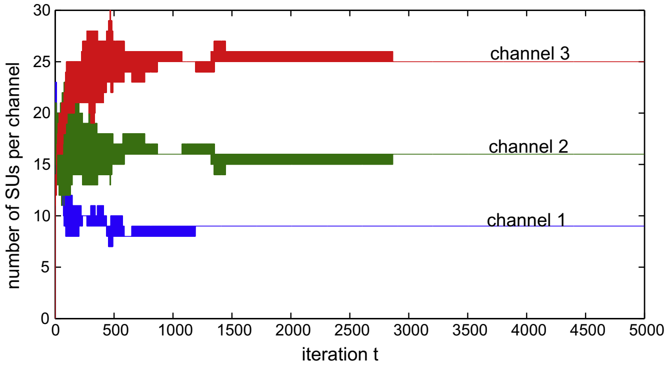

Fig. 6. PISAP on Network 1: number of SUs per channel as a function of the number of iterations.

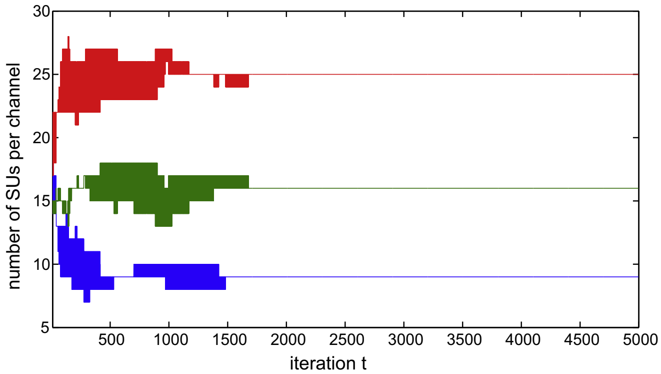

Fig. 7. DISAP on Network 1: number of SUs per channel as a function of the number of iterations.

8.2. System dynamics

In Fig. 5, the trajectories described by (6) and (11) are compared. The first part of the curves is characterized by important variations. This can be interpreted by the overlap of two replicator/aggregate monotone dynamics at odd and even instants, as explained in Section 6. We observe that, in the asymptotic case, DISAP outperforms PISAP as it is characterized by less pronounced wavelets and a faster convergence. However, both dynamics correctly converge to an evolutionary equilibrium. It is easy to check that the converged equilibrium is also the NE of G and the system optimum, which confirms our theoretic analysis. The dynamics presented in Fig. 5 are valid in an asymptotic case, when the number of SUs is large. We now turn our attention to small size scenarios.

8.3. Convergence with finite number of SUs

We study in this section the convergence of PISAP and DISAP on Network 1 ($N = 50$, $C = 3$). Figs. 6 and 7 show a realization of our algorithms. We notice that an imitation-stable equilibrium is achieved progressively following the dynamics characterized by (6) and (11). The equilibrium is furthermore very close to the system optimum: we can in fact check that, according to Theorem 1, the proportion of SUs choosing channels 1, 2 and 3 at the system optimum is 0.1875, 0.3125 and 0.5 respectively; in the simulation results we observe that there are 9, 16 and 25 SUs settling on channels 1, 2 and 3 respectively. We also notice on this example that DISAP convergence is faster than PISAP convergence.

We now focus on Network 2 ($N = 10$, $C = 2$) and compare T&E convergence behavior (Fig. 8)) to the trends of PISAP (Fig. 9) and DISAP (Fig. 10). It is easy to notice that T&E converges in a much slower and more chaotic way with respect to PISAP and DISAP. With T&E, the search of a NE may turn out to be extremely long (in the realization depicted in Fig. 8, e.g., convergence is achieved within 3.5×10^3 iterations). On the contrary, PISAP and DISAP converge within 75 and 32 iterations respectively.

8.4. System fairness

We now turn to the analysis of the fairness of the proposed spectrum access policies. To this end, we adopt the Jain's fairness index [40], which varies in [0,1] and reaches its maximum, when the resources are equally shared amongst users. Figs. 11 and 12, whose curves represent an average over 10^3 independent realizations on Network 2 of our algorithms and of T&E respectively, show that PISAP and DISAP clearly outperform T&E in

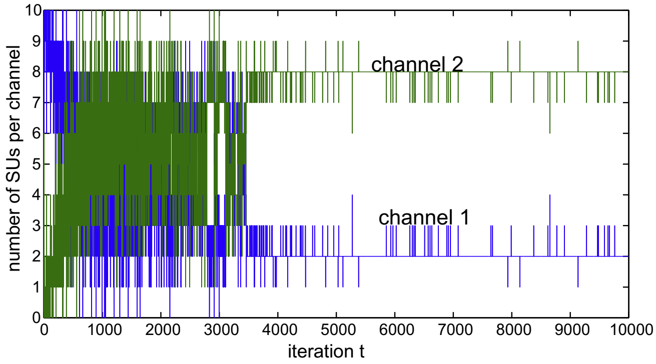

Fig. 8. T&E on Network 2: number of SUs per channel as a function of the number of iterations.

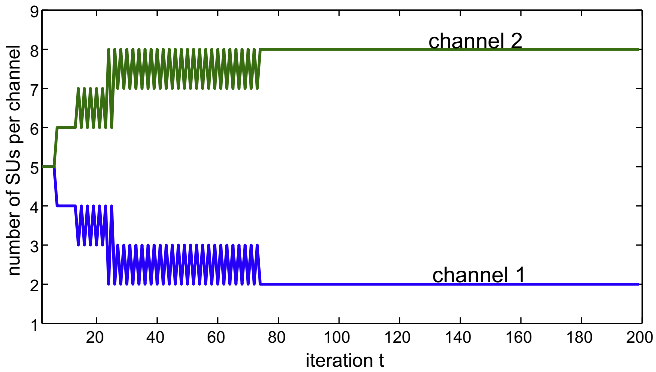

Fig. 9. PISAP on Network 2: number of SUs per channel as a function of the number of iterations.

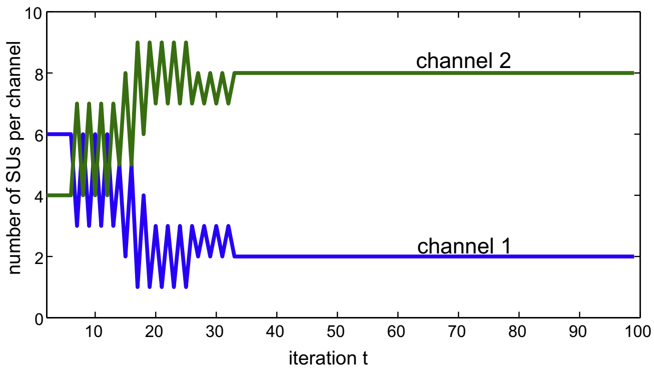

Fig. 10. DISAP on Network 2: number of SUs per channel as a function of the number of iterations.

terms both of fairness and convergence speed. In fact, while our system turns out to be very fair from the early iterations, T&E needs 6×10^3 iterations to get its system to reach a fairness value of 0.85. From Fig. 11, one can further infer that indeed DISAP converges more rapidly than PISAP: for example, a fairness index of 0.982 is reached at $t = 100$ by DISAP and at $t = 200$ by PISAP.

8.5. Switching cost

At last, we concentrate on the switching frequency of the three algorithms because switching may represent a significant cost for today's wireless devices in terms of delay, packet loss and protocol overhead. In Fig. 13, we define the switching cost at iteration t as the number of strategy switches between 0 and t. After 200 iterations, the

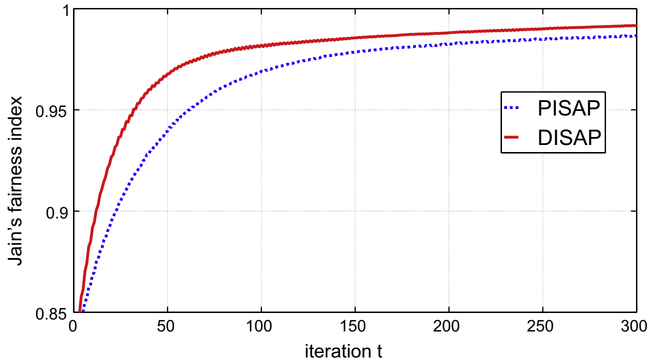

Fig. 11. PISAP and DISAP on Network 1: Jain's fairness index as a function of the number of iterations (average over 10^3 realizations).

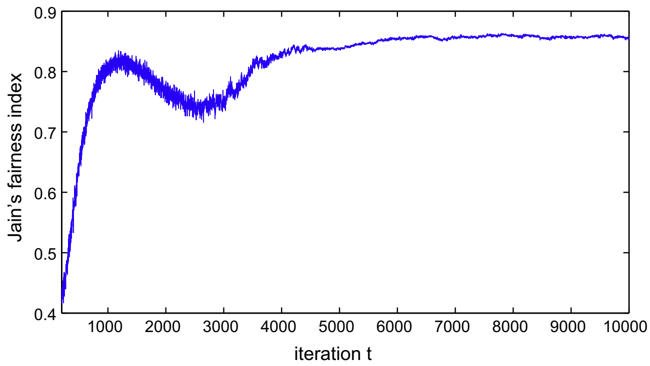

Fig. 12. T&E on Network 2: Jain's fairness index as a function of the number of iterations (average over 10^3 realizations).

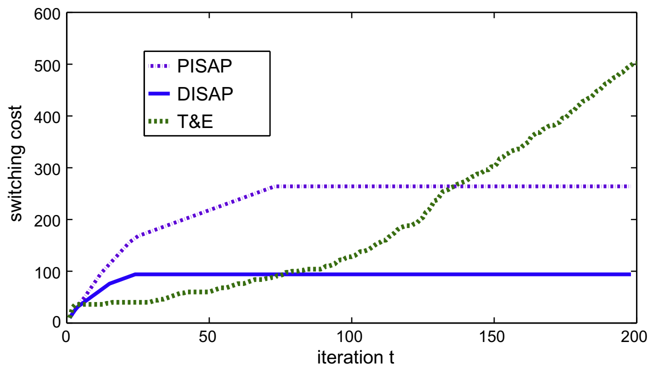

Fig. 13. Switching cost of PISAP, DISAP and T&E in Network 2.

switching cost of DISAP and PISAP has stabilized because convergence has been reached. On the contrary, T&E exhibits a fast growing cost.

8.6. Imperfect observations of PU activity

We assumed so far that cognitive radio users observe the channel activity of the primary user without errors. In this section, we investigate the performance of the proposed algorithms when the PU activity is *imperfectly* observed by the SUs. We denote by P_e the SU probability of error in detecting the PU activity and by Q_e the miss detection probability of an idle PU (probability of false alarm). The expected value of the payoff experienced by SUs on channel i can be written as follows:

$$\mathbb{E}[\pi_i(n_i)] = \sum_{m=0}^{n_i-1} \binom{n_i-1}{m} (1-Q_e)^m Q_e^{n_i-1-m} (1-Q_e) \frac{\mu_i}{m+1}, \tag{14}$$

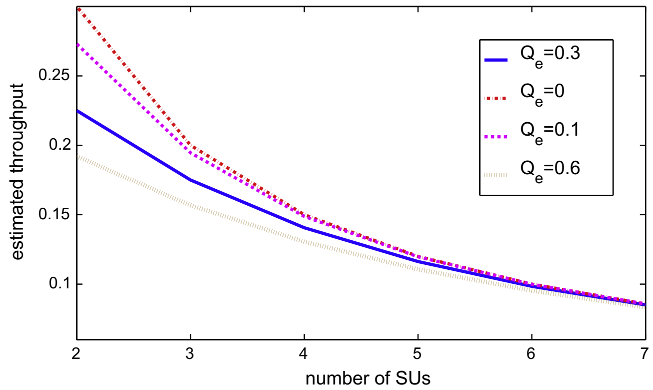

Fig. 14. Expected throughput deviation under sensing errors ($\mu_i = 0.6$).

which does not depend on P_e because a miss detection of the PU activity does not affect the throughput of any SU.

We now want to evaluate the impact of Q_e on the expected throughput estimates. To this end, we calculate the values taken by (14) for different values of Q_e and for different numbers of SUs. Results are shown in Fig. 14. Surprisingly, we see that the estimates under sensing errors rapidly converge to the values calculated for the ideal case with no miss detections (i.e., $Q_e = 0$). This is due to the fact that a trade-off arises. On the one hand, a SU, which is unable to detect a free slot experiences a penalty in its throughput. On the other hand, there are less SUs in average accessing free slots, which results in a higher throughput. As shown in Fig. 14, the two effects counterweight when the number of SUs gets larger. Hence, one can infer that in practice the impact of miss detections of the PU activity/inactivity is limited for a number of SUs on the same channel greater than 5.

9. Conclusion and further work

In this paper, we address the spectrum access problem in cognitive radio networks by applying population game theory and develop two imitation-based spectrum access policies. In our model, a SU can only imitate the other SUs operating on the same channel. This constraint makes the basic proportional imitation and double imitation rules irrelevant in our context. These two imitation rules are thus adapted to propose PISAP, a proportional imitation spectrum access policy, and DISAP, a double imitation spectrum access policy. A systematic theoretical analysis is presented on the induced imitation dynamics and the convergence properties of the proposed policies to the Nash equilibrium. Simulation results show the efficiency of our algorithms even for small size scenarios. It is also shown that PISAP and DISAP outperform Trial and Error in terms of convergence speed and fairness. As an important direction of the future work, we plan to investigate the imitation-based channel access problem in the more generic multi-hop scenario where SUs can imitate their neighbors and derive the relevant channel access policies.

Appendix A. Proof of Theorem 1

We first show that any point $\mathbf{x} = (x_i)_{i\in\mathcal{C}}$ cannot be a NE if there exists i_1 and i_2 such that $\pi_{i_1}(Nx_{i_1}) < \pi_{i_2}(Nx_{i_2})$. Otherwise, consider the strategy profile $\mathbf{x}'$ where ϵN SUs move from channel i_1 to i_2. For N large and with sufficient small ϵ, it follows from the continuity of $\pi_i(x_i)$ that $\pi_{i_1}(N(x_{i_1} - \epsilon)) < \pi_{i_2}(N(x_{i_2} + \epsilon))$, which indicates that by switching from i_1 to i_2, one can increase its payoff. We then proceed to show the second part of the theorem. To this end, let y denote the payoff of any SU at the NE, we have: $\mu_i S(x_i N) = y, \forall i \in \mathcal{C}$. It follows that $x_i N = S^{-1}\left(\frac{y}{\mu_i}\right)$. Noticing that $\sum_i x_i = 1$, at the NE, we have:

$$\sum_{i\in\mathcal{C}} S^{-1}\left(\frac{y}{\mu_i}\right) = N. \tag{A.1}$$

Since a NE is ensured to exist, (A.1) admits at least a solution y. Moreover, it follows from the strict monotonicity of S in Assumption 1 that its inverse function S^{-1} is also strictly monotonous. Hence (A.1) admits a unique solution. We thus complete the proof.

Appendix B. Proof of Theorem 2

We prove the statement for $t = 2$. The case for $t \geqslant 3$ is analogous to [30], which can be shown by induction and is therefore omitted.

Define the random variable $w_i^j(c)$ such that

$$w_i^j(c) = \begin{cases} 1 & \text{if SU } c \text{ is on channel } j \text{ at iteration } t = 1 \\ & \text{and migrates to channel } i \text{ at } t = 2, \\ 0 & \text{otherwise.} \end{cases} \tag{B.1}$$

We now distinguish two cases: proportional and double imitation.

B.1. Proportional imitation

By definition, if $j \neq s_c(1)$, it holds that $w_i^j(c) = 0$. Otherwise, c imitates with probability $\frac{n^k_{s_c(1)}}{n_{s_c(1)}}$ a SU that was using channel k at $t = 0$ and that is currently ($t = 1$) on the same channel as c ($s_c(1)$), and then migrates to channel i with probability $F^i_{s_c(0),k}$. Note that we allow for self-imitation in our algorithm. At initial states, all strategies are supposed to be chosen by at least one SU (N is large), so that $n_{s_c(1)} \neq 0$. We thus have:

$$\mathbb{P}\left[w^j_i(c) = 1\right] = \begin{cases} 0 & \text{if } j \neq s_c(1), \\ \sum_{k\in\mathcal{C}} \frac{n^k_{s_c(1)}}{n_{s_c(1)}} F^i_{s_c(0),k} & \text{otherwise.} \end{cases} \tag{B.2}$$

We can now derive the population proportions at iteration $t = 2$ as:

$$p^j_i(2) = \frac{1}{N}\sum_{c\in\mathcal{N}} w^j_i(c) \quad \forall i,j \in \mathcal{C}. \tag{B.3}$$

The expectations of these proportions can now be written as (using the Kronecker delta $\delta_{i,\,j}$):

$$\mathbb{E}[p^j_i(2)] = \frac{1}{N}\sum_{c\in\mathcal{N}} \mathbb{P}[w^j_i(c) = 1] \tag{B.4}$$

$$= \frac{1}{N}\sum_{c\in\mathcal{N},k\in\mathcal{C}} \frac{n^k_{s_c(1)}(1) F^i_{s_c(0),k}\delta_{j,s_c(1)}}{n_{s_c(1)}(1)} \tag{B.5}$$

$$= \frac{1}{N}\sum_{h,l,k\in\mathcal{C}} \frac{n^l_h(1) n^k_h(1) F^i_{l,k}\delta_{j,h}}{n_h(1)} \tag{B.6}$$

$$= \frac{1}{N}\sum_{l,k\in\mathcal{C}} \frac{n^l_j(1) n^k_j(1) F^i_{l,k}}{n_j(1)} \tag{B.7}$$

$$= \sum_{l,k\in\mathcal{C}} \frac{\tilde{x}^l_j(1)\tilde{x}^k_j(1)}{\tilde{x}_j(1)} F^i_{l,k}. \tag{B.8}$$

It follows that

$$\mathbb{E}[p_i(2)] = \sum_{j\in\mathcal{C}} \mathbb{E}[p^j_i(2)] = \sum_{j,l,k\in\mathcal{C}} \frac{\tilde{x}^l_j(1)\tilde{x}^k_j(1)}{\tilde{x}_j(1)} F^i_{l,k}. \tag{B.9}$$

As $w^j_i(c)$ and $w^j_i(d)$ are independent random variables for $c \neq d$ and since the variance of $w^j_i(c)$ is less than *1*, the variance of $p^j_i(2)$ and $p_i(2)$ for any $i,j \in \mathcal{C}$ are less than $1/N$ and C/N, respectively. It then follows the Bienaymé–Chebychev inequality that

$$\forall i \in \mathcal{C}, \quad \mathbb{P}[\{|p_i(2) - \mathbb{E}[p_i(2)]| > \delta\}] < \frac{C}{(N\delta)^2}. \tag{B.10}$$

Choosing N_0 such that $\frac{C}{(N_0\delta)^2} < \epsilon$ concludes the proof for $t = 2$. The proof can then be induced to any t as in [30].

B.2. Double imitation

If $j \neq s_c(1)$, it holds that $w^j_i(c) = 0$. Otherwise, c imitates with probability $\frac{n^k_{s_c(1)}}{N_{s_c(1)}}\frac{n^z_{s_c(1)}}{n_{s_c(1)}}$ two SUs that were using respectively channel k and channel z at $t = 0$ and that are currently ($t = 1$) on the same channel as c ($s_c(1)$), and then migrates to channel i with probability $F^i_{s_c(0),k,z}$.

The proof follows in the steps of the proportional imitation and only the main passages will be sketched out. We allow a SU to sample twice the same SU on the channel, so that:

$$\mathbb{P}\left[w^j_i(c) = 1\right] = \begin{cases} 0 & \text{if } j \neq s_c(1), \\ \sum_{k,z\in\mathcal{C}} \frac{n^k_{s_c(1)}}{n_{s_c(1)}}\frac{n^z_{s_c(1)}}{n_{s_c(1)}} F^i_{s_c(0),k,z} & \text{otherwise.} \end{cases} \tag{B.11}$$

We then derive the proportions expectations:

$$\mathbb{E}\left[p^j_i(2)\right] = \frac{1}{N}\sum_{c\in\mathcal{N}} \mathbb{P}[w^j_i(c) = 1] \tag{B.12}$$

$$= \frac{1}{N}\sum_{c\in\mathcal{N},k,z\in\mathcal{C}} \frac{n^k_{s_c(1)}(1)}{n_{s_c(1)}(1)}\frac{n^z_{s_c(1)}(1)}{n_{s_c(1)}(1)} F^i_{s_c(0),k,z}\delta_{j,s_c(1)} \tag{B.13}$$

$$= \sum_{l,k,z\in\mathcal{C}} \frac{\tilde{x}^l_j(1)\tilde{x}^k_j(1)\tilde{x}^z_j(1)}{[\tilde{x}_j(1)]^2} F^i_{l,k,z}. \tag{B.14}$$

It follows that:

$$\mathbb{E}[p_i(2)] = \sum_{j\in\mathcal{C}} \mathbb{E}\left[p^j_i(2)\right] \tag{B.15}$$

$$= \sum_{j,l,k,z\in\mathcal{C}} \frac{\tilde{x}^l_j(1)\tilde{x}^k_j(1)\tilde{x}^z_j(1)}{[\tilde{x}_j(1)]^2} F^i_{l,k,z}. \tag{B.16}$$

The rest of the proof for the double imitation follows the same way as that of proportional imitation.

Appendix C. Proof of Theorem 3

Recall the analysis in [30]. In this reference, Eq. (10) states that $F^j_{i,j} = F^i_{j,i} + \sigma[\pi_j - \pi_i]$. We can now characterize $\{F^i_{l,k}\}$ for PISAP as:

$$F^i_{l,k} = \begin{cases} 0 & \text{if } l,k \neq i, \\ F^l_{i,l} + \sigma[\pi_i(t-1) - \pi_l(t-1)] & \text{if } k = i \text{ and } l \neq i, \\ 1 - F^i_{k,i} - \sigma[\pi_k(t-1) - \pi_i(t-1)] & \text{if } l = i \text{ and } k \neq i, \\ 1 & \text{if } l = k = i. \end{cases}$$

The above four equations state that: (1) if none of the involved channels is i then the probability to switch to channel i is null (F is imitating); (2) the switching probability is proportional to the payoff difference; (3) if a SU does not imitate, it stays on the same channel; (4) if a SU imitates another SU with the same strategy, its strategy is not modified. Eq. (5) can now be written as follows:

$$\begin{aligned} x^i_i(t+1) &= \sum_{l\neq i} \frac{x^l_j(t)x^i_j(t)}{x_j(t)}(F^l_{i,l} + \sigma[\pi_i(t-1) - \pi_l(t-1)]) \\ &\quad + \sum_{k\neq i} \frac{x^i_j(t)x^k_j(t)}{x_j(t)}(1 - F^i_{i,k} - \sigma[\pi_k(t-1) - \pi_i(t-1)]) + \frac{x^{i2}_j}{x_j} \\ &= \sum_{l\neq i} \frac{x^l_j(t)x^i_j(t)}{x_j(t)}(1 + \sigma[\pi_i(t-1) - \pi_l(t-1)]) + \frac{x^{i2}_j}{x_j} \\ &= \sum_{l\neq i} \frac{x^l_j(t)x^i_j(t)}{x_j(t)}\sigma[\pi_i(t-1) - \pi_l(t-1)] + \sum_{l\in\mathcal{C}} \frac{x^l_j(t)x^i_j(t)}{x_j(t)} \\ &= x^i_j(t) + \sum_{l\in\mathcal{C}} \frac{x^l_j(t)x^i_j(t)}{x_j(t)}\sigma[\pi_i(t-1) - \pi_l(t-1)]. \end{aligned}$$

This concludes the proof.

Appendix D. Proof of Theorem 4

We prove the convergence of (9) by showing that the mapping described by (9) is a contraction. A contraction mapping is defined [41] as follows: let (X, d) be a metric space, f: $X \to X$ is a contraction if there exists a constant

$k \in [0,1)$ such that $\forall x, y \in X$, $d(f(x), f(y)) \leqslant kd(x, y)$, where $d(x, y) = \|x - y\| = \max_i |x_i - y_i|$. Such an f is called a contraction and admits a unique fixed point, to which the mapping described by f converges.

Noticing that

$$d(f(x), f(y)) = \|f(x) - f(y)\| \leqslant \left\|\frac{\partial f}{\partial x}\right\| d(x,y), \tag{D.1}$$

it suffices to show that the Jacobian $\left\|\frac{\partial f}{\partial x}\right\| \leqslant k$. In our case, it suffices to show that $\|J\|_\infty \leqslant k$, where $J = (J_{ij})_{i,j \in \mathcal{C}}$ is the Jacobian of the mapping described by one of the equation in (9), defined by $J_{ij} = \frac{\partial x_i(u)}{\partial x_j(u-1)}$.

Recall that $\pi_i = \frac{\mu_i}{N x_i}$ and $\bar{\pi} = \sum_l \frac{\mu_l}{N}$, (9) can be rewritten as:

$$x_i(u) = x_i(u-1) + \sigma\left[\frac{\mu_i}{N} - x_i(u-1)\sum_l \frac{\mu_l}{N}\right]. \tag{D.2}$$

It follows that

$$J_{ij} = \begin{cases} 1 - \sum_l \frac{\mu_l}{N} & \text{if } j = i, \\ 0 & \text{otherwise}. \end{cases} \tag{D.3}$$

Hence

$$\|J\|_\infty = \max_{i \in \mathcal{N}} \sum_{j \in \mathcal{N}} |J_{ij}| = 1 - \sum_l \frac{\mu_l}{N} < 1, \tag{D.4}$$

which shows that the mapping described by (9) is a contraction. It is further easy to check that the fixed point of (9) is $x^* = \frac{\mu_i}{\sum_{l \in \mathcal{N}} \mu_l}$, which is also the unique NE of G.

Appendix E. Proof of Theorem 5

We start from the following equation (we skip the reference to time on the right hand side after the first line for the sake of clarity):

$$x_i^j(t+1) = \sum_{l,k,z \in \mathcal{C}} \frac{x_j^l(t) x_j^k(t) x_j^z(t)}{[x_j(t)]^2} F^i_{l,k,z} \tag{E.1}$$

$$= \frac{x_j^i}{x_j^2} \sum_{k \neq i} x_j^{k2} [F^i_{i,k,k} + F^i_{k,i,k} + F^i_{k,k,i}] + \frac{x_j^{i2}}{x_j^2} \sum_{k \neq i} x_j^k [F^i_{k,i,i} + F^i_{i,k,i} + F^i_{i,i,k}] + \frac{x_j^i}{x_j^2} \sum_{k \neq i} \sum_{l \notin \{k,i\}} x_j^l x_j^k [F^i_{i,k,l} + F^i_{k,i,l} + F^i_{k,l,i}] + \frac{x_j^{i3}}{x_j^2}. \tag{E.2}$$

The second equality can be understood as follows. $F^i_{l,k,z} \neq 0$ only if at least one of the indices l, k, or z is equal to i. The first sum of the right hand side (RHS) is obtained when two indices are equal and different from i, the third one is equal to i. The second sum is obtained when one index is different from i and the two others are equal to i. The third sum is obtained when one index is equal to i and the two others are different and different from i. The last term corresponds to the case where all indices are equal to i (in this case, obviously, $F^i_{i,i,i} = 1$). Now we have:

$$F^i_{i,k,k} + F^i_{k,i,k} + F^i_{k,k,i} = 2F^i_{k,i,k} + 1 - F^k_{i,k,k}, \tag{E.3}$$

$$F^i_{k,i,i} + F^i_{i,k,i} + F^i_{i,i,k} = F^i_{k,i,i} + 2(1 - F^k_{i,i,k}), \tag{E.4}$$

$$F^i_{i,k,l} + F^i_{k,i,l} + F^i_{k,l,i} = 1 - F^{k,l}_{i,k,l} + F^i_{l,i,k} + F^i_{k,i,l}, \tag{E.5}$$

where $F^{k,l}_{i,k,l} = F^k_{i,k,l} + F^l_{i,k,l}$. Above, we used the fact that $\forall (i,j,k,l), F^l_{i,j,k} = F^l_{i,k,j}$ (i.e., there is no order in the sampling of two individuals) and $F^i_{i,k,l} + F^k_{i,k,l} + F^l_{i,k,l} = 1$ (i.e., with probability one, the SU goes to channel i, j or k at the next iteration).

Moreover, we note that:

$$\begin{aligned} &\frac{x_j^i}{x_j^2}\left[\sum_{k \neq i} x_j^{k2} + 2x_j^i \sum_{k \neq i} x_j^k + \sum_{k \neq i} \sum_{l \notin \{k,i\}} x_j^l x_j^k + x_j^{i2}\right] \\ &= \frac{x_j^i}{x_j^2}\left[\sum_k x_j^{k2} + 2x_j^i \sum_{k \neq i} x_j^k + \sum_{k \neq l} x_j^l x_j^k - x_j^i \sum_{l \neq i} x_j^l - x_j^i \sum_{k \neq i} x_j^k\right] \\ &= \frac{x_j^i}{x_j^2} \sum_{k,l} x_j^l x_j^k = x_j^i. \end{aligned} \tag{E.6}$$

We used here the fact that $\sum_k x_j^k = x_j$.

Eq. (E.2) can now be written (we skip the reference to time on the RHS, all x_j^i are functions of t):

$$\begin{aligned} x_i^j(t+1) = x_j^i &+ \frac{x_j^i}{x_j^2} \sum_{k \neq i} x_j^{k2} \left[2F^i_{k,i,k} - F^k_{i,k,k}\right] \\ &+ \frac{x_j^{i2}}{x_j^2} \sum_{k \neq i} x_j^k \left[F^i_{k,i,i} - 2F^k_{i,i,k}\right] \\ &+ \frac{x_j^i}{x_j^2} \sum_{k \neq i} \sum_{l \notin \{k,i\}} x_j^l x_j^k \left[F^i_{l,i,k} + F^i_{k,i,l} - F^{k,l}_{i,k,l}\right]. \end{aligned} \tag{E.7}$$

We now use the following property of the double imitation [34][3] for $i \notin \{j, k\}$:

$$\begin{aligned} F^{j,k}_{i,j,k} - F^i_{j,i,k} - F^i_{k,i,j} = {} & \frac{1}{2} Q(\pi_k(t-1))(\pi_j(t-1) - \pi_i(t-1)) \\ &+ \frac{1}{2} Q(\pi_j)(\pi_k(t-1) - \pi_i(t-1)). \end{aligned} \tag{E.8}$$

Payoffs π are functions of $t-1$ because imitation is based on the payoff obtained at the previous iteration). In particular, for $j = k$, we obtain:

$$F^k_{i,k,k} - 2F^i_{k,i,k} = Q(\pi_k(t-1))(\pi_k(t-1) - \pi_i(t-1)). \tag{E.9}$$

From these equations, we can simplify (E.7) into (skipping again reference to time on the RHS):

$$\begin{aligned} x_i^j(t+1) = x_j^i &+ \frac{x_j^i}{x_j^2} \sum_k x_j^{k2} Q(\pi_k)(\pi_i - \pi_k) \\ &+ \frac{x_j^{i2}}{x_j^2} \sum_k x_j^k Q(\pi_i)(\pi_i - \pi_k) \\ &+ \frac{x_j^i}{x_j^2} \sum_k \sum_{l \notin \{k,i\}} x_j^l x_j^k Q(\pi_l)(\pi_i - \pi_k). \end{aligned} \tag{E.10}$$

[3] In this reference, Eq. (3) of Theorem 1 is wrong. The correct formula is however given in the proof of the theorem in Appendix.

The term in the last double summation has been obtained by using (E.8), separating the expression in two double sums and interchanging indices j and k in the first double sum. Note also that all terms of the involved sums are null for $k = i$.

We now obtain:

$$x_i^j(t+1) = x_j^i + \frac{x_j^i}{x_j^2}\sum_k x_j^k(\pi_i - \pi_k)\left[x_j^k Q(\pi_k) + x_j^i Q(\pi_i) + \sum_{l\notin\{k,i\}} x_j^l Q(\pi_l)\right],$$
$$= x_j^i + x_j^i \sum_k \frac{x_j^k}{x_j}(\pi_i - \pi_k)\sum_l \frac{x_j^l}{x_j} Q(\pi_l) = x_j^i + x_j^i Q(\bar{\pi}_j)(\pi_i - \bar{\pi}_j), \tag{E.11}$$

where $\bar{\pi}_j(t-1) = \sum_k \frac{x_j^k(t)}{x_j(t)}\pi_k(t-1)$ can be interpreted as the average payoff at the previous iteration of SUs settling now on channel j. We now have:

$$x_i(t+1) = \sum_j x_i^j(t+1) = \sum_j \left[x_j^i(t) + x_j^i(t) Q(\bar{\pi}_j(t-1))(\pi_i(t-1) - \bar{\pi}_j(t-1))\right]$$
$$= x_i(t-1) + \sum_j x_j^i(t) Q(\bar{\pi}_j(t-1))(\pi_i(t-1) - \bar{\pi}_j(t-1)). \tag{E.12}$$

We used the fact that $\sum_j x_j^i(t+1) = x_i(t)$. This concludes the proof.

References

[1] S. Haykin, Cognitive radio: brain-empowered wireless communications, IEEE Journal on Selected Areas in Communications 23 (2) (2005) 201–220.
[2] M. Buddhikot, Understanding dynamic spectrum access: models, taxonomy and challenges, in: Proc. IEEE Dynamic Spectrum Access Networks (DySPAN), Dublin, Ireland, 2007.
[3] S. Iellamo, L. Chen, M. Coupechoux, A.V. Vasilakos, Imitation-based spectrum access policy for cognitive radio networks, in: Proc. International Symposium on Wireless Communication Systems (ISWCS), Paris, France, 2012.
[4] A. Mahajan, D. Teneketzis, Foundations and Applications of Sensor Management, Springer-Verlag, 2007. pp. 121–151 (Ch. Multi-armed Bandit Problems).
[5] A. Anandkumar, N. Michael, A. Tang, Opportunistic spectrum access with multiple users: learning under competition, in: Proc. IEEE International Conference on Computer Communication (INFOCOM), San Diego, CA USA, 2010.
[6] J. Neel, J. Reed, R. Gilles, Convergence of cognitive radio networks, in: Proc. IEEE Wireless Communications and Networking Conference (WCNC), Atlanta, Georgia USA, 2004.
[7] N. Nie, C. Comaniciu, Adaptive channel allocation spectrum etiquette for cognitive radio networks, ACM Mobile Networks and Applications (MONET) 11 (6) (2006) 779–797.
[8] Z. Han, C. Pandana, K. Liu, Distributive opportunistic spectrum access for cognitive radio using correlated equilibrium and no-regret learning, in: Proc. IEEE Wireless Communications and Networking Conference (WCNC), Hong Kong, China, 2007.
[9] L. Chen, S. Iellamo, M. Coupechoux, P. Godlewski, An auction framework for spectrum allocation with interference constraint in cognitive radio networks, in: Proc. IEEE International Conference on Computer Communication (INFOCOM), San Diego, California USA, 2010.
[10] J. Hofbauer, K. Sigmund, Evolutionary game dynamics, Bulletin of the American Mathematical Society 40 (4) (2003) 479–519.
[11] W.H. Sandholm, Population Games and Evolutionary Dynamics, The MIT Press, 2010.
[12] H. Tembine, E. Altman, R. El-Azouzi, Y. Hayel, Bio-inspired delayed evolutionary game dynamics with networking applications, Telecommunication Systems 47 (1) (2011) 137–152.
[13] P. Coucheney, C. Toutati, B. Gaujal, Fair and efficient user-network association algorithm for multi-technology wireless networks, in: Proc. IEEE International Conference on Computer Communication (INFOCOM), Rio de Janeiro, Brazil, 2009.
[14] S. Shakkottai, E. Altman, A. Kumar, Multihoming of users to access points in WLANs: a population game perspective, IEEE Journal on Selected Areas in Communications 25 (6) (2007) 1207–1215.
[15] D. Niyato, E. Hossain, Dynamics of network selection in heterogeneous wireless networks: an evolutionary game approach, IEEE Transactions on Vehicular Technology 58 (4) (2009) 2008–2017.
[16] H. Ackermann, P. Berenbrink, S. Fischer, M. Hoefer, Concurrent imitation dynamics in congestion games, in: Proc. ACM Symposium on Principles of Distributed Computing (PODC), Calgary, Canada, 2009.
[17] P. Berenbrik, T. Friedetzky, L. Goldberg, P. Goldberg, Distributed selfish load balancing, in: Proc. ACM-SIAM Symposium on Discrete Algorithms (SODA), San Francisco, CA, 2011.
[18] A. Ganesh, S. Lilienthal, D. Manjunath, A. Proutiere, F. Simatos, Load balancing via random local search in closed and open systems, in: Proc. ACM SIGMETRICS International Conference on Measurement and Modeling of Computer Systems, New York, NY, 2010.
[19] C. Alos-Ferrer, K.H. Schlag, The Handbook of Rational and Social Choice, Oxford University Press, 2009 (Ch. Imitation and Learning).
[20] X. Chen, J. Huang, Evolutionarily Stable Spectrum Access, IEEE Transactions on Mobile Computing, in press. http://ieeexplore.ieee.org/xpls/abs_all.jsp?arnumber=6185553&tag=1.
[21] X. Chen, J. Huang, Imitative spectrum access, in: Proc. International Symposium on Modeling and Optimization in Mobile, Ad Hoc, and Wireless Networks (WiOpt), Paderborn, Germany, 2012.
[22] S. Huang, X. Liu, Z. Ding, Opportunistic spectrum access in cognitive radio networks, in: Proc. IEEE International Conference on Computer Communication (INFOCOM), Phoenix, Arizona USA, 2008.
[23] M. Maskery, V. Krishnamurthy, Q. Zhao, Decentralized dynamic spectrum access for cognitive radios: cooperative design of a non-cooperative game, IEEE Transactions on Communications 57 (2) (2009) 459–469.
[24] S. Iellamo, L. Chen, M. Coupechoux, Imitation-based spectrum access policy for CSMA/CA-based cognitive radio networks, in: Proc. IEEE Wireless Communications and Networking Conference (WCNC), Paris, France, 2012.
[25] X. Chen, J. Huang, Spatial spectrum access game: Nash equilibria and distributed learning, in: Proc. ACM SIGMOBILE International Symposium on Mobile Ad Hoc Networking and Computing (MobiHoc), Hilton Head Island, South Carolina USA, 2012.
[26] L. Lai, H.E. Gamal, H. Jiang, H.V. Poor, Cognitive medium access: exploration, exploitation, and competition, IEEE Transactions on Mobile Computing 10 (2) (2011) 239–253.
[27] R.B. Myerson, Game Theory: Analysis of Conflict, Harvard University Press, Cambridge, MA, 1991.
[28] I. Milchtaich, Congestion games with player-specific payoff functions, Games and Economic Behavior 13 (1) (1996) 111–124.
[29] A. Haurie, P. Marcotte, On the relationship between Nash, Cournot and Wardrop equilibria, Networks 15 (3) (1985) 295–308.
[30] K.H. Schlag, Why imitate, and if so, how? A boundedly rational approach to multi-armed bandits, Journal of Economic Theory 78 (1) (1998) 130–156.
[31] C. Alos-Ferrer, F. Shi, Imitation with asymmetric memory, Economic Theory 49 (1) (2012) 193–215.
[32] B. Pradelski, H. Young, Learning efficient Nash equilibria in distributed systems, Games and Economic Behavior 75 (2) (2012) 882–897.
[33] J. Elias, F. Martignon, E. Altman, Joint pricing and cognitive radio network selection: a game theoretical approach, in: Proc. International Symposium on Modeling and Optimization in Mobile, Ad Hoc, and Wireless Networks (WiOpt), Paderborn, Germany, 2012.

[34] K.H. Schlag, Which one should i imitate?, Journal of Mathematical Economics 31 (4) (1999) 493–522
[35] W.H. Sandholm, Local stability under evolutionary game dynamics, Theoretical Economics 5 (1) (2010) 27–50.
[36] L. Sammuelson, J. Zhang, Evolutionary stability in asymmetric games, Journal of Economic Theory 57 (2) (1992) 363–391.
[37] C. Alós-Ferrer, S. Weidenholzer, Contagion and efficiency, Journal of Economic Theory 143 (1) (2008) 251–274.
[38] H.P. Young, Learning by trial and error, Games and Economic Behavior 65 (2) (2009) 626–643.
[39] B.S. Pradelski, H.P. Young, Efficiency and Equilibrium in Trial and Error Learning, Discussion Paper, Department of Economics, University of Oxford, 2010.
[40] R. Jain, D. Chiu, W. Hawe, A Quantitative Measure of Fairness and Discrimination for Resource Allocation in Shared Computer Systems, Research Report TR-301, DEC, 1984.
[41] R. Abraham, J. Marsden, T. Ratiu, Manifolds, Tensor Analysis, and Applications, Springer-Verlag, 1988.

Stefano Iellamo is currently a Ph.D. student at Telecom ParisTech. He completed his Master's degree in Telecommunications Engineering at Politecnico di Milano in 2009. His research activity, carried on at the Computer and Network Science department of Telecom ParisTech, mainly focuses on resources allocation for Cognitive Radio Networks.

Lin Chen received his B.E. degree in Radio Engineering from Southeast University, China in 2002 and the Engineer Diploma from Telecom ParisTech, Paris in 2005. He also holds a M.S. degree ofNetworking from the University of Paris 6. He currently works as associate professor in the department of computer science of the University of Paris-Sud XI. His main research interests include modeling and control for wireless networks, security and cooperation enforcement in wireless networks and game theory.

Marceau Coupechoux is Associate Professor at Telecom ParisTech since 2005. He obtained his master from Telecom ParisTech in 1999 and from University of Stuttgart, Germany in 2000, and his Ph.D. from Institut Eurecom, Sophia-Antipolis, France, in 2004. From 2000 to 2005, he was with Alcatel-Lucent (in Bell Labs former Research & Innovation and then in the Network Design department). In the Computer and Network Science department of Telecom ParisTech, he is working on cellular networks, wireless networks, ad hoc networks, cognitive networks, focusing mainly on layer 2 protocols, scheduling and resource management.

Optimal Sequential Wireless Relay Placement on a Random Lattice Path

Abhishek Sinha*, Arpan Chattopadhyay*, K. P. Naveen*, Marceau Coupechoux† and Anurag Kumar*
*Dept. of Electrical Communication Engineering, Indian Institute of Science, Bangalore 560012, India.
Email: {abhishek.sinha.iisc, arpanc.ju}@gmail.com, {naveenkp, anurag}@ece.iisc.ernet.in
†Telecom ParisTech and CNRS LTCI, Dept. of Informatique et Réseaux, 23, avenue d'Italie, 75013 Paris, France.
Email: marceau.coupechoux@telecom-paristech.fr

***Abstract*—Our work is motivated by the need for impromptu (or "as-you-go") deployment of relay nodes (for establishing a packet communication path with a control centre) by firemen/commandos while operating in an unknown environment. We consider a model, where a deployment operative steps along a random lattice path whose evolution is Markov. At each step, the path can randomly either continue in the same direction or take a turn "North" or "East," or come to an end, at which point a data source (e.g., a temperature sensor) has to be placed that will send packets to a control centre at the origin of the path. A decision has to be made at each step whether or not to place a wireless relay node. Assuming that the packet generation rate by the source is very low, and simple link-by-link scheduling, we consider the problem of relay placement so as to minimize the expectation of an end-to-end cost metric (a linear combination of the sum of convex hop costs and the number of relays placed). This impromptu relay placement problem is formulated as a total cost Markov decision process. First, we derive the optimal policy in terms of an optimal placement set and show that this set is characterized by a boundary beyond which it is optimal to place. Next, based on a simpler alternative one-step-look-ahead characterization of the optimal policy, we propose an algorithm which is proved to converge to the optimal placement set in a finite number of steps and which is faster than the traditional value iteration. We show by simulations that the distance based heuristic, usually assumed in the literature, is close to the optimal provided that the threshold distance is carefully chosen.**

***Index Terms*—Relay placement, Sensor networks, Markov decision processes, One-step-look-ahead.**

I. Introduction

Wireless networks, such as cellular networks or multihop ad hoc networks, would normally be deployed via a planning and design process. There are situations, however, that require the impromptu (or "as-you-go") deployment of a multihop wireless packet network. For example, such an impromptu approach would be required to deploy a wireless sensor network for situational awareness in emergency situations such as those faced by firemen or commandos (see [1], [2]). For example, as they attack a fire in a building, firemen might wish to place temperature sensors on fire-doors to monitor the spread of fire, and ensure a route for their own retreat; or commandos attempting to flush out terrorists might wish to place acoustic or passive infra-red sensors to monitor the movement of people in the building. As-you-go deployment may also be of interest when deploying a multi-hop wireless sensor network over a large terrain (such as a dense forest)

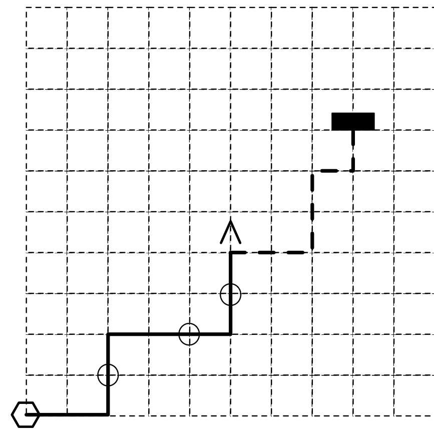

Fig. 1. A wireless network being deployed as a person steps along a random lattice path. Inverted **V**: location of the deployment person; solid line: path already covered; circles: deployed relays; thick dashed path: a possible evolution of the remaining path. The sensor to be placed at the end is also shown as the black rectangle.

in order to obtain a first-cut deployment which could then be augmented to a network with desired properties (connectivity and quality-of-service).

With the above larger motivation in mind, in this paper we are concerned with the rigorous formulation and solution of a problem of impromptu deployment of a multihop wireless network along a random lattice path, see Fig. 1. The path could represent the corridor of a large building, or even a trail in a forest. The objective is to create a multihop wireless path for packet communication from the end of the path to its beginning. The problem is formulated as an optimal sequential decision problem. The formulation gives rise to a total cost Markov decision process, which we study in detail in order to derive structural properties of the optimal policy. We also provide an efficient algorithm for calculating the optimal policy.

A. Related Work

Our study is motivated by "first responder" networks, a concept that has been around at least since 2001. In [2], Howard et al. provide heuristic algorithms for the problem of incremental deployment of sensors (such as surveillance cameras) with the objective of covering the deployment area. Their problem is related to that of self-deployment of autonomous robot teams and to the art-gallery problem. Creation of a communication network that is optimal in some sense is not an objective in [2]. In a somewhat similar vein, the work of Loukas et al. [3] is concerned with the dynamic locationing of robots that, in an emergency situation, can serve as wireless relays between the infrastructure and human-carried wireless devices. The problem of impromptu deployment of static wireless networks has been considered in [4], [5], [6], [7]. In [4], Naudts et al. provide a methodology in which, after a node is deployed, the next node to be deployed is turned on and begins to measure the signal strength to the last deployed node. When the signal strength drops below a predetermined level, the next node is deployed and so on. Souryal et al. provide a similar approach in [5], [6], where an extensive study of indoor RF link quality variation is provided, and a system is developed and demonstrated. The work reported in [7] is yet another example of the same approach for relay deployment. More recently, Liu et al. [8] describe a "breadcrumbs" system for aiding firefighters inside buildings, and is similar to our present paper in terms of the class of problems it addresses. In a survey article [1], Fischer et al. describe various localization technologies for assisting emergency responders, thus further motivating the class of problems we consider.

In our earlier work (Mondal et al. [9]) we took the first steps towards rigorously formulating and addressing the problem of impromptu optimal deployment of a multihop wireless network on a line. The line is of unknown length but prior information is available about its probability distribution; at each step, the line can come to an end with probability p, at which point a sensor has to be placed. Once placed, the sensor sends periodic measurement packets to a control centre near the start of the line. It is assumed that the measurement rate at the sensor is low, so that (with a very high probability) a packet is delivered to the control centre before the next packet is generated at the sensor. This so called "lone packet model" is realistic for situations in which the sensor makes a measurement every few seconds.

The objective of the sequential decision problem is to minimise a certain expected per packet cost (e.g., end-to-end delay or total energy expended by a node), which can be expressed as the sum of the costs over each hop, subject to a constraint on the number of relays used for the operation. It has been proved in [9] that an optimal placement policy solving the above mentioned problem is a threshold rule, i.e., there is a threshold r^* such that, after placing a relay, if the operative has walked r^* steps without the path ending, then a relay must be placed at r^*.

B. Outline and Our Contributions

In this paper, while continuing to assume (**a**) that a single operative moves step-by-step along a path, deciding to place or to not place a relay, (**b**) that the length of the path is a geometrically distributed random multiple of the step size, (**c**) that a source of packets is placed at the end of the path, (**d**) that the lone packet traffic model applies, and (**e**) that the total cost of a deployment is a linear combination of the sum of convex hop costs and the number of nodes placed, we extend

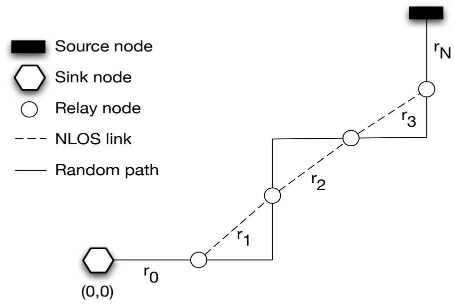

Fig. 2. A depiction of relay deployment along a random lattice path with NLOS propagation.

the work presented in [9] to the two-dimensional case. At each step, the line can take a right angle turn either to the "East" or to the "North" with known fixed probabilities. We assume a Non-Line-Of-Sight (NLOS) propagation model, where a radio link exists between two nodes placed anywhere on the path, see Fig. 2. The lone packet model is a natural first assumption, and would be useful in low-duty cycle monitoring applications. Once the network has been deployed, an analytical technique such as that presented in [10] can be used to estimate the actual packet carrying capacity of the network.

We will formally describe our system model and problem formulation in Section II. The following are our main contributions:

- We formulate the problem as a total cost Markov decision process (MDP), and characterize the optimal policies in terms of placement sets. We show that these optimal policies are threshold policies and thus the placement sets are characterized by boundaries in the two-dimensional lattice (Section III). Beyond these boundaries, it is optimal to place a relay.
- Noticing that placement instants are renewal points in the random process, we recognize and prove the One-Step-Look-Ahead (OSLA) characterization of the placement sets (Section IV).
- Based on the OSLA characterization, we propose an iterative algorithm, which converges to the optimal placement set in a finite number of steps (Section V). We have observed that this algorithm converges much faster than value iteration.
- In Section VII we provide several numerical results that illustrate the theoretical development. The relay placement approach proposed in [4], [5], [6], [7] would suggest a distance threshold based placement rule. We numerically obtain the optimal rule in this class, and find that the cost of this policy is numerically indistinguishable from that of the overall optimal policy provided by our theoretical development. It suggests that it might suffice to utilize a distance threshold policy. However, the distance threshold should be carefully designed taking into account the system parameters and the optimality objective.

For the ease of presentation we have moved most of the proofs to the Appendix.

II. System Model

We consider a deployment person, whose stride length is 1 unit, moving along a random path in the two-dimensional lattice, placing relays at some of the lattice points of the path and finally a source node at the end of the path. Once placed, the source node periodically generates measurement packets which are forwarded by the successive relays in a multihop fashion to the control centre located at $(0, 0)$; see Fig. 2.

A. Random Path

Let $\mathbb{Z}_+$ denote the set of nonnegative integers, and $\mathbb{Z}_+^2$ the nonnegative orthant of the two dimensional integer lattice. We will refer to the x direction as East and to the y direction as North. Starting from $(0, 0)$ there is a lattice path that takes random turns to the North or to the East (this is to avoid the path folding back onto itself, see Fig 2). Under this restriction, the path evolves as a stochastic process over $\mathbb{Z}_+^2$. When the deployment person has reached some lattice point, the path continues for one more step and terminates with probability p, or does not terminate with probability $1-p$. In either case, the next step is Eastward with probability q and Northward with probability $1 - q$. Thus, for instance, $(1 - p)q$ is the probability that the path proceeds Eastwards without ending. The person deploying the relays is assumed to keep a count of m and n, the number of steps taken in the x direction and in y direction, repectively, since the previous relay was placed. He is also assumed to know the probabilities p and q.

B. Cost Definition

In our model, we assume NLOS propagation, i.e., packet transmission can take place between any two successive relays even if they are not on the same straight line segment of the lattice path. In the building context, this would correspond to the walls being radio transparent. The model is also suitable when the deployment region is a thickly wooded forest where the deployment person is restricted to move only along some narrow path (lattice edges in our model).

For two successive relays separated by a distance r, we assign a cost of $d(r)$ which could be the average delay incurred over that hop (including transmission overheads and retransmission delays), or the power required to get a packet across the hop. For instance, in our numerical work we use the power cost, $d(r) = P_m + \gamma r^\eta$, where P_m is the minimum power required, γ represents an SNR constraint and η is the path-loss exponent. Now suppose N relays are placed such that the successive inter-relay distances are $r_0, r_1, \cdots, r_N$ (r_0 is the distance from the control centre at $(0, 0)$ and the first relay, and r_N is the distance from the last relay to the sensor placed at the end of the path) then the total cost of this placement is the sum of the one-hop costs $C = \sum_{i=0}^{N} d(r_i)$. The total cost being the sum of one-hop costs can be justified for the lone packet model since when a packet is being forwarded there is no other packet transmission taking place.

We now impose a few technical conditions on the one-hop cost function $d(\cdot)$: (**C1**) $d(0) > 0$, (**C2**) $d(r)$ is convex and increasing in r, and (**C3**) for any r and $\delta > 0$ the difference $d(r + \delta) - d(r)$ increases to ∞.

(**C1**) is imposed considering the fact that it requires a non-zero amount of delay or power for transmitting a packet between two nodes, however close they may be. (**C2**) and (**C3**) are properties we require to establish our results on the optimal policies. They are satisfied by the power cost, $P_m + \gamma r^\eta$, and also by the mean hop delay (see [11]).

We will overload the notation $d(\cdot)$ by denoting the one-hop cost between the locations $(0, 0)$ and $(x, y) \in \Re^2$ as simply $d(x, y)$ instead of $d(||(x, y) - (0, 0)||)$. Using the condition on $d(r)$ we prove the following convexity result of $d(x, y)$.

Lemma 1: The function $d(x, y)$ is convex in (x, y), where $(x, y) \in \mathbb{R}^2$.

Proof: This follows from the fact that $d(\cdot)$ is convex, non-decreasing in its argument. For a formal proof, see Appendix A-A. ■

We further impose the following condition on $d(x, y)$ where $(x, y) \in \Re^2$. We allow a general cost-function $d(x, y)$ endowed with the following property: (**C4**) The function $d(x, y)$ is positive, twice continuously partially differentiable in variables x and y and $\forall x, y \in \mathbb{R}_+$,

$$d_{xx}(x, y) > 0, \;\; d_{xy}(x, y) > 0, \;\; d_{yy}(x, y) > 0, \tag{1}$$

where $d_{xy}(x, y) = \frac{\partial^2 d(x,y)}{\partial x \partial y}$. These properties also hold for the mean delay and the power functions mentioned earlier.

Finally define, for $(m, n) \in \mathbb{Z}_+^2$, $\Delta_1(m, n) = d(m+1, n) - d(m, n)$ and $\Delta_2(m, n) = d(m, n + 1) - d(m, n)$.

Lemma 2: $\Delta_1(m, n)$ and $\Delta_2(m, n)$ are non-decreasing in both the coordinates m and n.

Proof: This follows directly from (1). See Appendix A-B for details. ■

C. Deployment Policies and Problem Formulation

A deployment policy π is a sequence of mappings (μ_k : $k \geq 0$), where at the k-th step of the path (provided that the path has not ended thus far) μ_k allows the deployment person to decide whether to *place* or *not to place* a relay where, in general, randomization over these two actions is allowed. The decision is based on the entire information available to the deployment person at the k-th step, namely the set of vertices traced by the path and the location of the previous vertices where relays were placed. Let Π represent the set of all policies. For a given policy $\pi \in \Pi$, let $\mathbb{E}_\pi$ represent the expectation operator under policy π. Let C denote the total cost incurred and N the total number of relays used. We are interested in solving the following problem,

$$\min_{\pi \in \Pi} \quad \mathbb{E}_\pi C + \lambda \mathbb{E}_\pi N, \tag{2}$$

where $\lambda > 0$ may be interpreted as the cost of a relay. Solving the problem in (2) can also help us solve the following constrained problem,

$$\begin{aligned} \min_{\pi \in \Pi} \qquad & \mathbb{E}_\pi C \\ \text{Subject to:} \quad & \mathbb{E}_\pi N \leq \rho_{avg}, \end{aligned} \tag{3}$$

where $\rho_{avg} > 0$ is a contraint on the average number of relays (we will describe this procedure in Section VI). First, in Sections III to V, we work towards obtaining an efficient solution to the problem in (2).

III. MDP Formulation and Solution

In this section we formulate the problem in (2) as a total cost infinite horizon MDP and derive the optimal policy in terms of optimal placement set. We show that this set is characterized by a two-dimensional boundary, upon crossing which it is optimal to place a relay.

A. States, Actions, State-Transitions and Cost Structure

We formulate the problem as a sequential decision process starting at the origin of the lattice path. The decision to place or not place a relay at the k-th step is based on $((M_k, N_k), Z_k)$, where (M_k, N_k) denotes the coordinates of the deployment person with respect to the previous relay and $Z_k \in \{\mathsf{e}, \mathsf{c}\}$; $Z_k = \mathsf{e}$ means that at step k the random lattice path has ended and $Z_k = \mathsf{c}$ means that the path will continue in the same direction for at least one more step. Thus, the state space is given by:

$$\mathcal{S} = \Big\{(m, n, z) : (m, n) \in \mathbb{Z}_+^2, z \in \{\mathsf{e}, \mathsf{c}\}\Big\} \cup \{\phi\}, \qquad (4)$$

where ϕ denotes the cost-free terminal state, i.e., the state after the end of the path has been discovered. The action taken at step k is denoted $U_k \in \{0, 1\}$, where $U_k = 1$ is the action to place a relay, and $U_k = 0$ is the action of not placing a relay. When the state is (m, n, c) and when action u is taken, the transition probabilities are given by:

- If u is 0 then,
  (i) $(m, n, \mathsf{c}) \longrightarrow (m + 1, n, \mathsf{c})$ w.p. $(1 - p)q$
  (ii) $(m, n, \mathsf{c}) \longrightarrow (m + 1, n, \mathsf{e})$ w.p. pq
  (iii) $(m, n, \mathsf{c}) \longrightarrow (m, n + 1, \mathsf{c})$ w.p. $(1 - p)(1 - q)$
  (iv) $(m, n, \mathsf{c}) \longrightarrow (m, n + 1, \mathsf{e})$ w.p. $p(1 - q)$.
- If u is 1 then
  (i) $(m, n, \mathsf{c}) \longrightarrow (1, 0, \mathsf{c})$ w.p. $(1 - p)q$
  (ii) $(m, n, \mathsf{c}) \longrightarrow (1, 0, \mathsf{e})$ w.p. pq
  (iii) $(m, n, \mathsf{c}) \longrightarrow (0, 1, \mathsf{c})$ w.p. $(1 - p)(1 - q)$
  (iv) $(m, n, \mathsf{c}) \longrightarrow (0, 1, \mathsf{e})$ w.p. $p(1 - q)$.

If $Z_k = \mathsf{e}$ then the only allowable action is $u = 1$ and we enter into the state ϕ. If the current state is ϕ, we stay in the same cost-free termination state irrespective of the control u. The one step cost when the state is $s \in \mathcal{S}$ is given by:

$$c(s, u) = \begin{cases} d(m, n) & \text{if } s = (m, n, \mathsf{e}), \\ \lambda + d(m, n) & \text{if } u = 1 \text{ and } s = (m, n, \mathsf{c}), \\ 0 & \text{if } u = 0 \text{ or } s = \phi. \end{cases}$$

For simplicity we write the state (m, n, c) as simply (m, n).

B. Optimal Placement Set $\mathcal{P}_\lambda$

Let $J_\lambda(m, n)$ denote the optimal cost-to-go when the current state is (m, n). When at some step the state is (m, n) the deployment person has to decide whether to place or not place a relay at the current step. J_λ is the solution of the Bellman equation [12, Page 137, Prop. 1.1],

$$J_\lambda(m, n) = \min\{c_p(m, n), c_{np}(m, n)\}, \qquad (5)$$

where $c_p(m, n)$ and $c_{np}(m, n)$ denote the expected cost incurred when the decision is to *place* and *not place* a relay, respectively. $c_p(m, n)$ is given by

$$\begin{aligned} c_p(m, n) \quad &= \quad \lambda + d(m, n) + (1 - p)(1 - q)J_\lambda(0, 1) \\ &\quad\; + (1 - p)qJ_\lambda(1, 0) + pd(1). \end{aligned} \qquad (6)$$

The term $\lambda + d(m, n)$ in the above expression is the one step cost which is first incurred when a relay is placed. The remaining terms are the average cost-to-go from the next step. The term $(1-p)(1-q)J_\lambda(0, 1)$ can be understood as follows: $(1-p)(1-q)$ is the probability that the path proceeds Eastward without ending. Thus the state at the next step is $(0, 1, \mathsf{c})$ w.p. $(1 - p)(1 - q)$, the optimal cost-to-go from which is, $J_\lambda(0, 1)$. Similarly for the term $(1 - p)qJ_\lambda(1, 0)$, $(1 - p)q$ is the probability that the path will proceed, without ending, towards the North (thus the next state is $(1, 0, \mathsf{c})$) and $J_\lambda(1, 0)$ is the cost-to-go from the next state. Finally, in the term $pd(1)$, p is the probability that the path will end, either proceeding East or North, at the next step and $d(1)$ is the cost of the last link. Following a similar explanation, the expression for $c_{np}(m, n)$ can be written as:

$$\begin{aligned} &c_{np}(m, n) = \\ &\quad (1 - p)qJ_\lambda(m + 1, n) + (1 - p)(1 - q)J_\lambda(m, n + 1) \\ &\quad + pqd(m + 1, n) + p(1 - q)d(m, n + 1). \end{aligned} \qquad (7)$$

We define the optimal placement set $\mathcal{P}_\lambda$ as the set of all lattice points (m, n), where it is optimal to place rather than to not place a relay. Formally,

$$\mathcal{P}_\lambda = \Big\{(m, n) : c_p(m, n) \le c_{np}(m, n)\Big\}. \qquad (8)$$

In this definition, if the costs of placing and not-placing are the same, we have arbitrarily chosen to place at that point.

The above result yields the following main theorem of this section which characterizes the optimal placement set $\mathcal{P}_\lambda$ in terms of a boundary.

Theorem 1: The optimal placement set $\mathcal{P}_\lambda$ is characterized by a boundary, i.e., there exist mappings $m^* : \mathbb{Z}_+ \to \mathbb{Z}_+$ and $n^* : \mathbb{Z}_+ \to \mathbb{Z}_+$ such that:

$$\begin{aligned} \mathcal{P}_\lambda \quad &= \quad \bigcup_{n \in \mathbb{Z}_+} \{(m, n) : m \ge m^*(n)\} &\qquad (9) \\ &= \quad \bigcup_{m \in \mathbb{Z}_+} \{(m, n) : n \ge n^*(m)\}. &\qquad (10) \end{aligned}$$

Proof Outline: The proof utilizes the conditions **C2** and **C3** imposed on the cost function $d(\cdot)$. First, using (6) and (7) in (8) and rearranging we alternatively write $\mathcal{P}_\lambda$ as, $\mathcal{P}_\lambda = \{(m, n) : F(m, n) \ge K\}$, where K is a constant and $F(\cdot, \cdot)$ is some function of m and n. Then, we complete the proof by showing that $F(m, n)$ is non-decreasing in both m and n. This requires us to prove (using an induction argument) that

$H_\lambda(m,n) := J_\lambda(m,n) - d(m,n)$ is non-decreasing in m and n. Also, Lemma 2 has to be used here. For a formal proof see Appendix B. ■

Remark: Though the optimal placement set $\mathcal{P}_\lambda$ was characterized nicely in terms of a boundary $m^*(\cdot)$ and $n^*(\cdot)$, a naive approach of computing this boundary, using value iteration to obtain $J_\lambda(m,n)$ (for several values of $(m,n) \in \mathbb{Z}_+^2$), would be computationally intensive. Our effort in the next section (Section IV) is towards obtaining an alternate simplified representation for $\mathcal{P}_\lambda$ using which we propose an algorithm in Section V, which is guaranteed to return $\mathcal{P}_\lambda$ in a finite (in practice, small) number of steps.

IV. Optimal Stopping Formulation

We observe that the points where the path has not ended, and a relay is placed, are renewal points of the decision process. This motivates us to think of the decision process after a relay is placed as an optimal stopping problem with *termination cost* $J_\lambda(0,0)$ (which is the optimal cost-to-go from a relay placement point). Let $\overline{\mathcal{P}}_\lambda$ denote the placement set corresponding to the OSLA rule (to be defined next). In this section we prove our next main result that $\mathcal{P}_\lambda = \overline{\mathcal{P}}_\lambda$.

A. One-Step-Look-Ahead Stopping Set $\overline{\mathcal{P}}_\lambda$

Under the OSLA rule, a relay is placed at state (m,n,c) if and only if the "cost $c_1(m,n)$ of *stopping* (i.e., placing a relay) at the current step" is less than the "cost $c_2(m,n)$ of continuing (without placing relay at the current step) for one more step, and then stopping (i.e., placing a relay at the next step)". The expressions for the costs $c_1(m,n)$ and $c_2(m,n)$ can be written as:

$$c_1(m,n) = \lambda + d(m,n) + J_\lambda(0,0)$$

and

$$\begin{aligned} c_2(m,n) = \\ & pq(d(m+1,n) + p(1-q)d(m,n+1)) + (1-p) \\ & \Big(qd(m+1,n) + (1-q)d(m,n+1) + \lambda + J_\lambda(0,0)\Big). \end{aligned}$$

Then we define the OSLA placement set $\overline{\mathcal{P}}_\lambda$ as:

$$\overline{\mathcal{P}}_\lambda = \{(m,n) \in \mathbb{Z}_+^2 : c_1(m,n) \le c_2(m,n)\}.$$

Substituting for $c_1(m,n)$ and $c_2(m,n)$ and simplifying we obtain:

$$\overline{\mathcal{P}}_\lambda = \Big\{(m,n) \in \mathbb{Z}_+^2 : p(\lambda + J_\lambda(0,0)) \le \Delta_q(m,n)\Big\}, \quad (11)$$

where $\Delta_q(m,n) = q\Delta_1(m,n) + (1-q)\Delta_2(m,n)$.

Theorem 2: The OSLA rule is a threshold policy, i.e., there exist mappings $\bar{m} : \mathbb{Z}_+ \to \mathbb{Z}_+$ and $\bar{n} : \mathbb{Z}_+ \to \mathbb{Z}_+$, which define the one-step placement set $\overline{\mathcal{P}}_\lambda$ as follows,

$$\begin{aligned} \overline{\mathcal{P}}_\lambda &= \bigcup_{n \in \mathbb{Z}_+} \{(m,n) : m \ge \bar{m}(n)\} \quad (12) \\ &= \bigcup_{m \in \mathbb{Z}_+} \{(m,n) : n \ge \bar{n}(m)\}. \quad (13) \end{aligned}$$

Proof: Noticing that in (11) $\Delta_q(m,n)$ is non-decreasing in (m,n) and $p(\lambda + J_\lambda(0,0))$ is a constant, the proof follows along the lines of the proof of Theorem 1. ■

Now, we present the main theorem of this section.

Theorem 3:

$$\mathcal{P}_\lambda = \overline{\mathcal{P}}_\lambda.$$

Proof: See Appendix C. ■

Remark: The characterization in (11) is much simpler than the one in (20) once the value of $J_\lambda(0,0)$ is given. In the following subsection, we define a function $g(\cdot)$ and express $J_\lambda(0,0)$ as the minimum value of this function.

B. Computation of $J_\lambda(0,0)$

Let us start by defining a collection of placement sets indexed by $h \ge 0$:

$$\mathcal{P}(h) = \{(m,n) \in \mathbb{Z}_+^2 : p(\lambda + h) \le \Delta_q(m,n)\}. \quad (14)$$

Referring to (11), note that $\mathcal{P}(J_\lambda(0,0)) = \overline{\mathcal{P}}_\lambda$. Let $g(h)$ denote the cost-to-go, starting from $(0,0)$, if the placement set $\mathcal{P}(h)$ is employed. Then, since $J_\lambda(0,0)$ is the optimal cost-to-go and $\mathcal{P}_\lambda \in \{\mathcal{P}(h)\}_{h\ge 0}$, we have $J_\lambda(0,0) = \min_{h\ge 0} g(h)$.

To compute $g(h)$, we proceed by defining the boundary $\mathcal{B}(h)$ of $\mathcal{P}(h)$ as follows:

$$\begin{aligned} \mathcal{B}(h) = \{&(m,n) \in \mathcal{P}(h) : (m-1,n) \in \mathcal{P}^c(h) \text{ or} \\ &(m,n-1) \in \mathcal{P}^c(h)\}, \end{aligned} \quad (15)$$

where $\mathcal{P}^c(h) := \mathbb{Z}_+^2 - \mathcal{P}(h)$.

Suppose the corridor ends at some $(m,n) \in \mathcal{P}^c(h) \cup \mathcal{B}(h)$, then only a cost of $d(m,n)$ is incurred. Otherwise (i.e., if the corridor reaches some $(m,n) \in \mathcal{B}(h)$ and continues), using a renewal argument, a cost of $d(m,n) + \lambda + g(h)$ is incurred, where $d(m,n) + \lambda$ is the cost of placing a relay and $g(h)$ is the future cost-to-go. We can thus write:

$$\begin{aligned} g(h) = & \sum_{(m,n) \in \mathcal{P}^c(h) \cup \mathcal{B}(h)} \mathbb{P}((m,n),\mathsf{e}) d(m,n) + \\ & \sum_{(m,n) \in \mathcal{B}(h)} \mathbb{P}((m,n),\mathsf{c})(g(h) + \lambda + d(m,n)), \end{aligned} \quad (16)$$

where $\mathbb{P}((m,n),\mathsf{e})$ is the probability of the corridor ending at (m,n) and $\mathbb{P}((m,n),\mathsf{c})$ is the probability of the corridor reaching the boundary and continuing. Solving for $g(h)$, we obtain:

$$\begin{aligned} g(h) = & \frac{1}{1 - \sum_{(m,n)\in\mathcal{B}(h)} \mathbb{P}((m,n),\mathsf{c})} \times \\ & \Bigg(\sum_{(m,n) \in \mathcal{P}^c(h) \cup \mathcal{B}(h)} \mathbb{P}((m,n),\mathsf{e}) d(m,n) + \\ & \sum_{(m,n) \in \mathcal{B}(h)} \mathbb{P}((m,n),\mathsf{c})(\lambda + d(m,n)) \Bigg). \end{aligned} \quad (17)$$

The above expression is extensively used in our algorithm proposed in the next section.

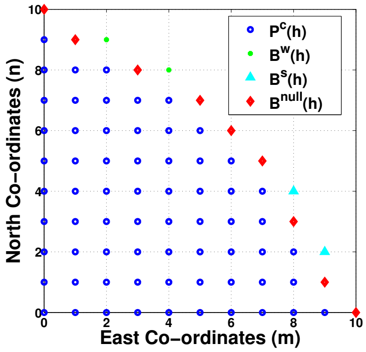

Fig. 3. Example of placement set of the form in (14): 'o' denotes lattice points outside the placement set; lattice points on the boundary can be partitioned into three sets according to the direction, from which they can be reached.

We conclude this subsection by deriving the expression for the probabilities $\mathbb{P}((m,n),\mathsf{e})$ and $\mathbb{P}((m,n),\mathsf{c})$. Let us partition the boundary $\mathcal{B}(h)$ into three mutually disjoint sets:

$$\begin{aligned}\mathcal{B}^w(h) &= \{(m,n)\in\mathcal{B}(h) : (m-1,n)\in\mathcal{B}(h)\}\\ \mathcal{B}^s(h) &= \{(m,n)\in\mathcal{B}(h) : (m,n-1)\in\mathcal{B}(h)\}\\ \mathcal{B}^{null}(h) &= \{(m,n)\in\mathcal{B}(h) : (m-1,n)\notin\mathcal{B}(h) \text{ and}\\ &\qquad (m,n-1)\notin\mathcal{B}(h)\}.\end{aligned}$$

For a depiction of the various boundary points, see Fig. 3. Now, $\mathbb{P}((m,n),\mathsf{e})$ can be written as:

$$\mathbb{P}((m,n),\mathsf{e}) = \begin{cases} \binom{m+n}{m}p(1-p)^{m+n-1}q^m(1-q)^n \\ \qquad\qquad \text{if } (m,n)\in\mathcal{P}^c(h)\cup\mathcal{B}^{null}(h) \\ \binom{m+n-1}{m}p(1-p)^{m+n-1}q^m(1-q)^n \text{ if } (m,n)\in\mathcal{B}^w(h) \\ \binom{m+n-1}{m-1}p(1-p)^{m+n-1}q^m(1-q)^n \text{ if } (m,n)\in\mathcal{B}^s(h). \end{cases}$$

This can be understood as follows. Any point $(m,n)\in\mathcal{P}^c(h)\cup\mathcal{B}^{null}(h)$ can be reached from West or South. $\binom{m+n}{m}$ is the number of possible paths for reaching (m,n). Each such path has to go m times Eastwards (thus the term q^m) and n times Northwards (thus the term $(1-q)^n$) and finally ending at (m,n) (thus the term $p(1-p)^{m+n-1}$). Any point $(m,n)\in\mathcal{B}^w(h)$ can be reached only from South point $(m,n-1)$. The probability of reaching $(m,n-1)$ without ending is $\binom{m+n-1}{m}(1-p)^{m+n-1}q^m(1-q)^{n-1}$. Then, the corridor reaches (m,n) and ends with probability $p(1-q)$. $\mathbb{P}((m,n),\mathsf{e})$ for $(m,n)\in\mathcal{B}^s(h)$ can be obtained analogously.

Similarly, $\mathbb{P}((m,n),\mathsf{c})$ can be written as:

$$\mathbb{P}((m,n),\mathsf{c}) = \begin{cases} \binom{m+n}{m}(1-p)^{m+n}q^m(1-q)^n \\ \qquad\qquad \text{if } (m,n)\in\mathcal{P}^c(h)\cup\mathcal{B}^{null}(h) \\ \binom{m+n-1}{m}(1-p)^{m+n}q^m(1-q)^n \text{ if } (m,n)\in\mathcal{B}^w(h) \\ \binom{m+n-1}{m-1}(1-p)^{m+n}q^m(1-q)^n \text{ if } (m,n)\in\mathcal{B}^s(h). \end{cases}$$

V. OSLA Based Fixed Point Iteration Algorithm

In this section, we present an efficient fixed point iteration algorithm (Algorithm 1) using the OSLA rule in (11) for obtaining the optimal placement set, $\mathcal{P}_\lambda$, and the optimal cost-to-go, $J_\lambda(0,0)$. There are two advantages of our algorithm over the naive approach of directly trying to minimize the function $g(\cdot)$ to obtain $J_\lambda(0,0)$ (recall that $J_\lambda(0,0)=\min_{h\geq 0} g(h)$):

- On the theoretical side, this iterative algorithm avoids explicit optimization altogether, which, otherwise would be performed numerically over a continuous range. Without any structure on the objective function, direct numerical minimization of $g(\cdot)$ is difficult and often unsatisfactory, as it invariably uses some sort of heuristic search over this continuous range.
- On the practical side, this algorithm is proved to converge within a finite number of iterations and observed to be extremely fast (requires 3 to 4 iterations typically).

The following is our Algorithm which we refer to as the OSLA Based Fixed Point Iteration Algorithm.

Algorithm 1 OSLA Based Fixed Point Iteration Algorithm

Require: $0<p<1,\ 0\leq q\leq 1,\ \lambda\geq 0$

```
k = 0, h^(k) = 0
while 1 do
    P(h^(k)) ← {(m,n) ∈ Z_+^2 : p(λ + h^(k)) ≤ Δ_q(m,n)}
    Compute g(h^(k)) using (17)
    if g(h^(k)) == h^(k) then
        Break;
    end if
    h^(k+1) ← g(h^(k))
    k ← k + 1
end while
return g(h^(k)), P(h^(k))
```

We now prove the correctness and finite termination properties of our algorithm. First, we define $g^* := J_\lambda(0,0) = \min_{h\geq 0} g(h)$. Now consider a sample plot of the function $g(h)$ in Fig. 4. From Fig. 4(a) observe that whenever $h>g^*$ (which is around 150), $h>g(h)$. Also, Fig. 4(b) (where we have plotted the functions $g(h)$ and $l(h)=h$) suggests that $g(h)$ has a unique fixed point. We formally prove these results.

Lemma 3: If $h>g^*$ then $h>g(h)$.

Proof: This follows from the manipulation of (17). See Appendix D for details. ■

Lemma 4: $g(h)$ has a unique fixed point.

Proof: From (14) and (11), we observe that $\mathcal{P}(J_\lambda(0,0)) = \overline{\mathcal{P}}_\lambda$. From Theorem 3, $\overline{\mathcal{P}}_\lambda$ is the optimal placement set and thus the cost-to-go of using $\mathcal{P}(J_\lambda(0,0))$ is $J_\lambda(0,0)$, i.e., $g(J_\lambda(0,0)) = J_\lambda(0,0)$. Hence, $J_\lambda(0,0)=g^*$ is a fixed point of $g(\cdot)$. Now, any $h>g^*$ cannot be a fixed point since, in this case, $h>g(h)$ from Lemma 3. On the other hand, any $h<g^*$ is such that $h<g^*\leq g(h)$ because g^* is the optimal cost-to-go. Hence, g^* is the unique fixed point of $g(\cdot)$. ■

We are now ready to prove the convergence property of our Algorithm.

Lemma 5: 1) The sequence $\{h^{(k)}\}_{k\geq 1}$ (in Algorithm 1) is non-increasing, i.e., $h^{(k+1)}\leq h^{(k)}$, with the equality sign holding if and only if $h^{(k)}=g^*$.

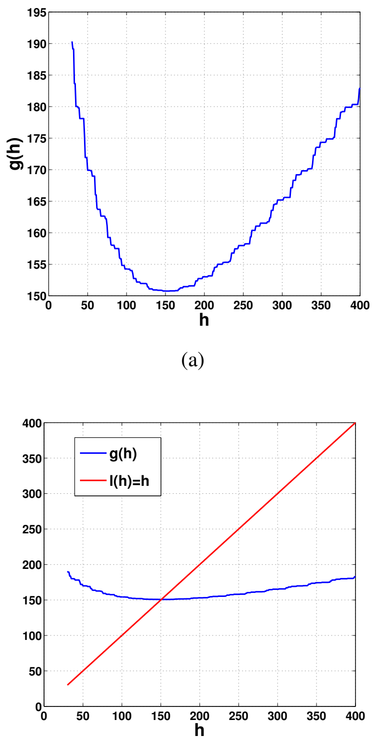

(a)

(b)

Fig. 4. (a) Cost-to-go $g(h)$ as a function of h (b) Zoom on the cost-to-go $g(h)$ as a function of h. These plots are for $p = 0.02$, $q = 0.5$, and $\lambda = 41$.

2) The sequence $\{\mathcal{P}^c(h^{(k)})\}_{k\geq 1}$ is non-increasing, i.e., $\mathcal{P}^c(h^{(k+1)}) \subseteq \mathcal{P}^c(h^{(k)})$, where the containment is strict whenever $\mathcal{P}^c(h^{(k+1)}) \subsetneq {\mathcal{P}_\lambda}^c$.

Proof: 1) Note first that $h^{(k)} \geq g^*$ for $k \geq 1$ because $h^{(k)} = g(h^{(k-1)}) \geq g^*$. Then, for $k \geq 1$, we have either $h^{(k)} = g^*$ or $h^{(k)} > g^*$. In the first case $h^{(k+1)} = g(h^{(k)}) = g(g^*) = g^* = h^{(k)}$ and we can stop, whereas in the second case, from Lemma 3 we have $h^{(k+1)} = g(h^{(k)}) < h^{(k)}$.

2) From (14), $h_2 > h_1$ implies $\mathcal{P}^c(h_1) \subseteq \mathcal{P}^c(h_2)$. Hence, as $\{h^{(k)}\}_{k\geq 1}$ is non-increasing (from Part 1)), $\{\mathcal{P}^c(h^{(k)})\}_{k\geq 1}$ is also non-increasing.

Suppose $\mathcal{P}^c(h^{(k+1)}) = \mathcal{P}^c(h^{(k)})$ then $g(h^{(k+1)}) = g(h^{(k)}) = h^{(k+1)}$ (second equality is by the definition of $\{h^{(k)}\}$), which implies $h^{(k+1)} = g^*$ (since $g(\cdot)$ has a unique fixed point, see Lemma 4). Thus, $\mathcal{P}^c(h^{(k+1)}) = {\mathcal{P}_\lambda}^c$. ■

Theorem 4: Algorithm 1 returns g^* and ${\mathcal{P}_\lambda}^c$ in a finite number of steps.

Proof: Noting that $h^{(1)} = g(h^{(0)}) \geq g^*$ and using (14), we have ${\mathcal{P}_\lambda}^c \subseteq \mathcal{P}^c(h^{(1)})$. Either ${\mathcal{P}_\lambda}^c = \mathcal{P}^c(h^{(1)})$, in which case the algorithm stops. Otherwise, note that both sets, ${\mathcal{P}_\lambda}^c$ and $\mathcal{P}^c(h^{(1)})$ contain a finite number of lattice points (from the definition of $\mathcal{P}(h)$ in (14)). Using Lemma 5, $\mathcal{P}^c(h^{(k)})$ converges to ${\mathcal{P}_\lambda}^c$ in at most $|\mathcal{P}^c(h^{(1)}) - {\mathcal{P}_\lambda}^c| < \infty$ iterations. Once $\mathcal{P}^c(h^{(k)})$ converges to $\mathcal{P}_\lambda$, the algorithm stops and returns the optimal cost-to-go g^*. ■

VI. Solving the Constrained Problem

In this section, we devise a method to solve the constrained problem in (3) using the solution of the unconstrained problem (2) provided by Algorithm 1. This method is applied in Section VII-B where, imposing a constraint on the average number of relays, we compare the performance of a distance based heuristic with the optimal.

We begin with the following standard result which relates the solutions of the problems in (2) and (3).

Lemma 6: Let $\pi_\lambda^* \in \Pi$ be an optimal policy for the unconstrained problem in (2) such that $\mathbb{E}_{\pi_\lambda^*} N = \rho_{avg}$. Then π_λ^* is also optimal for the constrained problem in (3).

However, the above lemma is useful only when we are able to exhibit a λ such that $\mathbb{E}_{\pi_\lambda^*} N = \rho_{avg}$. The subsequent development in this section is towards obtaining the solution to the more general case.

The expected number of relays used by the optimal policy, π_λ^*, which uses the optimal placement set $\mathcal{P}_\lambda$, can be computed as:

$$\mathbb{E}_{\pi_\lambda^*} N = \frac{\sum_{(m,n)\in\mathcal{B}_\lambda} \mathbb{P}((m,n),\mathsf{c})}{1 - \sum_{(m,n)\in\mathcal{B}_\lambda} \mathbb{P}((m,n),\mathsf{c})}, \tag{18}$$

where $\mathbb{P}((m,n),\mathsf{c})$ is the reaching probability corresponding to $\mathcal{P}_\lambda$ and $\mathcal{B}_\lambda$ is the boundary of $\mathcal{P}_\lambda$. A plot of $\mathbb{E}_{\pi_\lambda^*} N$ vs. λ is given in Fig. 5. We make the following observations about $\mathbb{E}_{\pi_\lambda^*} N$.

1) $\mathbb{E}_{\pi_\lambda^*} N$ decreases with λ; this is as expected, since as each relay becomes "costlier" fewer relays are used on the average.

2) Even when $\lambda = 0$, $\mathbb{E}_{\pi_\lambda^*} N$ is finite. This is because $d(0) > 0$, i.e., there is a positive cost for a 0 length link. Define the value of $\mathbb{E}_{\pi_\lambda^*} N$ with $\lambda = 0$ to be $\rho_{\max}$.

3) $\mathbb{E}_{\pi_\lambda^*} N$ vs. λ is a piecewise constant function. This occurs because the relay placement positions are discrete. For a range of values of λ the same threshold is optimal. This structure is also evident from the results based on the optimal stopping formulation and the OSLA rule in Section IV. It follows that for a value of λ at which there is a step in the plot, there are two optimal deterministic policies, $\underline{\pi}$ and $\overline{\pi}$, for the relaxed problem. Let $\underline{\rho} = \mathbb{E}_{\underline{\pi}} N$ and $\overline{\rho} = \mathbb{E}_{\overline{\pi}} N$.

We have the following structure of the optimal policy for the constrained problem:

Theorem 5: 1) For $\rho_{avg} \geq \rho_{max}$ the optimal placement set is obtained for $\lambda = 0$, i.e., is $\mathcal{P}_0$.

2) For $\rho_{avg} < \rho_{max}$, if there is a λ such that (a) $\mathbb{E}_{\pi_\lambda^*} N = \rho_{avg}$ then the optimal policy is π_λ^*, or (b) $\underline{\rho} < \rho_{avg} < \overline{\rho}$ then the optimal policy is obtained by mixing $\underline{\pi}$ and $\overline{\pi}$.

Proof: 1) is straight forward. For proof of 2)-(a), see Lemma 6. Considering now 2)-(b), define $0 < \alpha < 1$ such that $(1-\alpha)\underline{\rho} + \alpha\overline{\rho} = \rho_{avg}$. We obtain a mixing policy π_m by choosing $\underline{\pi}$ w.p. $1-\alpha$ and $\overline{\pi}$ w.p. α at the beginning of the deployment. For any policy π we have the following standard

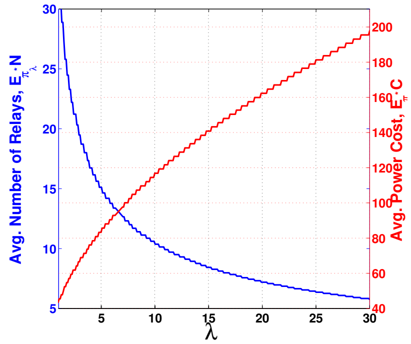

Fig. 5. Average number of relays $\mathbb{E}_{\pi_\lambda^*}N$ (left) and average power cost $\mathbb{E}_{\pi_\lambda^*}C$ (right) as a function of λ ($p = 0.002$, $q = 0.5$ and $\eta = 2$).

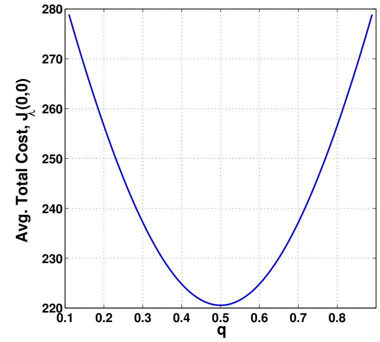

Fig. 7. Average total cost $J_\lambda(0, 0)$ as a function of q ($p = 0.002$ and $\eta = 2$).

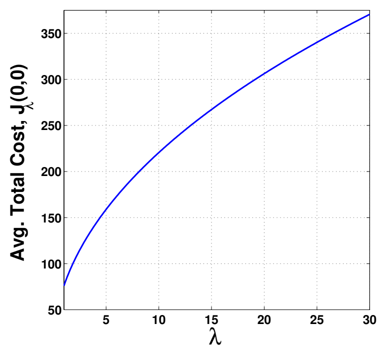

Fig. 6. Average total cost $J_\lambda(0, 0)$ as a function of λ ($p = 0.002$, $q = 0.5$ and $\eta = 2$).

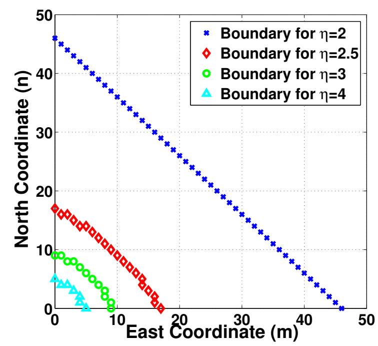

Fig. 8. Boundaries for various values of the path-loss exponent η ($p = 0.002$, $q = 0.5$).

argument:

$$\begin{aligned}
&\mathbb{E}_{\pi_m} C + \lambda \mathbb{E}_{\pi_m} N \\
&= (1-\alpha)(\mathbb{E}_{\underline{\pi}} C + \lambda \underline{\rho}) + \alpha(\mathbb{E}_{\overline{\pi}} C + \lambda \overline{\rho}) \\
&\leq (1-\alpha)(\mathbb{E}_{\pi} C + \lambda \mathbb{E}_{\pi} N) + \alpha(\mathbb{E}_{\pi} C + \lambda \mathbb{E}_{\pi} N) \\
&= \mathbb{E}_{\pi} C + \lambda \mathbb{E}_{\pi} N. \qquad (19)
\end{aligned}$$

The inequality is because $\underline{\pi}$ and $\overline{\pi}$ are both optimal for the problem (2) with relay price λ. Thus, we have shown that π_m is also optimal for the relaxed problem. Using this along with $\mathbb{E}_{\pi_m} N = \rho_{avg}$ in Lemma 6, we conclude the proof. ■

VII. Numerical Work

For our numerical work we use the one-hop power function $d(r) = P_m + \gamma r^\eta$, with $P_m = 0.1$, $\gamma = 0.01$. We first study the effect of parameter variation on the various costs. Next, we compare the performance of a distance based heuristic with the optimal.

A. Effect of Parameter Variation

In Fig. 3, we have already shown an optimal placement boundary for $p = 0.002$, $q = 0.5$, and $\eta = 3$. Since $q = 0.5$ the boundary is symmetric about the $m = n$ line.

In Fig. 5, we plot $E_{\pi_\lambda^*}N$ and $E_{\pi_\lambda^*}C$ vs. λ. The plot of $J_\lambda(0, 0)$ vs. λ is in Fig. 6. These plots are for $p = 0.002$ and $q = 0.5$. Since λ is the cost per relay, as expected, $E_{\pi_\lambda^*}N$ decreases as λ increases. We observe that $E_{\pi_\lambda^*}C$ and the optimal total cost $J_\lambda(0, 0)$ increase as λ increases. A close examination of Fig. 5 reveals that both the plots are step functions. This is due to the discrete placement at lattice points, which results in the same placement boundary being optimal for a range of λ values. Thus, as seen in Section VI, at the λ values, where there is jump in $E_{\pi_\lambda^*}N$, a random mixture of two policies is needed.

Fig. 7 shows the variation of the total optimal cost $J_\lambda(0, 0)$ with q. The variation is symmetric about $q = 0.5$. For a given probability p of the path ending, $q = 0.5$ results in the path folding frequently. In such a case, since NLOS propagation is permitted, and the path-loss is isotropic, fewer relays are required to be placed. On the other hand, when q is close to 0 or to 1 the path takes fewer turns and more relays are needed, leading to larger values of the total cost.

In Fig. 8 we show the variation of optimal boundaries with η. As η, the path-loss exponent, increases the hop cost increases for a given hop distance. This results in relays needing to be placed more frequently. As can be seen the placement boundaries shrink with increasing η. We also notice that the placement boundary for $\eta = 2$ is a straight line; indeed this provable result holds for $\eta = 2$ for any values of p and q.

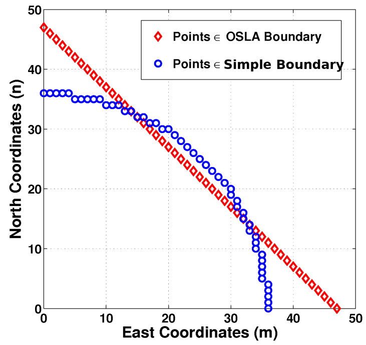

Fig. 9. Boundary of the optimal placement set (OSLA boundary) and boundary derived from the heuristic policy ($p = 0.002$, $q = 0.5$ and $\eta = 2$).

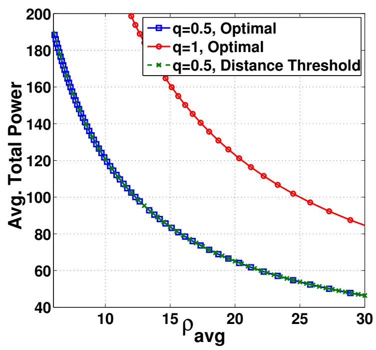

Fig. 10. Average total power as a function of ρ for the optimal policy ($q = 0.5$ and $q = 1$, which corresponds to the straight line) and for the heuristic ($q = 0.5$) for $p = 0.002$ and $\eta = 2$.

B. Comparison with the Distance based Heuristic

We recall from the literature survey in Section I that prior work invariably proposed the policy of placing a relay after the RF signal strength from the previous relay dropped below a threshold. For isotropic propagation (as we have assumed in this paper), this is equivalent to placing the relay after a circular boundary is crossed. With this in mind, we obtained the *optimal constant distance placement policy* (called *the heuristic* hereafter) numerically in a manner similar to what is described in Section IV-B. A sample result is provided in Fig. 9, for the parameters $p = 0.002$, $q = 0.5$ and $\eta = 2$. We observe that if the path were to evolve roughly Eastward or Northward then the heuristic will result in many more relays being placed. On the other hand, if the path evolves diagonally (which has higher probability) then the two placement boundaries will result in similar placement decisions.

This observation shows up in Fig. 10, where we show the cost incurred by the optimal policy (for $q = 0.5$ and for $q = 1$, which corresponds to a straight line corridor) and the heuristic ($q = 0.5$) vs. ρ for the constrained problem. As expected, the cost is much larger for $q = 1$ since the path does not fold. We find that for $q = 0.5$ the optimal placement boundary and the heuristic provide costs that are almost indistinguishable at this scale. We have performed simulations by varying the system parameters and observed the same good performance of the optimal constant distance placement policy. This suggests that the heuristic policy performs well provided that the threshold distance is optimally chosen with respect to the system parameters.

VIII. Conclusion

We considered the problem of placing relays on a random lattice path to optimize a linear combination of average power cost and average number of relays deployed. The optimal placement policy was proved to be of threshold nature (Theorem 1). We further proved the optimality of the OSLA rule (in Theorem 3). We have also devised an OLSA based fixed point iteration algorithm (Algorithm 1), which we have proved to converge to the optimal placement set in a finite number of steps. Through numerical work we observed that the performance (in terms of average power incurred for a given relay constraint) of the optimal policy is closed to that of the distance threshold policy provided that the threshold distance is optimally chosen with respect to the system parameters.

References

[1] C. Fischer and H. Gellersen, "Location and Navigation Support for Emergency Responders: A Survey," *IEEE Pervasive Computing*, vol. 9, no. 1, pp. 38–49, Jan.-Mar. 2010.

[2] A. Howard, M. J. Matarić, and S. Sukhat Gaurav, "An Incremental Self-Deployment Algorithm for Mobile Sensor Networks," *Kluwer Autonomous Robots*, vol. 13, no. 2, pp. 113–126, Sept. 2002.

[3] G. Loukas, S. Timotheou, and E. Gelenbe, "Robotic Wireless Network Connection of Civilians for Emergency Response Operations," in *Proc. of the IEEE International Symposium on Computer and Information Sciences (ISCIS)*, Istanbul, Turkey, Oct. 2008.

[4] D. Naudts, S. Bouckaert, J. Bergs, A. Schouttcet, C. Blondia, I. Moerman, and P. Demeester, "A Wireless Mesh Monitoring and Planning Tool for Emergency Services," in *Proc. of the IEEE Workshop on End-to-End Monitoring Techniques and Services (E2EMON)*, Munich, Germany, May 2007.

[5] M. R. Souryal, J. Geissbuehler, L. E. Miller, and N. Moayeri, "Real-Time Deployment of Multihop Relays for Range Extension," in *Proc. of the ACM International Conference on Mobile Systems, Applications and Services (MobiSys)*, San Juan, Puerto Rico, June 2007.

[6] M. R. Souryal, A. Wapf, and N. Moayeri, "Rapidly-Deployable Mesh Network Testbed," in *Proc. of the IEEE Conference on Global Telecommunications (GLOBECOM)*, Honolulu, Hawai, USA, Nov. 2009.

[7] T. Aurisch and J. Tölle, "Relay Placement for Ad-hoc Networks in Crisis and Emergency Scenarios," in *Proc. of the Information Systems and Technology Panel (IST) Symposium*. Bucharest, Romania: NATO Science and Technology Organization, May 2009.

[8] H. Liu, J. Li, Z. Xie, S. Lin, K. Whitehouse, J. A. Stankovic, and D. Siu, "Automatic and Robust Breadcrumb System Deployment for Indoor Firefighter Applications," in *Proc. of the ACM International Conference on Mobile Systems, Applications and Services (MobiSys)*, San Francisco, California, USA, June 2010.

[9] P. Mondal, K. P. Naveen, and A. Kumar, "Optimal Deployment of Impromptu Wireless Sensor Networks," in *Proc. of the IEEE National Conference on Communications (NCC)*, Kharagpur, India, Feb. 2012.

[10] R. Srivastava and A. Kumar, "Performance Analysis of Beacon-Less IEEE 802.15.4 Multi-Hop Networks," in *Proc. of the IEEE International Conference on Communication Systems and Networks (COMSNETS)*, Bangalore, India, Jan. 2012.

[11] P. Mondal, "Optimal Deployment of Impromptu Wireless Sensor Networks," Master's thesis, Indian Institute of Science, Bangalore, 2011.

[12] D. P. Bertsekas, *Dynamic Programming and Optimal Control, Vol-II, 3rd Edition*. Athena Scientific, Belmont, Massachusetts, 1995.

[13] S. Boyd and L. Vandenberghe, *Convex Optimization*. Cambridge University Press, 2004.

APPENDIX A
PROOF OF LEMMAS IN SECTION II

A. Proof of Lemma 1

Proof: Any norm is convex so that the function $g(x,y) \equiv \sqrt{x^2+y^2}$ is convex in (x,y). The delay function $d(\cdot)$ is also assumed to be convex and non-decreasing in its argument. Hence by using the composition rule [13, Section 3.2.4], we conclude that the function $d(x,y) \equiv d(\sqrt{x^2+y^2})$ is convex in $(x,y) \in \mathbb{R}^2$. ■

B. Proof of Lemma 2

Proof: It is easier to prove the lemma allowing the arguments m and n take values from the Real line. We have,

$$\Delta_1(x,y) = d(x+\delta,y) - d(x,y)$$

Partially differentiating both sides w.r.t. x, we get

$$\begin{aligned}\frac{\partial \Delta_1(x,y)}{\partial x} &= d_x(x+\delta,y) - d_x(x,y) \\ &= \delta d_{xx}(\zeta,y) \text{ where } x<\zeta<x+\delta \\ &> 0,\end{aligned}$$

where the equality follows from the application of Lagrange's Mean Value Theorem to the function $d_x(.,y)$ and the inequality is due to assumption in (1). The above proves the fact that $\Delta_1(x,y)$ is non-decreasing in x.

To prove that $\Delta_1(x,y)$ is non-decreasing in y, we partially differentiate $\Delta_1(x,y)$ w.r.t. y and obtain

$$\begin{aligned}\frac{\partial \Delta_1(x,y)}{\partial y} &= d_y(x+\delta,y) - d_y(x,y) \\ &= \delta d_{xy}(\eta,y) \text{ where } x<\eta<x+\delta \\ &> 0,\end{aligned}$$

where the equality follows from the application of Lagrange's Mean Value Theorem to the function $d_y(.,y)$ and the inequality is due to assumption in (1). This shows that the function $\Delta_1(x,y)$ is non-decreasing in both the coordinates x and y. In a similar way it can also be shown that $\Delta_2(x,y)$ is non-decreasing in x and y under the assumption made in (1). This completes the proof. ■

APPENDIX B
PROOF OF THEOREM 1

We begin by defining $H_\lambda(m,n) := J_\lambda(m,n) - d(m,n)$. Substituting for $c_p(m,n)$ and $c_{np}(m,n)$ (from (6) and (7), respectively) into (8) and rearranging we obtain (recall the definitions of $\Delta_1(m,n)$ and $\Delta_2(m,n)$ from Section II):

$$\begin{aligned}\mathcal{P}_\lambda = \\ &\Big\{(m,n): (1-p)(qH_\lambda(m+1,n)+(1-q)H_\lambda(m,n+1)) \\ &+p(q\Delta_1(m,n)+(1-q)\Delta_2(m,n)) \geq \lambda + \\ &(1-p)qJ_\lambda(1,0)+(1-p)(1-q)J_\lambda(0,1)+pd(1)\Big\}.\end{aligned} \tag{20}$$

Lemma 7: For a fixed λ, $H_\lambda(m,n)$ is non-decreasing in both $m \in \mathbb{Z}_+$ and $n \in \mathbb{Z}_+$.

Proof: Consider a sequential relay placement problem where we have K steps to go. The corridor length is the minimum of K and of a geometric random variable with parameter p. The problem be formulated as a finite horizon MDP with horizon length K. For any given (m,n), $J_K(m,n)$, $K \geq 2$ is obtained recursively:

$$\begin{aligned}&J_K(m,n) = \min\{c_p(m,n), c_{np}(m,n)\} \\ &= \min\{\lambda + d(m,n) + (1-p)qJ_{K-1}(1,0) + pqd(1) + \\ &\quad (1-p)(1-q)J_{K-1}(0,1) + p(1-q)d(1), \\ &\quad (1-p)qJ_{K-1}(m+1,n) + pqd(m+1,n) + \\ &\quad (1-p)(1-q)J_{K-1}(m,n+1) + p(1-q)d(m,n+1)\}.\end{aligned}$$

For $K=1$, since a sensor must be placed at the next step, we have $J_1(m,n) = \min\{\lambda + d(m,n) + d(1), qd(m+1,n) + (1-q)d(m,n+1)\}$. Therefore,

$$\begin{aligned}&H_1(m,n) := J_1(m,n) - d(m,n) \\ &= \min\{\lambda + d(1), q\Delta_1(m,n) + (1-q)\Delta_2(m,n)\}.\end{aligned}$$

From Lemma 2, it follows that $H_1(m,n)$ is non-decreasing in both m and n. Now we make the induction hypothesis and assume that $H_{K-1}(m,n)$ is non-decreasing in m and n. We have:

$$\begin{aligned}&H_K(m,n) = J_K(m,n) - d(m,n) \\ &= \min\{\lambda + (1-p)qJ_{K-1}(1,0) + pqd(1) + \\ &\quad (1-p)(1-q)J_{K-1}(0,1) + p(1-q)d(1), (1-p) \\ &\quad (qH_{K-1}(m+1,n) + (1-q)H_{K-1}(m,n+1)) + \\ &\quad q\Delta_1(m,n) + (1-q)\Delta_2(m,n)\}.\end{aligned}$$

By the induction hypothesis and Lemma 2, it follows that $H_K(m,n)$ is non-decreasing in both m and n. The proof is complete by taking the limit as $K \to \infty$. ■

We are now ready to prove Theorem 1.

Proof of Theorem 1: Referring to (20), utilizing Lemma 7 and the Lemma 2, it follows that for a fixed $n \in \mathbb{Z}_+$, the LHS (Left Hand Side) of (20), describing the placement set $\mathcal{P}_\lambda$ is an increasing function of m, while the RHS (Right Hand Side) is a *finite* constant. Also, because of the assumed properties of the function $d(.)$, $\Delta_1(m,n) \to \infty$ as $m \to \infty$, for any fixed n. Hence it follows that there exists an $m^*(n) \in \mathbb{Z}_+$ such that $(m,n) \in \mathcal{P}_\lambda \quad \forall m \geq m^*(n)$. Hence we may write $P_\lambda = \bigcup_{n \in \mathbb{Z}_+}\{(m,n) | m \geq m^*(n)\}$. The second characterization follows by similar arguments. ■

APPENDIX C
PROOF OF THEOREM 3

We require the following lemmas to prove Theorem 3.

Lemma 8: $\mathcal{P}_\lambda \subset \overline{\mathcal{P}}_\lambda$

Proof: Suppose that $(m,n) \in \mathcal{P}_\lambda$. Then from (9) $(m+1,n) \in \mathcal{P}_\lambda$ and from (10), $(m,n+1) \in \mathcal{P}_\lambda$. Since $(m,n) \in$

$\mathcal{P}_\lambda$, we have from (6), (7) and (8) that

$$\lambda+d(m,n)+(1-p)qJ_\lambda(1,0)+pqd(1)+(1-p)(1-q)\times J_\lambda(0,1)+p(1-q)d(1)\leq(1-p)qJ_\lambda(m+1,n)+pq\times d(m+1,n)+(1-p)(1-q)J_\lambda(m,n+1)+p(1-q)d(m,n+1). \tag{21}$$

Also we may argue that at the state $(0,0)$, it is optimal not to place. Indeed, if it had been optimal to place at the state $(0,0)$, at the next step, we return to the same state, viz., $(0,0)$. Now, because of the stationarity of the optimal policy, we would keep placing relays at the same point, and since "relay-cost" $\lambda>0$ and $d(0,0)>0$, the expected cost for this policy would be ∞. Hence,

$$J_\lambda(0,0)=(1-p)qJ_\lambda(1,0)+pqd(1)+(1-p)(1-q)J_\lambda(0,1)+p(1-q)d(1). \tag{22}$$

Since $(m+1,n)\in\mathcal{P}_\lambda$ and $(m,n+1)\in\mathcal{P}_\lambda$, we have (noticing that it is optimal to place at these points and utilizing (6) and (22)),

$$J_\lambda(m+1,n) = \lambda+d(m+1,n)+J_\lambda(0,0) \tag{23}$$
$$J_\lambda(m,n+1) = \lambda+d(m,n+1)+J_\lambda(0,0). \tag{24}$$

Now, using (22), (23) and (24) in (21), we obtain:

$$p(\lambda+J_\lambda(0,0)) \leq q\Delta_1(m,n)+(1-q)\Delta_2(m,n). \tag{25}$$

This proves that $(m,n)\in\bar{\mathcal{P}}_\lambda$ and hence $\mathcal{P}_\lambda\subset\overline{\mathcal{P}}_\lambda$ ■

Using the above Lemma and from (9), (10), (12), (13) we can conclude that:

$$n^*(m)\geq\overline{n}(m)\quad\forall m\in\mathbb{Z}_+ \tag{26}$$
$$m^*(n)\geq\overline{m}(n)\quad\forall n\in\mathbb{Z}_+. \tag{27}$$

Lemma 9: If $(m,n)\in\overline{\mathcal{P}}_\lambda$ is such that $(m,n+1)\in\mathcal{P}_\lambda$ and $(m+1,n)\in\mathcal{P}_\lambda$, then $(m,n)\in\mathcal{P}_\lambda$

Proof: Since $(m,n)\in\bar{\mathcal{P}}_\lambda$, we have from (11),

$$p(\lambda+J_\lambda(0,0))\leq q\Delta_1(m,n)+(1-q)\Delta_2(m,n). \tag{28}$$

Now $(m,n+1)\in\mathcal{P}_\lambda$, and $(m+1,n)\in\mathcal{P}_\lambda$, hence we have from (23) and (24):

$$J_\lambda(m+1,n) = \lambda+d(m+1,n)+J_\lambda(0,0)$$
$$J_\lambda(m,n+1) = \lambda+d(m,n+1)+J_\lambda(0,0).$$

The expression (22) is always true. Now using (22) and the above two equations in inequality (28), we obtain (21), which proves that $(m,n)\in\mathcal{P}_\lambda$. ■

Lemma 10: If $(m,n)\in\mathcal{P}_\lambda$ (resp. $\overline{\mathcal{P}}_\lambda$), then $(m+k,n)\in\mathcal{P}_\lambda$ (resp. $\overline{\mathcal{P}}_\lambda$) and $(m,n+k)\in\mathcal{P}_\lambda$ (resp. $\overline{\mathcal{P}}_\lambda$) for any $k\in\mathbb{Z}_+$.

Proof: The proof follows easily because the LHS of (20) is increasing in both m and n while the RHS is a constant. Similarly, the RHS of (11) is increasing in both m and n while the LHS is a constant. ■

We can now prove the main theorem.

Proof of Theorem 3: We need to show that inequalities in (26) and (27) are equalities. For any $m\in\mathbb{Z}_+$, suppose that in (26) $n^*(m)>n^*(m)-1\geq\bar{n}(m)$. Then we have the following inclusions:

$$\begin{aligned}(m,n^*(m)) &\in \mathcal{P}_\lambda\\ (m,n^*(m)-1) &\in \overline{\mathcal{P}}_\lambda\\ (m,n^*(m)-1) &\notin \mathcal{P}_\lambda.\end{aligned} \tag{29}$$

Let us index the collection of lattice-points $(m+i,n^*(m)-1)$ by $N_i, i\in\mathbb{Z}_+$. Since $(m,n^*(m)-1)\in\overline{\mathcal{P}}_\lambda$, from Lemma 10, it follows that $N_i\in\overline{\mathcal{P}}_\lambda$. From (29), $N_0\notin\mathcal{P}_\lambda$.

Then, the optimal policy being a threshold policy, we know that there exists a finite $k>0$, s.t. $N_k\in\mathcal{P}_\lambda$, i.e.,

$$(m+k,n^*(m)-1)\in\mathcal{P}_\lambda. \tag{30}$$

Again from Lemma 10, since $(m,n^*(m))\in\mathcal{P}_\lambda$, we have for any $k>0$:

$$(m+k-1,n^*(m)) \in \mathcal{P}_\lambda. \tag{31}$$

Now we see that for the point N_{k-1}, the conditions of Lemma 9 are satisfied. Hence $N_{k-1}\in\mathcal{P}_\lambda$. If $k=1$, we already have a contradiction since $N_0\notin\mathcal{P}_\lambda$. Otherwise for $k>1$, using Lemma 10 and $N_{k-1}\in\mathcal{P}_\lambda$, we can show that N_{k-2} is subject to the conditions of Lemma 9 implying that $N_{k-2}\in\mathcal{P}_\lambda$. By iteration, we finally obtain that $N_0\in\mathcal{P}_\lambda$, which contradicts (29) and proves the result. ■

Appendix D
Proof of Lemma 3

We start by showing the following lemma.

Lemma 11: For *any* placement set $\mathcal{P}(h)$ of the form in (14), we have:

$$\sum_{(m,n)\in\mathcal{P}^c(h)} r(m,n)\Big(\Delta_q(m,n)-p(\lambda+g(h))\Big) + d(0,0)+\lambda=0, \tag{32}$$

where $r(m,n)=(1-p)^{m+n}\binom{m+n}{m}q^m(1-q)^n$.

Proof: We first introduce some notations and definitions.

Let us define a path σ as a possible realization of the corridor, starting from $(0,0)$ and let $\mathbb{P}(\sigma)$ be the probability of such a path. The set of all paths is denoted by Σ. Let Σ_{mn} denote the set of all paths that end at $(m,n)\in\mathcal{P}^c(h)\cup\mathcal{B}(h)$ and $\Sigma_{mn}(c)$ the set of all paths that hit $(m,n)\in\mathcal{B}(h)$ and continue.

Let us denote the set of edges whose both end vertices belong to the set $\mathcal{P}^c(h)\cup\mathcal{B}(h)$ by E. A path σ is completely characterized by its edge set E_σ.

The reaching probability, $r(m,n)$, of a point (m,n) is defined as the probability that a random path σ *reaches* the point (m,n) and continues for at least one step. Hence, $r(m,n)=(1-p)^{m+n}\binom{m+n}{m}q^m(1-q)^n$.

The incremental cost function $\delta:E\longrightarrow\mathbb{R}_+$ is defined as follows:

$$\delta(e)=\begin{cases}d(m+1,n)-d(m,n)=\Delta_1(m,n)\\ \qquad\text{if } e=\{(m,n),(m+1,n)\}\\ d(m,n+1)-d(m,n)=\Delta_2(m,n)\\ \qquad\text{if } e=\{(m,n),(m,n+1)\}.\end{cases} \tag{33}$$

For $(m,n) \in \sigma$, the incremental cost function allows us to write:

$$d(m,n) = \sum_{e \in E_\sigma \cap E} \delta(e) + d(0,0). \tag{34}$$

Now consider

$$\begin{aligned}
&\sum_{\mathcal{P}^c(h)\cup\mathcal{B}(h)} \mathbb{P}((m,n),\mathsf{e}) d(m,n) + \sum_{\mathcal{B}(h)} \mathbb{P}((m,n),\mathsf{c}) d(m,n) \\
&= \sum_{\mathcal{P}^c(h)\cup\mathcal{B}(h)} \sum_{\sigma\in\Sigma_{mn}} \mathbb{P}(\sigma)\Bigg(\sum_{e\in E_\sigma} \delta(e) + d(0,0)\Bigg) + \\
&\quad \sum_{\mathcal{B}(h)} \sum_{\sigma\in\Sigma_{mn}(c)} \mathbb{P}(\sigma)\Bigg(\sum_{e\in E_\sigma\cap E} \delta(e) + d(0,0)\Bigg) \\
&= \sum_{e\in E} \delta(e) \sum_{\sigma\in\Sigma : e\in E_\sigma} \mathbb{P}(\sigma) + d(0,0) \\
&= \sum_{e\in E} \delta(e) t(e) + d(0,0),
\end{aligned} \tag{35}$$

where by $t(e)$ we denote the probability that a random path goes through the edge $e \in E$.

Now if e is horizontal, i.e., $e = \{(m,n),(m+1,n)\}, (m,n) \in \mathcal{P}^c(h)$, we have $t(e) = qr(m,n)$ and $\delta(e) = \Delta_1(m,n)$. Similarly if e is vertical, i.e., $e = \{(m,n),(m,n+1)\}, (m,n) \in \mathcal{P}^c(h)$, we have $t(e) = (1-q)r(m,n)$ and $\delta(e) = \Delta_2(m,n)$. Using these relations, we may rewrite (35) as follows:

$$\begin{aligned}
&\sum_{\mathcal{P}^c(h)} r(m,n)\Bigg(q\Delta_1(m,n) + (1-q)\Delta_2(m,n)\Bigg) + d(0,0) \\
&= \sum_{\mathcal{P}^c(h)} r(m,n)\Delta_q(m,n) + d(0,0).
\end{aligned} \tag{36}$$

Now consider the probability $\sum_{(m,n)\in\mathcal{B}(h)} \mathbb{P}((m,n),\mathsf{c})$. It is the probability that a random path continues beyond the boundary $\mathcal{B}(h)$. Hence we may write

$$\begin{aligned}
\sum_{\mathcal{B}(h)} \mathbb{P}((m,n),\mathsf{c}) &= 1 - \sum_{\mathcal{P}^c(h)\cup\mathcal{B}(h)} \mathbb{P}((m,n),\mathsf{e}) \\
&= 1 - \sum_{\mathcal{P}^c(h)} r(m,n)p.
\end{aligned} \tag{37}$$

Using (36) and (37) in (17) and simplifying, we obtain the result. ■

Proof of Lemma 3:

We recall the definition of $\mathcal{P}^c(h)$.

$$\mathcal{P}^c(h) = \{(m,n) \in \mathbb{Z}_+^2 : p(\lambda + h) > \Delta_q(m,n)\}. \tag{38}$$

Since $h > g^*$, we immediately conclude that ${\mathcal{P}_\lambda}^c \subset \mathcal{P}^c(h)$. From (32) in Lemma 11, we may write for the optimal placement set $\mathcal{P}_\lambda$:

$$\begin{aligned}
\sum_{{\mathcal{P}_\lambda}^c} r(m,n)\Delta_q(m,n) &= p(\lambda+g^*) \sum_{{\mathcal{P}_\lambda}^c} r(m,n) \\
&\quad -(d(0,0)+\lambda).
\end{aligned} \tag{39}$$

We may similarly write for the placement set $\mathcal{P}(h)$:

$$\begin{aligned}
\sum_{\mathcal{P}^c(h)} r(m,n)\Delta_q(m,n) &= p(\lambda+g(h)) \sum_{\mathcal{P}^c(h)} r(m,n) \\
&\quad -(d(0,0)+\lambda).
\end{aligned} \tag{40}$$

Now, since ${\mathcal{P}_\lambda}^c \subset \mathcal{P}^c(h)$, we may expand the LHS of (40) as follows:

$$\begin{aligned}
&\sum_{\mathcal{P}^c(h)} r(m,n)\Delta_q(m,n) \\
&= \sum_{\mathcal{P}_\lambda^c} r(m,n)\Delta_q(m,n) + \sum_{\mathcal{P}^c(h)\setminus\mathcal{P}_\lambda^c} r(m,n)\Delta_q(m,n) \\
&< \sum_{\mathcal{P}_\lambda^c} r(m,n)\Delta_q(m,n) + p(\lambda+h) \sum_{\mathcal{P}^c(h)\setminus\mathcal{P}_\lambda^c} r(m,n) \\
&= p(\lambda+g^*) \sum_{\mathcal{P}_\lambda^c} r(m,n) - (d(0,0)+\lambda) \\
&\quad + p(\lambda+h) \sum_{\mathcal{P}^c(h)\setminus\mathcal{P}_\lambda^c} r(m,n),
\end{aligned} \tag{41}$$

where, for the inequality, we used (38) and for (41), we have substituted the value for the quantity from (39). We may alternatively write the RHS of (40) as:

$$\begin{aligned}
&p(\lambda+g(h)) \sum_{\mathcal{P}^c(h)} r(m,n) - (d(0,0)+\lambda) \\
&= p(\lambda+g(h))\Bigg(\sum_{{\mathcal{P}_\lambda}^c} r(m,n) + \sum_{\mathcal{P}^c(h)\setminus{\mathcal{P}_\lambda}^c} r(m,n)\Bigg) \\
&\quad - (d(0,0)+\lambda).
\end{aligned} \tag{42}$$

Now comparing (41) and (42) and rearranging, we may write:

$$p(g(h)-g^*) \sum_{{\mathcal{P}_\lambda}^c} r(m,n) < p(h-g(h)) \sum_{\mathcal{P}^c(h)\setminus{\mathcal{P}_\lambda}^c} r(m,n) \tag{43}$$

Now $\sum_{\mathcal{P}^c(h)\setminus{\mathcal{P}_\lambda}^c} r(m,n) = 0$ if and only if $\mathcal{P}^c(h)\setminus{\mathcal{P}_\lambda}^c = \varnothing$, i.e., $\mathcal{P}(h) = \mathcal{P}_\lambda$. In this case we get $g(h) = g^* < h$. On the other hand, if $\sum_{\mathcal{P}^c(h)\setminus{\mathcal{P}_\lambda}^c} r(m,n) > 0$, since $g^* \le g(h)$, from the inequality (43), we conclude that $h > g(h)$. ■